PROGRAMA DE PÓS-GRADUAÇÃO EM CIÊNCIAS BIOLÓGICAS: BIOQUÍMICA

DEPARTAMENTO DE BIOQUÍMICA

INSTITUTO DE CIÊNCIAS BÁSICAS DA SAÚDE

UNIVERSIDADE FEDERAL DO RIO GRANDE DO SUL

Tese de Doutorado

# Modulação do metabolismo mitocondrial como estratégia terapêutica e profilática no traumatismo cranioencefálico: Abordagens farmacológicas e comportamentais em modelos pré-clínicos

Randhall Bruce Kreismann Carteri

Porto Alegre

2019

PROGRAMA DE PÓS-GRADUAÇÃO EM CIÊNCIAS BIOLÓGICAS: BIOQUÍMICA

DEPARTAMENTO DE BIOQUÍMICA

INSTITUTO DE CIÊNCIAS BÁSICAS DA SAÚDE

UNIVERSIDADE FEDERAL DO RIO GRANDE DO SUL

Tese de Doutorado

# Modulação do metabolismo mitocondrial como estratégia terapêutica e profilática no traumatismo cranioencefálico: Abordagens farmacológicas e comportamentais em modelos pré-clínicos

Tese apresentada ao Programa de Pós - Graduação em Ciências Biológicas - Bioquímica da Universidade Federal do Rio Grande do Sul, como requisito parcial à obtenção do grau de Doutor em Bioquímica.

**Randhall Bruce Kreismann Carteri**

Orientador: Prof. Dr. Luis Valmor Cruz Portela

Porto Alegre

2019

*“Did I ever tell you what the definition of insanity is? Insanity is doing the exact... same thing... over and over again expecting... changes... That. Is. Crazy. ”*

*- Vaas Montenegro*

**Agradecimentos**

Em primeiro lugar, agradeço a minha família, *José Luis* e *Karin,* meus pais, aqueles que com doação integral e suporte inabalável auxiliaram minha vida toda. Aos meus avós, *Alda*, *Nely* e *Nelson* que também acompanharam o processo. Ao meu filho *Dimitri,* minha maior motivação nos momentos de dificuldade. Obrigado por me tornar melhor. Obrigado por fazer meus dias melhores.

Agradeço o professor doutor *Luis Valmor Cruz Portela*, pelo suporte em todas as esferas necessárias e tornando possível completar a jornada sem querer cometer "*auto-suicídio de mim mesmo*". Agradeço também a *toda família Portela* pelo acolhimento. Aos colegas do *Neurotrauma Lab*, amigos, pelo suporte e auxílio nessa caminhada. Obrigado *Afonso*, *Nathan* e *Marcelo* pela amizade, paciência e parceria no desenvolvimento dos trabalhos aqui apresentados e muitos outros que vão surgir. Agradeço a *Mônia* e a *Marceli,* pela parceria para experimentos e por muito me ensinarem sobre ensinar. Agradeço a *Lizia*, pela ajuda para a conclusão dos trabalhos, pela paciência com as confusões e por confiar (aparentemente) em mim. Finalmente, agradeço aos recém-chegados, *Wanda*, *Luiza* e *Wesley*, pela ajuda na reta final. Podem ter certeza que escolheram o melhor lugar para crescer em vários aspectos. Agradeço ao professor *Marcelo Ganzella*, pela disponibilidade e paciência, no auxílio com técnicas e pelos ensinamentos. Agradeço ao professor *Antônio Galina* pela inspiração, por todo incentivo e ensinamentos, ao professor *Jean Pierre* pelo envolvimento e ajuda que me possibilitaram crescimento profissional. Agradeço também a professora *Gisele Hansel* por desde o início ajudar no que fosse possível e se envolver com a realização de muitos trabalhos. Agradeço também ao professor *Douglas Smith* por confiar no potencial dos nossos trabalhos e enriquecer nossa produção com sua colaboração.

Agradeço a Professora *Lisiane* por também me ajudar ao longo do processo e também ajudar no desenvolvimento dos trabalhos. Agradeço a todos integrantes de seu grupo, *Amanda*, *Daniela*, *Catiane* e *Marcus*, não somente pelo café de cada dia, mas pela paciência em disponibilizar espaço e materiais, além de "abraçarem a causa" e ajudarem no desenvolvimento de trabalhos. Agradeço ao Professor *Renato* pelas inúmeras discussões sobre bioquímica e futebol durante o café matinal. És meu ídolo no departamento!

Agradeço ao professor *Fábio* pelo apoio em diversos momentos. Agradeço muito ao *Marco Antônio* pelo suporte e parceria para abraçar as ideias e elevar nossos trabalhos para um nível superior. Agradeço ao professor *Diogo Souza* pela ajuda sempre que solicitada. Agradeço também a professora *Débora Guerini* pelo auxílio durante os semestres de aulas e por se envolver também com nossos trabalhos. Ainda, agradeço aos professores *Fátima Guma*, *Clóvis Wannmacher* e *David Driemeier* pelo auxílio que proporcionou aprimorar o desenvolvimento dos trabalhos desta tese. Ainda, obviamente, agradeço também aos colegas *Franciele Rohden*, *Itiane Franceschi* e *Marcia Hammerschmitt* pelo profissionalismo e ajuda nos trabalhos.

Finalmente, agradeço a *Fabíola e todo pessoal do biotério* pelo trabalho diário que facilita nossa vida. Ao todo pessoal da secretaria, principalmente a *Cléia* e o *Giordano* por sempre ajudar a resolver minhas confusões burocráticas. Agradeço também ao pessoal da segurança por toda simpatia e paciência com os horários atípicos. O Departamento de bioquímica só funciona por causa de vocês!

Em resumo agradeço a todos que de forma direta ou indireta contribuíram para que esse trabalho fosse desenvolvido. Já dizia o sábio professor *Tuiskon Dick*: "O produto da tese não são os artigos e sim o aluno". Portanto, o resultado desse trabalho só existe por influência de todos vocês.

Muito Obrigado!

# APRESENTAÇÃO

Esta tese está organizada em três Partes, cada uma sendo constituída dos seguintes itens:

**Parte I:** Resumo, Resumo em inglês (abstract), Lista de abreviações, Introdução e Objetivos;

**Parte II:** Resultados, apresentados na forma capítulos constituídos de artigos científicos, sendo que cada capítulo contém um breve prefácio;

**Parte III:** Discussão, Conclusão, Anexos e Referências bibliográficas citadas na Introdução da Parte I, e Discussão da Parte III.

Na seção "Anexos" estão os artigos científicos em preparação que foram também desenvolvidos durante o período de doutoramento que tem conteúdo dissociado do tema central da tese (Anexo I e Anexo II) e artigos científicos com enfoque clínico publicados durante a tese (Anexo III e Anexo IV). Os trabalhos elaborados nesta tese foram desenvolvidos no Laboratório de Neurotrauma e Biomarcadores, no Departamento de Bioquímica da Universidade Federal do Rio Grande do Sul (UFRGS), sob a orientação do Dr. Luis Valmor Cruz Portela.

**SUMÁRIO**

# PARTE I

**Resumo**

Carteri, Randhall Bruce Kreismann. Modulação do metabolismo mitocondrial como estratégia terapêutica e profilática no traumatismo cranioencefálico: Abordagens farmacológicas e comportamentais em modelos pré-clínicos. Tese de Doutorado, Programa de Pós- graduação em Ciências Biológica: Bioquímica, Universidade Federal do Rio Grande do Sul. Porto Alegre, Brasil, 2019.

O traumatismo cranioencefálico (TCE) está associado a um metabolismo mitocondrial cerebral e conectividade metabólica prejudicados. Assim, considerando a importância da mitocôndria como um determinante dos desfechos clínicos e neurológicos associados ao TCE, postulamos que estratégias farmacológicas e de pré-condicionamento das mitocôndrias de células neurais poderiam ser uma alternativa para se opor a neurodegeneração. Ainda, modulamos a atividade mitocondrial com esteroides anabólicos androgênicos (EAA), particularmente a testosterona (TS) e decanoato de nandrolona (NAND). Esta abordagem se baseia no potencial anabólico destas substâncias, muito relacionado a melhoria do metabolismo oxidativo, como já descrito previamente em atletas. Nesta tese, avançamos no entendimento dos efeitos de doses suprafisiológicas de esteroides anabólicos androgênicos (EAA) sobre mitocôndrias de órgãos como coração e fígado, e também em mitocôndrias sinápticas e extrasinápticas. Avaliamos também, o potencial farmacológico da TS em camundongos submetidos a um modelo de TCE grave denominado impacto cortical controlado (CCI). Desenvolvemos um modelo de concussão relacionada ao esporte para estudo de encefalopatia traumática crônica (ETC) em roedores além do impacto da combinação entre exercício físico e abuso de EAA na neuroenergética. Investigamos também se diferentes "volumes" de exercício físico poderiam promover adaptações neuroenergéticas mitocondriais capazes de evitar as perdas cognitivas comumente descritas no TCE grave. Finalmente, utilizamos um protocolo de jejum intermitente (IF) como estratégia nutricional de pré-condicionamento mitocondrial e avaliamos *in vivo* a conectividade metabólica entre áreas cerebrais, e a memória espacial. Nesta tese, concluímos que a TS beneficia o metabolismo mitocondrial pósTCE grave, e que estratégias profiláticas como exercício e IF promovem adaptações neuroenergéticas relevantes na prevenção e recuperação do dano cerebral.

**Palavras – chave:** Trauma cranioencefálico, mitocôndria, nutrição, exercício, bioquímica.

**Abstract**

Carteri, Randhall Bruce Kreismann. Modulation of mitochondrial metabolism as a therapeutic and prophylactic strategy in traumatic brain injury: Pharmacological and behavioral approaches in preclinical models. PhD Thesis, Post-graduation Program of Biological Sciences: Biochemistry, Universidade Federal do Rio Grande do Sul. Porto Alegre, Brazil, 2019.

Traumatic Brain Injury (TBI) is associated with impaired cerebral mitochondrial metabolism and metabolic connectivity. Thus, considering the importance of mitochondria as a determinant of the clinical and neurological outcomes associated with TBI, we postulated that pharmacological and preconditioning strategies aiming mitochondria of neural cells could be an alternative to oppose neurodegeneration. Furthermore, we modulated mitochondrial activity with androgenic anabolic steroids (AAS), particularly testosterone (TS) and nandrolone decanoate (NAND). This approach is based on the anabolic potential of these substances, closely related to the improvement of oxidative metabolism, as previously described in athletes. In this thesis, we advance the understanding of the effects of supraphysiological doses of anabolic androgenic steroids (AAS) on mitochondria of organs such as heart and liver, as well as on synaptic and extrasynaptic mitochondria. We also evaluated the pharmacological potential of TS in mice submitted to a severe TBI model called controlled cortical impact (CCI). We developed a model of sports-related concussion to study chronic traumatic encephalopathy (CTE) in rodents and also the impact of the combination of physical exercise and AAS abuse on neuroenergetics. We also investigated whether different "volumes" of physical exercise could promote mitochondrial neuroenergetic adaptations capable of avoiding the cognitive losses commonly described in severe TBI. Finally, we used an intermittent fasting protocol (IF) as a nutritional strategy for mitochondrial preconditioning and evaluated in vivo the metabolic connectivity between brain areas and spatial memory. In this thesis, we conclude that TS benefits the mitochondrial metabolism after severe ECT, and that prophylactic strategies such as exercise and IF promote relevant neuroenergetic adaptations in the prevention and recovery of brain damage.

**Key words:** Head trauma, mitochondria, nutrition, exercise, biochemistry

**Lista de abreviaturas**

TCE - Traumatismo Cranioencefalico

EAA - Esteroides anabolizantes androgênicos

TS - Testosterona

NAND - Nandrolona

CCI - Impacto cortical controlado

ETC - Encefalopatia traumática crônica

IF - Jejum intermitente

SUS - Sistema único de saúde

$Ca^{2+}$ - Cálcio

ATP - Adenosina trifosfato

SNC - Sistema nervoso central

ERO - Espécies reativas de oxigênio

POR - Porinas

VDAC - Canal de ânion dependente de voltagem

TOM - Translocases

Mnf1 - Mitofusina 1

Mnf2 - Mitofusina 2

FIS1 - Proteína de fissão mitocondrial 1

Bcl-2 - Linfoma de célula beta-2

BAK - Antagonista/Assassino de *Bcl-2*

OPA1 - Proteína da atrofia óptica 1

MICOS - Sistema de organização da crista mitocondrial

MAM - Membrana do retículo endoplasmático associada à mitocôndria

JIM - Junções intermitocondriais

IM - Espaço intermembranas

TIM - Translocases de membrana interna

PARL - Proteína semelhante a rombóide associada à presenilinas

ROMO1 - Modulador de espécies reativas 1

m-AAA - proteases de ATP da matriz mitocondrial

PHB-SLP2 - Proteína semelhante a proibitina-estomatina 2

TCA - Ciclo do ácido tricarboxílico

NADH - Dinucleótido de nicotinamida e adenina reduzido

$FADH_2$ - Dinucleótido de flavina e adenina

$H^+$ - Hidrogênio

$\Delta\Psi m$ - Potencial de membrana mitocondrial

$\Delta pH$ - Diferencial químico do gradiente prótons

UCP - Proteína desacopladora

ANT - Adenina nucleotídeo translocase

$H_2PO^{4-}$ - Fosfato Diácido

FT - Fosfato diácido translocase

$O_2^{\bullet-}$ - Superóxido

$OH^{\bullet-}$ - Radical hidroxil

$^1O_2$ - Oxigênio singleto

$H_2O_2$ - Peróxido de hidrogênio

SOD - Superóxido dismutase

GPx - Glutationa peroxidase

CAT - catalase

mtDNA - DNA mitocondrial

$ONOO^{\bullet-}$ - Peroxinitrito

$NAD^+$ - Dinucleótido de nicotinamida e adenina oxidado

ADP - Adenosina difosfato

μM - Micromol

MCU - Canal iônico de cálcio mitocondrial

$Na^+$ - Sódio

NCLX - Trocador de sódio-cálcio (lítio) mitocondrial

MA - Lançadeira malato-aspartato

G3PDH - Glicerol-3-Fosfato desidrogenase

DRP1 - Proteína relacionada à dinamina 1

Mff - Fator de Fusão Mitocondrial

Bcl-xL - Linfoma de célula beta extra grande

BAX - Proteína X associada a Bcl-2

FDG-PET - Tomografia por emissão de pósitrons com [$^{18}$F]-fluorodesoxiglucose

MC - Conectividade metabólica

ROI - Região de Interesse

FDA - Administração de alimentos e medicamentos dos Estados Unidos

AR - Receptor androgênico

ER - Receptores estrogênicos

DHT - Diidrotestosterona

SNZ - Stanozolol

ANVISA - Agência Nacional de Vigilância Sanitária

PIC - Pressão intracraniana

kcal - Quilocaloria

kg - Quilograma

mg - Miligrama

dL - Decilitros

g - Gramas

CREB - proteína de ligação responsiva ao AMP cíclico

BDNF - Fator neurotrófico derivado do cérebro

RD - Restrição dietética

AD - *ad libitum*

IMS - Troca metabólica intermitente

WADA - Agência Mundial *Anti-Doping*

NMDAr - Receptor N-metil-D-Aspartato

PC - Protocolo de concussão

## Introdução

Atualmente reconhecido como um importante problema de saúde pública, o traumatismo cranioencefálico (TCE) comumente resulta em disfunção neurológica persistente (Rosenfeld *et al.*, 2012; Meaney *et al.*, 2014). O TCE é definido por uma alteração da função normal cerebral, resultante de forças biomecânicas (**Figura 1**), causada por uma rápida aceleração ou desaceleração do cérebro, decorrente de acidentes com motocicletas ou automóveis; impacto resultante da batida do cérebro devido a quedas, acidentes de motocicletas e automóveis ou em esportes de impacto; uma mudança de pressão e deslocamento de ar devido a explosões; e também pela penetração de projéteis ou de objetos no cérebro (Blennow *et al.*, 2012; Rosenfeld *et al.*, 2012). As alterações fisiopatológicas iniciais resultantes de danos mecânicos primários podem desencadear efeitos deletérios secundários, incluindo neurodegeneração progressiva (Blennow *et al.*, 2012). No entanto, os mecanismos celulares e moleculares envolvidos nessas mudanças progressivas são pouco compreendidos (Meng *et al.*, 2017; Johnson *et al.*, 2018). Portanto, tem sido sugerido que a disfunção neurometabólica persistente pode estar por trás de algumas das características patológicas do TCE crônico.

**Figura 1 - Forças biomecânicas associadas com o traumatismo cranioencefálico.**

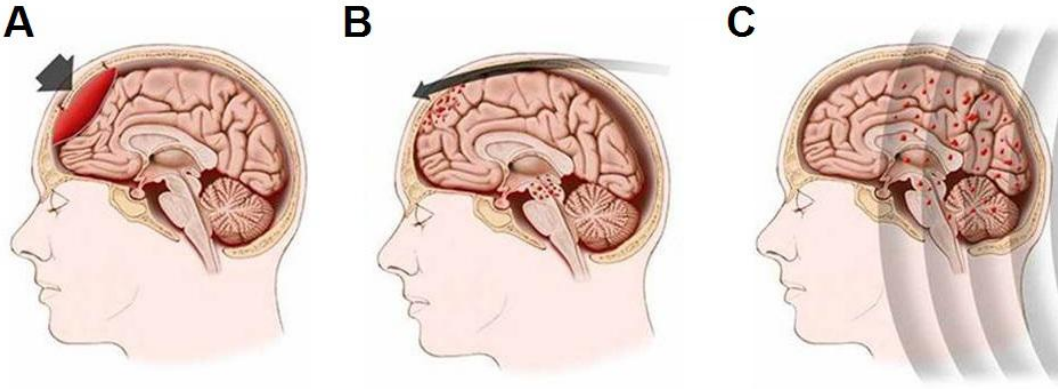


A) Impacto Cortical direto podendo ser penetrante ou não; B) Aceleração e desaceleração da cabeça; C) Ondas mecânicas ocasionadas por impactos e/ou explosões. Fonte: Adaptado de Blennow et al. 2012.

## Incidência de TCE

A incidência do TCE tem sido crescente em países em desenvolvimento principalmente devido aos acidentes de trânsito. Também, o envelhecimento da população

mundial tem dado origem a um aumento das lesões cerebrais traumáticas devido a quedas (Blennow *et al.*, 2012). O Brasil é um dos líderes mundiais na incidência de TCE. No ano de 2013, estimou-se cerca de 500 casos para cada 100.000 habitantes. No estado do Rio Grande do Sul, 75 % das causas de TCE são decorrentes de acidentes de trânsito, envolvendo atropelamentos, acidentes de carro e motos. O risco de TCE é especialmente elevado entre os adolescentes, adultos jovens, pessoas com idade inferior a 2 anos e superior a 75 anos. A faixa etária de maior incidência está entre 15 e 24 anos, sendo mais prevalente no sexo masculino. A mortalidade geral relacionada ao TCE grave está em torno de 30-50%, sendo que 90% destas ocorrem nas primeiras 48 h após o insulto (Blennow *et al.*, 2012). Em 2012 o valor total despendido pelo SUS (Sistema Único de Saúde) para atendimento de danos cerebrais por causas externas (que incluem o TCE) foi maior que 1 bilhão de reais com 998.994 internações. O custo médio da internação foi R$ 1.079,60 e a média de permanência no hospital foi de 5,3 dias. Esses dados sobre custos e valores pagos pelo SUS não incluem os custos ambulatoriais e de clínicas de reabilitação. Somam-se a estes, medicamentos, materiais necessários aos cuidados domiciliares, cuidador, transporte e aqueles indiretos referentes aos dias não trabalhados pelos pacientes e familiares (Fukujima, 2013). Portanto, o TCE e suas consequências são atualmente considerados problemas de saúde pública no Brasil e no mundo.

É importante também considerar que atletas profissionais envolvidos em esportes de contato ou com risco de colisão estão expostos a um amplo espectro de traumatismos cranianos, que muitas vezes não são tratados e nem tampouco relatados (Langlois *et al.*, 2006). No entanto, investigações neuropatológicas *post-mortem* em atletas profissionais identificaram depósitos de proteína tau fosforilada, hipoteticamente uma consequência direta de TCE repetidos relacionados com o esporte nomeada “concussão relacionada ao esporte” (Mez *et al.*, 2017). Consequentemente, esse fenômeno culminou na identificação de uma nova tauopatia neurodegenerativa progressiva nomeada “Encefalopatia Traumática Crônica” (ETC), desencadeada por lesões cerebrais traumáticas leves repetidas resultando em comprometimento da função cerebral e alterações neuropsicólogicas, sugerindo que o TCE leve repetido levaria a um início precoce de neurodegeneração (Kulbe e Hall, 2017). Enquanto os sintomas da ETC são comumente observados clinicamente, os mecanismos indutores associados ainda não estão claros. Devido ao fato de que a maioria das cascatas bioquímicas envolvidas na progressão da neurodegeneração é estudada em modelos de TCE aplicados a animais não exercitados, é possível limitar a sua aplicabilidade no contexto do

esporte. Assim, não existem modelos animais que considerem o exercício como variável visando estudar a ETC causada por concussão relacionada ao esporte até o momento, negligenciando um fator de confusão (Shahim et al., 2018). Portanto, essa lacuna na literatura permanece como um possível alvo de investigações.

### *Pesquisa translacional do TCE*

O TCE é classificado como leve, moderado e severo, podendo levar a morte prematura, alterações cognitivas e neuropsiquiátricas comprometendo, muitas vezes, a qualidade de vida dos indivíduos sobreviventes (Meaney *et al.*, 2014; Levin e Diaz-Arrastia, 2015). Essa classificação é uma combinação de diferentes critérios (**quadro 1**), onde quando o paciente atender critérios em mais de uma categoria de gravidade, a gravidade mais alta será determinada (Brasure *et al.*, 2012). Destaca-se também a Escala de Coma de Glasgow (usando a melhor pontuação nas primeiras 24 horas) como a ferramenta qualitativa mais utilizada. O nível de gravidade tem valor prognóstico, porém não necessariamente prediz o nível final de funcionamento do paciente.

**Quadro 1. Critérios para a classificação da gravidade do TCE em humanos.**

| Humanos | | | |
|---|---|---|---|
| **Critério** | **Leve/Concussão** | **Moderado** | **Grave** |
| **Imagem Estrutural** | Normal | Normal ou anormal | |
| **Perda de Consciência** | 0 a 30 minutos | > 30 minutos e <24 horas | > 24 horas |
| **Alteração da consciência / estado mental** | Breve ou até 24 horas> | >24 horas. Gravidade baseada em outros critérios | |
| **Amnésia pós-traumática** | 0-1 dia | > 1 e <7 dias | > 7 dias |
| **Escala de Coma de Glasgow*** | 13-15 | 9-12 | <9 |

* melhor pontuação disponível nas primeiras 24 horas. Fonte: Adaptado de (Brasure *et al.*, 2012).

O modelo de impacto cortical controlado (CCI, do inglês *controlled cortical impact*) em camundongos é amplamente utilizado para estudar mecanismos fisiopatológicos associados ao TCE. O modelo CCI proporciona alta reprodutibilidade, graças a possibilidade de controle de critérios (**quadro 2**) para a indução de lesão visando diferentes gravidades de TCE (Siebold *et al.*, 2018).

| Quadro 2. Critérios para a classificação da gravidade do TCE no modelo de CCI em camundongos. | | | |
|---|---|---|---|
| **CCI em camundongos** | | | |
| **Critério** | **Leve/Concussão** | **Moderado** | **Grave** |
| **Perda do tecido** | Nenhuma ou confinada à camada cortical | Lesão cortical evidente estendendo-se ao tecido subcortical | Lesão cortical e hipocampal evidente |
| **Escore de gravidade neurológica** | Déficits menores <24h | Déficits substanciais <72h seguidos de recuperação completa ou déficits menores sustentados | Déficits substanciais> 72h |
| **Déficits cognitivos** | Déficits menores <1 semana com recuperação completa | Déficits substanciais <1 semana seguidos por déficits menores ou recuperação completa | Déficits substanciais> 1 semana sem recuperação completa |
| **Parâmetros cirúrgicos*** | Depressão cortical <0,5mm velocidade <4,0m/s. Sem craniotomia | Depressão cortical 1.0–1.5mm, velocidades 4.0–5.0m/s | Depressão cortical> 2.0mm, velocidades> 5.0m/s |
| * Equipamento acoplado a estereotáxico, *myNeuroLab*® (Leica, St. Louis, MO, USA).<br>Fonte: Adaptado de (Siebold *et al.*, 2018). | | | |

## Mecanismos bioquímicos envolvidos no dano após TCE

Os mecanismos fisiopatológicos associados ao TCE envolvem a lesão primária resultante do dano mecânico ou inercial a substância branca e cinzenta com ruptura das membranas celulares, liberação do seu conteúdo e lesão axonal difusa (Dash *et al.*, 2010; Roozenbeek *et al.*, 2013). O dano secundário se refere à progressão das alterações associadas ao dano primário cerebral resultando em diversas alterações neurológicas podendo resultar em consequências devastadoras ao longo da vida. No dano secundário, a ativação persistente de uma série de cascatas de eventos neurotóxicos, desencadeia a progressão do dano estrutural, a perda de função e conectividade neuronal, culminando com a morte de células neurais adjacentes ao foco da lesão (**figura 2**) (Roozenbeek *et al.*, 2013).

A extensão e severidade dos danos secundários são proporcionais à intensidade do trauma e do local do insulto primário. Entre os mecanismos que sustentam o dano secundário estão o aumento excessivo de glutamato extracelular (excitotoxicidade), prejuízos na homeostasia da cálcio ($Ca^{2+}$), resposta inflamatória persistente, disfunção mitocondrial, deficiência neuroenergética, desbalanço redox, disfunção do sistema vascular, isquemia e acúmulo de proteínas no axônio (Hemphill *et al.*, 2015). Desse modo, o interesse emergente na função mitocondrial no TCE reforça a estabelecida importância histórica desta organela na literatura científica.

**Figura 2 – Cascata de dano secundário associada ao TCE.**

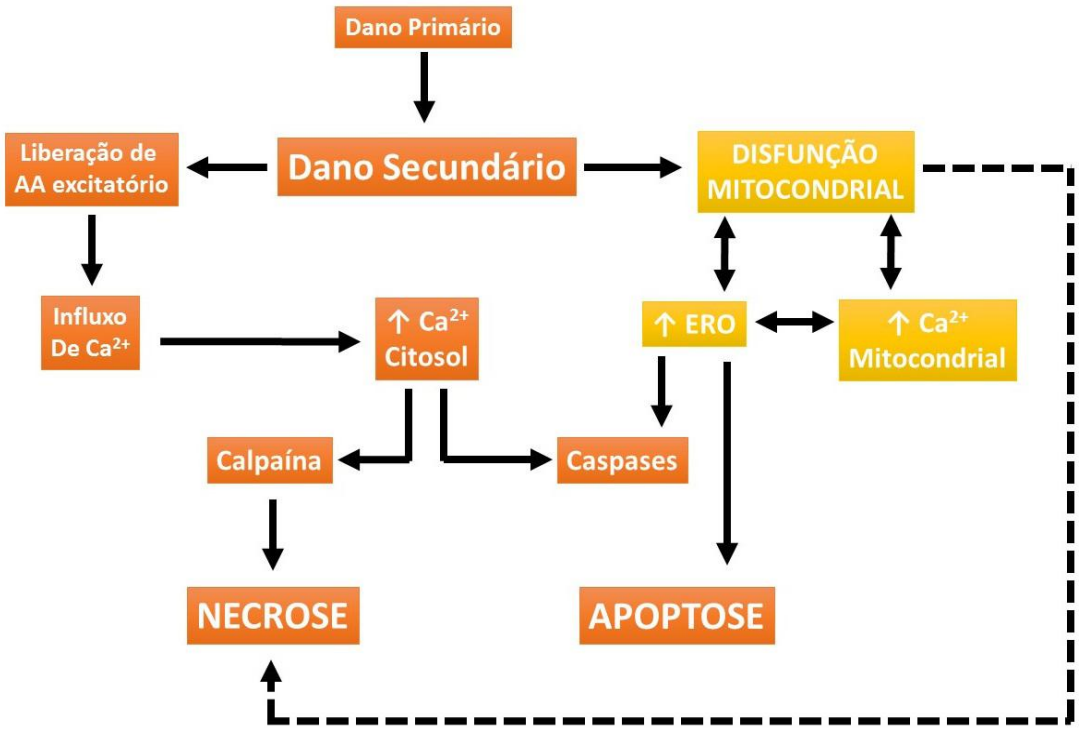


As forças biomecânicas do trauma causam uma deformação tecidual (dano primário), seguido da disrregulação do fluxo sanguíneo e liberação excessiva de neurotransmissores (AA) excitatórios. Ainda, o aumento das concentrações intracelulares de $Ca^{2+}$, ativam proteases (calpainas) que degradam o citoesqueleto neuronal. Paralelamente, a sobrecarga de $Ca^{2+}$ na mitocôndria desregula o metabolismo, a produção de espécies reativas de oxigênio (ERO) e ativa vias de sinalização de morte apoptótica e por necrose. Fonte: Adaptado de (Cheng *et al.*, 2012).

## Mitocôndria: da sua descoberta até sua importância como um alvo terapêutico no TCE

Muito antes de seu reconhecimento como uma organela vital, o primeiro relato envolvendo as mitocôndrias foi feito por Friedrich Gustav Jacob Henle, que descreveu grânulos subcelulares por uma variedade de nomes, como plastocôndrias e microssomas, usando microscopia de luz em 1841 (Müller e Henle, 1841).

Posteriormente, Richard Altmann, em 1890, alegou uma semelhança entre bactérias e organelas de aspecto granular, sugerindo que estes eram componentes autônomos celulares, denominados bioblastos: um estado de organização química da matéria que era maior que a molécula, mas menor que a célula, descrito como "a menor unidade morfológica do material organizado" (Altmann, 1890). Altmann propôs que os bioblastos já foram células vivas que agora viviam dentro de células eucarióticas. Foi Carl Benda, em 1898, quem nomeou as mitocôndrias como organelas “semelhantes a grãos” - *mitos* (do grego, "fio") e *chondrion* (do grego, "grãos"), com base em uma tendência de formação de cadeias em formatos de grãos (Benda, 1898).

As mitocôndrias são organelas de células eucarióticas delimitadas por duas membranas e por cristas que consomem oxigênio para produzir ATP (adenosina trifosfato), realizam a síntese de metabólitos vitais, homeostase de cálcio e mecanismos de morte celular (Khacho *et al.*, 2019). No sistema nervoso central (SNC), as mitocôndrias normais funcionam como um centro de integração entre múltiplas funções que determinam a homeostase das células neurais. As lesões que levam à disfunção mitocondrial podem dessincronizar as funções celulares, contribuindo assim para a fisiopatologia dos distúrbios cerebrais (Khacho *et al.*, 2019). O cérebro tem altas taxas de gasto de energia e o acoplamento do sistema de transporte de elétrons mitocondrial com a fosforilação oxidativa fornece a maior parte da energia necessária para manter funções como neurotransmissão, homeostase iônica e dos potenciais de membrana (Gilmer *et al.*, 2009; Hiebert *et al.*, 2015). O metabolismo mitocondrial produz moléculas de sinalização como espécies reativas de oxigênio (ERO), regulando os níveis de cálcio e controla o perfil de expressão de efetores pró-apoptóticos intrínsecos. O conjunto dessas funções é comumente referido como "função mitocondrial", embora tal definição ainda seja limitada pela complexidade de relação entre tais componentes (Brand e Nicholls, 2011).

A mitocôndria apresenta duas membranas na sua estrutura: A membrana externa, que separa a organela do citosol e a membrana interna, envolvendo a matriz mitocondrial definindo assim três diferentes regiões especializadas (Cogliati *et al.*, 2016). A membrana externa separa as mitocôndrias do citosol, permitindo a passagem de metabólitos através de porinas (POR) do canal iônicos dependente de voltagem (VDAC) e de proteínas que compõem a família das translocases da membrana externa (TOM, do inglês *Translocases of outter membrane*) (Kühlbrandt, 2015). Outras proteínas da membrana externa regulam a dinâmica mitocondrial, principalmente as mitofusinas 1 e 2 (Mfn1 e Mfn2) e a FIS1 (do inglês *mitochondrial fission protein 1*) e também proteínas da família Bcl-2 (do inglês, *B-cell lymphoma-2*) como por exemplo, BAK (do inglês *Bcl-2 homologous antagonist killer*). Proteínas da membrana externa também interagem com proteínas da membrana interna: a proteína Gαq/11 interage com a proteína da atrofia óptica 1 (OPA1) e a proteína SAM (do inglês *Sorting Assembly Machinery*) interage com o complexo MICOS (do inglês, *mitochondrial cristae organizing system*) (Cogliati *et al.*, 2016). Além disso, a membrana externa também tem regiões específicas para interação com outras organelas: membrana do retículo endoplasmático associada à mitocôndria (MAM do inglês Mitochondrial Associated – Endoplasmic Reticulum Membrane), que interage com o retículo endoplasmático

(Demetriadou *et al.*, 2017); e as junções intermitocondriais (JIM), que interagem com outras mitocôndrias (Picard *et al.*, 2015).

O espaço intermembranas (IM) é delimitado pela membrana interna, onde a estrutura forma as cristas mitocondriais que separam o IM da matriz da mitocôndria (Cogliati *et al.*, 2016). A membrana interna contém as proteínas da família das translocases de membrana interna (TIM, do inglês *Translocases of the Inner Membrane*), que transportam proteínas para a matriz, a proteína OPA1 e a cardiolipina (um fosfatidilglicerol), essenciais para a correta montagem e localização das proteínas da membrana interna. A OPA1 é regulada por Gαq/11 (da membrana externa) além de outras proteínas da membrana interna como a PARL (Presenilins-associated rhomboid-like protein), ROMO1 (do inglês *reactive oxygen species modulator 1*), e pelas proteases de ATP da matriz (m-AAA), sendo controladas pelo complexo PHB–SLP2 (do inglês, *prohibitin–stomatin-like protein 2*) que se ancora na cardiolipina (Cogliati *et al.*, 2016). A interação dessas proteínas garante a funcionalidade das cristas, sua estrutura e a disposição dos complexos do sistema de transporte de elétrons (Frey e Mannella, 2000) Portanto, as cristas são estruturas fundamentais para as mitocôndrias e não são simplesmente invaginações; essas estruturas são separadas do espaço intermembrana por junções tubulares estreitas reguladas por diferentes proteínas, principalmente a OPA1 e o complexo MICOS, formando compartimentos especializados para limitar a difusão de moléculas importantes para o sistema do transporte de elétrons e garantindo o máximo de funcionalidade (Cogliati *et al.*, 2013).

Conceitualmente, a oxidação mitocondrial de substratos metabólicos no ciclo do ácido tricarboxílico (TCA, do inglês *Tricarboxylic Acid Cycle*), ou do citosol via lançadeiras malato-aspartato, direciona o fluxo de elétrons advindos de NADH (Dinucleótido de nicotinamida e adenina reduzido) e $FADH_2$ (Dinucleótido de flavina e adenina reduzido) através dos complexos respiratórios para o oxigênio e, concomitantemente, gera um gradiente de prótons de hidrogênio e a síntese de ATP. Os complexos respiratórios que compõem o sistema de transporte de elétrons são localizados na membrana interna da mitocôndria o Complexo I (NADH ubiquinona oxidoredutase ou NADH desidrogenase); Complexo II (sucinato ubequinona oxidoredutase ou sucinato desidrogenase), Complexo III (ubiquinol-citocromo C oxidoredutase); o complexo IV (citocromo C oxidase) onde ocorre o consumo de $O_2$ e finalmente, o complexo V, F1-FOATP sintase, onde ocorre a síntese de ATP.

Os complexos do sistema de transporte de elétrons se organizam na forma de supercomplexos ao longo das cristas (**figura 3**), podendo apresentar diferentes conjuntos de

complexos (por exemplo: I,III, IV e V; II,III,IV e V; além do clássico descrito de I até V), sempre notoriamente convergindo para dímeros de F1FO ATP Sintase localizados na extremidade das cristas (Cogliati *et al.*, 2016).

**Figura 3 – O sistema de transporte de elétrons mitocondrial.**

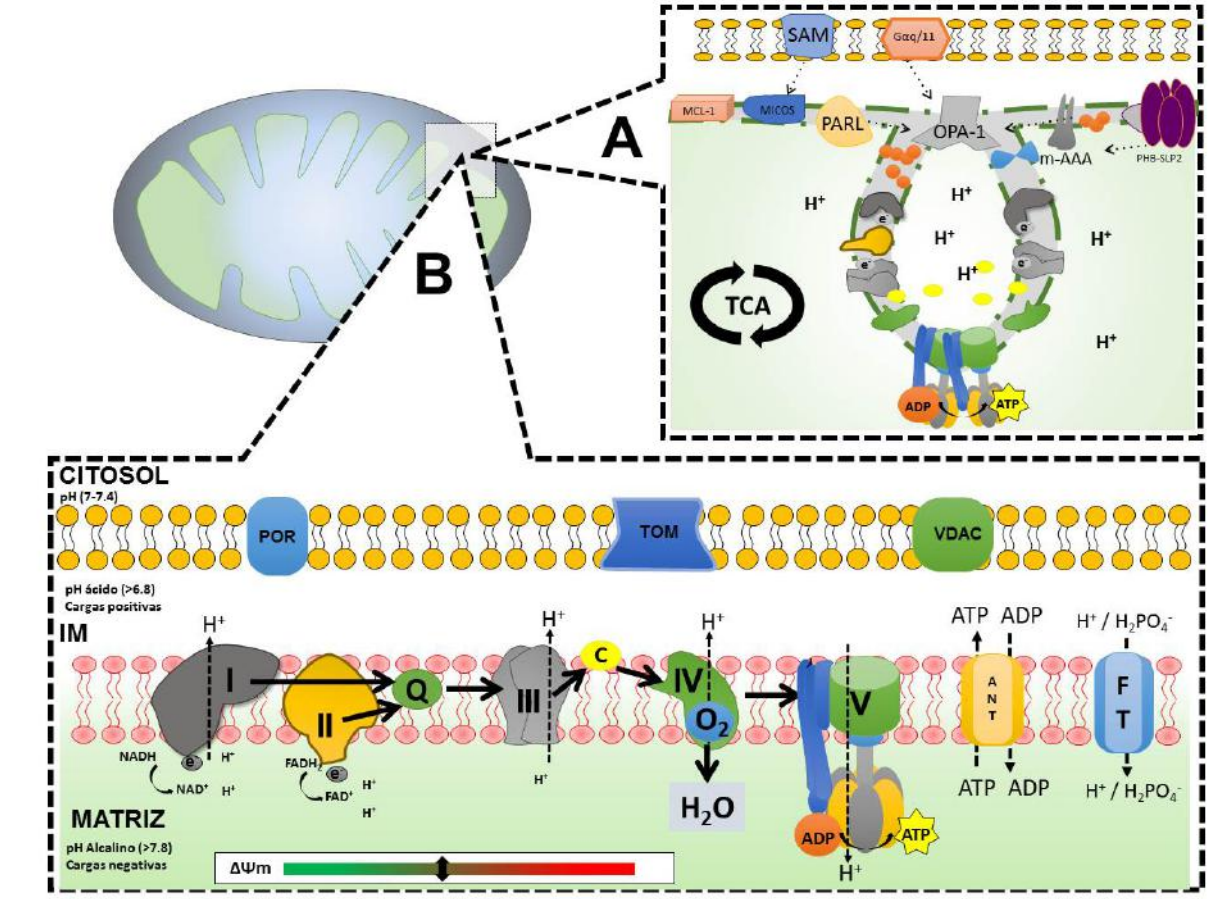


A mitocôndria é envolta por uma membrana externa, apresenta diferentes proteínas, que participam da dinâmica mitocondrial. Na ilustração dos conceitos mais atuais (A), os complexos do sistema de transporte de elétrons se organizam em supercomplexos com diferentes configurações (I –V e I, III, IV e V) que convergem para a F1-FOATP sintase, geralmente localizada em dímeros nas cristas mitocondriais. Na ilustração clássica (B), observa-se as principais proteínas da membrana externa responsáveis por fluxo de metabólitos, como as porinas (POR, onde podem passar pequenas moléculas de até 5 kDa), os canais voltagem-dependente (VDAC) e as translocases de membrana externa (TOM). O espaço intermembrana apresenta um pH mais ácido (cerca de 6.8) por possuir predominância de cargas positivas, devido ao bombeamento de prótons $H^+$ dos complexos I, III e IV. A membrana mitocondrial interna apresenta os componentes do sistema de transporte de elétrons (complexos I-V) o fluxo de elétrons do complexo I e II para ubequinona (junção Q) são independentes (Fluxo convergente). O espaço da matriz abriga diversas enzimas do ciclo de Krebs, e apresenta pH mais alcalino (cerca de 7,8). Para síntese de ATP, a Adenina Nucleotídeo Translocase (ANT; realiza transporte de ADP para Matriz a ATP para intermembrana) e a Fosfato Diácido Translocase (FT; permite deslocamento de $H^+$ por concentração menor na matriz e $H_2PO^{4-}$ para fornecer grupos fosfato para sintetizar ATP) são importantes componentes da membrana mitocondrial interna. Fonte: Adaptado de (Cogliati *et al.*, 2016).

Um componente vital desse processo é a força proton-motriz, que é a combinação do potencial de membrana mitocondrial ($\Delta\Psi m$; gerado pelo bombeamento de prótons de $H^+$) da matriz para o espaço intramembranas através dos complexos I, III e IV) e o diferencial químico do gradiente de $H^+$ ($\Delta pH$). A força protón-motriz permite que a ocorra a síntese de ATP no complexo V e o retorno de prótons para a matriz. A força próton-motriz é influenciada por vazamento de prótons, de forma induzível via ação de proteínas desacopladoras (UCP, do inglês *uncoupling proteins*), ou não-induzível (patológico). O complexo II, através da oxidação de sucinato também doa elétrons para o ubequinona e consequentemente para o complexo III, de forma independente do complexo I. Esse fenômeno é denominado "Fluxo convergente" e é de vital importância para compreender o funcionamento do sistema de transporte para síntese de ATP (Gneiger, E, 2014).

**Figura 4 – Metabolismo do oxigênio e de espécies reativas de oxigênio.**

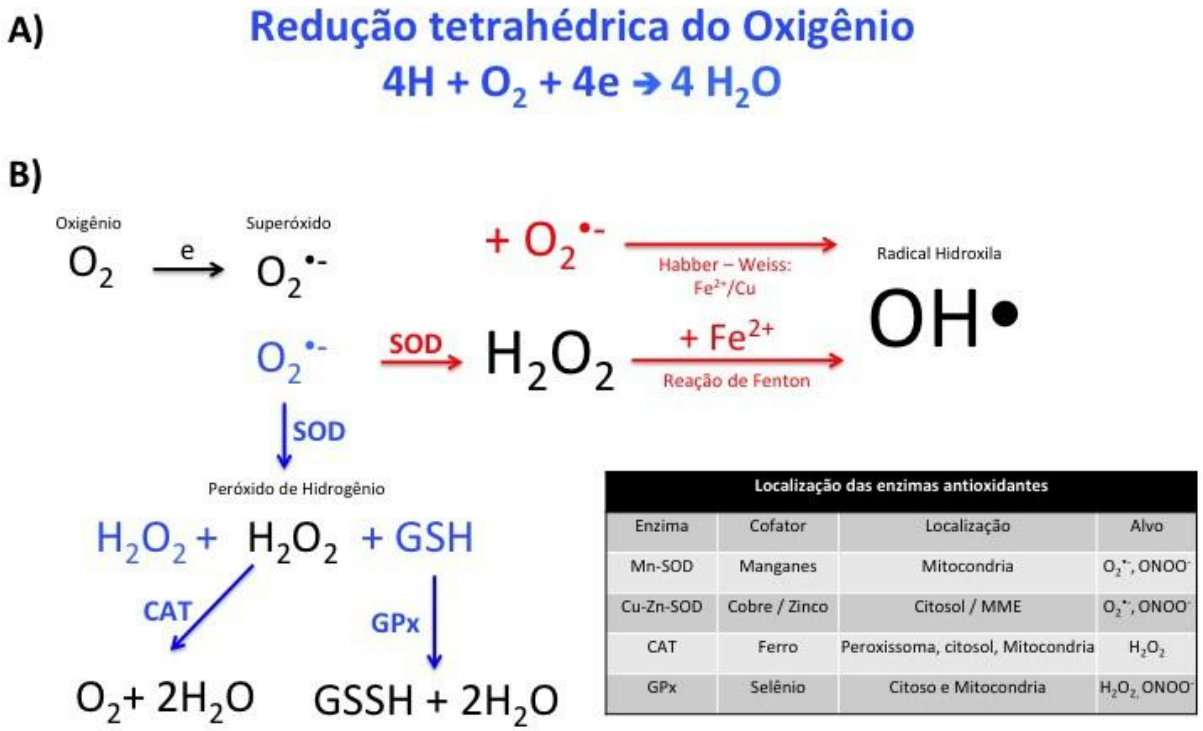


No sistema de transporte, o oxigênio é reduzido gerando água (A). Entretanto, o oxigênio pode receber elétrons e formar superóxido ($O_2^{\bullet-}$), que é rapidamente metabolizado pela enzima superóxido dismutase (SOD), gerando peróxido de hidrogênio ($H_2O_2$). O $H_2O_2$ é um importante sinalizador celular e pode sofrer diversos caminhos: neutralização pelas enzimas glutationa peroxidase (GPx; gerando dissulfeto de glutationa e água) ou catalase (CAT; gerando oxigênio e água). O $H_2O_2$ pode gerar o radical hidroxila ($OH^{\bullet-}$) pelas reações de Haber-Weiss ou reação de Fenton (B). O quadro destaca a localização das enzimas do sistema antioxidante e seus alvos. $ONOO^{\bullet-}$: peroxinitrito. Fonte: Adaptado de (Carteri, 2016).

O sistema de transporte também produz as ERO (**figura 4**), subprodutos fisiológicos do metabolismo normal do oxigênio. Categoricamente, ERO incluem radicais livres, principalmente superóxido ($O_2^{\bullet -}$), radical hidroxila ($OH^{\bullet -}$) e oxigênio singleto ($^1O_2$), bem como espécies não-radicais, como o peróxido de hidrogênio ($H_2O_2$). Em condições fisiológicas, vários antioxidantes endógenos previnem o dano oxidativo, principalmente as enzimas superóxido dismutase (SOD), glutationa peroxidase (GPx), catalase (CAT). No cenário do TCE, diversos componentes do sistema antioxidante do SNC são prejudicados resultando em danos celulares oxidativos essencialmente comprometendo a integridade e permeabilidade de membranas celulares por peroxidação lipídica, a oxidação de proteínas e DNA além da inibição do sistema de transporte de elétrons (Halliwell, 2006). Classicamente, a superprodução de ROS está associada com a hiperpolarização de $\Delta\Psi m$, a liberação de fatores pró-apoptóticos como o citocromo c e ativação de caspases, além do fato do DNA mitocondrial (mtDNA) também ser sensível ao dano oxidativo contribuindo também para a apoptose (Cornelius *et al.*, 2013).

A regulação do metabolismo oxidativo mitocondrial ocorre pela complexa interação de concentração de substratos, razão NADH/$NAD^+$, razão ATP/ADP e, mais recentemente, por concentrações de cálcio. A mitocôndria apresenta baixas concentrações de cálcio, respondendo a aumentos na concentração de cálcio no citosol podendo variar de 0,1 até 10 μM (Calì *et al.*, 2012)

A entrada de $Ca^{2+}$ na matriz mitocondrial é mediada através da abertura de um canal iônico de cálcio mitocondrial (MCU), que efetivamente detecta os níveis de cálcio extra mitocondrial e o importa através da membrana interna, dissipando parcialmente o potencial de membrana mitocondrial ($\Delta\Psi m$). Isso ocorre em paralelo a ativação de três enzimas da matriz mitocondrial (Piruvato desidrogenase, Isocitrato desidrogenase e alfa-cetoglutarato desidrogenase) além de regular as lançadeiras malato-aspartato, lançadeira glicerol 3 fosfato e diretamente o complexo III e V do sistema de transporte de elétrons (Glancy e Balaban, 2012; Tarasov *et al.*, 2012).

O $Ca^{2+}$ regula a respiração independentemente da demanda de ATP (Weber, 2012). Para manter a homeostase de cálcio, o trocador de sódio ($Na^+$)-cálcio (lítio) mitocondrial (NCLX) equilibra o influxo pela extrusão de um íon $Ca^{2+}$ na troca com três íons sódio (Jafri e Kumar, 2014).

**Figura 5 – Influxo/efluxo de cálcio na mitocôndria e processos mitocondriais regulados por cálcio.**

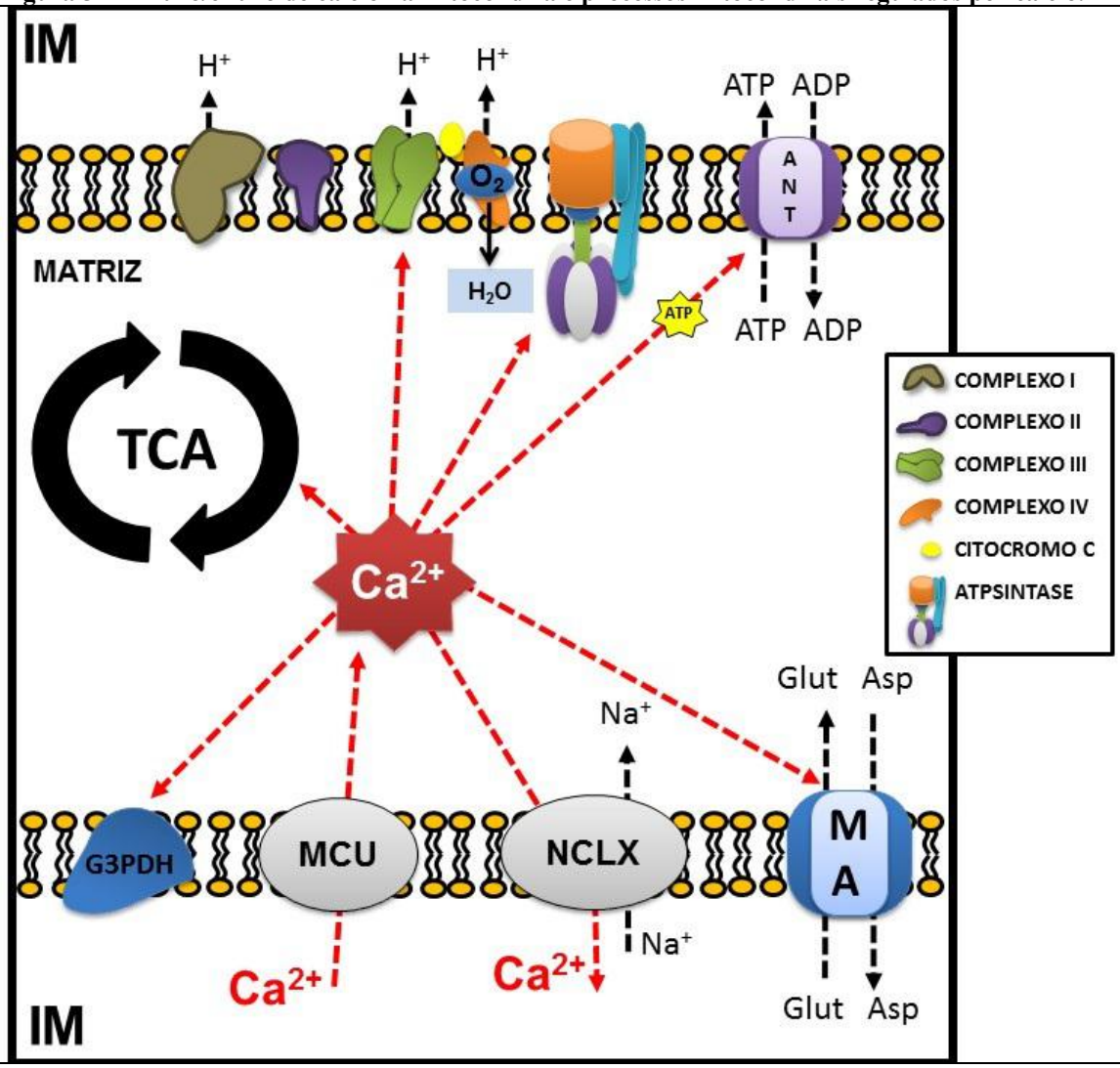


O influxo de cálcio do espaço intermembranas (IM) para a matriz ocorre pelo MCU, e regula diretamente enzimas envolvidas com o ciclo do ácido tricarboxílico (TCA; Piruvato Desidrogenase, Isocitrato desidrogenase e alfacetoglutarato desidrogenase) e também as lançadeira malato-aspartato (MA) e Glicerol-3-Fosfato Desidrogenase (G3PDH), aumentando substratos para o sistema de transporte. O cálcio regula também diretamente complexos do sistema de transporte de elétrons (complexo III-V) e a adenina nucleotídeo translocase. O efluxo de cálcio ocorre pelo NCLX (trocador de sódio-cálcio (lítio) mitocondrial) equilibrando as concentrações de cálcio na mitocondria. Fonte: Adaptado de (Zoccarato *et al.*, 2004).

Aumentos moderados na concentração de $Ca^{2+}$ mitocondrial são necessários e suficientes para ajustar a produção de ATP à demanda celular, mas a sobrecarga mitocondrial de $Ca^{2+}$ leva à ruptura da integridade da membrana mitocondrial e dano oxidativo irreversível diminuindo a capacidade de produção de ATP (Zoccarato *et al.*, 2004). Esse fenômeno resulta essencialmente de três mecanismos: (I) aumento da captação mitocondrial de $Ca^{2+}$, após efluxo do retículo endoplasmático e influxo de $Ca^{2+}$ do espaço extracelular; (II) redução da extrusão de $Ca^{2+}$ através do NCLX; e (III) alterações do tamponamento mitocondrial de $Ca^{2+}$ (**figura 5**). Portanto, o comprometimento da homeostase do cálcio mitocondrial é uma

característica reconhecida das fases iniciais da neurodegeneração, com implicação direta no TCE, ocorrendo efeitos sinérgicos entre ruptura do potencial de membrana mitocondrial, sobrecarga de cálcio e ERO na mediação do dano celular após o TCE (Mattson, 2007; Calì *et al.*, 2012).

Sabendo da importância e complexa relação entre ΔΨm, produção de ERO, homeostase do cálcio e a síntese de ATP, outro ponto importante é como a mitocôndria reage a alterações nesses componentes: a mitocôndria é uma organela dinâmica, com um ciclo de vida envolvendo também dois processos denominados fusão e fissão. Ambos processos são fundamentais para a manutenção da função mitocondrial, a fim de adaptar a morfologia e formar uma rede interconectada dinâmica, mantendo a integridade e qualidade mitocondrial (Twig *et al.*, 2008). O ciclo de vida das mitocôndrias é composto por períodos distintos: o período solitário, pré-fusão, formação de rede e período pós-fusão (**figura 6**). As mitocôndrias de mamíferos exibem uma breve fusão caracteristicamente seguida de fissão. A fissão e a fusão seletiva regem a segregação mitocondrial e a eliminação por autofagia, sendo intimamente relacionadas com a redução do potencial de membrana mitocondrial, levando a despolarização mitocondrial (Ishihara *et al.*, 2003).

A dinâmica desses processos permite que mitocôndrias retenham um potencial de membrana mais estável após a fissão, embora ele possa variar em até 5 mV em relação ao período solitário. Portanto, a fissão resulta em mitocôndrias funcionalmente diferentes. Para que a fissão ocorra, a proteína DRP1 (do inglês *Dynamin-related protein 1*) interage com duas proteínas ancoradas na membrana mitocondrial externa: o Fator de Fusão Mitocondrial (Mff; do inglês *mitochondrial fission factor*) e a FIS1, em menor escala (Elgass *et al.*, 2013). Em contra-partida, a fusão combina o conteúdo da mitocôndria original e requer um potencial de membrana mitocondrial intacto, regenerando as mitocôndrias danificadas. Além disso, a fusão permite a rápida difusão das proteínas da matriz mitocondrial combinada com uma migração mais lenta dos componentes da membrana interna e externa. Em mamíferos, a fusão mitocondrial é dependente de diferentes GTPases da família das dinaminas: na membrana mitocondrial interna, a OPA1 e as mitofusinas da membrana mitocondrial externa (Mnf1 e Mnf2). Um detalhamento maior desses mecanismos estão fora do escopo dessa tese, porém o leitor pode se beneficiar em recorrer a revisões recentes (Elgass *et al.*, 2013; Escobar-Henriques e Anton, 2013; Pfanner *et al.*, 2019).

**Figura 6 – O ciclo de vida dinâmico da mitocôndria e os processos de fusão e fissão.**

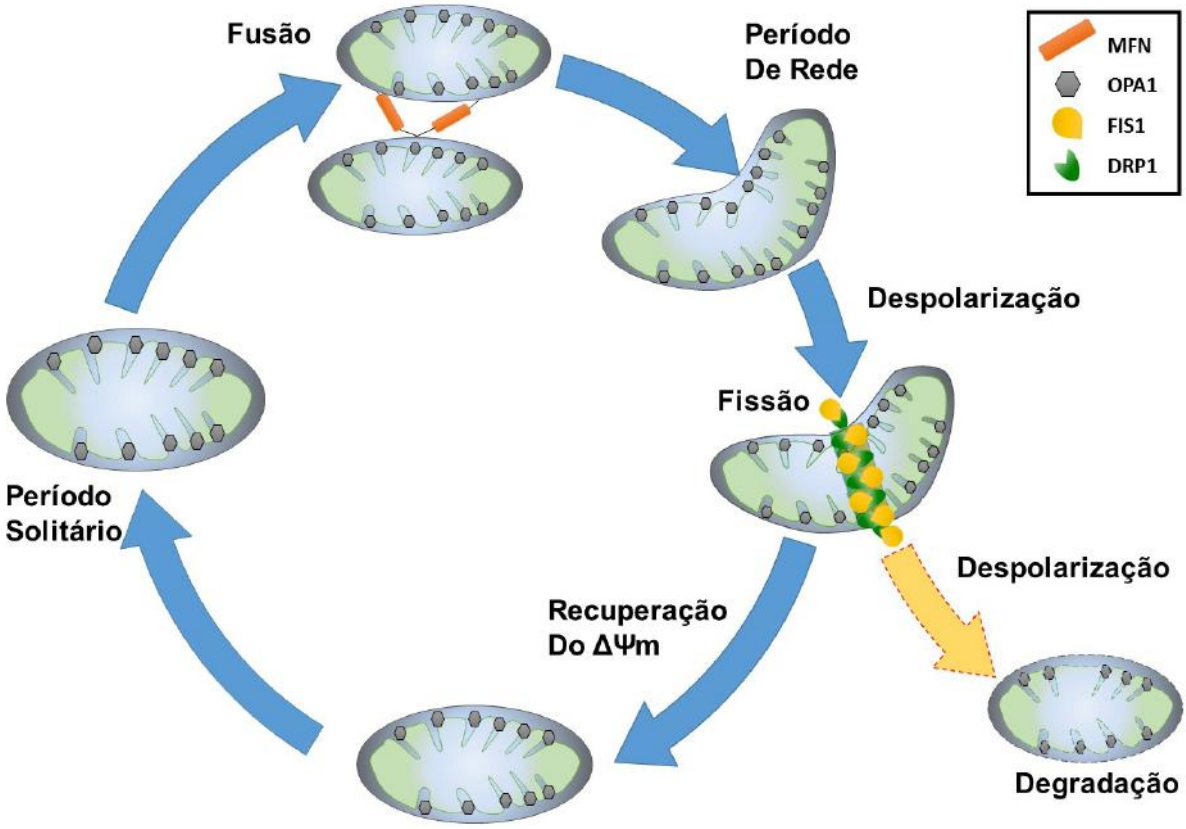


A mitocôndria muda ciclicamente entre um estado solitário, pós-fusão (rede) e um estado pós-fissão (solitário). A perda de potencial resulta em fusão, que é rápida e desencadeia a fissão. Após um evento de fissão, as mitocôndrias geradas podem manter seu potencial de membrana intacto (Recuperação) ou seguir com despolarização, sendo então direcionada para vias de degradação Fonte: Adaptado de (Twig *et al.*, 2008).

## A sinalização mitocondrial para a apoptose

A sinalização mitocondrial que resulta em apoptose (morte celular programada) decorre da interação de concentração do $Ca^{2+}$ com proteínas da família Bcl-2. As proteínas anti-apoptóticas Bcl-2 e Bcl-XL (do inglês, *B-cell lymphoma-extra large*) reduzem as concentrações de $Ca^{2+}$ no retículo endosplasmático e regulam positivamente a mitocondria para manutenção da homeostase celular. Isso é póssível graças a sua localização na membrana de ambas organelas. De maneira oposta, as proteínas BAX (do inglês *Bcl-2-associated X protein*) e BAK, pertencentes a mesma família, tem efeito pró-apoptótico (Mattson, 2007; Calì *et al.*, 2012).

A regulação dessa via é diretamente proporcional as concentrações de cálcio liberadas pelo retículo endoplasmático. Um aumento exacerbado se reflete no influxo na mitocondria, resultando em abertura do poro de transição de permeabilidade e consequentemente na mudança na morfologia, liberação de citocromo c e ativação de caspases, proteases

determinantes do estímulo pró-apoptótico (Mattson, 2007; Calì *et al.*, 2012).

Em modelos de TCE experimental, a disfunção mitocondrial tem sido comumente descrita como uma fonte de crise metabólica celular (Gilmer *et al.*, 2009; Hiebert *et al.*, 2015). Acredita-se que isso reflita, em parte, o aumento patológico nas concentrações de cálcio intracelular, que por sua vez é sequestrado pelas mitocôndrias. No entanto, esse tamponamento de cálcio geram uma diminuição da capacidade das mitocôndrias em produzir ATP. O hipometabolismo resultante pode dessincronizar as funções celulares concomitante ao aumento de espécies reativas de oxigênio (Pandya *et al.*, 2013; Vekaria *et al.*, 2017). Com o aumento do cálcio excedendo a capacidade de sequestro mitocondrial, a destruição seletiva do citoesqueleto pode levar à morte celular por neurodegeneração apoptótica (Johnson *et al.*, 2016). O excesso de cálcio ativa da familia das calpaínas (principalmente, calpaína-2) que por um mecanismos associado a ação das proteínas da família das caspases induz a fragmentação de proteínas estruturais do citoesqueleto neuronal, como a alfa-espectrina além de estimular a hiperfosforilação de Tau, biomarcadores moleculares clássicos de neurodegeneração (Ji *et al.*, 2012). A associação desses mecanismos explica parcialmente como o TCE pode resultar em diferentes doenças neuropsiquiátricas, como ansiedade, depressão, alcoolismo e doença de Alzheimer (Blennow *et al.*, 2012; Sivanandam e Thakur, 2012; Johnson e Stewart, 2015). Adicionalmente, também explica parcialmente o fato de grupos específicos que sofrem repetidas lesões na cabeça (atletas de esporte de contato e veteranos de guerra) apresentarem maior risco de desenvolvimento de tais distúrbios em comparação com indivíduos normais (Hanten *et al.*, 2013).

Enquanto o alto consumo de energia é um aspecto importante da comunicação neuronal normal (Hyder *et al.*, 2013), o TCE induz hipometabolismo em áreas cerebrais específicas (Nakashima *et al.*, 2007) associados com desfechos neuropsicológicos e neurodegeneração em longo prazo (Scholl *et al.*, 2015; Daulatzai, 2017). Tais doenças associadas ao TCE podem surgir também de neurônios distantes exibindo comprometimento metabólico. A tomografia por emissão de pósitrons com [$^{18}$F]-fluorodesoxiglicose (FDG-PET) é uma ferramenta clínica estabelecida medindo a taxa de metabolismo cerebral de glicose (Phelps *et al.*, 1979), interpretada como o acoplamento entre a transmissão sináptica e o consumo local de glicose (Magistretti, 2006). Além disso, FDG-PET pode fornecer uma análise integrativa do metabolismo cerebral total, nomeada "conectividade metabólica" (MC; do inglês "*metabolic connectivity*"), que pode ser estimada com a correlação dos valores de captação de glicose entre diferentes regiões anatômicas de interesse (ROI; do inglês "*Region*

*of Interest*"), onde a magnitude da correlação é proporcional à associação funcional (Horwitz *et al.*, 1984). Essa ferramenta pode ser explorada visando compreender os efeitos metabólicos do TCE em diferentes modelos experimentais, tal como na busca de terapias ou também de estratégias de prevenção de piores desfechos. Assim, a mitocôndria no TCE serve como um nexo para o destino neuronal: sobreviver ou perecer (Winklhofer *et al.*, 2008).

**Figura 7 – Modelo de diagnóstico mitocondrial proposto pela presente tese.**

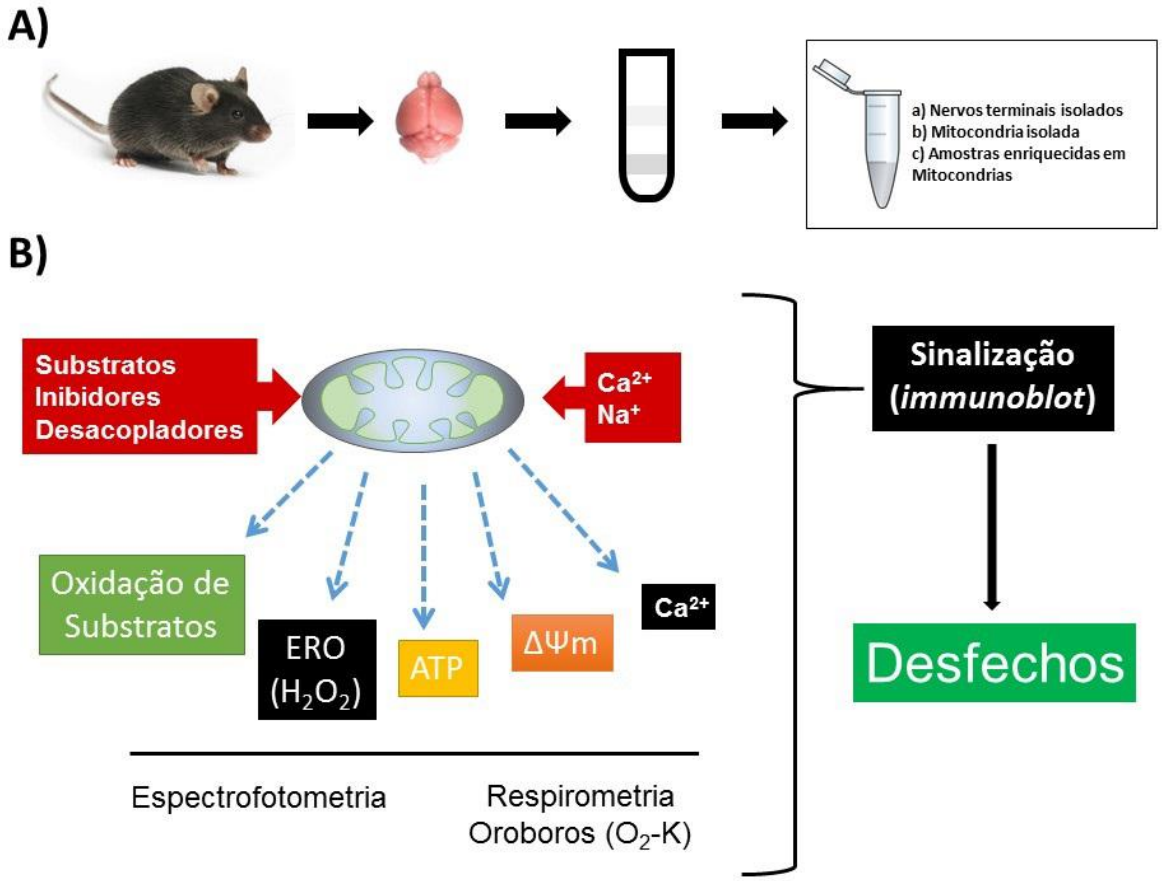


A presente tese propõe também um modelo de diagnóstico mitocondrial nos estudos pré-clinicos em roedores, avaliando o consumo de oxigênio e a capacidade de síntese de ATP através da respirometria de alta-resolução. Essa análise é complementada com ensaios espectrofotométricos para a avaliação da síntese de peróxido de hidrogênio e demais espécies reativas, a avaliação da dinâmica de potencial de membrana e também a capacidade de manejo de cálcio. Ainda, técnicas para avaliar a sinalização celular como imunoblot ou imunohistoquímica podem adicionar componentes mecanísticos para explicar os desfechos. Fonte: Adaptado de Fisher-Wellman et al., 2018.

Dada a complexidade das funções da mitocôndria, diferentes ferramentas podem ser combinadas para otimizar estudos visando explorar mecanismos mitocondriais em diferentes contextos fisiológicos, incluindo o TCE. Nesse sentido, é importante considerar a amostra escolhida e buscar realizar uma combinação de análises abrangendo as diferentes funções da mitocôndria. A presente tese propõe um modelo de diagnóstico mitocondrial nos estudos pré-

clinicos em roedores baseado em diferentes diretrizes sobre análise de função mitocôndria (Connolly *et al.*, 2018; Fisher-Wellman *et al.*, 2018). Inicialmente ocorre a preparação de amostras (nervos terminais isolados, mitocôndrias extra-sinápticas ou homogenatos enriquecidos de mitocôndria), para posterior avalição do consumo de oxigênio e a capacidade de síntese de ATP através da respirometria de alta-resolução. Essa análise é complementada com ensaios espectrofotométricos para a avaliação da síntese de peróxido de hidrogênio e demais espécies reativas, a avaliação da dinâmica de potencial de membrana e também a capacidade de manejo de cálcio. Ainda, técnicas para avaliar a captação de glicose, a sinalização celular como imunoblot ou imunohistoquímica podem adicionar componentes mecanísticos para explicar os desfechos (**figura 7**).

**Figura 8 – Mecanismos de dano resultantes do Traumatismo Cranioencefálico e propostas profiláticas e terapêuticas.**

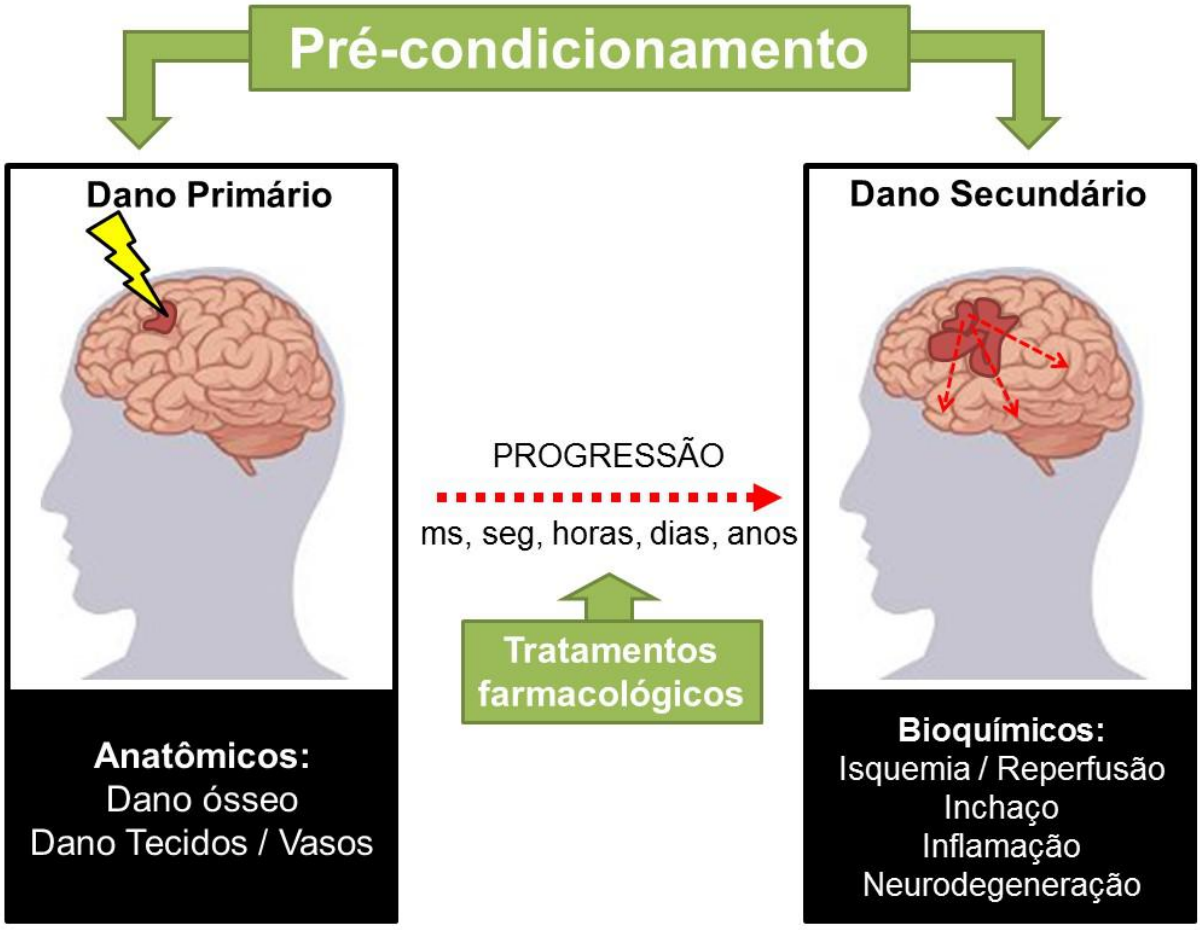


Mecanismos relacionados com a progressão de dano neurodegenerativos associados ao TCE e oportunidades de intervenção. Fonte: Adaptado de Blennow et al. 2012.

Embora evidências conceituais abundantes estejam atualmente considerando as mitocôndrias cerebrais como um potencial alvo terapêutico contra a neurodegeneração, até o momento não há nenhuma intervenção farmacológica disponível com eficácia comprovada (Schon e Przedborski, 2011; Gajavelli *et al.*, 2015). Nesse contexto, com o avanço significativo nos últimos anos na descrição dos mecanismos fisiopatológicos envolvidos com a neurodegeneração pós-TCE, a literatura atual busca como estes podem ser influenciados por estratégias farmacológicas ou comportamentais, antes ou após o TCE (**figura 8**). Assim, foi proposto que o TCE prepara os neurônios para morrer devido à confluência da disfunção mitocondrial e subsequentes processos degenerativos (Ji *et al.*, 2012). Desse modo, a mitocôndria se torna um alvo terapêutico em estratégias que visam garantir melhores resultados funcionais (Schon e Przedborski, 2011; Blennow *et al.*, 2012; Gajavelli *et al.*, 2015) onde as intervenções farmacológicas falharam repetidamente. Assim, além de exercício físico e nutrição, agentes farmacológicos aprovados pela *Food and Drug Administration* (FDA) com benefícios reconhecidos para as mitocôndrias de tecidos periféricos merecem agora ser explorados em relação aos seus potenciais benefícios cerebrais contra as consequências a curto e longo prazo do TCE (Cheng *et al.*, 2012).

**Distúrbios hormonais envolvidos no dano após TCE**

Após um único ou repetidos TCE, muitas manifestações clínicas são também insidiosas. Entre elas, o hipopituitarismo é uma condição que pode influenciar diretamente no processo de recuperação e nos desfechos neurológicos, devido predominantemente a diminuição de hormônios anabólicos (Bondanelli *et al.*, 2007) (Klose e Feldt-Rasmussen, 2015). O primeiro caso de hipopituitarismo induzido por traumatismo cranioencefálico (TCE) foi relatado em 1918, onde um homem adulto jovem, sofreu uma injúria severa e apresentou anormalidades endócrinas que perduraram por anos após o acidente (Cyran, 1918). Os mecanismos fisiopatológicos da deficiência hormonal após o TCE permanecem apenas parcialmente conhecidos, podendo ser consequência dos mecanismos primários (lesão mecânica direta) ou secundários (hipometabolismo, disfunção energética, hipóxia e edema cerebral) causando restrição do fluxo nos vasos portais hipofisários longos após a injúria (Klose e Feldt-Rasmussen, 2015). É relatado que cerca de um terço dos pacientes com traumatismo craniano fatal apresentam necrose da glândula pituitária anterior (Salehi *et al.*, 2007). Adicionalmente, níveis de testosterona no cérebro se correlacionam inversamente com

a formação de edema e déficits neurológicos após o TCE (Lopez-Rodriguez *et al.*, 2016), e menores níveis de testosterona estão associados com perturbações na bioenergética mitocondrial hipocampal, que podem ser revertidas após a terapia de reposição androgênica ter sido iniciada (Hioki *et al.*, 2014). A avaliação da função hipofisária após o TCE é dificultada por alterações hormonais e efeitos de diferentes drogas na fase inicial de cuidados intensivos, sendo que o hipopituitarismo não tratado é um fator que contribui para os problemas neurológicos crônicos observados em muitos pacientes anabólicos (Klose e Feldt-Rasmussen, 2015).

**Esteróides Anabólicos Androgênicos e TCE**

Atualmente a terapia de reposição de testosterona é um relevante adjuvante na garantia de saúde masculina ao longo do processo de envelhecimento, resultando em diversos benefícios (Giagulli *et al.*, 2016). Com base nisso, é natural considerar que os esteroides anabolizantes androgênicos (EAA), podem exercer benefícios metabólicos em células neurais e assim poderiam ter aplicabilidade relevante na terapia pós TCE (Cheng *et al.*, 2012). Particularmente, a testosterona é um hormônio gonadal que melhora o metabolismo cerebral da glicose, plasticidade sináptica (Hatanaka *et al.*, 2015), defesas antioxidantes, aumentando a sobrevivência celular após diferentes modelos de lesão (Fanaei *et al.*, 2014) pela diminuição dos estímulos pró-apoptóticos (Hioki *et al.*, 2014; Gurer *et al.*, 2015).

Os EAA são compostos sintéticos derivados da testosterona que podem ser divididos em diferentes classes (**figura 9a**) de acordo com as modificações na molécula original (Pope *et al.*, 2014). Estes compostos exercem efeitos anabólicos sistêmicos, incluindo aumento na síntese de proteínas e construção tecidual combinados com efeitos androgênicos estimulando características sexuais secundárias (Busardo *et al.*, 2015). Muitas modificações podem ser feitas na molécula de testosterona, alterando desta maneira suas características farmacológicas, conforme demonstrado na **figura 9b** (Kicman, 2008).

**Figura 9 – Diferentes classes de esteroides anabolizantes androgênicos.**

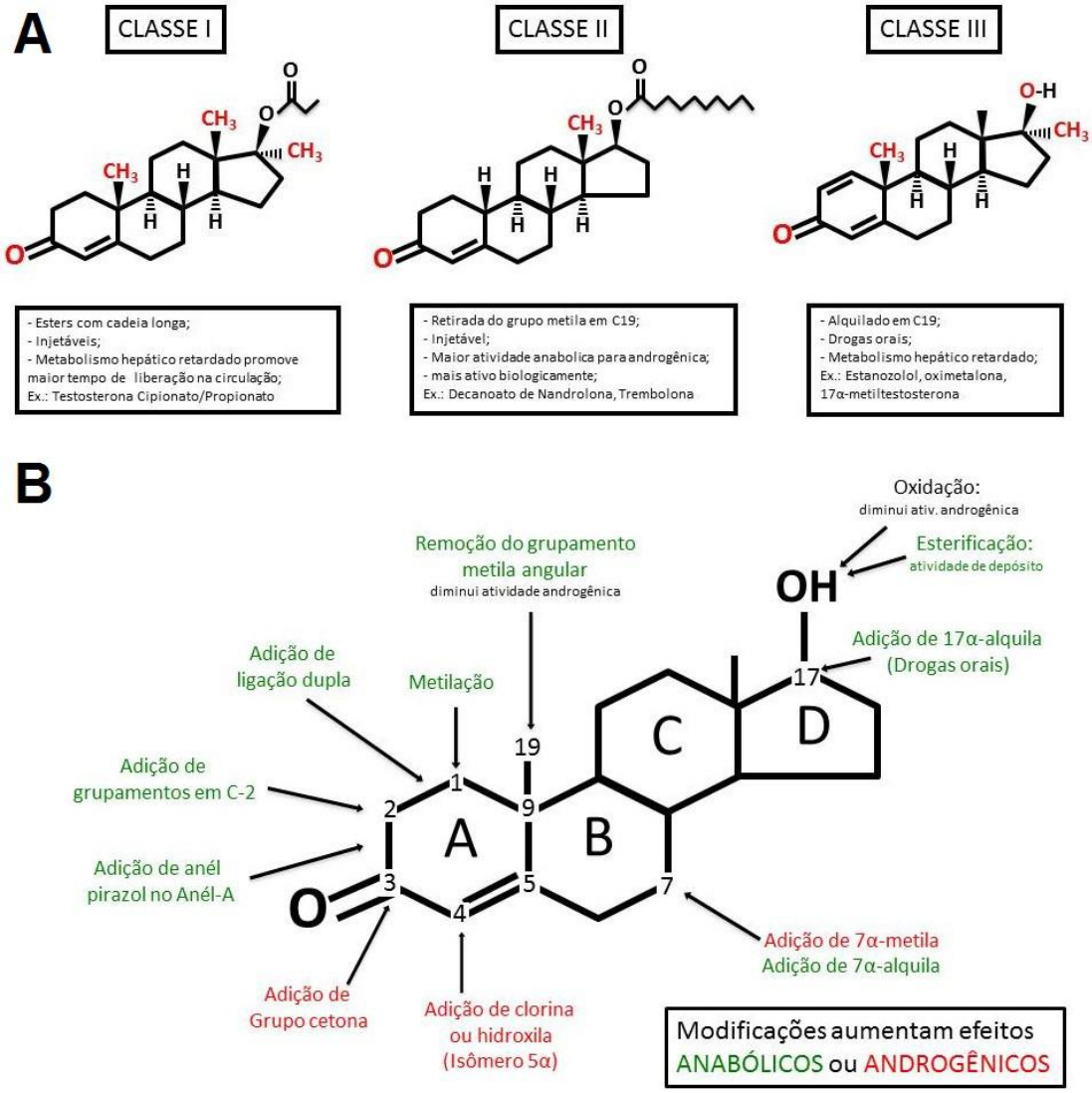


Classes de esteroides anabolizantes androgênicos e modificações possíveis na molécula de testosterona. As três principais classes de esteróides androgênicos anabólicos e suas características específicas (A). Modificações específicas na molécula de testosterona modificam o potencial anabólico ou androgênico do fármaco (B). Adaptado de (Oberlander e Henderson, 2012) e (Kicman, 2008)

Os EAA exercem seus efeitos através da ligação ao receptor androgênico (AR) ou aos receptores estrogênicos (ER) que também são expressos nas mitocôndrias. Primeiramente, a enzima 5-alfa-redutase converte a testosterona (TS) em diidrotestosterona (DHT), que se liga ao AR com uma maior afinidade quando comparada a testosterona, enquanto a enzima aromatase converte a testosterona em estradiol. A nandrolona (NAND), um EAA bastante estudado tem potencial anabólico superior ao androgênico em comparação com a testosterona: sendo também substrato para a 5-alfa-redutase, o metabólito resultante tem afinidade menor

ao AR (Sundaram *et al.*, 1995) (Bergink *et al.*, 1985). No entanto, usuários que abusam de EAA geralmente combinam hormônios diferentes na forma de "coquetéis" e também em "ciclos" (**figura 10**), o que dificulta o estabelecimento da toxicidade individual de um fármaco para um órgão específico (Oberlander e Henderson, 2012).

Historicamente, a noção de melhora fisiológica induzida por EAA pode ser datada de antigas teorias egípcias e gregas anteriores à ciência moderna, onde se considerava que o uso de compostos relacionados a hormônios tinham poderes de cura e aumento de desempenho físico. Embora a primeira evidência científica dessa noção surgisse apenas no final do século XVIII, tais teorias levaram à descoberta de vários aspectos dos efeitos fisiológicos hormonais. Na edição de 1899 do "*Comptes rendus des séances de la Société de biologie*", o professor M.G. Variot publicou os resultados de um conjunto de experimentos indicando os efeitos da injeção de extrato de testículo animal em indivíduos do sexo masculino, relatando aumento da força, apetite e desejo sexual. Na mesma edição, o Dr. Brown-Séquard relatou os resultados da auto injeção do mesmo extrato aos 72 anos de idade, aumentando sua própria força e disposição, levantando hipóteses de vários mecanismos possíveis e estimulando novas investigações sobre suas especulações. Esses relatos iniciaram um século de pesquisas sobre os efeitos sistêmicos dos esteroides anabolizantes. Embora os efeitos metabólicos dos EAA tenham sido amplamente estudados no coração, fígado e músculo esquelético, estudos abordando os efeitos potenciais na neurotrasmissão e no metabolismo cerebral são recentes e focados principalmente na exploração dos efeitos comportamentais. Destaca-se que a maioria dos estudos com EAA são focados na toxicidade devido a utilização abusiva, no entanto o potencial uso terapêutico destes fármacos em diferentes lesões cerebrais ou em estratégias de reposição hormonal tem, atualmente, recebido maior atenção (Kang *et al.*, 2014). Embora a TS e seus derivados sintéticos como a NAND, sejam substâncias frequentemente utilizadas nos esportes de alto rendimento como "drogas de aumento de desempenho", são altamente lipofílicas, tem fácil penetração no cérebro onde podem mediar efeitos genômicos e não genômicas, suas propriedades anabólicas para as células neurais é muitas vezes negligenciada e seus efeitos tóxicos muitas vezes são superestimados ou não reconhecidos. Um aspecto dessa discussão é a sua possível influencia nos mecanismos patofisiológicos do ETC (Pope *et al.*, 2014).

**Figura 10 – Exemplo de uso comum relatado por usuários de esteroides anabolizantes androgênicos.**

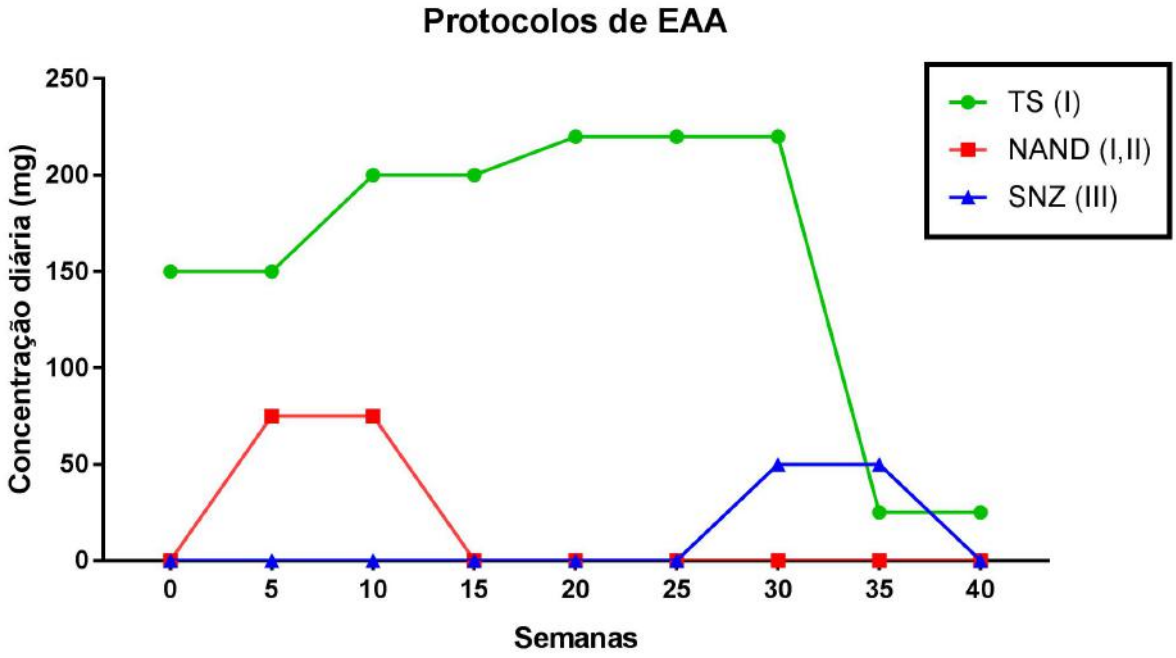


Diferentes EAA são combinados e a dose é variável ao longo do uso prolongado dessas substâncias. As drogas comumente abusadas são a testosterona, da classe I (TS), Nandrolona (NAND), de classe II e o Stanozolol (SNZ), de classe III. Adaptado de (Oberlander e Henderson, 2012).

Portanto, embora o uso crônico de esteroides resulte em efeitos específicos na melhora do desempenho e recuperação principalmente relacionado ao tecido muscular esquelético (Geyer *et al.*, 2014), o abuso também poderia levar a comprometimento da função cerebral, e até mesmo antagonizar os efeitos benéficos do exercício no metabolismo cerebral (Novaes Gomes *et al.*, 2014). Particularmente, estudos associando EAA e TCE ainda são inconclusivos, mostrando nenhum efeito (Mills *et al.*, 2012) ou aumento de dano (Bolton Hall *et al.*, 2016). Embora existam evidências proeminentes de efeitos deletérios de doses supra fisiológicas crônicas de EAA para viabilidade de células neuronais e neurogênese (Ma e Liu, 2015) (Novaes Gomes *et al.*, 2014), existem relatos apontando efeitos benéficos contra diferentes insultos cerebrais (Gouras *et al.*, 2000; Chisu *et al.*, 2006; Fanaei *et al.*, 2014; Hioki *et al.*, 2014; Gurer *et al.*, 2015; Toro-Urrego *et al.*, 2016). Estas controvérsias, estimulam um melhor entendimento do perfil neurotóxico e neuroprotetor dessas substâncias, quando usadas em doses controladas ou suprafisiológicas.

O conjunto de evidências em modelos pré-clinicos reforçam a hipótese de que a testosterona, um medicamento aprovado pela FDA (USA) e pela Agência Nacional de

Vigilância Sanitária (ANVISA, Brasil), abrange propriedades terapêuticas e características lipofílicas capazes de promover efeitos terapêuticos benéficos no TCE, embora, como já foi reforçado anteriormente, isso seja uma possibilidade ainda inexplorada (Pantziarka *et al.*, 2018). Entretanto, um aspecto importante que tem sido amplamente discutido em relação aos estudos pré-clínicos com fármacos para a terapia do TCE, é a dificuldade de replicação dos resultados ou a ausência de modelos adequados (Smith, D. H. *et al.*, 2019). Esta questão foi levada em conta nesta tese, com o desenvolvimento de um protocolo para investigar especificamente as condições ambientais da concussão relacionada ao esporte, além dos efeitos do uso abusivo de EAA (TS+NAND) combinados (Bolouri e Zetterberg, 2015).

***Manejo terapêutico e dietoterápico no TCE***

A terapia farmacológica aprovada pelo FDA e ANVISA para o tratamento de pacientes com TCE é limitada. O maior desafio reside no fato de que o dano induzido pelo TCE emerge de múltiplos mecanismos combinados, resultando em vários sintomas agudos e crônicos. Portanto, seria bastante peculiar se uma única droga pudesse ter como alvo os muitos mecanismos celulares e moleculares envolvidos nos desfechos do TCE, sugerindo que os tratamentos com drogas sinérgicas poderiam ter maior eficácia terapêutica do que drogas individuais. Existe uma lacuna evidente na literatura em relação a agentes farmacológicos específicos para melhorar a recuperação após lesão cerebral traumática. Embora muitos candidatos potenciais tenham surgido em estudos pré-clínicos, evidências sólidas de grandes ensaios multicêntricos randomizados controlados são escassos. Amantadina, metilfenidato e inibidores da acetilcolinesterase são drogas promissoras para melhora dos desfechos neurológicos (Diaz-Arrastia *et al.*, 2014).

Uma dificuldade no manejo do paciente com TCE é o controle glicêmico, pois a hiperglicemia persistente em pacientes com TCE é comum e correlaciona-se também com a gravidade da lesão e o desfecho clínico. Em um estudo envolvendo um total de 228 pacientes com TCE severo tratados com insulina, durante a primeira semana a glicemia de 90-144 mg / dL foi associada com menor mortalidade e pressão intracraniana (PIC) em comparação com glicemia mantida entre 63-117 mg/dL. No entanto, na segunda semana os grupos reverteram os desfechos, onde o grupo de 63-117 mg / dL demonstrou uma diminuição da incidência de elevação da PIC e reduziu as complicações infecciosas ao contrário do que aconteceu com pacientes mantidos na maior faixa de glicemia (Meier *et al.*, 2008). O grau de severidade

também influencia no controle glicêmico e no desfecho. Enquanto a glicemia <108-200 mg / dL poderia reduzir a mortalidade em pacientes com TCE leve, em pacientes com TCE severo, o alvo ideal de glicemia pode ser maior 140-180 mg / dL (Bilotta e Rosa, 2012). Consequentemente, o debate sobre os níveis de glicemia no TCE ainda é controverso e precisa ser explorado mais a fundo. Considerando que a ingestão calórica afeta diretamente a homeostase da glicose, sendo que pacientes alimentados via enteral ou parental comumente apresentam valores de glicemia em torno de 200 mg/dL a restrição de calorias poderia promover benefícios também por melhorar a homeostase da glicemia (Shi *et al.*, 2016).

Adicionalmente, a importância da nutrição transcende o fornecimento adequado de nutrientes e calorias para o paciente após o TCE, podendo garantir não somente a evolução clínica, mas também atenuar a progressão do dano induzido pelo trauma. Entre as variáveis na prescrição de dieta no trauma, a quantidade calórica visa garantir o funcionamento das funções vitais do organismo. Nesse contexto, as diretrizes apontam que a manipulação da ingestão calórica pode influenciar em diversos fatores associados ao desfecho pós-TCE. A base para a prescrição nutricional no TCE é limitada e conflitante, baseada em recomendações associadas ao politrauma. O paciente após TCE enfrenta alto catabolismo (Perel *et al.*, 2006). A nutrição imediata (iniciando 24 horas após o evento) proporciona diminuição na mortalidade, segundo dados de 797 pacientes em 22 centros, onde o aumento de 10 kcal/kg/dia diminuiu o risco de morte, sendo metade quando comparado com pacientes que não foram alimentados. É importante ressaltar que a maioria dos pacientes (62%) não atingiram 25 kcal/kg/dia e os que não foram alimentados apresentaram risco de morte quatro vezes maior (Hartl *et al.*, 2008).

Em ambiente de tratamento intensivo, a restrição calórica é usualmente recomendada até o paciente atingir estabilidade hemodinâmica, ao mesmo tempo em que se busca atingir o total calórico recomendado em um período de sete dias. A aplicação da restrição calórica controlada (entre 60-70% do total calórico recomendado) diminui o risco de morte comparado com restrição mais severa (80-90% do recomendado), porém, as recomendações sobre a ingestão calórica variam entre 10 – 50 kcal/kg/dia (Arabi *et al.*, 2011).

Uma dificuldade no TCE é a estimativa do gasto de energia, que aumenta com a lesão em proporção ao grau de resposta inflamatória sistêmica, variando geralmente de aumento de até 100% no TCE e outras injurias graves. Geralmente uma faixa de 25-30 kcal/kg/dia é recomendada, sendo a equação de Harris-Benedict que considera estatura, sexo e idade a mais utilizada. Entretanto, ambos os valores possivelmente subestimam a real necessidade calórica,

e também apresentam menor probabilidade de gerar hiperglicemia nas primeiras duas semanas após a injúria (Mcevoy *et al.*, 2009). Se a estimativa for necessária, a equação de Penn State é atualmente considerada a mais precisa, com uma precisão maior que 70% (Frankenfield *et al.*, 2004). Visando retenção de tecido após a lesão, tanto o aporte calórico quanto o proteico é necessário, embora mesmo com o aporte proteico no limite superior (até 1,5 g / kg / dia), a retenção total de massa muscular é muitas vezes impossível na fase aguda da lesão devido ao impacto da resposta inflamatória sistêmica no catabolismo proteico (Jensen *et al.*, 2010)

***Estratégias de pré-condicionamento neuronal: impacto no TCE***

O conceito de "pré-condicionamento" foi introduzido em 1964, descrevendo um efeito onde a estimulação abaixo do limiar de um determinado insulto resulta em proteção subsequente ao mesmo insulto (Janoff, 1964). O avanço nesse campo de pesquisa demonstrou que pequenas doses de estímulos nocivos como isquemia, baixas concentrações de espécies reativas de oxigênio e hipóxia mostraram ser capazes de induzir respostas neuroprotetoras associadas ao pré-condicionamento (Yang *et al.*, 2018) (Dawson e Dawson, 2000).

Atualmente, o eixo CREB (do inglês, cAMP response element-binding protein)-BDNF (do inglês, *Brain-derived neurotrophic fator*) é considerado um importante efetor molecular do pré-condicionamento, promovendo o crescimento dos neurônios durante o desenvolvimento do cérebro, a plasticidade sináptica, aprendizagem e memória além de sobrevivência neuronal a diferentes insultos (Müller *et al.*, 2011) (Ortega-Martínez, 2015) (Correia, Santos*, et al.*, 2010).

Duas formas distintas de pré-condicionamento são conhecidas: "pré-condicionamento imediato" (ocorrendo imediatamente após o estímulo) e "pré-condicionamento tardio". Ambos envolvem alterações celulares relacionadas à atividade ou função de enzimas, mensageiros secundários e canais iônicos (Correia, Carvalho*, et al.*, 2010). Entretanto, o "pré-condicionamento tardio" é dependente de processos relacionados com a expressão gênica e também de síntese proteica *de novo* (Cadet e Krasnova, 2009).

É importante considerar que os hábitos alimentares têm papel fundamental na saúde cerebral, podendo exercer efeitos profiláticos em relação a insultos cerebrais. De um ponto de vista translacional, tanto o exercício quanto estratégias de restrição dietética (RD) são atrativas devido aos benefícios já terem sido evidenciado em roedores e humanos em ensaios

clínicos (Tinsley e La Bounty, 2015). O exercício físico é um indutor efetivo do pré-condicionamento neuronal por meio do aumento dos fatores neurotróficos, juntamente com a melhora em vários mecanismos associados à atividade mitocondrial, o que supostamente resulta em melhores prognósticos após o TCE (Mota *et al.*, 2012) (Chio *et al.*, 2017) (Zhao *et al.*, 2015).

No contesto nutricional, a RD já demonstrou também induzir maior resistência neuronal a diferentes injúrias cerebrais (Camandola e Mattson, 2017; Mattson *et al.*, 2018). Estudos em roedores também apoiam a noção de que o envelhecimento cerebral e a neurodegeneração estão fortemente ligados ao equilíbrio metabólico e energético (Pani, 2015). Diferentes paradigmas de restrição calórica podem ser utilizados em modelos animais, como a alimentação diária limitada, onde os animais recebem uma porção diária de alimentos que geralmente é 30-40% menor que o consumo *ad libitum* (AL) de um grupo controle, resultando em restrição calórica controlada e redução correspondente no peso corporal. No segundo paradigma, os animais são submetidos a jejum intermitente (IF; do inglês "*Intermittent Fasting*") em dias alternados, que geralmente é isocalórico, resultando em diferentes benefícios metabólicos (Xie *et al.*, 2017). Ambos os paradigmas de restrição calórica afetam a longevidade através de mecanismos comuns, incluindo modificações no peso corporal, níveis de insulina e glicose sérica em jejum, além de melhorar o metabolismo energético e as defesas antioxidantes (Brown-Borg e Rakoczy, 2013), onde a modulação do metabolismo mitocondrial é evidente (Descamps *et al.*, 2005; Qiu *et al.*, 2010). Dessa forma, os roedores mantidos em longos períodos de IF exibem maior resistência neuronal a diferentes insultos, incluindo crises epilépticas e acidente vascular cerebral (Goodrick *et al.*, 1990; Anson *et al.*, 2003). Evidências de neuroproteção foram demonstradas com 24 horas de RD em roedores após TCE. Entretanto, o mesmo não foi demonstrado para lesão severa após impacto cortical controlado (Davis *et al.*, 2008). Assim, ainda não existem dados suficientes para se determinar a relevância desta intervenção no metabolismo cerebral após um TCE severo.

Recentemente, foi proposto que o exercício e jejum intermitente causam reprogramação metabólica cerebral (Hiebert *et al.*, 2015) por um efeito nomeado "Troca metabólica intermitente" (IMS; do inglês "*Intermittent Metabolic Switch*"). Esse efeito decorre de um desafio bioenergético (alta utilização de substratos e/ou produção de corpos cetônicos) induzindo vias relacionadas ao estresse metabólico seguido de uma recuperação (como ressíntese de reservas de glicose após o acesso alimentar) induzindo vias relacionadas

com a neurogênese (Mattson *et al.*, 2018). Os efeitos do IMS levam a mecanismos de adaptação promovendo maior resistência e plasticidade neuronal, além da melhora da função mitocondrial (López-Lluch *et al.*, 2006; Amigo *et al.*, 2017). Em resumo, os circuitos neuronais e diversos mecanismos respondem aos desafios bioenergéticos intermitentes de forma que aumentam a plasticidade sináptica e a neurogênese, melhoram a função cognitiva e aumentam a resistência neuronal aos estresses metabólicos, oxidativos e excitotóxicos (**figura 11**).

**Figura 11 - O exercício e o jejum intermitente exercem efeitos com a alternância entre substratos energéticos e estímulos de desafio bioenergético e recuperação.**

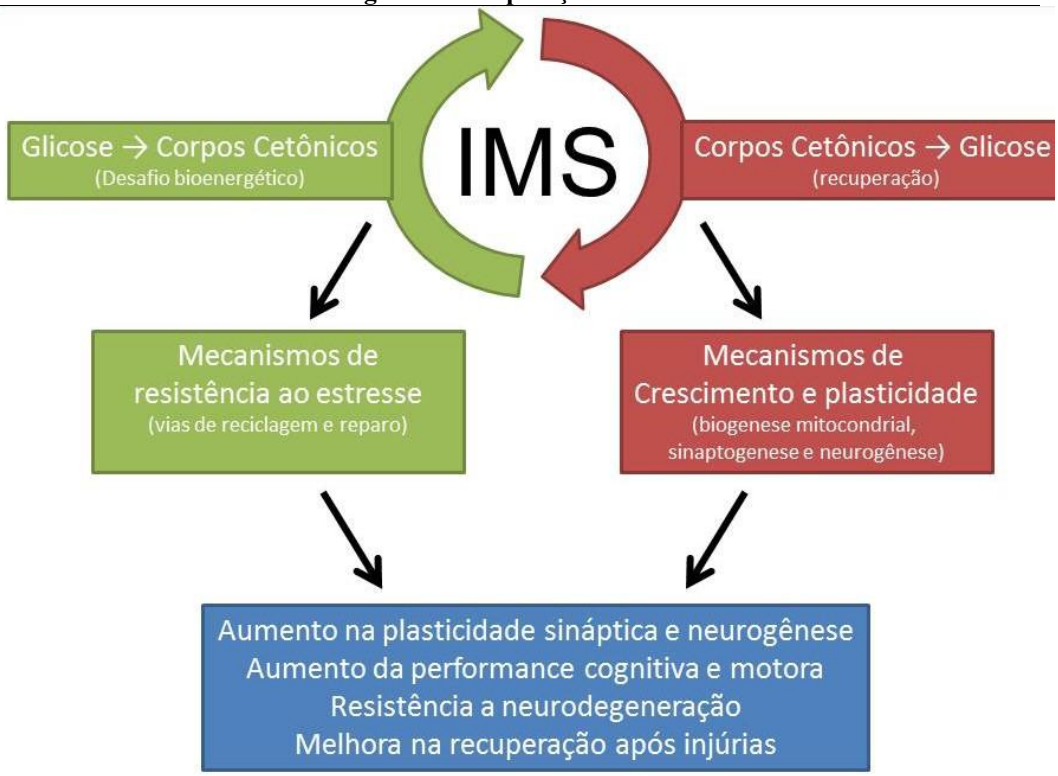


Alternância de substratos (IMS; do inglês "*Intermittent Metabolic Switch*") onde ocorre a alternância da utilização de corpos cetônicos (produzidos pelo fígado durante a restrição alimentar) e utilização de glicose induz mecanismos potencialmente benéficos para a recuperação de injúrias cerebrais. Modificado de Mattson *et al*. 2018

Portanto, como a literatura sobre a fisiopatologia e o tratamento do TCE ainda contém lacunas significativas em relação a organelas especificas, estratégias farmacológicas terapêuticas e a importância de medidas profiláticas particularmente endereçadas para a melhoria da capacidade neuroenergética, o objetivo da presente tese foi investigar os a mitocôndria como um "*hub*" celular determinante de desfechos neurometabólicos e moleculares capaz de influenciar desfechos neurológicos após o TCE. Para tanto, aprofundamos o conhecimento dos efeitos periféricos e centrais dos EAA e exploramos

estratégias profiláticas e terapêuticas endereçadas a modulação da atividade mitocondrial após TCE severo em camundongos.

## OBJETIVOS

### Objetivo geral:

Investigar o potencial de intervenções terapêuticas e profiláticas em mecanismos mitocondriais neurometabólicos, apoptóticos e na memória em camundongos submetidos a diferentes protocolos de traumatismo cranioencefálico.

### Objetivos específicos:

a) Avaliar efeitos periféricos de diferentes EAA no metabolismo mitocondrial;
b) Avaliar efeitos cerebrais de diferentes EAA em populações mitocondriais específicas no sistema nervoso central;
c) Avaliar o potencial terapêutico de EAA no detrimento metabólico após o TCE;
d) Propor um modelo de TCE repetido em roedores para estudo da concussão relacionada ao esporte;
e) Avaliar o potencial de pré-condicionamento pelo exercício físico no TCE grave e investigar a influência do "volume" de exercício na neuroenergética mitocondrial, sinalização apoptótica, sinalização neurotrófica e memória espacial;
f) Avaliar o potencial de pré-condicionamento do jejum intermitente no TCE grave em desfechos neurometabólicos e cognitivos.

# PARTE II

Nesta seção os resultados serão apresentados em capítulos compostos por um breve prefácio seguido de um artigo científico.

Os capítulos I-II demonstram os resultados de estudos experimentais desta tese visando o entendimento de mecanismos mitocondriais em coração e fígado de diferentes EAA.

O capítulo III é composto pelo estudo dos efeitos terapêuticos da testosterona no TCE grave e o capítulo IV propõe um modelo animal para estudo da concussão no esporte e encefalopatia traumática crônica (ETC), além de investigar mecanismos associados com o uso crônico de uma combinação de EAA nesse contexto.

O capítulo V investiga os efeitos profiláticos de diferentes volumes de exercício na bioenergética mitocondrial, sinalização neurotrófica e memória após TCE grave.

O capítulo VI demonstra um protocolo de jejum intermitente como estratégia profilática para os desfechos neurometabólicos e comportamentais associados a um TCE grave.

**Capítulo I:** *Impaired oxidative metabolism and redox imbalance induced by anabolic androgenic steroids precede structural damage in the heart and liver.*

No capitulo I apresentamos o artigo submetido ao periódico "*Chemico-Biological Interactions*".

A busca de uma alternativa farmacológica para a terapia do TCE envolveu, em primeiro lugar, a avaliação dos efeitos de doses suprafisiológicas de EAA sobre as mitocôndrias do fígado e coração. Para tanto, utilizamos doses supra fisiológicas de decanoato de nandrolona (NAND) e cipionato de testosterona (TS), e investigamos os parâmetros mitocondriais associados a oxidação de substratos e acoplamento energético, além de parâmetros de estresse oxidativo e análises histopatológicas.

Demonstramos que o tratamento com NAND ou TS levam a respostas mitocondriais distintas no fígado e coração. Houve uma modulação positiva da TS sobre o metabolismo mitocondrial, regulação redox e homeostase do cálcio, enquanto a NAND resultou em efeitos predominantemente negativos sobre estes parâmetros.

Ainda, reforçamos que as alterações metabólicas causadas pela NAND precedem alterações na morfologia desses órgãos.

# Manuscript Details

| | |
|---|---|
| **Manuscript number** | CHEMBIOINT_2018_1638 |
| **Title** | Impaired oxidative metabolism and redox imbalance induced by anabolic androgenic steroids precede structural damage in the heart and liver |
| **Article type** | Research Paper |


**Abstract**

Supraphysiological doses of anabolic androgenic steroids (AAS) may cause morphological abnormalities particularly to the heart and liver that may only represent the later-stage of cumulative damage caused by dysfunctional organelles and maladaptive biochemical responses over time. Here, we investigated whether supraphysiological doses of Testosterone (Test) and nandrolone decanoate (Nand) trigger early-onset alterations in the mitochondrial bioenergetic machinery and redox homeostasis coupled with histopathological alterations to the heart and liver of adult mice. CF1 albino mice were treated daily with 15 mg/kg of Nand or Test or oil (vehicle) for 19 days. Preparations enriched in mitochondria from heart and liver were used to perform assays of Ca2+ influx/eflux, membrane potential (ΔΨm), oxygen consumption coupled with ATP synthesis, and H2O2 production. Heart and liver tissues were also collected for haematoxylin and eosin staining and analysis of oxidative stress biomarkers. Nand and Test do not affected tissues morphology. Nand significantly impaired mitochondrial Ca2+ influx and ΔΨm in heart and liver relative to other groups. Relative to control, Nand decreases the oxygen consumption rates and ATP synthesis in the liver; while both Test and Nand, increased H2O2 levels in heart and liver. In addition, Nand increased the biomarkers of oxidative damage to lipids and proteins (TBARS and carbonils) in both organs and decreased glutathione metabolism and glutathione peroxidase activity. In summary, supraphysiological doses of Nand, and in less extension Test, impaired mitochondrial calcium influx, membrane potential, and bioenergetics, associated with perturbations in the redox homeostasis. Since there was no clear histopathological damage we conclude that impairment oxidative energy support and redox imbalance precedes structural damage to the heart and liver.



| | |
|---|---|
| **Keywords** | Testosterone; nandrolone decanoate; mitochondrial dysfunction; impaired metabolism; oxidative stress. |
| **Taxonomy** | Mitochondrial Toxicity, Biochemical Neurotoxicology, Toxicology |
| **Manuscript category** | Biochemical toxicology |



| | |
|---|---|
| **Corresponding Author** | Luis Portela |
| **Corresponding Author's Institution** | Universidade Federal do Rio Grande do Sul |
| **Order of Authors** | Randhall B. Carteri, Afonso Kopczinski, Marcelo S. Rodolphi, Nathan R. Strogulski, Clovis M. D. Wannmacher, Itiane Diehl de Franceschi, Márcia Elisa Hammerschmitt, David Driemeier, Luis Portela |
| **Suggested reviewers** | Vittorio Fineschi, Nipon Chattipakorn, Maria Irigoyen |

# Impaired oxidative metabolism and redox imbalance induced by anabolic androgenic steroids precede structural damage in the heart and liver

Randhall B. Carteri[1], Afonso Kopczinski[1], Marcelo S. Rodolphi[1], Nathan R. Strogulski,[1] Clovis M. D. Wannmacher,[1] Ithiane D. Franceschini,[1] Marcia E. Hammerschmitt,[2] David Driemeier,[2] Luis V. Portela,[1*].

[1] PPG-Ciências Biológicas Bioquímica, Departamento de Bioquímica, Instituto de Ciências Básicas da Saúde, Universidade Federal do Rio Grande do Sul - UFRGS, Porto Alegre, RS, Brasil

[2] Setor de Patologia Veterinária, Faculdade de Veterinária da Universidade Federal do Rio Grande do Sul - UFRGS, Porto Alegre, RS, Brasil

* Corresponding author:

Dr. Luis Valmor Portela

Departament of Biochemistry, ICBS

Laboratory of Neurotrauma and Biomarkers

Federal University of Rio Grande do Sul

Porto Alegre, RS, Brasil

CEP 90095-003

Tel. +55 51 33085557

Fax. + 5551 33085557

**Abstract**

Supraphysiological doses of anabolic androgenic steroids (AAS) may cause morphological abnormalities particularly to the heart and liver that may only represent the later-stage of cumulative damage caused by dysfunctional organelles and maladaptive biochemical responses over time. Here, we investigated whether supraphysiological doses of Testosterone (Test) and nandrolone decanoate (Nand) trigger early-onset alterations in the mitochondrial bioenergetic machinery and redox homeostasis coupled with histopathological alterations to the heart and liver of adult mice. CF1 albino mice were treated daily with 15 mg/kg of Nand or Test or oil (vehicle) for 19 days. Preparations enriched in mitochondria from heart and liver were used to perform assays of Ca2+ influx/eflux, membrane potential (Δ□m), oxygen consumption coupled with ATP synthesis, and H2O2 production. Heart and liver tissues were also collected for haematoxylin and eosin staining and analysis of oxidative stress biomarkers. Nand and Test do not affected tissues morphology. Nand significantly impaired mitochondrial Ca2+ influx and Δ□m in heart and liver relative to other groups. Relative to control, Nand decreases the oxygen consumption rates and ATP synthesis in the liver; while both Test and Nand, increased $H_2O_2$ levels in heart and liver. In addition, Nand increased the biomarkers of oxidative damage to lipids and proteins (TBARS and carbonils) in both organs and decreased glutathione metabolism and glutathione peroxidase activity. In summary, supraphysiological doses of Nand, and in lower extension Test, impaired mitochondrial calcium influx, membrane potential, and bioenergetics, associated with perturbations in the redox homeostasis. Since there was no clear histopathological

damage we conclude that impairment oxidative energy support and redox imbalance precedes structural damage to the heart and liver.

**Highlights**

- Nineteen-days testosterone and nandrolone do not alter heart and liver structure
- Nandrolone impairs mitochondrial $Ca^{2+}$ influx and membrane potential
- Nandrolone decreases oxidative phosphorylation and increases $H_2O_2$ production
- Nandrolone, and in lower extension testosterone causes oxidative damage to the heart and liver.
- Mitochondrial dysfunction precedes structural damage to heart and liver

**Keywords:** Testosterone; nandrolone decanoate; mitochondrial dysfunction; impaired metabolism; oxidative stress.

## 1. Introduction

Testosterone (Test) and nandrolone decanoate (Nand) are anabolic androgenic steroids (AAS) able to burst biochemical reactions thereby providing anabolic benefits [1]. The illegal use of these substances mainly by young individuals aiming to improve athletic performance, increase in skeletal muscle mass and/or for aesthetical purposes has been associated with structural alterations, particularly reported in heart and liver [2], [3], [4]. However, these findings may only represent the later stage of cumulative damage caused by dysfunctional organelles and maladaptive biochemical responses over time.

While at physiological levels AAS mediate global improvements in the energy metabolism, the administration of supraphysiological doses causes reactive oxygen

species (ROS) overproduction along with oxidative damage, which is suggestive of mitochondrial dysfunction [5], [6], [7], [8]. Actually, myocardium and liver are enriched in mitochondria and present a high oxygen consumption rate implying their reliance on oxidative metabolism [9], [10]. In addition to oxygen availability, the $Ca^{2+}$ levels also regulates oxidative energy metabolism [11], [12]. The influx of $Ca^{2+}$ into the mitochondrial matrix occurs through the calcium uniporter (MCU) and leads to the activation of dehidrogenases and the dissipation of membrane potential (Δ□m). On opposite, the sodium–calcium-lithium exchanger (NCLX), promotes the antiport transportation of one $Ca^{2+}$ ion from matrix in the exchange for three sodium ions ($Na^{+}$) [12]. Although this mechanism is proposed to be the main responsible for the mitochondrial $Ca^{2+}$ efflux in heart and neurons, thus serving as the key homeostatic regulator, it's physiological relevance in liver still remains obscure as well as whether it is affected by AAS [13]. It is known that sustained $Ca^{2+}$ load leads to mitochondrial swelling, accompanied by ATP consumption rather than production, dissipation of proton-motive gradient as heat and exacerbated production of ROS, which together may cause cellular death [14].

Therefore, although postmortem studies with humans and rodents after prolonged AAS abuse show visible anatomical and histological abnormalities in the heart and liver, the early biochemical mechanisms triggering such alterations are not clearly elucidated.

Here, we investigated whether supraphysiological doses of Test and Nand trigger early-onset alterations in the mitochondrial bioenergetic machinery and redox homeostasis coupled with damage to the heart and liver of adult mice.

## 2. Methods

### 2.1. Animals and treatment protocol

Male 90 days old albino CF1 mice were obtained from Foundation for Health Science Research (FEPPS, Porto Alegre/RS, Brazil). Animals (4-5 per cage) were placed into a controlled temperature room (22 ºC ± 1) under a 12h light/12h dark cycle (lights on at 7 a.m.) and had free access to food and water. The treatment consisted of a daily 15 mg/kg subcutaneously injection of nandrolone decanoate (Organon Pharmaceuticals) (Nand group) or testosterone cypionate (Sigma-pharma) (Test group) or equivalent volume of vehicle (corn oil) (Veh group), for 19 days. The Ethical Committee on the Care and Use of Experimental Animal Resources, UFRGS, Brazil number 22436, approved all experiments. Animal weight was assessed before and after treatment. Treatment duration was chosen based on a previous study by our group, where significant biochemical and behavioral alterations were observed at 19 days after Nand administration [15]. Test administration was based on publish papers by others [16]. The experimental timeline is showed in Figure 1 A.

### 2.2. Maximal exercise capacity test

Mice from a separate group were tested 2 h after the last treatment day to ensure classical benefits of AAS on physical performance. Test and Nand injected animals were allocated individually on a sealed electrical treadmill; with shock bars with adjustable voltage (set at 3.0 mA) placed close to the rear paws. Prior to the test procedures, animals were familiarized to the treadmill using 5 min exposures per day for two days, with a fixed speed of 16 m/min with shock bars on. The test for the maximum capacity was performed in stages with crescent speed as follows: a starting stage the speed of 8 m/min

for 3 min, followed by increments of 4 m/min every three minutes until reaching the maximum speed of 40 m/min. The test was terminated if the mouse remained in the shock area for 5 seconds, or if the test lasted 36 min with the mouse running at 40 m/min

2.3. Histopathological analysis

Twenty-four hours after the last 19 days injection a group of mice were euthanized and tissues were immersed in 4% paraformaldehyde followed by the collection of heart and liver used for histopathological analysis using hematoxylin and eosin (H&E) staining. Briefly, tissue samples were fixed in 10 % neutral buffered formaldehyde, then processed in paraffin blocks, cut into 3 μm thick sections and stained with hematoxylin and eosin (HE) for the visualization of cellular structures with optical microscopy (Nikon, Eclipse E600, 400x) [17].

2.4. Preparation of tissue enriched in mitochondria

Liver and heart tissues were collected 24 h after the last injection and homogenized in a specific buffer (320 mM sucrose, 1mM EDTA, pH 7.4) using a pre-cooled glass potter. Following a first 5 minutes centrifugation step (600 *x*g for liver and 800 *x*g for heart) at 4 °C, resulting supernatant was further centrifuged (12.000 *x*g for liver and 9500 *x*g for heart) and mitochondria enriched pellet were resuspended and used for immediate respirometry analysis, $Ca^{2+}$ handling, mitochondrial membrane potential and hydrogen peroxide production [18], [19]. Posterior protein quantification was performed using bicinchoninic acid assay (Pierce Biotechnology™, Rockford, IL, USA Catalog number: 23225) [20]. The samples were frozen at − 80 °C for protein quantification. All spectrophotometric analyses were performed in duplicates (coefficient

of variation between duplicates was < 3 %) and corrected for the absorbance measured in the homogenization buffer only.

2.5. Mitochondrial $Ca^{2+}$ handling

Mitochondrial calcium influx and efflux was assessed indirectly by spectrophotometric analysis (λ=540 nm) (Spectra Max M5, Molecular Devices) of mitochondrial swelling, induced by colloid-osmotic force of $Ca^{2+}$ influx at proteins localized in the mitochondrial matrix. This assumes that mitochondrial $Ca^{2+}$ influx leads to swelling reducing light scattering in this specific wavelength, and consequently absorbance, whilst in corollary shrinkage leads to increased absorbance. Mitochondria-enriched homogenates (50 uL) from liver and heart were added to standard swelling incubation medium (100 mM KCl, 50 mM Sucrose, 10 mM HEPES and 5 mM $KH_2PO_4$) and the basal mitochondrial swelling was monitored during 3 min in microplates. Mitochondrial energy substrates, 3.5 mM pyruvate, 4.5 mM malate, 4.5 mM glutamate, 1.2 mM succinate (PMGS) and 100 uM of adenosine diphosphate (ADP) were added to energize mitochondria and support ATP synthesis, to assess oxidative phosphorylation-driven mitochondrial shrinkage during 5 min. Afterward, calcium ($CaCl_2$, 20 mM) was added to induce large-amplitude swelling driven by the colloid osmotic force of $Ca^{2+}$ influx at proteins localized in the mitochondrial matrix. The modifications in the absorbance caused by the $Ca^{2+}$ influx were monitored for 10 min. After calcium-induced mitochondrial swelling, we assessed NCLX $Ca^{2+}$ efflux mechanism as indicated by mitochondrial shrinkage induced by the addition of $Na^+$ (NaCl 30 mM) to the medium, monitored for 10 min [21]. All results were normalized for the protein content, and were calculated for the percentage of variation in the absorbance after the addition of

substrates (PMGSA) relative to basal; after addition of $Ca^{2+}$ relative to (PMGSA); and after addition of $Na^{+}$ relative to $Ca^{2+}$.

2.6. Mitochondrial Membrane Potential ($\Delta\Psi_m$)

The $\Delta\Psi_m$ was measured through the fluorescence signal emitted by the cationic dye, safranin-*O*. Mitochondria-enriched homogenates from the liver and heart were incubated in the respiration buffer (100 mM KCI, 75 mM mannitol, 25 mM sucrose, 5 mM phosphate, 0.05 mM EDTA, and 10 mM Tris-HC1, pH 7.4) used for the respirometry protocol, additionally supplemented with 10 μM safranin-*O*. The fluorescence was detected with an excitation wavelength of 495 nm and an emission wavelength of 586 nm (Spectra Max M5, Molecular Devices). Increased fluorescence units mirror decreased $\Delta\Psi_m$ whereas decreased fluorescence units indicate increased $\Delta\Psi_m$. Baseline $\Delta\Psi_m$ was measured without addition of substrates and inhibitors in the incubation medium.

Further to baseline, substrates PMGS were incubated to modulate the activity of mitochondrial respiratory complex I and II, and consequently $\Delta\Psi$m in State IV respiration. Increased oxygen consumption coupled with ATP synthesis by the $F_1$Fo-ATP synthase (respiratory Complex V) along with decreased $\Delta\Psi_m$ (State III) was mirrored by addition of ADP (2.5 mM) after the addition of PMGS. Proton ionophore Carbonyl cyanide 4-trifluoromethoxy-phenylhydrazone (FCCP 1 μM), was used as a chemical mitochondrial uncoupler, triggering decreases in the $\Delta\Psi_m$ and oxidative phosphorylation, while stimulating the maximal mitochondrial oxygen consumption (State $III_{(U)}$). The addition of sodium azide ($NaN_6$; 20 mM), an inhibitor of mitochondrial respiratory complex IV (cytochrome c oxidase), was used to decrease ATP synthesis and disrupt

mitochondrial membrane potential (ROX). Moreover, we used the data achieved through the sequential manipulation of mitochondrial respiratory rates with the components PMGS, ADP, FCCP and ROX to calculate the percentage of variation in the $\Delta\Psi_m$ for each achieved state relative to the previous state. Data are reported as percentage of variation of arbitrary fluorescence units (AFUs) and were normalized to protein content [22].

2.7. Mitochondrial respiratory protocol

Oxygen consumption measurements were performed in the tissue homogenates using respiration buffer. Oxygen consumption per tissue mass was measured using the high-resolution Oxygraph-2k system and recorded real-time using DatLab software (Oroboros, Innsbruck, Austria). The results were normalized to the protein content. The experiments were performed at 37°C in a 2-ml chamber, with a modified multi-substrate titration protocol as previously described in detail elsewhere [23].

Following 5 minutes for establishing routine respiration values, the multi-substrate titration protocol started. The protocol consisted of sequential addition of pyruvate, malate, glutamate and succinate (PMGS; 10, 10, 20 and 10 mM, respectively) to obtain State IV respiration (CI and CII – linked); Sub sequentially, adenosine diphosphate (ADP, 2.5 mM) was titrated to obtain Maximal OxPHOS capacity (StateIII) in saturating ADP concentrations and non-mitochondrial respiration (ROX) after addition of potassium cyanide (KCN, 5 mM).

Respiratory fluxes were corrected automatically for instrumental background by DatLab taking into account oxygen consumption of the oxygen sensor and oxygen diffusion out of or into the oxygraph chamber measured at experimental conditions in

incubation medium without biological sample. ROX was extracted from all of the above-mentioned states and tissue-mass specific oxygen fluxes were compared in different substrate and coupling states.

We calculated the respiratory control ratio (RCR = StateIII/StateIV) obtained in the CI and CII-linked substrate state. For statistical analysis, RCR was transformed to its flux control factor (FCF), which is the OXPHOS coupling efficiency (calculated as State III-StateIV)/StateIII), which mathematically expresses the changes of flux in a single step of the SUIT protocol, normalized for the high flux as a specific reference state [20], [23].

2.8. Mitochondrial $H_2O_2$ production

The pattern of mitochondrial production of hydrogen peroxide ($H_2O_2$) was assessed in the tissue homogenates through the Amplex® Red Hydrogen Peroxidase Assay kit (Invitrogen, Carlsbad, CA, USA) (n=10 per group) as instructed by the manufacturer. The same substrates, uncoupler and inhibitors used in the respirometry protocol were incubated sequentially in the respiration buffer supplemented with 10 μM Amplex® Red and 2 units/mL horseradish peroxidase to assess $H_2O_2$ generation in 96 well microplates. Similarly to oxygen consumption, $H_2O_2$ production was assessed in a sequential series of mitochondrial states, where the routine $H_2O_2$ production was measured without the presence of energetic substrates in the incubation medium. Then, PMGS was provided to the samples, as the substrate to stimulate mitochondrial respiration leading to State IV, ADP to analyze $H_2O_2$ production whilst maximum functional capacity of mitochondria to produce ATP is induced (State III), in the presence of oligomycin (ATP Synthase inhibitor; $StateIV_{(omy)}$), and the proton ionophore FCCP (Carbonyl cyanide 4-trifluoromethoxy-phenylhydrazone, a reversible inhibitor of

mitochondrial oxidative phosphorylation; State $III_{(U)}$) to estimate the maximal mitochondrial electron transport system capacity. Sodium Azide was used to assess non-mitochondrial $H_2O_2$ production (ROX). Fluorescence was monitored at excitation (563 nm) and emission (587 nm) wavelengths with a Spectra Max M5 microplate reader (Molecular Devices, USA) [24].

2.9. Oxidative stress biomarkers

Twenty-four hours after the last 19 days injection a group of mice were anesthetized with ketamine and xylazine (70 and 10 mg/kg, respectively) and immediately perfused with phosphate buffer saline (PBS) to remove blood cells followed by the collection of heart and liver used to measure the activity of the enzymes involved in $H_2O_2$ production (Superoxide dismutase - SOD) and degradation (glutathione peroxidase – GP*x*); the expression levels of the mitochondrial enzyme manganese superoxide dismutase (MnSOD), and total ROS production, altogether here designated as oxidative stress biomarkers. The protein content of the homogenates was determined by bicinchoninic acid assay (Pierce Biotechnology™, Rockford, IL, USA Catalog number: 23225).

The measurements were performed, as follows:

2.9.1. 2’7’-Dihydro-dichlorofluorescein ($H_2$DCF-DA) Oxidation Assay

The measure of global reactive oxygen species (ROS) production in the ipsilateral cortex homogenates was performed according to LeBel et al. by using reduced $H_2$DCF-DA. To avoid photobleacing samples were incubated for 30 min protected from light at 37 ºC in medium supplemented with 20 mM sodium phosphate, 140 mM KCl buffer pH 7.4 and 100 μM reduced 2'7'-Dichlorofluorescein diacetate ($H_2$DCF-DA) solution in a 96

wells microplate. The product of $H_2$DCF oxidation by ROS is fluorescent, thus fluorescence intensity is proportional to the amount of ROS formed. Fluorescence was measured using excitation and emission wavelengths of 480 and 535 nm, respectively. The calibration curve was performed with standard DCF (0.25–10 μM), and the levels of ROS were expressed as nmol of DCF formed per mg of protein [25].

2.9.2. Thiobarbituric Acid Reactive Substances (TBARS) Assay

TBARS levels were measured as Ohkawa and others [26]. This method measures the malondialdehyde (MDA), a product of lipoperoxidation caused mostly by hydroxyl free radicals. Briefly, to microtube were added, in the following order: heart or liver tissues; 8.1 % sodium dodecyl sulphate; 20% acetic acid in aqueous solution (v/v) pH 3.5 and 0.8 % thiobarbituric acid. Reaction was carried out in a boiling water bath for one hour. The mixture was allowed to cool water for 5 min and centrifuged at 750 x g for 10 min. The resulting supernatant pink stained TBARS were spectrophotometrically quantified as absorbance in 532 nm wavelength. A calibration curve was generated using 1,1,3,3-tetramethoxypropane as a standard. Results are expressed and calculated as nmol of TBA-RS per mg of protein.

2.9.3. Carbonyls Protein Assay

Protein carbonyl content was assayed by the method described by Reznick and Packer [27]. Protein carbonyls react with dinitrophenylhydrazine (DNPH) forming dinitrophenylhydrazone, a yellow compound, measured spectrophotometrically at 370 nm. Briefly, samples were incubated with 10 mM DNPH (prepared in 2 M HCl) protected from light for 1 hour and vortexed every 15 min. After this, 20% (w/v) trichloroacetic acid (TCA) was added and centrifuged at 10.000 x g for 3 min. The

supernatant was discarded, and the pellet was washed with ethyl acetate/ethanol 1:1 (v/v), vortexed, and centrifuged at 10.000 x g for 3 min. The supernatant was discarded, and the pellet re-suspended in 6 M guanidine (prepared in a 20 mM potassium phosphate solution pH 2.3). The samples were vortexed and kept at 60°C for 15 min. After this, samples were centrifuged, and the supernatants read spectrophotometrically at 370 nm. Total carbonylation was calculated using a molar extinction coefficient of 22,000 $M^{-1}cm^{-1}$. Results are expressed as nmol of carbonyls formed per mg of protein.

2.9.4. Total Sulfhydryl Content Assay

The sulfhydryl assay is based on the reduction of 5,5-0-dithio-bis (2-nitrobenzoic acid) (DTNB) by thiols, generating a yellow derivative (TNB) whose absorption is measured spectrophotometrically at 412 nm [28]. Results were calculated as nmol of TNB per mg of protein.

2.9.5. GSH/GSSG Ratio Assay

Glutathione reduced (GSH) and oxidized (GSSG) forms were determined fluorometrically as described by Hissin and Hilf, [29] using o-phthaldialdehyde (OPT) as the fluorescent reagent and, from which, the GSH/GSSG ratio was calculated. GSH reacts with OPT at pH 8.0 and GSSG at pH 12.0. To prevent GSH interference in GSSG measurement, N-ethylmaleimide (NEM) is added, forming a complex with GSH. Fluorescence was measured using excitation and emission wavelengths of 350 and 420 nm, respectively. A calibration curve was generated using GSH and GSSH as a standard. Results were calculated as nmol of GSH or GSSG per mg of protein.

2.9.6. Superoxide Dismutase (SOD) Activity Assay

SOD activity was determined based on the capacity of autoxidation of pyrogallol, a process highly dependent on superoxide radical [30]. The inhibition of autoxidation of this compound occurs in the presence of SOD, whose activity can then be indirectly assayed spectrophotometrically at 420 nm. A calibration curve was performed with purified SOD as standard. A 50 % inhibition of pyrogallol autoxidation is defined as one unit of SOD, and the specific activity was expressed as SOD units per mg of protein. The expression level of MnSOD was analyzed through western blotting (see the section below).

2.9.7. Catalase (CAT) Activity Assay

CAT activity was assayed according to Aebi [31] by measuring the absorbance decrease of $H_2O_2$ at 240 nm. The reaction medium contained 20 mM $H_2O_2$, 0.1 % Triton X-100, 10 mM potassium phosphate buffer, pH 7.0 and supernatant sample. One CAT unit is defined as 1 μmol of hydrogen peroxide consumed per min, and the specific activity is calculated as CAT units per mg of protein.

2.9.8. Glutathione Peroxidase (GPx) Assay

The GP*x* activity in the homogenates was measured using tert-butylhydroperoxide as substrate [32]. The enzyme activity was determined by monitoring the nicotinamide adenosine dinucleotide phosphate (NADPH) disappearance at 340 nm. The medium contain 100 mM potassium phosphate, 1 mM ethylenediaminetetraacetic acid buffer pH 7.7, 0.4 mM azide, 2 mM glutathione reduced, 0.15 U/mL glutathione reductase, 0.1 mM NADPH, 0.5 mM tert-butyl-hydroperoxide, and supernatant sample. One GP*x* unit is defined as 1 μmol of NADPH consumed per minute. The specific activity was expressed as micromole of NADPH consumed per minute per mg of protein.

*2.10. Statistical analysis*

Results were calculated and expressed as the mean ± S.E.M. Normality of data was assessed with shapiro-wilk test. Difference between groups was analyzed with one-way analysis of variance (ANOVA) followed by tukey's post hoc test. Kruskal-Wallis was used for nonparametric comparisons. All procedures were performed using GraphPad Prism 6.0 software. The differences were considered statistically significant at $p < 0.05$.

## 3. Results

3.1. Nand and Test improved exercise performance

As early symptoms of drug toxicity animals may display decrease food and water intake, muscle weakness and consequently loose their weight. Here we showed that Nand administration increased body weight (Figure 1B) compared to Veh (Mean diff = 3.23, $p = 0.025$) and Test (Mean diff = 2.35, $p = 0.03$). However, both AAS exerted similar effects on physical performance, such as increasing the total time on the running wheel (Figure 1C) and total distance run (D) compared to Veh ($p < 0.01$).

3.2. Nand and Test do not affect tissue morphology

At later stages subjects exposed to high doses of AAS commonly display cardiomegaly, left ventricular hypertrophy, fibrosis and necrosis [2], [4], whereas hepatic alterations include fatty deposition, hepatomegaly, macrophage infiltration, and fibrosis [4], [33]. We performed histopathological evaluation through hematoxylin and eosin staining of heart (Figure A, B and C) and liver (Figure D, E and F) sections and found no apparent significant alterations in the cell nuclei, cytoplasm, connective tissue or blood

vessels. Visual observation of the isolated organs demonstrated no evidences of fatty acid deposition, and no differences in the net weight of heart and liver (data not shown). Also, no microscopic evidences of necrosis could be seen in the sections. Similarly, there were no hepatocellular lesions indicated by vacuolization, sinusoidal dilatation or cell infiltration in control and AAS groups.

3.3. Nand impairs mitochondrial $Ca^{2+}$ influx

Cardiac tissue mitochondria from Nand group displayed exacerbated mitochondrial swelling (Supp. Material A) in the resting states and after addition of substrates (PMGSA) compared to Veh, ($p$ = 0.06). After the addition of $Ca^{2+}$, the swelling increased in all groups; however, Nand showed the lower increase compared to Veh and Test groups (Figure 3A; Mean diff = 11.93, $p < 0.0001$ and Mean diff = 13.21, $p < 0.0001$; respectively). After the addition of $Na^{+}$ to the incubation medium all groups extruded $Ca^{2+}$, indicating preserved functional capacity of mitochondrial NCLX channel.

Similar responses were observed in liver mitochondria (Figure 3B). No differences were observed in absorbance at baseline and after the addition of substrates (PMGSA; Supp. Material B). Mitochondrial swelling increased in all groups after the addition of $Ca^{2+}$ albeit the effect was more pronounced in the Test compared to Veh and Nand groups (Figure 3B; Mean diff = 9.974, $p < 0.0001$ and Mean diff = 11.59, $p < 0.0001$; respectively). No differences were observed after the addition of $Na^{+}$ to the incubation medium, indicating normal functioning of the mitochondria NCLX channel. Taken together, these results indicate that exposure to Test and Nand differentially modulates calcium uptake by the mitochondria from heart and liver.

The estimated percentage of absorbance in the influx and efflux for Nand group was between -10 % ($Ca^{2+}$) and +10 % ($Na^{+}$) respectively, whereas in the Veh and Test groups were approximately -23 % ($Ca^{2+}$) and +10 % ($Na^{+}$). Considering the physiological properties of $Ca^{2+}$ ions to the mitochondrial membrane potential and activity of oxidative enzymes, we conjectured if these differences in $Ca^{2+}$ handling might affect such functional roles.

3.4. Nand disturbs the mitochondrial membrane potential ($\Delta\Psi_m$)

We showed that exposure to Nand impaired the $\Delta\Psi_m$ dynamics in both heart and liver mitochondria.

The resting state fluorescence in the heart preparations decreased in Nand (increased $\Delta\Psi_m$) compared to Veh and Test groups ($p = 0.06$ and $p = 0.04$ respectively, supp. Material C). After the addition of the metabolic substrates (PMGS) (StateIV), the fluorescence was significantly higher (decreased $\Delta\Psi_m$) in Nand compared to Veh and Test (supp. Material C). These results implies in decreased $\Delta\Psi_m$ formation in Nand group (Figure 3C; Mean diff = 27.99, $p < 0.0001$, and Mean diff = 27.4, $p < 0.0001$, respectively).

No significant differences in fluorescence were observed among groups after ADP addition (StateIII). Fluorescence was significantly higher in Nand compared to Veh and Test after the addition of oligomycin (Omy) to inhibit ATP synthase ($p < 0.0001$, supp. Material D). Uncoupler addition (FCCP) ($StateIII_U$) resulted in reduced variation of $\Delta\Psi_m$ in Nand relative to Veh and Test groups (Figure 3C; Mean diff = 54.88, $p < 0.0001$, and Mean diff = 44.79, $p < 0.0001$, respectively). As expected, the addition of sodium cyanide (CN) (ROX) completely dissipated the $\Delta\Psi_m$.

Furthermore, in liver Nand decreased safranin-o fluorescence (increased $\Delta\Box_m$) in the resting state compared to Veh and Test ($p < 0.0001$, supp. Material D). After the addition of metabolic substrates (StateIV) there was an increase in fluorescence (decreased $\Delta\Box_m$) in Nand relative to Veh and Test (Figure 3D; Mean diff = 43.19, $p < 0.0001$, and Mean diff = 35.43, $p = 0.0002$, respectively). No significant differences in absolute fluorescence were observed among groups after ADP addition (StateIII). Uncoupler addition (FCCP) ($StateIII_U$) resulted in reduced variation of $\Delta\Box_m$ in Nand compared to Veh (Figure 3D; Mean diff = 20.61, $p = 0.03$). Addition of sodium cyanide (CN) completely dissipated the $\Delta\Box_m$.

The present results indicate that in comparison to Veh and Test, Nand caused more prominent disruption in the $\Delta\Box_m$ dynamics (formation and dissipation) in both liver and heart and further, Test sustained the $\Delta\Box_m$ dynamics at level of controls.

3.5. Nand decreases the mitochondrial oxygen consumption rates and ATP synthesis in the liver but not in the heart

A normal $\Delta\psi_m$ dynamics is a vital component to the mitochondrial electron transport chain and ATP production via the oxidative phosphorylation in the Complex V [22], [23]. We further explored the effects of AAS in the bioenergetic responses of mitochondria from heart and liver. Assessment of mitochondrial oxygen consumption rate (OCR) in the heart (Figure 4A) showed no difference in the coupling states (IV, III and ROX), resulting in no significant changes in the oxidative phosphorylation coupling efficiency (OxPHOS) (Figure 4B).

However, Nand and Test reduced liver mitochondrial OCR in the respiratory State III (Figure 4C; Mean diff = 3.67.5, p = 0.01, and Mean diff = 3.80, p = 0.007,

respectively); however only Nand implicated in reduced oxidative phosphorylation coupling efficiency (Figure 4D; Mean diff = 0.31, p = 0.005, and Mean diff = 0.22, p = 0.048, respectively). Although, heart and liver displayed impaired mitochondrial $Ca^{2+}$ handling and $\Delta\Psi_m$ dynamics due to Nand, these alterations do not impact oxygen consumption in hepatic tissue.

3.6. Test and Nand increase mitochondrial hydrogen peroxide ($H_2O_2$) production in heart and liver tissues.

In the heart, Nand and Test significantly increased $H_2O_2$ levels relative to Veh (Figure 5A) in all coupling states ($p < 0.001$). Similarly, Nand and Test increased liver mitochondrial $H_2O_2$ levels in all coupling states (Figure 5B) relative to VEH group ($p < 0.001$). Further, the effect of Nand was significantly higher than Test.

3.7. Nand increases oxidative damage biomarkers in the heart and liver

Relative to Veh and Test, Nand significantly increased total ROS (Figure 6A; Mean diff = 36.33, p = 0.014 and Mean diff = 37.02, p = 0.025), TBARS (Figure 6B; Mean diff = 0.27, p = 0.05 and Mean diff = 0.38, p = 0.001) and protein carbonyls (Figure 6C; Mean diff = 1.187, p = 0.038 and Mean diff = 1.362, p = 0.021) in the heart. In addition, Nand decreased sulfhydryl levels (Figure 6D) in relation to Veh and Test (Mean diff = 21.42, p = 0.036 and Mean diff = 25.3, p = 0.020).

In the liver, Nand increased total ROS levels (Figure 6E; Mean diff = 30.92, p = 0.009) and TBARS (Figure 6F; Mean diff = 1.35, p = 0.01). There were no significant differences between groups regarding the protein carbonyls (Figure 6G), while levels of sulfhydryl groups decreased in Nand group (Mean diff = 40.2, p = 0.0005 and Mean diff = 29.42, p = 0.008) (Figure 6H).

3.8. Nand and Test modulates glutathione metabolism

In the heart tissue, both Test and Nand significantly decreased the reduced form (GSH) (Figure 7A; Mean diff = 10.01, p = 0.005 and Mean diff = 9.04, p = 0.01) and the oxidized form of glutathione (GSSG) relative to Veh (Figure 7B; Mean diff = 2.34, p = 0.038 and Mean diff = 2.25, p = 0.029). However, the GSH:GSSG ratio was only decreased in Nand group (Figure 7C; Mean diff = 0.99, p = 0.02).

Similar effects were observed in the liver tissue, as both Test and Nand decreased GSH (Figure 7D; Mean diff = 25.25, p = 0.0002 and Mean diff = 17.45, p = 0.008) and GSSG (Figure 7E; Mean diff = 4.42, p = 0.011 and Mean diff = 3.38, p = 0.004) compared to Veh. However, Nand displayed a significant decrease in the GSH:GSSG ratio relative to Veh and Test (Figure 7F; Mean diff = 1.49, p = 0.018 and Mean diff = 1.39, p = 0.028, respectively).

3.9. Exposure to Nand and Test affects antioxidant enzymes activity in heart and liver

Nand and Test did not lead to altered activity of SOD in both heart (Figure 8A) and liver (Figure 8D). Furthermore, treatment with Nand was capable of reducing CAT activity in the heart (Figure 8 B; Mean diff = 2.442, p = 0.001 and Mean diff = 1.73, p = 0.023, respectively) while no alterations were observed in the liver. Nand and Test reduced the activity of GP*x* in the heart (Figure 8C; Mean diff = 6.73, p = 0.004 and Mean diff = 6.08, p = 0.012), and liver tissues (Figure 8F; Mean diff = 67.43, p = 0.002 and Mean diff = 47.93, p = 0.023).

## 4. Discussion

In this study, we looked for AAS-specific effects in particular components of the mitochondrial machinery that impacts ATP and ROS production. The results showed that supraphysiological doses of Nand and Test, two widely used AAS drugs in the field of sports, caused a distinct impact on mitochondria of the heart and liver. However, Nand produced the highest setting of undesirable effects, albeit were not correlated with marked histopathological damage.

AAS exert their cellular effects through binding to the androgen (AR) or estrogen receptors (ER) that are also expressed in mitochondria. Primarily, the enzyme 5-alpha reductase converts testosterone to dihydrotestosterone (DHT), which binds to the AR with a higher affinity compared to Test meanwhile aromatase enzyme converts Test to estradiol. Nand has higher anabolic compared to androgenic effects, and is also a substrate for 5-alpha reductase albeit its metabolite has weaker AR affinity [34], [35]. However, AAS abusers often combine different hormones, which makes difficult to establish individual drug toxicity to a specific organ [36]. It is important to notice that Test and Nand are FDA approved drugs with potentialities that were not exhausted yet as recent clinical trials are exploring the benefits of Test against neurodegenerative disorders and aged-associated cognitive decline [37], [38], [39] implying that a better understanding in terms of tissue-specific toxicology is still necessary.

A common effect showed by Nand and Test was the increased physical performance observed in non-exercise trained mice. Indeed, previous studies showed that AAS increases the tolerance to fatigue in exercise tests suggesting improved skeletal muscle strength [40], [41]. We also confirm that Test does not significantly affected body weight.

The absence of weight loss and symptoms of locomotor deficits paralleled with apparently normal histopathological examination by haematoxylin and eosin staining. Our result is opposed to several reports indicating Nand induced myocyte hypertrophy and increased matrix collagen deposition culminating in cardiac remodeling and subsequent cardiac injury [42], [43], [44]. These histopathological alterations are intimately dependent on higher doses and prolonged exposure [45], [46]; however, early-onset biochemical alterations serving as substrates for the initiation and/or progression of tissues injury may have been missed by these studies. In similar fashion, there were no abnormalities in the liver tissue, which is conflicting with the findings reported with methylandrostanolone and stazonol [47], [48]. However, others have shown that rodents treated with Test displayed normal hepatic morphology along with hepatocytes organized in cellular cords surrounded by sinusoidal capillaries with narrow lumens, strengthening the idea that tissue-specific histopathological toxicity depends on type of AAS, duration, and drug regimen [49], [50]. Moreover, a previous work of our group confirmed that 19-days of Nand administration heightened aggressive behavior mechanistic linked with increased glutamatergic excitability. These changes were not accompanied by alterations in blood markers of liver damage or spatial memory deficits [15].[20] Thus, the lack of pronounced histopathological tissue abnormalities showed here reinforce the need of searching for sensitive and tissue specific biochemical mechanisms in the prodromal phase of the heart and liver damage.

Based on this, we look for perturbations in the oxidative metabolism, once mitochondria are very sensitive to environmental changes and finely tuning energy requirements of the cells with ATP synthesis, in response to hormones and ionic

messengers [51]. Numerous studies have demonstrated that in response to AAS administration, the intracellular $Ca^{2+}$ levels increases, which may have detrimental or beneficial effects for the mitochondrial metabolism. The intramitochondrial $Ca^{2+}$ signals activate dehydrogenases enzymes thereby improving oxidative phosphorylation and redox balance. Remarkably, the mitochondrial $Ca^{2+}$ influx also affects the net charge across the mitochondrial internal membrane and $\Delta\psi_m$ depolarization [52], [53]. Further, disruptions of $\Delta\psi m$ dynamics due to impaired control of the $Ca^{2+}$ influx/efflux may disrupt ATP synthesis and serve as intrinsic apoptotic stimuli [54]. Our results indicated that Nand impaired the mitochondrial $Ca^{2+}$ influx and $\Delta\psi_m$ dynamics (formation and dissipation) in the heart and liver mitochondria. This provides additional evidence for the role of androgen receptors in mediating toxic effects of Nand via a deficient $Ca^{2+}$ influx; meanwhile the efflux via Na+ dependent NCLX is normal [55].

Given the functional proximity between $Ca^{2+}$ handling, $\Delta\psi_m$, and the activity of oxidative complexes activity and $F_1F_O$-ATP synthase, we challenged mitochondrial metabolism in a high-resolution respiratometric analysis protocol. In cardiac tissue, no significant alterations were found in the OCR or oxidative phosphorylation coupling efficiency, which provides the degree of metabolic coupling between ETS and oxidative phosphorylation by the $F_1F_O$-ATP synthase [18]. However, State III OCR was significantly impaired in the liver mitochondria in response to both Nand and Test, culminating in decreased OxPHOS coupling efficiency. These results support the decrease ETS enzymes activity of the liver mitochondria reported after stanozolol treatment [7], and provides further targets for mitotoxicity induced by AAS.

Oxidative stress is known to play a crucial role in the pathogenesis of several

heart and liver diseases, and is also potentially involved in both genomic and non-genomic actions of different AAS [56], [57], [58]. Classically, uncoupling between mitochondrial ETS and OxPHOS is considered an abundant source of reactive oxygen species (ROS), like the $H_2O_2$, which is also mechanistic linked with $\Delta\psi m$ [59]. In the present study we demonstrated that both Nand and Test increase mitochondrial $H_2O_2$ production in the liver and heart, albeit the increment induced by Test displayed a lower magnitude. In the heart, the increase in the $H_2O_2$ level was not associated with deficient oxidative phosphorylation, suggesting a compensatory mechanism at a cost of high rates of oxygen consumption (see Figure 4A). In agreement with this conjecture, the mitochondrial $H_2O_2$ production was also higher in the heart compared to liver.

As a response to increased ROS levels the enzymatic and non-enzymatic antioxidant defenses are employed to prevent and limit the initiation and propagation of free radical chain reactions, and hence, the tissue damage [51]. We found that the activity of the enzyme GP*x* that metabolizes $H_2O_2$ to $H_2O$ was decreased by Nand and Test, albeit the balance of GP*x* coactivator (GSH/GSSG ratio) was decreased only due to Nand administration (see Figures 7C and F, and 8C and F). Thus, it seems that impaired activity of both GP*x* and CAT induced by Nand in the heart contributes to the more pronounced $H_2O_2$ levels and total ROS, coupled with oxidative damage to membranes (TBARS) and proteins (Carbonyls).

Several studies report redox imbalance induced by AAS treatment, suggesting distinct and different patterns of systemic or local redox response according to the substance investigated [60], [61]. Recent data support a cardioprotective effect induced by Test in both *in vivo* and *in vitro* models of cardiac injury [62], [63] contrary to evidences of

detrimental effects exerted by Nand [64]. Test deprivation has been shown to negatively affect cardiovascular function and Nand administration was associated with suppressed Test production [8], [65]. Therefore, the observed effects in mitochondrial metabolism could be partially explained by the different metabolism of these compounds, as Nand binds to androgen receptors with a greater binding affinity compared to testosterone, and with an increased anabolic, or myotrophic, activity rate compared to its androgenic activity [66]. Additionally, the low 5-alpha reductase activity in the heart suggests that both, the decrease in endogenous testosterone production and ND binding to the AR could directly or indirectly impact mitochondrial machinery [35]. Actually, we demonstrated that Nand increased oxidative damage, along with detrimental effects in the antioxidant system, which is consistent with previous reports [64], [67]. However, we do not found oxidative damage to the heart caused by Test, thereby adding controversy to the literature about the time and dose-effects on this tissue [68].

Therefore, supraphysiological doses of Nand, and in lower extension Test, impaired mitochondrial $Ca^{2+}$ handling, $\Delta\psi m$ dynamics and ATP synthesis, which was associated with perturbations in the redox homeostasis. Since there was no clear histopathological damage we conclude that impairment oxidative energy support and redox imbalance precedes structural damage to the heart and liver.

**Acknowledgements**

This work was supported by the Brazilian grants of Conselho Nacional de Desenvolvimento Científico e Tecnológico (CNPq) #426796/2016-0 and 141100/2013-3, CNPq-Instituto Nacional de Neurociência Translacional-INNT #465346/2014-6,

FAPERGS/PRONEX#16/2551-0000499-4 and also by the Conselho de Aperfeiçoamento de Pessoal de Nível Superior (CAPES) #1663.

**References**

[1] H.G. Pope, Jr., R.I. Wood, A. Rogol, F. Nyberg, L. Bowers, S. Bhasin, Adverse health consequences of performance-enhancing drugs: an Endocrine Society scientific statement, Endocrine reviews, 35 (2014) 341-375.

[2] A.L. Baggish, R.B. Weiner, G. Kanayama, J.I. Hudson, M.H. Picard, A.M. Hutter, Jr., H.G. Pope, Jr., Long-term anabolic-androgenic steroid use is associated with left ventricular dysfunction, Circulation Heart Failure, 3 (2010) 472-476.

[3] KL Soe, M Soe, C Gluud, Liver pathology associated with the use of anabolic-androgenic steroid, Liver, 12 (1992) 73-79.

[4] E. Nieschlag, E. Vorona, Doping with anabolic androgenic steroids (AAS): Adverse effects on non-reproductive organs and functions, Reviews in Endocrine and Metabolic Disorders, 16 (2015) 199-211.

[5] S.P. Frankenfeld, L.P. Oliveira, V.H. Ortenzi, I.C.C. Rego-Monteiro, E.A. Chaves, A.C. Ferreira, A.C. Leitão, D.P. Carvalho, R.S. Fortunato, The Anabolic Androgenic Steroid Nandrolone Decanoate Disrupts Redox Homeostasis in Liver, Heart and Kidney of Male Wistar Rats, PLoS ONE, 9 (2014) e102699.

[6] E. Sadowska-Krepa, B. Klapcinska, S. Jagsz, A. Nowara, I. Szoltysek-Boldys, M. Chalimoniuk, J. Langfort, S.J. Chrapusta, High-dose testosterone enanthate

supplementation boosts oxidative stress, but exerts little effect on the antioxidant barrier in sedentary adolescent male rat liver, Pharmacological reports: PR, 69 (2017) 673-678.

[7] F. Molano, A. Saborido, J. Delgado, M. Moran, A. Megias, Rat liver lysosomal and mitochondrial activities are modified by anabolic-androgenic steroids, Medicine and science in sports and exercise, 31 (1999) 243-250.

[8] W. Pongkan, S.C. Chattipakorn, N. Chattipakorn, Chronic testosterone replacement exerts cardioprotection against cardiac ischemia-reperfusion injury by attenuating mitochondrial dysfunction in testosterone-deprived rats, PloS one, 10 (2015) e0122503.

[9] C. Garcia-Ruiz, J.C. Fernandez-Checa, Mitochondrial Oxidative Stress and Antioxidants Balance in Fatty Liver Disease, Hepatology communications, 2 (2018) 1425-1439.

[10] D.A. Brown, J.B. Perry, M.E. Allen, H.N. Sabbah, B.L. Stauffer, S.R. Shaikh, J.G.F. Cleland, W.S. Colucci, J. Butler, A.A. Voors, S.D. Anker, B. Pitt, B. Pieske, G. Filippatos, S.J. Greene, M. Gheorghiade, Mitochondrial function as a therapeutic target in heart failure, Nature reviews. Cardiology, 14 (2017) 238-250.

[11] J. Rieusset, Endoplasmic reticulum-mitochondria calcium signaling in hepatic metabolic diseases, Biochimica et Biophysica Acta (BBA) - Molecular Cell Research, 1864 (2017) 865-876.

[12] M.S. Jafri, R. Kumar, Modeling Mitochondrial Function and Its Role in Disease, Progress in molecular biology and translational science, 123 (2014) 103-125.

[13] B. Kim, S. Matsuoka, Cytoplasmic Na+-dependent modulation of mitochondrial Ca2+ via electrogenic mitochondrial Na+-Ca2+ exchange, J Physiol 586 (2008) 1683-1697.

[14] E.A. Schon, S. Przedborski, Mitochondria: the next (neurode)generation, Neuron, 70 (2011) 1033-1053.

[15] E. Kalinine, E.R. Zimmer, K.C. Zenki, I. Kalinine, V. Kazlauckas, C.B. Haas, G. Hansel, A.R. Zimmer, D.O. Souza, A.P. Muller, L.V. Portela, Nandrolone-induced aggressive behavior is associated with alterations in extracellular glutamate homeostasis in mice, Hormones and behavior, 66 (2014) 383-392.

[16] K.R. Bonson, R.G. Johnson, D. Fiorella, R.A. Rabin, J.C. Winter. Serotonergic control of androgen-induced dominance, Pharmacol biochemical behavior, 49 (1994) 313-322.

[17] A.H. Fischer, K.A. Jacobson, J. Rose, R. Zeller, Hematoxylin and eosin staining of tissue and cell sections, CSH protocols, 2008 (2008) pdb.prot4986.

[18] E. Gnaiger, Mitochondrial pathways and respiratory control. An introduction to OXPHOS analysis. , 4th ed., OROBOROS MiPNet Publications, Innsbruck, 2014.

[19] J. Burtscher, L. Zangrandi, C. Schwarzer, E. Gnaiger, Differences in mitochondrial function in homogenated samples from healthy and epileptic specific brain tissues revealed by high-resolution respirometry, Mitochondrion, 25 (2015) 104-112.

[20] O.H. Lowry, N.J. Rosebrough, A.L. Farr, R.J. Randall, Protein measurement with the Folin phenol reagent, The Journal of biological chemistry, 193 (1951) 265-275.

[21] T.S. Luongo, J.P. Lambert, P. Gross, M. Nwokedi, A.A. Lombardi, S. Shanmughapriya, A.C. Carpenter, D. Kolmetzky, E. Gao, J.H. van Berlo, E.J. Tsai, J.D. Molkentin, X. Chen, M. Madesh, S.R. Houser, J.W. Elrod, The mitochondrial Na(+)/Ca(2+) exchanger is essential for Ca(2+) homeostasis and viability, Nature 545 (2017) 93-97.

[22] L.V. Portela, A.W. Brochier, C.B. Haas, A.K. de Carvalho, J.A. Gnoato, E.R. Zimmer, E. Kalinine, L. Pellerin, A.P. Muller, Hyperpalatable Diet and Physical Exercise Modulate the Expression of the Glial Monocarboxylate Transporters MCT1 and 4, Mol neurobiology, 54 (2017) 5807-5814.

[23] E. Gnaiger, Mitochondrial pathways and respiratory control. An introduction to OXPHOS analysis. , 4th ed., OROBOROS MiPNet Publications, Innsbruck, 2014.

[24] A.P. Muller, C.B. Haas, J. Camacho-Pereira, A.W. Brochier, J. Gnoatto, E.R. Zimmer, D.O. Souza, A. Galina, L.V. Portela, Insulin prevents mitochondrial generation of $H_2O_2$ in rat brain, Experimental neurology, 247 (2013) 66-72.

[25] C.P. LeBel, H. Ischiropoulos, S.C. Bondy, Evaluation of the probe 2',7'-dichlorofluorescin as an indicator of reactive oxygen species formation and oxidative stress, Chemical research in toxicology, 5 (1992) 227-231.

[26] H. Ohkawa, N. Ohishi, K. Yagi, Assay for lipid peroxides in animal tissues by thiobarbituric acid reaction, Analytical biochemistry, 95 (1979) 351-358.

[27] A.Z. Reznick, L. Packer, Oxidative damage to proteins: spectrophotometric method for carbonyl assay, Methods in enzymology, 233 (1994) 357-363.

[28] M.Y. Aksenov, W.R. Markesbery, Changes in thiol content and expression of glutathione redox system genes in the hippocampus and cerebellum in Alzheimer's disease, Neuroscience letters, 302 (2001) 141-145.

[29] P.J. Hissin, R. Hilf, A fluorometric method for determination of oxidized and reduced glutathione in tissues, Analytical biochemistry, 74 (1976) 214-226.

[30] S.L. Marklund, Pyrogallol autoxidation, CRC Press Inc., Boca Raton, 1985.

[31] H. Aebi, Catalase in vitro, Methods in enzymology, 105 (1984) 121-126.

[32] A. Wendel, Glutathione peroxidase, Methods in enzymology, 77 (1981) 325-333.

[33] P. Bond, W. Llewellyn, P. Van Mol, Anabolic androgenic steroid-induced hepatotoxicity, Medical hypotheses, 93 (2016) 150-153.

[34] K. Sundaram, N. Kumar, C. Monder, C.W. Bardin, Different patterns of metabolism determine the relative anabolic activity of 19-norandrogens, The Journal of steroid biochemistry and molecular biology, 53 (1995) 253-257.

[35] E.W. Bergink, P.S.L. Janssen, E.W. Turpun, J. Van Der Vies, Comparison of the receptor binding properties of nandrolone and testosterone under in vitro and in vivo conditions, Journal of Steroid Biochemistry, 22 (1985) 831-836.

[36] J.G. Oberlander, L.P. Henderson, The Sturm und Drang of anabolic steroid use: angst, anxiety, and aggression, Trends in neurosciences, 35 (2012) 382-392.

[37] P. Pantziarka, M. Pirmohamed, N. Mirza, New uses for old drugs, BMJ, 361 (2018).

[38] O. Beauchet, Testosterone and cognitive function: current clinical evidence of a relationship, European journal of endocrinology, 155 (2006) 773-781.

[39] V.A. Giagulli, E. Guastamacchia, B. Licchelli, V. Triggiani, Serum Testosterone and Cognitive Function in Ageing Male: Updating the Evidence, Recent patents on endocrine, metabolic & immune drug discovery, 10 (2016) 22-30.

[40] T. Tamaki, S. Uchiyama, Y. Uchiyama, A. Akatsuka, R.R. Roy, V.R. Edgerton, Anabolic steroids increase exercise tolerance, American Journal of Physiology-Endocrinology and Metabolism, 280 (2001) E973-E981.

[41] C.G. Van Zyl, T.D. Noakes, M.I. Lambert, Anabolic-androgenic steroid increases running endurance in rats, Medicine and science in sports and exercise, 27 (1995) 1385-1389.

[42] P. Frati, F.P. Busardo, L. Cipolloni, E.D. Dominicis, V. Fineschi, Anabolic Androgenic Steroid (AAS) related deaths: autoptic, histopathological and toxicological findings, Current neuropharmacology, 13 (2015) 146-159.

[43] M. Montisci, R. El Mazloum, G. Cecchetto, C. Terranova, S.D. Ferrara, G. Thiene, C. Basso, Anabolic androgenic steroids abuse and cardiac death in athletes: morphological and toxicological findings in four fatal cases, Forensic science international, 217 (2012) e13-18.

[44] J.V. Franquni, A.M. do Nascimento, E.M. de Lima, G.A. Brasil, O.A. Heringer, K.O. Cassaro, T.V. da Cunha, C. Musso, M.C. Silva Santos, I.C. Kalil, D.C. Endringer, G.A. Boechat, N.S. Bissoli, T.U. de Andrade, Nandrolone decanoate determines cardiac remodelling and injury by an imbalance in cardiac inflammatory cytokines and ACE activity, blunting of the Bezold-Jarisch reflex, resulting in the development of hypertension, Steroids, 78 (2013) 379-385.

[45] E. Emer, O. Yildiz, M. Seyrek, S. Demirkol, T. Topal, B. Kurt, A. Sayal, High-dose testosterone and dehydroepiandrosterone induce cardiotoxicity in rats: Assessment of echocardiographic, morphologic, and oxidative stress parameters, Human & experimental toxicology, 35 (2016) 562-572.

[46] A. Bueno, F.B. Carvalho, J.M. Gutierres, C. Lhamas, C.M. Andrade, A comparative study of the effect of the dose and exposure duration of anabolic androgenic steroids on behavior, cholinergic regulation, and oxidative stress in rats, PLoS ONE, 12 (2017).

[47] L.D. Boada, M. Zumbado, S. Torres, A. Lopez, B.N. Diaz-Chico, J.J. Cabrera, O.P. Luzardo, Evaluation of acute and chronic hepatotoxic effects exerted by anabolic-

androgenic steroid stanozolol in adult male rats, Archives of toxicology, 73 (1999) 465-472.

[48] A. Saborido, F. Molano, A. Megias, Effect of training and anabolic-androgenic steroids on drug metabolism in rat liver, Medicine and science in sports and exercise, 25 (1993) 815-822.

[49] J.D.B. Santos, A.A.S. Mendonça, R.C. Sousa, T.G.S. Silva, S.M. Bigonha, E.C. Santos, R.V. Gonçalves, R.D. Novaes, Food-drug interaction: Anabolic steroids aggravate hepatic lipotoxicity and nonalcoholic fatty liver disease induced by trans fatty acids, Food and Chemical Toxicology, 116 (2018) 360-368.

[50] G.H. Marquardt, C.I. Fisher, P. Levy, R.M. Dowben, Effect of anabolic steroids on liver function tests and creatine excretion, Jama, 175 (1961) 851-853.

[51] M. Schieber, N.S. Chandel, ROS function in redox signaling and oxidative stress, Current biology : CB, 24 (2014) R453-R462.

[52] L. Contreras, I. Drago, E. Zampese, T. Pozzan, Mitochondria: the calcium connection, Biochimica et biophysica acta, 1797 (2010) 607-618.

[53] M. Schieber, N.S. Chandel, ROS function in redox signaling and oxidative stress, Current biology : CB, 24 (2014) R453-R462.

[54] E. Gottlieb, S.M. Armour, M.H. Harris, C.B. Thompson, Mitochondrial membrane potential regulates matrix configuration and cytochrome c release during apoptosis, Cell death and differentiation, 10 (2003) 709-717.

[55] J.M. Vicencio, M. Estrada, D. Galvis, R. Bravo, A.E. Contreras, D. Rotter, G. Szabadkai, J.A. Hill, B.A. Rothermel, E. Jaimovich, S. Lavandero, Anabolic Androgenic

Steroids and Intracellular Calcium Signaling: A Mini Review on Mechanisms and Physiological Implications, Mini reviews in medicinal chemistry, 11 (2011) 390-398.

[56] H. Cichoż-Lach, A. Michalak, Oxidative stress as a crucial factor in liver diseases, World Journal of Gastroenterology : WJG, 20 (2014) 8082-8091.

[57] T. Münzel, G.G. Camici, C. Maack, N.R. Bonetti, V. Fuster, J.C. Kovacic, Impact of Oxidative Stress on the Heart and Vasculature, Journal of the American College of Cardiology, 70 (2017) 212.

[58] C.D. Foradori, M.J. Weiser, R.J. Handa, Non-genomic actions of androgens, Frontiers in neuroendocrinology, 29 (2008) 169-181.

[59] A.E. Vercesi, R.F. Castilho, A.J. Kowaltowski, H.C.F. de Oliveira, N.C. de Souza-Pinto, T.R. Figueira, E.N.B. Busanello, Mitochondrial calcium transport and the redox nature of the calcium-induced membrane permeability transition, Free Radical Biology and Medicine, 129 (2018) 1-24.

[60] I. Germanakis, K. Tsarouhas, P. Fragkiadaki, C. Tsitsimpikou, N. Goutzourelas, M.C. Champsas, D. Stagos, E. Rentoukas, A.M. Tsatsakis, Oxidative stress and myocardial dysfunction in young rabbits after short term anabolic steroids administration, Food and chemical toxicology : an international journal published for the British Industrial Biological Research Association, 61 (2013) 101-105.

[61] A. Pey, A. Saborido, I. Blazquez, J. Delgado, A. Megias, Effects of prolonged stanozolol treatment on antioxidant enzyme activities, oxidative stress markers, and heat shock protein HSP72 levels in rat liver, The Journal of steroid biochemistry and molecular biology, 87 (2003) 269-277.

[62] S. Tsang, J. Liu, T.M. Wong, Testosterone and cardioprotection against myocardial ischemia, Cardiovascular & hematological disorders drug targets, 7 (2007) 119-125.

[63] M. Wang, Y. Wang, A. Abarbanell, J. Tan, B. Weil, J. Herrmann, D.R. Meldrum, Both endogenous and exogenous testosterone decrease myocardial STAT3 activation and SOCS3 expression after acute ischemia and reperfusion, Surgery, 146 (2009) 138-144.

[64] F. Vasilaki, C. Tsitsimpikou, K. Tsarouhas, I. Germanakis, M. Tzardi, M. Kavvalakis, E. Ozcagli, D. Kouretas, A.M. Tsatsakis, Cardiotoxicity in rabbits after long-term nandrolone decanoate administration, Toxicology letters, 241 (2016) 143-151.

[65] C. Pomara, R. Barone, A. Marino Gammazza, C. Sangiorgi, F. Barone, A. Pitruzzella, N. Locorotondo, F. Di Gaudio, M. Salerno, F. Maglietta, A.L. Sarni, V. Di Felice, F. Cappello, E. Turillazzi, Effects of Nandrolone Stimulation on Testosterone Biosynthesis in Leydig Cells, Journal of cellular physiology, 231 (2016) 1385-1391.

[66] A.T. Kicman, Pharmacology of anabolic steroids, British journal of pharmacology, 154 (2008) 502-521.

[67] E.A. Chaves, P.P. Pereira-Junior, R.S. Fortunato, M.O. Masuda, A.C. de Carvalho, D.P. de Carvalho, M.F. Oliveira, J.H. Nascimento, Nandrolone decanoate impairs exercise-induced cardioprotection: role of antioxidant enzymes, The Journal of steroid biochemistry and molecular biology, 99 (2006) 223-230.

[68] E. Sadowska-Krępa, B. Kłapcińska, S. Jagsz, A. Sobczak, S.J. Chrapusta, M. Chalimoniuk, P. Grieb, S. Poprzęcki, J. Langfort, High-Dose Testosterone Propionate Treatment Reverses the Effects of Endurance Training on Myocardial Antioxidant Defenses in Adolescent Male Rats, Cardiovascular Toxicology, 11 (2011) 118-127.

**Figure captions**

**Figure 1. Experimental timeline, body weight and exercise performance.** The experimental design (A). The percentage of gain in body weight at day twenty relative to day one was significant higher in ND group (B). The maximal exercise capacity indicated by total time on running wheel (C) and distance run (D) were increased by Nand and Test. *Denotes significant difference compared to Veh; # denotes significant difference comparing Nand with Test (* and # $p < 0.05$).

**Figure 2. Histopathological analysis.** Multifocal and discrete vacuolization of hepatocytes in vehicle (Veh), nandrolone decanoate (Nand) and testosterone (Test) treated animals. Haematoxylin & Eosin, magnitude 400x.

**Figure 3. Mitocondrial $Ca^{2+}$ handling and mitochondrial membrane potential after Nandrolone decanoate (Nand) and testosterone (Test) administration.** Nand group displayed lower $Ca^{2+}$ uptake (swelling) by the heart (A) and liver (B). The extrusion of $Ca^{2+}$ (shrinkage) through the Na+ dependent channel (NCLX) was not affected in the heart (A) and liver (B). Nand also impaired the $\Delta\Psi_m$ dynamics (formation and dissipation) in heart (C) and liver (D), in different mitochondrial respiratory states equivalent to the activity of oxidative complexes I and II (State IV, PMGS), Complex V (State III, PMGS+ADP), Complex V Uncoupled (State $III_U$, PMGS+ADP+FCCP), and non-mitochondrial respiration (ROX, CN). P, Pyruvate; M, Malate; G, Glutamate; S, Succinate; FCCP, Carbonilcyanide p-triflouromethoxyphenylhydrazone. *Denotes significant difference compared to Veh; # denotes significant difference comparing Nand

with Test (* and # $p < 0.05$).

**Figure 4. Nandrolone decanoate (Nand) and Testosterone (Test) effect on mitochondrial ATP synthesis.** The oxygen consumption rate (OCR) in the State III respiration (F1FO ATP synthase Complex V activity) and oxidative phosphorylation coupling efficiency (OxPhos C.E.) were decreased in the liver (C and D) but not in the heart (A and B). *Denotes significant difference compared to Veh.

**Figure 5. Nandrolone decanoate (Nand) and Testosterone (Test) increases mitochondrial $H_2O_2$ production.** Nand and Test caused a prominent increase in mitochondrial $H_2O_2$ production in the heart (A) and liver (B) in relation to Veh. However, in comparison to Nand, Test group displayed a significant lower increment in the heart and liver. *Denotes significant difference compared to Veh; # denotes significant difference comparing Nand with Test (* and # $p < 0.05$).

**Figure 6. Nand increases oxidative damage biomarkers.** Nand but not Test significantly increased total ROS levels (A), TBARS (B), carbonyls (C) and decreased sulfhydryl groups (D) in the heart. Nand also increased ROS levels (E), TBARS (F), and decreased sulfhydryl groups in the liver (H), but not affected carbonyl levels (G). *Denotes significant difference compared to Veh; # denotes significant difference comparing Nand with Test (* and # $p < 0.05$).

**Figure 7. Nand and Test affect glutathione metabolism.** The levels of GSH (A and D), GSSH (B and E) were decreased by Nand and Test in the heart and liver, while the GSH:GSSH ratio (C and F) was maintained at level of Veh by Test in both tissues. *Denotes significant difference compared to Veh; # denotes significant difference comparing Nand with Test (* and # $p < 0.05$).

**Figure 8. Nand and Test selectively impacts the antioxidant enzymes activity in the heart and liver.** The activity of glutathione peroxidase (GPX) decreased similarly in the heart (C) and liver (F) due to both, Nand and Test administration. Only Nand significantly decreased CAT activity (B) in the heart tissue. SOD and CAT activities in the liver were not significantly affected by the treatments. SOD: Superoxide dismutase; CAT: catalase. *Denotes significant difference compared to Veh; # denotes significant difference comparing Nand with Test (* and # $p < 0.05$).

A

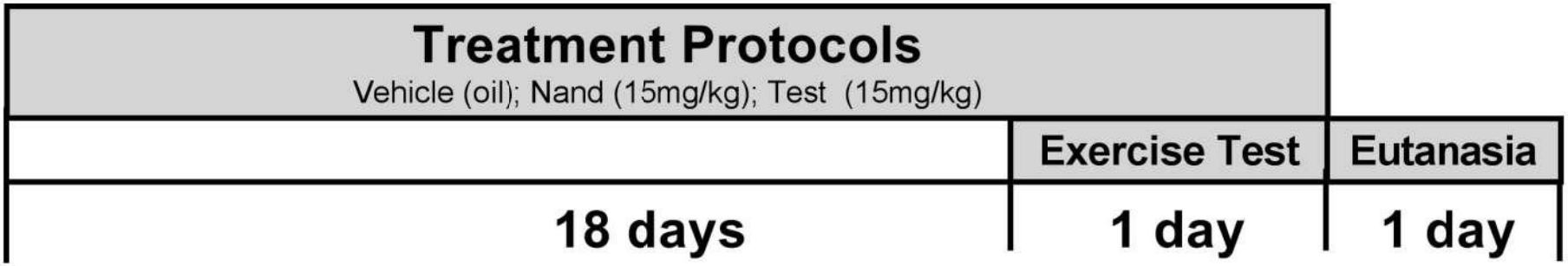
Treatment Protocols
Vehicle (oil); Nand (15mg/kg); Test (15mg/kg)
Exercise Test
Eutanasia
18 days
1 day
1 day

B

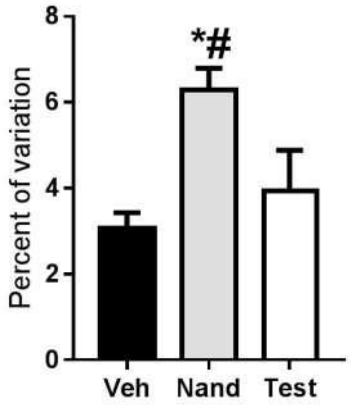
(%) Weight Change
Percent of variation
0
2
4
6
8
*#
Veh
Nand
Test

C

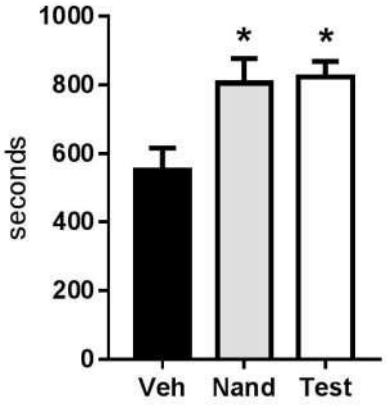
Exercise Total Time
seconds
0
200
400
600
800
1000
*
*
Veh
Nand
Test

D

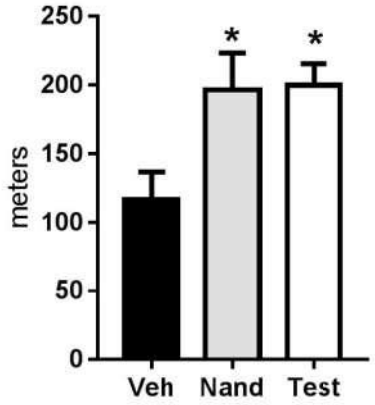
Exercise Total Distance
meters
0
50
100
150
200
250
*
*
Veh
Nand
Test

# HEART

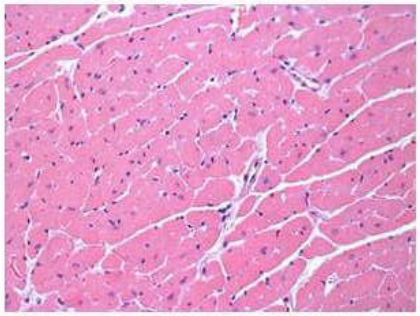

VEH

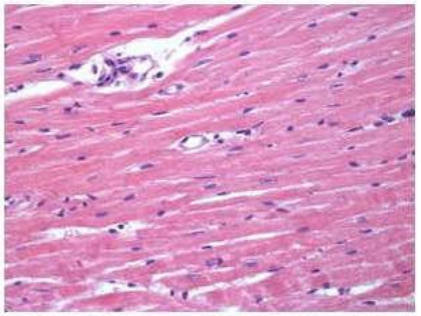

NAND

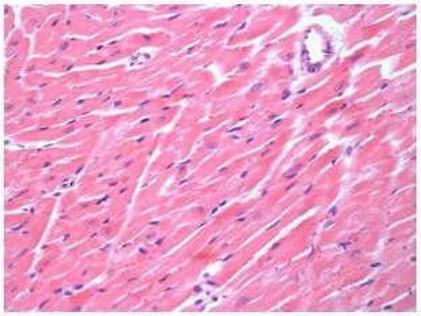

TEST

# LIVER

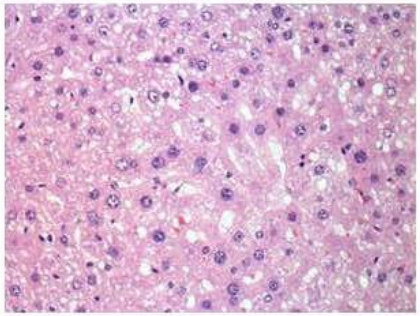

VEH

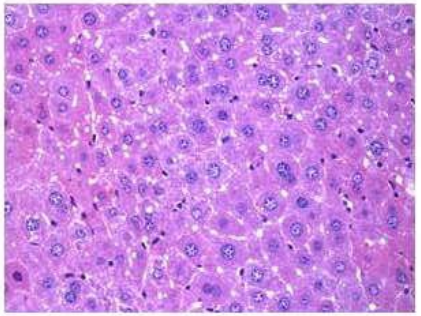

NAND

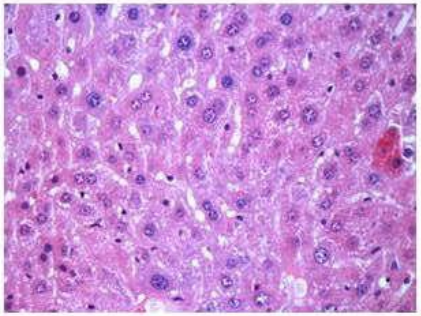

TEST

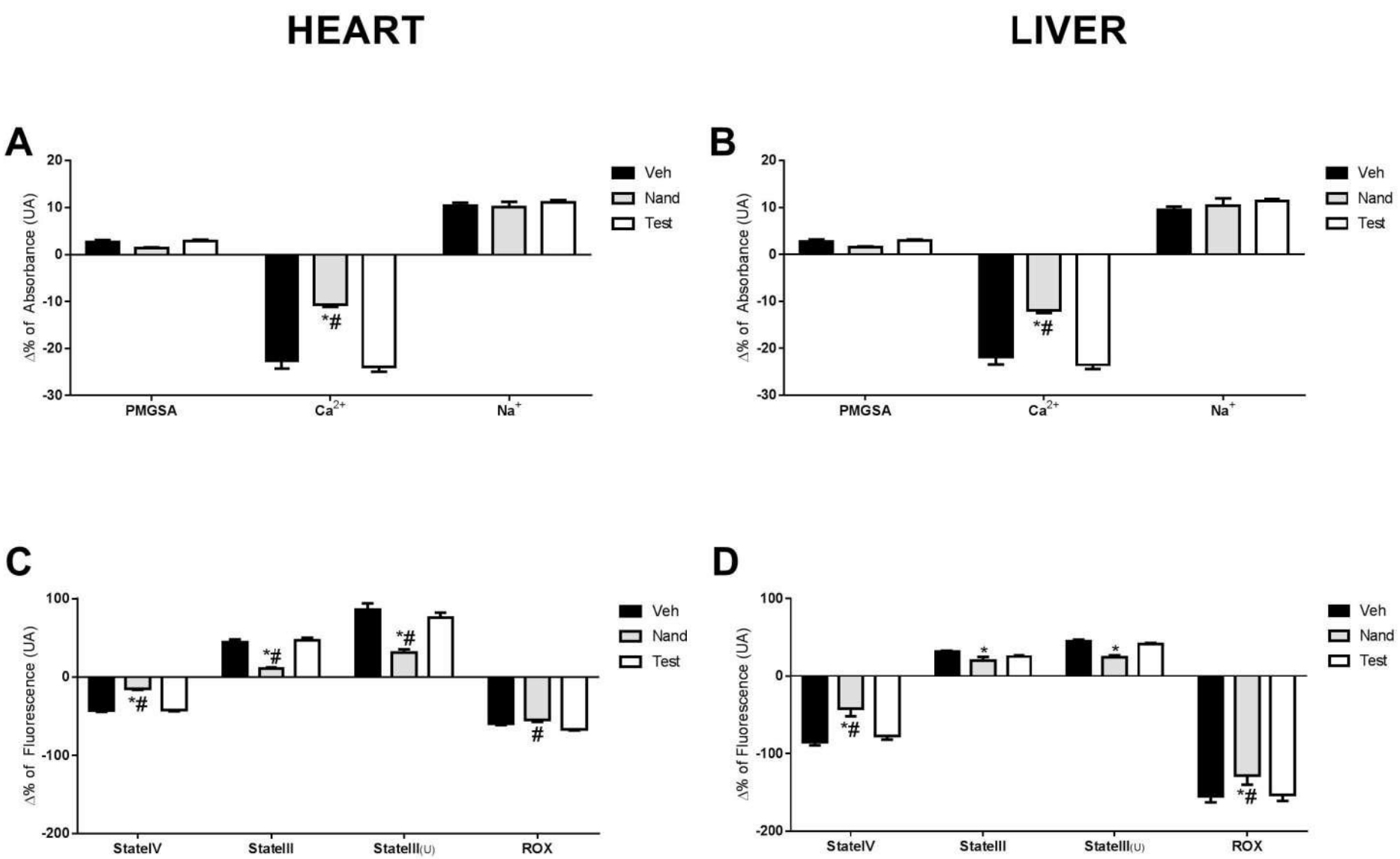
HEART
LIVER
A
B
C
D
Δ% of Absorbance (UA)
Δ% of Fluorescence (UA)
Veh
Nand
Test
PMGSA
Ca2+
Na+
StateIV
StateIII
StateIII(U)
ROX
*#
*
#

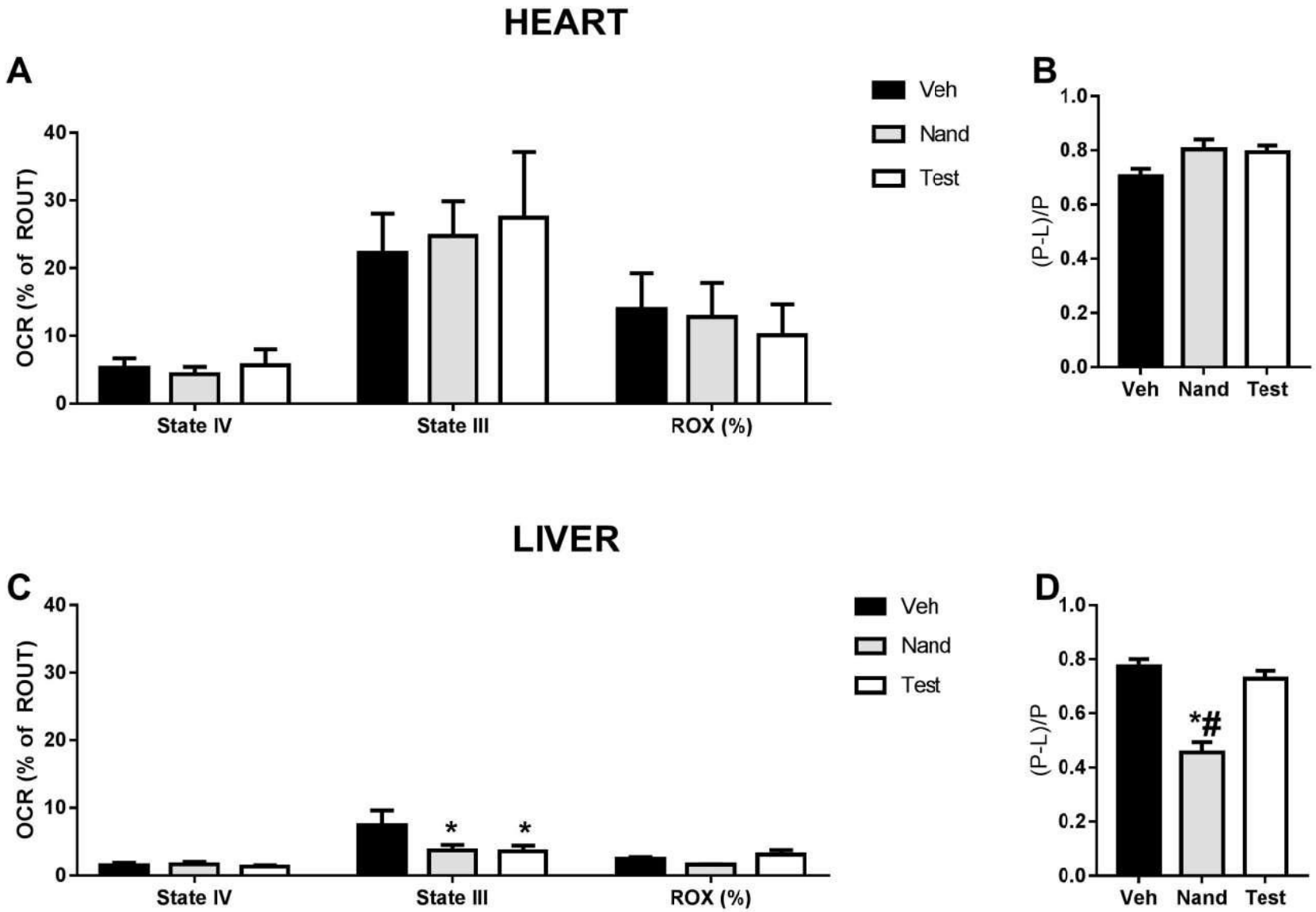
HEART
A
OCR (% of ROUT)
40
30
20
10
0
State IV
State III
ROX (%)
Veh
Nand
Test
B
(P-L)/P
1.0
0.8
0.6
0.4
0.2
0.0
Veh
Nand
Test
LIVER
C
OCR (% of ROUT)
40
30
20
10
0
*
*
State IV
State III
ROX (%)
Veh
Nand
Test
D
(P-L)/P
1.0
0.8
0.6
0.4
0.2
0.0
*#
Veh
Nand
Test

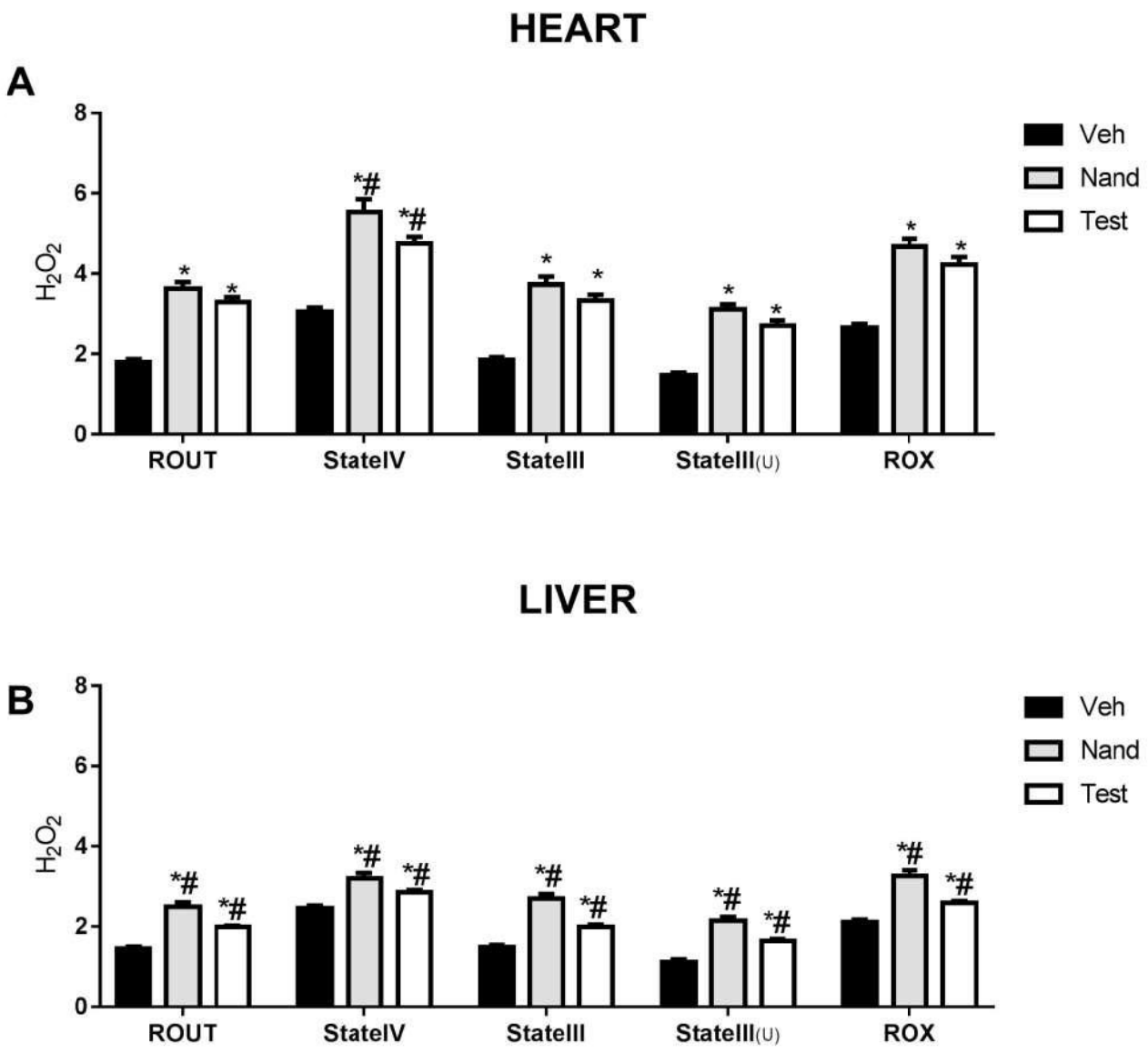
HEART
A
$H_2O_2$
0
2
4
6
8
ROUT
StateIV
StateIII
StateIII(U)
ROX
Veh
Nand
Test
LIVER
B
$H_2O_2$
0
2
4
6
8
ROUT
StateIV
StateIII
StateIII(U)
ROX
Veh
Nand
Test

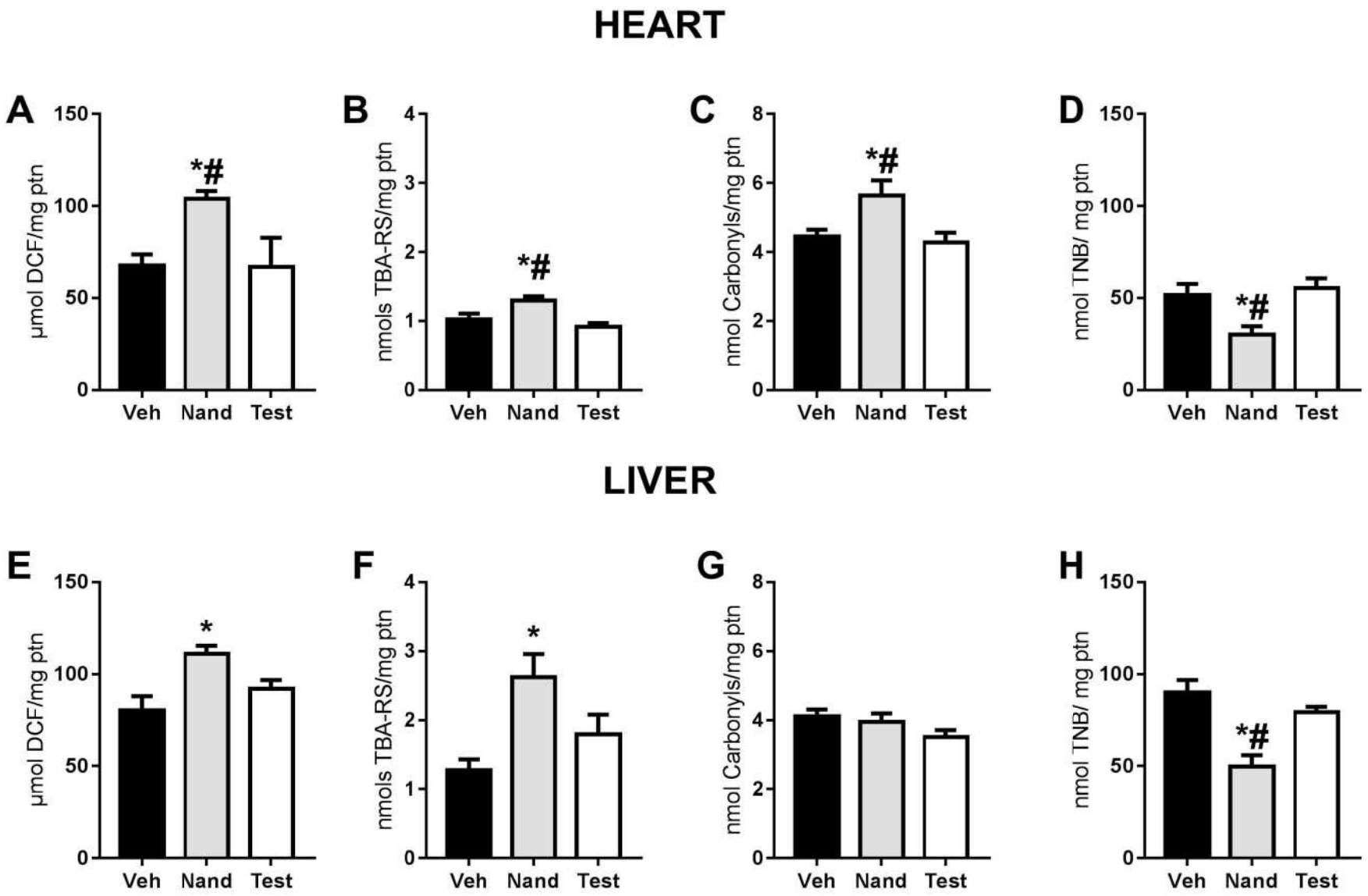
HEART
A
µmol DCF/mg ptn
150
100
50
0
*#
Veh
Nand
Test
B
nmols TBA-RS/mg ptn
4
3
2
1
0
*#
Veh
Nand
Test
C
nmol Carbonyls/mg ptn
8
6
4
2
0
*#
Veh
Nand
Test
D
nmol TNB/ mg ptn
150
100
50
0
*#
Veh
Nand
Test
LIVER
E
µmol DCF/mg ptn
150
100
50
0
*
Veh
Nand
Test
F
nmols TBA-RS/mg ptn
4
3
2
1
0
*
Veh
Nand
Test
G
nmol Carbonyls/mg ptn
8
6
4
2
0
Veh
Nand
Test
H
nmol TNB/ mg ptn
150
100
50
0
*#
Veh
Nand
Test

## HEART

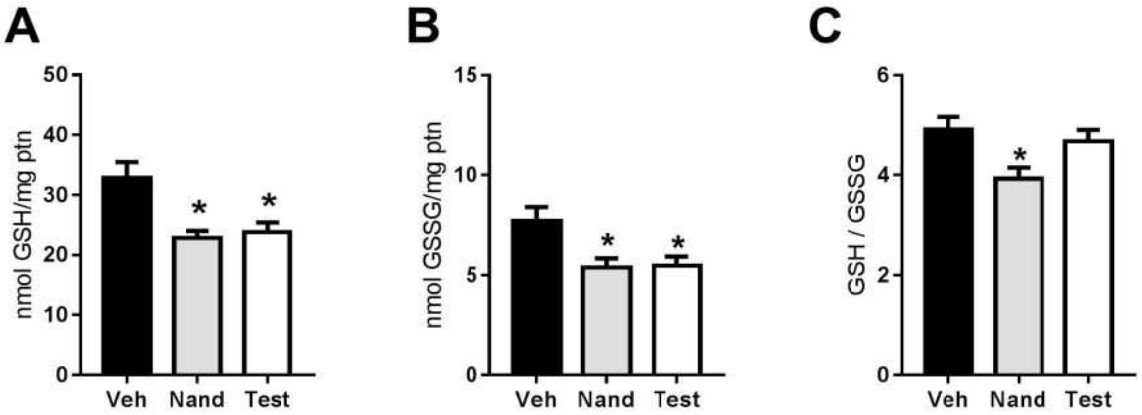
A
nmol GSH/mg ptn
50
40
30
20
10
0
Veh
Nand
Test
*
*
B
nmol GSSG/mg ptn
15
10
5
0
Veh
Nand
Test
*
*
C
GSH / GSSG
6
4
2
0
Veh
Nand
Test
*

## LIVER

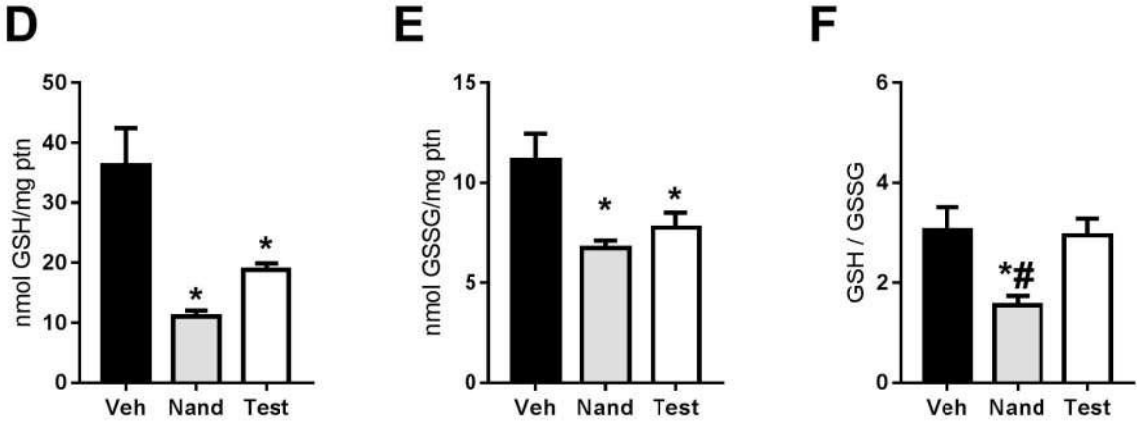
D
nmol GSH/mg ptn
50
40
30
20
10
0
Veh
Nand
Test
*
*
E
nmol GSSG/mg ptn
15
10
5
0
Veh
Nand
Test
*
*
F
GSH / GSSG
6
4
2
0
Veh
Nand
Test
*#

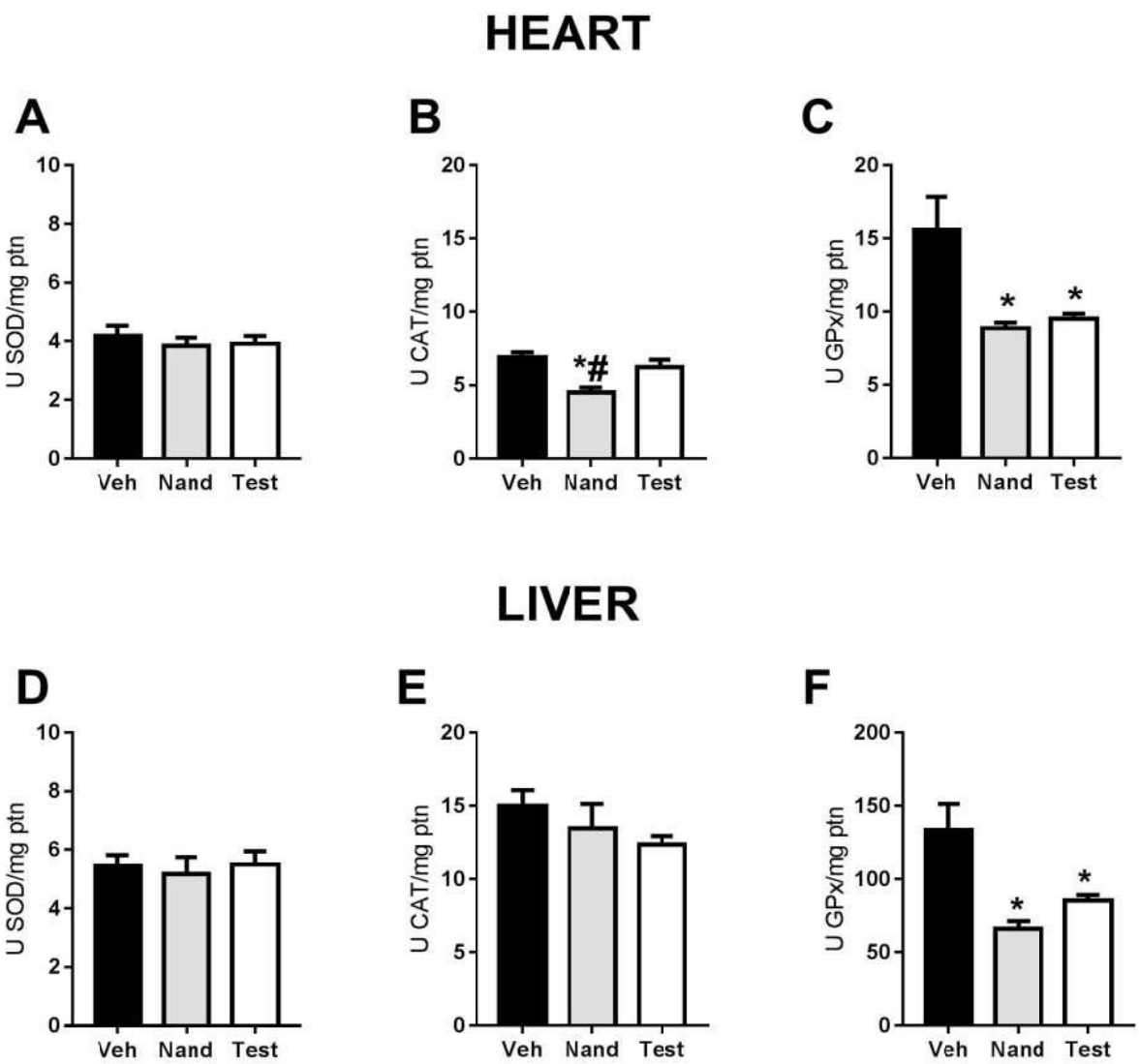
HEART
A
U SOD/mg ptn
10
8
6
4
2
0
Veh
Nand
Test
B
U CAT/mg ptn
20
15
10
5
0
*#
Veh
Nand
Test
C
U GPx/mg ptn
20
15
10
5
0
*
*
Veh
Nand
Test
LIVER
D
U SOD/mg ptn
10
8
6
4
2
0
Veh
Nand
Test
E
U CAT/mg ptn
20
15
10
5
0
Veh
Nand
Test
F
U GPx/mg ptn
200
150
100
50
0
*
*
Veh
Nand
Test

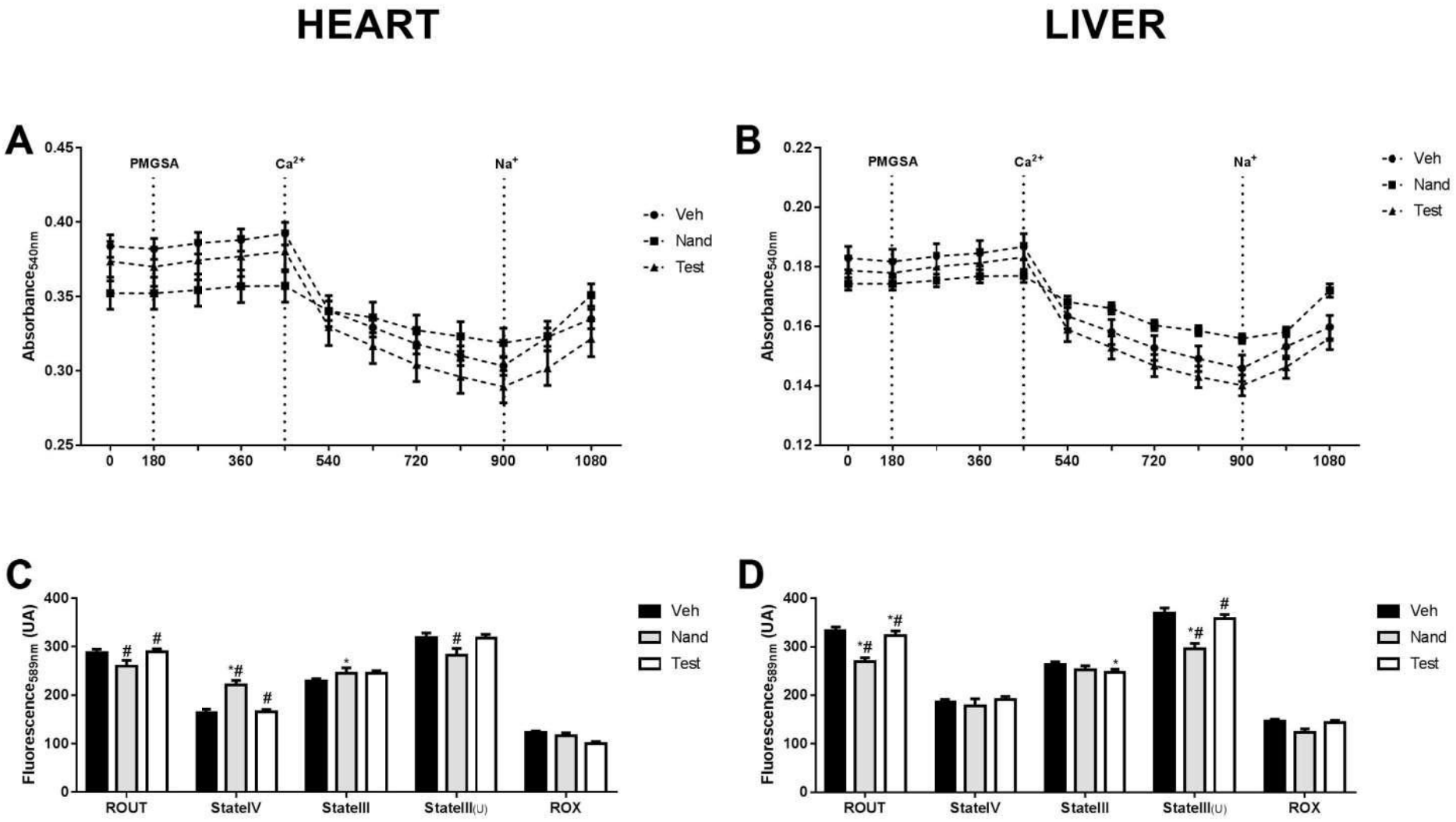
HEART
LIVER
A
B
C
D
PMGSA
Ca2+
Na+
Absorbance540nm
Fluorescence589nm (UA)
Veh
Nand
Test
ROUT
StateIV
StateIII
StateIII(U)
ROX

**Capítulo II:** *Anabolic androgen steroids effects on bioenergetics responsiveness of synaptic and extrasynaptic mitochondria.*

No capitulo II apresentamos o artigo publicado no periódico "*Toxicology Letters*".

No capítulo I evidenciamos que diferentes EAA induzem alterações distintas relacionadas ao metabolismo mitocondrial, regulação redox e homeostase de cálcio no coração e no fígado. No estudo presente, buscamos investigar as alterações induzidas por ambos EAA em populações específicas de mitocôndrias do sistema nervoso central (sináptica e extra sináptica), investigando a bioenergética, parâmetros redox, homeostase de cálcio expressão de Tau fosforilada e memória espacial.

Demonstramos que mitocôndrias sinápticas e extra sinápticas exibem uma resposta distinta aos esteroides anabolizantes. A nandrolona prejudicou a capacidade da mitocôndria de regular os níveis de cálcio e o potencial de membrana resultando em maior produção de peróxido de hidrogênio e também maior fosforilação de Tau, um indicador de neurodegenaração.

Os resultados obtidos reforçaram a aplicabilidade da TS para modular a atividade metabólica mitocondrial cerebral com uma aparente baixa toxicidade periférica. Considerando os efeitos secundários deletérios do TCE sobre o metabolismo cerebral, investimos em uma abordagem farmacológica com TS no TCE. Além disso, os efeitos deletérios da nandrolona na homeostase de cálcio e na fosforilação de proteína Tau abrem precedentes para investigações envolvendo outros mecanismos associados com neurodegeneração, embora no tempo avaliado não detectamos prejuízos na memória.


Title: Anabolic-androgen steroids effects on bioenergetics responsiveness of synaptic and extrasynaptic mitochondria

Authors: Randhall B. Carteri, Afonso Kopzynski, Lizia Nardi Menegassi, Marcelo Salimen Rodolphi, Nathan Ryzewski Strogulski, Luis Valmor Portela

PII: S0378-4274(19)30062-1
DOI: https://doi.org/10.1016/j.toxlet.2019.03.004
Reference: TOXLET 10430

To appear in: *Toxicology Letters*

Received date: 10 January 2019
Revised date: 5 March 2019
Accepted date: 7 March 2019

Please cite this article as: Carteri RB, Kopzynski A, Menegassi LN, Salimen Rodolphi M, Strogulski NR, Portela LV, Anabolic-androgen steroids effects on bioenergetics responsiveness of synaptic and extrasynaptic mitochondria, *Toxicology Letters* (2019), https://doi.org/10.1016/j.toxlet.2019.03.004

# Anabolic-androgen steroids effects on bioenergetics responsiveness of synaptic and extrasynaptic mitochondria

**Running title: Synaptic and extrasynaptic mitochondria bioenergetics**

Randhall B Carteri, *MSc*,[1] Afonso Kopzynski,[1] Lizia Nardi Menegassi,[1] Marcelo Salimen Rodolphi *MSc*,[1] Nathan Ryzewski Strogulski, *MSc*,[1] & Luis Valmor Portela, *PhD*[1*]

[1] Laboratório de Neurotrauma e Biomarcadores - Departamento de Bioquímica, Programa de Pós-Graduação em Bioquímica, ICBS, Universidade Federal do Rio Grande do Sul - UFRGS, Porto Alegre, RS, Brazil.

**Correspondent author:**

*** Dr. Luis V. Portela,**

Department of Biochemistry,

ICBS, UFRGS. Rua Ramiro Barcelos, 2600 anexo

90035-003, Porto Alegre, RS, Brazil.

Tel: 55 51 33085558; Fax: 55 51 33085544;

E-mail: roskaportela@gmail.com

## Highlights

- Synaptic and extrasynaptic mitochondria display distinct response to anabolic steroids
- Nandrolone impaired mitochondrial $Ca^{2+}$ control and membrane potential

- Nandrolone increased mitochondrial $H_2O_2$ production and Tau hypersphosphorylation
- Testosterone positively modulated mitochondrial bioenergetics respiratory outcomes
- Anabolic steroids did not impair spatial memory

**Abstract:**

**We hypothesized that supraphysiological administration of the anabolic-androgenic steroids (AAS) like testosterone (TEST) and nandrolone decanoate (NAND) might differentially affect synaptic and extrasynaptic components of mitochondrial bioenergetics, thereby resulting in memory impairment. Oil (VEH), NAND or TEST (15 mg/Kg) were daily administered to male CF-1 albino mice for 19-days. We evaluated in the synaptosomes and extrasynaptic mitochondria, Ca2+ influx/efflux, membrane potential ΔΨm, oxidative respiratory states, dehydrogenases activity, H2O2 production, Tau phosphorylation, and spatial memory in the Morris water maze (MWM). In synaptosomes, both AAS increased Ca2+influx and Na+ dependent efflux. In extrasynaptic mitochondria NAND increased the Ca2+influx. NAND prominently impaired ΔΨm formation and dissipation in synaptosomal and extrasynaptical mitochondria, while the effect of TEST was less pronounced. TEST increased the Reserve Respiratory Capacity in synaptosomes, and NAND decreased dehydrogenases activity in synaptic and extrasynaptic mitochondria. Also, NAND increased H2O2 production by synaptosomes and extrasynaptic mitochondria. NAND increased pTauSer396 in synaptosomes. Both AAS did not impair memory**

**performance on MWM. We highlight that high doses of NAND cause neurotoxic effects to components of synaptic and extrasynaptic mitochondrial bioenergetics, like calcium influx, membrane potential and H2O2 production. TEST was less neurotoxic to synaptic and extrasynaptic mitochondrial bioenergetics responses.**

**Keywords: Testosterone, nandrolone decanoate, synaptic, extrasynaptic, Ca2+ handling, mitochondrial bioenergetics, memory.**

## 1. Introduction

The anabolic-androgenic steroids (AAS) like testosterone (TEST) and nandrolone decanoate (NAND) are recognized for their potent trophic properties to the skeletal muscle (Phillis et al., 2007; Pozzi et al., 2013; Sundaram et al., 1995). However, both TEST and NAND easily cross from peripheral blood to the brain where their metabolism can occur in the hypothalamus, cortex, and hippocampus, areas of the brain implicated in emotional and cognitive process (Kalinine et al., 2014; Midzak et al., 2009; Wang and Stocco, 2005). It has been extensively demonstrated that hippocampal dendritic connectivity is critical for the neurochemical processes involved in memory formation, and even in the adulthood this brain region receives the influence of steroids to mediate mechanisms of memory (Geinisman et al., 2001; Kasai et al., 2003). Also, it should be considered that synaptic communication requires a massive energy support to maintain the electrochemical gradients, trafficking of synaptic vesicles and neurotransmitters recycling (Devine and Kittler, 2018; Volgyi et al., 2015). This brings to light the role of

mitochondria from the hippocampal synaptic terminals as a metabolic mediator of the effects of AAS, including in the memory processing (Oettinghaus et al., 2016).

Moreover, as a downstream effector of intracellular Ca2+, mitochondria responds in different manners depending on its synaptic or extrasynaptic locations, though its direct relationship with specific metabolic signatures leading to cell death or survival is a current matter of debate (Stauch et al., 2014; Volgyi et al., 2015; Yarana et al., 2012). The fast dynamics of neuronal firing and ionic flux across the synapses, implies that mitochondria should adapt itself to $Ca^{2+}$ waves and "read" the energy demands associated with neuronal activity. Thus, a transient mitochondrial $Ca^{2+}$ influx/efflux positively influences the membrane potential dynamics (formation and dissipation), activity of matrix dehydrogenases and oxidative complexes, ultimately increasing ATP synthesis (MacAskill et al., 2010). On opposite, deficient mitochondrial $Ca^{2+}$ regulation evokes energy dissipation coupled with exacerbated reactive oxygen production, thus impairing synaptic function (Devine and Kittler, 2018).

In this context, the mitochondrial $Ca^{2+}$ levels, membrane potential and oxidative complexes activity might have potential implications to both, the desired neurotrophic effects induced by therapeutic doses of AAS, or alternatively to the appearance of neurotoxic effects when submitted to high doses (Gruenewald and Matsumoto, 2003; Pope et al., 2014). The latter, is particularly important because the increased number of healthy young women and men that make self-administration of supraphysiological doses of AAS for both aesthetical purposes and gain of athletic performance (Kanayama and Pope, 2018) without recognizing the putative neurotoxic risks, i.e., particularly to neuroenergetics (Frankenfeld et al., 2014). Although supraphysiological doses of AAS

have been associated with increased physical performance due to heightened energy production by skeletal muscle mitochondria, such energy boost may cause functional stress to this organelle (Magnusson et al., 2009; Novaes Gomes et al., 2014; Pieretti et al., 2013). At synaptic level, where mitochondria are considered more vulnerable to damage, a burst of oxidative metabolism could not necessarily result in benefits. Thus, it remains an open question whether or not supraphysiological doses of AAS might enhance energy production specifically in synaptic and extrasynaptic mitochondria, which conceptually could mirror a mechanism of neural plasticity or neurotoxicity, respectively.

This study was designed to unravel whether supraphysiological doses of NAND and TEST impair synaptic and extrasynaptic mitochondrial $Ca^{2+}$ handling and bioenergetics responsiveness, thereby affecting memory formation.

## 2. Methods

### *2.1.Animals and treatment protocol*

Male 70 days old CF1 mice (n= 30 animals, n=6-10 per group) were obtained from (CREAL, Porto Alegre/RS, Brazil). Animals (4-5 per cage) were placed into a controlled temperature room (22ºC ± 1) under a 12 h light/12h dark cycle (lights on at 7 a.m.) and had free access to food and water. The 19-days-long treatment consisted of a daily injection of either 15 mg/kg nandrolone decanoate (Schering-Plough®, Kenilworth, NJ, USA) (NAND group), testosterone cypionate (Sigma Pharma EMS™, Hortolândia, SP, Brazil) (TEST group) or corn oil as vehicle (SALADA™, Bunge Alimentos™, São Paulo, SP, Brazil) (VEH group). These dosages reportedly induce behavioral alterations

in mice, and translate the abusive supraphysiological administration aiming esthetical and performance enhancement in humans (Bonson et al., 1994; Kalinine et al., 2014; Martinez-Sanchis et al., 1998).. Steroids were diluted in corn oil to a 15 mg/ml concentration, allowing 15 mg/kg dosage to be administered through subcutaneous 1 ml/kg injection. One day after the last injection animals were placed in a closed chamber containing veterinary use grade isoflurane (Isoforin™, Cristália™, Itapira, SP, Brazil). As anesthesia was achieved mice were euthanized by decapitation, cerebral hemispheres removed and dissected over ice-cold homogenization buffer (EDTA 2 mM, 0.001 %, Tris HCl 50 mM, (pH 7,4), sucrose 320 mM, and Triton X-100 1 %). All animal experimentation procedures were previously submitted and approved in ethical and scientific validity by the Committee on the Care and Use of Experimental Animal Resources, UFRGS, Brazil number 22436, and performed aiming comfort and well-being of animals, according to the Brazilian Law Number 11749, Oct 8th, 2008, regarding the ethical guidelines for animal use in scientific research and education.".

*2.2.Morris Water Maze*

The spatial memory was evaluated through Morris Water Maze task as previously described (Kalinine et al., 2014; Muller et al., 2011). Animals of each group (n = 10 per group) were trained daily in a four-trial MWM to find a hidden platform; followed by one-day test phase without the platform. The time spent in the target quadrant was measured. Videos were obtained and analyzed using the Any-Maze® (Stoelting ™, Wood Dale, IL, USA) (Muller et al., 2011)

*2.3.Synaptosomes and extrasynaptic mitochondria isolation*

The left cerebral hemisphere was rapidly removed and homogenized in 500µL of isolation buffer (320mM sucrose, 10mM Tris, 0,1% BSA, pH 7.4) with 10 strokes of a 7 mL glass Douce tissue homogenizer. Briefly, homogenized tissue is submitted to a 1330 *g x* 3 min centrifugation in isolation buffer. Posteriorly, supernatant is removed and centrifuged for 10 min at 21200 *g*. The formed pellet is resuspended in a 15% Percoll® (GE Healthcare®, Little Chalfont, UK) solution and submitted to a discontinuous Percoll® gradients centrifugation at 30700 *g x* 5 min, with 23% and 40% Percoll® bands, respectively enriched in synaptossomes and extrasynaptic mitochondria, as previously described (Muller et al., 2013; Sims, 1990; Sims and Anderson, 2008). Posterior to separation, both enriched bands are separately centrifuged at 16500 *g* x 10 min and supernatant debris removed; also, extrasynaptic mitochondrial enrichment required 6900g x 10 min. Samples were then resuspended in a sucrose and Tris buffer (320mM sucrose, 10mM Tris, pH 7.4) and immediately used for the respirometry, $Ca^{2+}$ handling, mitochondrial membrane potential ($\Delta\Psi m$), and hydrogen peroxide assays. Aliquots of the samples were used for protein quantification.

*2.4.Mitochondrial calcium handling*

To assess mitochondrial calcium influx and efflux, we measured the absorbance spectrophotometrically at 540 nm (Spectra Max M5®, Molecular Devices®, San Jose, CA, USA). Isolated synaptosomes and extrasynaptic mitochondria were added to standard swelling incubation medium (100 mM KCl, 50 mM Sucrose, 10 mM HEPES and 5 mM KH2PO4) and basal mitochondrial absorbance was monitored during 3min.

Mitochondrial substrates were added to support ATP production (3,5 mM pyruvate, 4,5 mM malate, 4,5mM glutamate, 1,2 mM succinate and 100 uM ADP) and the mitochondrial absorbance during coupled oxidative phosphorylation (PMGSA) was monitored during 5 min. Subsequentially, 10 mM $Ca^{2+}$ was added to induce swelling due to influx into the mitochondrial matrix ($Ca^{2+}$). The mitochondrial calcium efflux through the sodium–calcium-lithium exchanger (NCLX), was monitored (10 min) after addition of 25 mM $Na^{+}$. For a mitochondrial enriched suspension, swelling and shrinkage leads to a decrease and increase in absorbance respectively (Nunez-Figueredo et al., 2014). The results are expressed as absorbance in 540 nm.

*2.5.Mitochondrial Membrane Potential (ΔΨm)*

The ΔΨm was measured by using the fluorescence signal of the cationic dye, Safranin-O (Sigma-Aldrich, Aldrich,® Saint Louis, MO, USA). Isolated synaptosomes and extrasynaptic mitochondria were incubated in the respiration buffer used in the respirometry protocol supplemented with 10 μM safranin-O. Fluorescence was detected with an excitation wavelength of 495 nm and an emission wavelength of 586 nm (Spectra Max M5®, Molecular Devices®, San Jose, CA, USA). Data are reported as arbitrary fluorescence units (AFUs) (Portela et al., 2016).

*2.6.High Resolution Respirometry Respiratory protocol*

Oxygen consumption rate (OCR) measurements were performed using Oxygraph-2k system with DatLab™ software (Oroboros Instruments™, Innsbruck, Austria) and normalized to the protein content. Isolated synaptosomes and extrasynaptic mitochondria

were incubated to a standard respiration buffer (100 mM KCI, 75 mM mannitol, 25 mM sucrose, 5 mM phosphate, 0.05 mM EDTA, and 10 mM Tris-HC1, pH 7.4). All experiments were performed at 37°C in a 2-ml chamber, with a modified multi-substrate titration protocol as previously described in detail elsewhere (Gnaiger, 2014)

Following 5 minutes for establishing ROUTINE (ROUT) respiration values, the multi-substrate titration protocol started with sequential addition of pyruvate, malate, and glutamate (10, 10, and 20 mM, respectively) and 10 mM Succinate to obtain LEAK respiration (L); Adenosine diphosphate (ADP, 2.5 mM) was titrated to obtain OxPHOS capacity (P); Stepwise titration of the protonophore Carbonyl cyanide-4-(trifluoromethoxy)phenylhydrazone (FCCP, 0.5 μM steps) yields the capacity of the electron transfer system (E) and residual oxygen consumption (ROX) after both antimycin-A and cyanide (AA, 2mM and KCN, 5 mM). We calculated the biochemical OXPHOS coupling efficiency ((P-L)/P); the OXPHOS control ratio, ≈P/E = (P-L)/E, and reserve respiratory capacity (RRC; ETS capacity - ROUTINE)(Burtscher et al., 2015; Gnaiger, 2014).

*2.7.Mitochondrial dehydrogenase activity – MTT assay*

Dehydrogenase activity was measured by the colorimetric [3(4,5-dimethylthiazol-2- yl)- 2,5-diphenyl tetrazolium bromide] (MTT, Sigma-Aldrich,® Saint Louis, MO, USA) method (Hansen et al., 1989). The results were expressed as percentage of control.

*2.8.Mitochondrial $H_2O_2$ production*

The mitochondrial production of hydrogen peroxide ($H_2O_2$) was assessed with the AmplexRed® (Invitrogen®, Paisley, UK) hydrogen peroxide assay kit in isolated synaptosomes and extrasynaptic mitochondria (n=10 per group) as instructed by manufacturer. The same substrates, uncouplers and inhibitors used for respirometry were incubated sequentially in the same respiration buffer supplemented with 10 µM AmplexRed® and 2 units/mL horseradish peroxidase to assess $H_2O_2$ generation. Fluorescence was monitored at excitation (563 nm) and emission (587 nm) wavelengths with a Spectra Max M5 microplate reader (Spectra Max M5®, Molecular Devices®, San Jose, CA, USA) (Portela et al., 2016). Data are expressed as RFU/sec/mg protein.

*2.9.Western blotting*

Soon after the euthanasia, the left cortex and hippocampus were dissected and homogenized in a buffer solution (EDTA 2 mM, protease and phosphatase inhibitor cocktails I and II (Sigma®, St. Louis, MO, USA) 0.001 %, Tris HCl 50 mM, (pH 7,4), sucrose 320 mM, and Triton X-100 1 %) and centrifuged (1300 g/ 3 min). Supernatant was collected and protein concentration normalized with sample buffer (Bromophenol blue 0.01 g% w/v, Tris 0.06M, Glycerol 25% v/v, SDS 2% w/v, pH 6.8). Samples of 20 µg of protein (n=6-8 per group) were separated by electrophoresis on a 10% or 12% polyacrylamide gel and electrotransferred to Nitrocellulose membranes (Amersham®, GE Healthcare®, Little Chalfont, UK) as previously reported (Muller et al., 2011). Membrane blockage steps and antibody dilutions where performed as appointed in the specific Datasheets provided with primary antibodies Anti-Tau phospho-S396 (ABCAM®, Cambridge, UK; 1:1000; ref. ab109390) and Anti-Tau antibody (ABCAM®, Cambridge,

UK; 1:1000; ref. ab32057). HRP-linked Secondary antibody incubation was performed according to manufacturer appointments (Anti-Rabbit IgG, Sigma-Aldrich®, St. Louis, MO USA, 1:2000, ref A0545), followed by chemiluminescent reaction with Clarity® Kit (BioRad®, Hercules, CA, USA). Protein expression was quantified using Image J® software (Rockville, USA). The values of optic density were expressed as % of control.

*2.10. Protein quantification*

The Pierce™ BCA Protein Assay Kit (Thermo Scientific®, Waltham, MA, USA) (Catalog number: 23225) was used for quantification of protein contents of the synaptosomes and extrasynaptic mitochondria preparations.

*2.11. Statistical Analysis*

Results were calculated and expressed as the mean ± S.E.M. Normality of data was assessed with Shapiro-Wilk test. To analyze the differences between groups, we used one-way analysis of variance (ANOVA) followed by a post-hoc Tukey test. All procedures were performed using Prism® 6.0 (GraphPad Software®, San Diego, CA, USA) software. The differences were considered statistically significant at $p < 0.05$.

## 3. Results

### *3.1.Chronic exposure to Nandrolone and Testosterone does not impair spatial memory*

Owing that metabolic dysfunction, increased $H_2O_2$ levels and Tau hyperphosphorylation could lead to cognitive deficits we submitted animal to the Morris Water Maze task to evaluate learning and memory performance. Remarkably, we observed no differences neither during the training days (acquisition phase, Supplementary Figure 1A) nor in the test phase according to the evaluated trial parameters (Suppl. Figure 1B and C).

*3.2. AAS differentially affect mitochondrial calcium efflux*

After the addition of substrates (PMGSA and $Ca^{2+}$, both NAND and TEST in synaptic mitochondria, showed higher influx when compared to VEH (Figure 1A and C; Mean diff = 11.76, p = 0.0001 and Mean diff = 4.398, p = 0.0001; respectively), indicating an increased mitochondrial swelling. NAND group showed a significantly higher variation when compared to TEST group (Figure 1 C; Mean diff = 7.361, p = 0.0001). After the addition of $Na^+$ to the incubation medium all groups presented mitochondrial $Ca^{2+}$ extrusion (Figure 1A and C), which was higher in both NAND and TEST groups compared to VEH (Figure 1C; Mean diff = 8.285, p = 0.0001 and Mean diff = 4.49, p = 0.0001; respectively). This effect was significantly higher in NAND when compared to TEST group (Figure 1C; Mean diff = 3.795, p = 0.0001).

In extrasynaptic mitochondria (Figure 1B and D), the absorbance decreased in all groups however it was higher in NAND groups compared to VEH and TEST (Figure 1B and D; Mean diff = 5.366.285, p = 0.0001 and Mean diff = 4.238, p = 0.0042; respectively), indicating increased mitochondrial swelling (Figure 1B). No differences were observed comparing VEH to TEST group (Figure 1D; Mean diff = 1.129, p =

0.6505). After the addition of $Na^+$ all groups presented mitochondrial $Ca^{2+}$ extrusion, and no significant differences in variation among groups were observed, indicating normal functional capacity of NCLX channel and mitochondrial shrinkage.

Taken together, these results indicate that exposure to NAND modulates $Ca^{2+}$ uptake in both synaptic and extrasynaptic mitochondria. Also, NAND induces increased extrusion of $Ca^{2+}$ in both synaptic but not in extrasynaptic mitochondria. TEST increased $Ca^{2+}$ influx and extrusion in synaptic mitochondria. Remarkably, both AAS improved the $Na^+$-dependent control of $Ca^{2+}$ levels within the mitochondria matrix implying in benefits for the NCLX function in synaptosomes.

*3.3.Anabolic-androgen steroids impact synaptic and extrasynaptic $\Delta\Psi m$*

We showed that chronic AAS treatment affects the $\Delta\Psi_m$ in both synaptic and extrasynaptic mitochondria. During evaluation of synaptosomes in the resting state, NAND showed decreased fluorescence (increased $\Delta\Psi_m$) compared to both VEH and TEST (Figure 2A; Mean diff = 47.15, p = 0.0001, and Mean diff = 32.32, p = 0.0027). After the addition of the metabolic substrates (PMGS), fluorescence was significantly higher in NAND compared to both VEH and TEST (Figure 2A; Mean diff = 67.19, p = 0.0001, and Mean diff = 62.58, p = 0.0001, respectively). This resulted in decreased $\Delta\Psi_m$ formation in NAND compared to both VEH and TEST (Figure 2C; Mean diff = 67.19, p = 0.0001, and Mean diff = 62.58, p = 0.0001). No significant differences in fluorescence were observed among groups after ADP addition (Figure 2A) albeit $\Delta\Psi_m$ dissipation to oxidative phosphorylation was significantly decreased in NAND compared to both VEH and TEST (Figure 2C; Mean diff = 40.34, p = 0.0001, and Mean diff = 25.83, p = 0.0001,

respectively). Uncoupler addition (FCCP) resulted in reduced fluorescence in NAND compared to VEH and TEST (Figure 2A; Mean diff = 52.94, p = 0.0001, and Mean diff = 37.52, p = 0.0002). Although TEST group showed significantly higher variation of $\Delta\Psi_m$ compared to NAND (Figure 2 C; Mean diff = 33.5, p = 0.0001), both NAND and TEST presented impaired dissipation of $\Delta\Psi_m$ compared to VEH (Figure 2C; Mean diff = 48.95, p = 0.0001, and Mean diff = 15.44, p = 0.03, respectively). No significant differences were observed among groups after sodium cyanide addition to completely dissipate $\Delta\Psi_m$.

Extra-synaptic mitochondria showed a very similar profile in $\Delta\Psi_m$. In the resting state, NAND showed decreased fluorescence (increased $\Delta\Psi_m$) compared to both VEH and TEST (Figure 2B; Mean diff = 51.67, p = 0.0043, and Mean diff = 45.31, p = 0.0143). After the addition of the metabolic substrates (PMGS) fluorescence was significantly higher in NAND compared to both VEH and TEST (Figure 2B; Mean diff = 72.36, p = 0.0001, and Mean diff = 61.58, p = 0.0001, respectively). This results in decreased $\Delta\Psi_m$ formation in NAND compared to both VEH and TEST (Figure 2D; Mean diff = 34.54, p = 0.0001, and Mean diff = 30.06, p = 0.0001). No significant differences in fluorescence were observed among groups after ADP addition or after the addition of oligomycin (Figure 2B). However, $\Delta\Psi_m$ dissipation to ATP synthesis was significantly decreased in NAND compared to both VEH and TEST (Figure 2D; Mean diff = 41.66, p = 0.0001, and Mean diff = 27.14, p = 0.0002, respectively). After the uncoupler addition (FCCP), reduced fluorescence in NAND compared to VEH and TEST (Figure 2B; Mean diff = 59.6, p = 0.0008, and Mean diff = 54.09, p = 0.0026) was observed. Similarly, to synaptosomes, the TEST group showed significantly higher variation of $\Delta\Psi_m$ compared to NAND (Figure 02 D; Mean diff = 33.86, p = 0.0001), both NAND and TEST

presented impaired dissipation of $\Delta\Psi_m$ compared to VEH (Figure 2D; Mean diff = 49.31, p = 0.0001, and Mean diff = 15.24, p = 0.0408, respectively). No significant differences were observed among groups after sodium cyanide addition to completely dissipate $\Delta\Psi_m$.

The present results indicate that chronic exposure to nandrolone and testosterone affect ΔΨm in distinct fashions, both resulting in impaired coupling states in synaptic and extra-synaptic mitochondria.

### *3.4. Anabolic-androgen steroids influence synaptic and extrasynaptic mitochondrial respiratory states*

The normal dynamics of $\Delta\psi_m$ is a vital component to mitochondrial ATP generation via the oxidative phosphorylation (Figueira et al., 2012). We further explored the effects of different AAS in bioenergetic parameters assessed in synaptossomal and extrasynaptic mitochondria. In synaptic mitochondrial preparations, both the Leak state and OxPhos state did not present differences between groups, culminating in no differences in the OxPhos coupling efficiency (Figure 3B). In the ETS state, TEST increased OCR when compared to both VEH and NAND (Mean diff = 1480, p = 0.0001, and Mean diff = 1348, p = 0.001, respectively), with no differences observed comparing NAND to VEH. TEST increased RRC (Figure 3C) when compared to both VEH and NAND (Mean diff = 1518, p = 0.02, and Mean diff = 1570, p = 0.01, respectively).

Extrasynaptic mitochondria OCR (Figure 3E) showed a distinct response. NAND decreased OCR in the Oxphos state compared only to VEH (p = 0.0436). However, no differences among groups were observed neither in the Leak, ETS or ROX states, nor in the OxPhos coupling efficiency (Figure 3F) and RRC (Figure 3G). Given that

mitochondrial bioenergetics also depend on dehydrogenase enzymes, we further explored this through the MTT assay. Remarkably, NAND induced decreased the activity of dehydrogenases in both synaptosomes (Figure 3D; Mean diff = 46.72, p = 0.0001; Mean diff = 39.58, p= 0.007; VEH and TEST respectively) and extra-synaptic mitochondria (Figure 3H; Mean diff = 54.99, p = 0.007; Mean diff = 49.6, p = 0.018; VEH and TEST respectively).

### *3.5.Exposure to anabolic-androgen steroids increases synaptic and extrasynaptic mitochondrial hydrogen peroxide production*

In synaptosomes, $H_2O_2$ levels (Figure 5A) were increased at baseline by NAND compared to VEH and TEST (Mean diff = 0.686, p = 0.001 and Mean diff = 0.606, p = 0.001, respectively), while TEST did not present difference from VEH (p = 0.678). The addition of the CI-and CII-linked mitochondrial substrates (PMGS) increased $H_2O_2$ production, significantly higher only in the NAND group compared only to TEST (Mean diff = 0.25, $p$ = 0.02). The addition of ADP culminating in higher $O_2$ consumption, evoked a significantly higher $H_2O_2$ production in NAND compared to VEH and TEST (Mean diff = 0.663, $p$ = 0.001 and Mean diff = 0.615, $p$ = 0.001, respectively). Uncoupler addition yielded significantly higher $H_2O_2$ production in NAND compared to VEH and TEST (Mean diff = 0.667, $p$ = 0.001 and Mean diff = 0.512, $p$ = 0.001, respectively). The same was observed after cyanide addition to inhibit complex IV.

Extrasynaptic mitochondria showed a very similar pattern to the observed in synaptossomes (Figure 5B). Production of $H_2O_2$ was increased at baseline by NAND only when compared to VEH (Mean diff = 0.397, p = 0.002), while VEH and TEST were

not significantly different (p= 0.28). The addition of the CI-and CII-linked mitochondrial substrates (PMGS) increased $H_2O_2$ production, which was significantly higher in the NAND group compared to both VEH and TEST (Mean diff = 0.433, p = 0.001 and Mean diff = 0.426, p = 0.001, respectively). Addition of ADP induced a significantly higher $H_2O_2$ production in NAND compared to VEH and TEST (Mean diff = 0.947, p = 0.001 and Mean diff = 0.807, p = 0.001, respectively). Also, NAND induced significantly higher $H_2O_2$ production compared to VEH and TEST after addition of both uncoupler (E), and cyanide (ROX) ($p$ = 0.001 in all comparisons) with no differences observed between VEH and TEST. Remarkably, only NAND increased hydrogen peroxide production in different mitochondrial respiration states.

### *3.6.Nandrolone increases Tau phosphorylation*

Further, we explored whether increased $H_2O_2$ could parallel with increased Tau phosphorylation, a molecular hallmark of neurodegeneration. Strikingly, NAND induced increased pTau(Ser396)/Total Tau ratio in the cortex as compared to both TEST and VEH (Mean diff = 326.2, p=0.007; Mean diff = 208.5, p = 0.05; VEH and TEST respectively) but not in the hippocampus (p= 0.25).

## 4. Discussion

Here, we found that NAND and TEST modulate synaptic and extrasynaptic mitochondrial parameters linked with bioenergetics in distinct ways. To date NAND caused the highest neurotoxic effects, albeit none induced synaptic or extrasynaptic modifications paralleled with impaired spatial memory performance.

It should be taken into consideration that brain mitochondria present dissimilar characteristics relative to their synaptic and extrasynaptic localization (Stauch et al., 2014; Yarana et al., 2012) that, depending on the stimuli may affect its functions. Particularly, it is assumed that synaptic mitochondria exhibit increased susceptibility to oxidative damage, and higher vulnerability to calcium load compared to extrasynaptic mitochondria (Stauch et al., 2014; Yarana et al., 2012), which could result in different response patterns to supraphysiological doses of AAS. Actually, it was previously demonstrated that NAND and TEST administered alone or in cocktails, increased glutamatergic activity, mainly through overactivation of the *N-methyl-D-aspartate* (NMDA) receptor calcium channel (Maria Carrillo, 2012; Kalinine et al 2014). The overactivation of these receptors through AAS' like NAND and TEST hence, could contribute to elevate mitochondrial $Ca^{2+}$, leading to energy deficits and oxidative damage associated with neurodegeneration (Lin and Beal, 2006; Nicholls, 2003, 2010).

The mitochondrial $Ca^{2+}$ homeostasis involves the outer mitochondrial membrane voltage dependent anion channel (VDAC) and the inner mitochondrial membrane calcium uniporter (MCU), controlling $Ca^{2+}$ uptake with a sufficiently high $\Delta\Psi m$ whereas the efflux is mainly dependent on the inner membrane $Na^{+}$/ $Ca^{2+}$/$Li^{+}$ exchanger (NCLX) (Contreras et al., 2010). In the present study, $Ca^{2+}$ influx was predominantly altered by both AAS in synaptic preparations, and only by NAND in extrasynaptic preparations, whereas the efflux was increased by AAS in synaptic preparations only. The $\Delta\Psi m$ generation was impaired by both AAS in synaptosomal and extrasynaptic preparations albeit NAND displayed more striking effects, which is likely attributed to the aforementioned increased $Ca^{2+}$ influx. It should be considered that concomitant

disruptions of $Ca^{2+}$ control and ΔΨm may serve as a trigger for H2O2 production, oxidative damage and apoptotic stimuli (Duchen, 2000; Gottlieb et al., 2003; Tan and Colombini, 2007). Under the present experimental scenario, it is plausible to suggest that $Ca^{2+}$ overload following high doses of NAND is connected with deficient ΔΨm formation and dissipation (Celsi et al., 2009), and has implications to the increased hydrogen peroxide ($H_2O_2$) production, which may serve as an apoptotic signal. Actually, supraphysiological doses of AAS can induce neuronal apoptosis (Ma and Liu, 2015), and impair hippocampal neurogenesis (Novaes Gomes et al., 2014). However, lower doses of AAS may protect brain protect against insults by increasing neurotrophic signaling, neurogenesis and decreasing oxidative stress (Chisu et al., 2006; Fanaei et al., 2014; Gouras et al., 2000; Gurer et al., 2015; Hioki et al., 2014; Toro-Urrego et al., 2016). This sort of "Janus-faced" effects reinforces the importance to further explore how the AAS dose and time regimen is related with subcellular compartmentalization of mitochondrial bioenergetics. Here, we found that NAND but not TEST, significantly increased mitochondrial $H_2O_2$ production at synaptic and extrasynaptic sites in different coupling states, implying that mitochondria dysfunction indeed mediates neurotoxicity induced by NAND. On the other hand, the increase of RRC in synaptic fractions (the difference between ATP produced by oxidative phosphorylation at baseline and at maximal activity) after TEST indicates increased capacity of substrate oxidation, which is here a proxy indicator of compartmentalized metabolic adaptions.

Although a previously published work of our group showed no difference in the MTT assay for cell viability in slices after NAND, in this work we highlight the specific responses in two mitochondrial enriched preparations, synaptosomes and extrasynaptic

samples (Kalinine et al., 2014). Here, diminished MTT levels by NAND in synaptic and extrasynaptic fractions, indicates reduction of mitochondrial dehydrogenases activity; and interestingly, this effect parallels with mitochondrial dysfunction. This highlights the importance of compartmentalized analysis to avoid underestimation of neurochemical toxicity induced by AAS. Since decreased MTT levels are commonly associated with neurodegeneration, we confirmed this assumption, showing that only NAND induced Tau hyperphosphorylation in cortex, albeit not in the hippocampus.

Although supraphysiological doses of NAND elicited increased biomarkers of neurotoxicity, here we did not find alterations in the spatial memory performance (Supplementary file). Spatial memory function requires high levels of neural cells connectivity and energy support, and is considered dependent on brain hippocampal structures (Buckner et al., 2005; Lustig et al., 2003). Based on this, we assumed that the mitochondrial alterations here described could only represent a prodromal phase of neurotoxicity induced by AAS abuse, thereby still causing low impact to the hippocampal circuits.

Most of the current literature has investigated the effects of testosterone therapy in aged or castrated rodents (Frye and Seliga, 2001; Isgor and Sengelaub, 2003), often pointing that testosterone deprivation decreases cognitive function; however, there are conflicting reports regarding whether exogenous AAS supplementation may promote gain of cognitive function or at least delay its decline (Gouchie and Kimura, 1991; Goudsmit et al., 1990; Vazquez-Pereyra et al., 1995; Zhang et al., 2013). Also, studies evaluating the potential toxic effect of AAS on brain mitochondria are scarce, albeit there

are evidences of neurofunctional alterations, such as altered behavior phenotypes and decreased connectivity (Kaufman et al., 2015; Westlye et al., 2017), and neurodegenerative processes (Ma and Liu, 2015). Moreover, the effects of AAS on learning and memory performance have been a matter of debate regarding the appropriate dose, time regimen, and memory paradigm (Spritzer et al., 2011).

## Conclusion

Here we highlight that high doses of NAND cause neurotoxic effects to components of synaptic and extrasynaptic mitochondrial bioenergetics, impairing calcium influx, membrane potential dynamics and increasing $H_2O_2$ production. These alterations did not culminate in cognitive disfunction.

## Acknowledgements

This work was supported by the Brazilian grants of Conselho Nacional de Desenvolvimento Científico e Tecnológico (CNPq) #426796/2016-0 and 141100/2013-3, CNPq-Instituto Nacional de Neurociência Translacional-INNT #465346/2014-6, FAPERGS/PRONEX#16/2551-0000499-4 and also by the Conselho de Aperfeiçoamento de Pessoal de Nível Superior (CAPES) #1663.

## References

Bonson, K.R., Johnson, R.G., Fiorella, D., Rabin, R.A., Winter, J.C., 1994. Serotonergic control of androgen-induced dominance. Pharmacology, biochemistry, and behavior 49, 313-322.

Brand, Martin D., Nicholls, David G., 2011. Assessing mitochondrial dysfunction in cells. Biochemical Journal 435, 297-312.

Buckner, R.L., Snyder, A.Z., Shannon, B.J., LaRossa, G., Sachs, R., Fotenos, A.F., Sheline, Y.I., Klunk, W.E., Mathis, C.A., Morris, J.C., Mintun, M.A., 2005. Molecular, Structural, and Functional Characterization of Alzheimer's Disease: Evidence for a Relationship between Default Activity, Amyloid, and Memory. The Journal of Neuroscience 25, 7709-7717.

Burtscher, J., Zangrandi, L., Schwarzer, C., Gnaiger, E., 2015. Differences in mitochondrial function in homogenated samples from healthy and epileptic specific brain tissues revealed by high-resolution respirometry. Mitochondrion 25, 104-112.

Celsi, F., Pizzo, P., Brini, M., Leo, S., Fotino, C., Pinton, P., Rizzuto, R., 2009. Mitochondria, calcium and cell death: A deadly triad in neurodegeneration. Biochimica et biophysica acta 1787, 335-344.

Chisu, V., Manca, P., Lepore, G., Gadau, S., Zedda, M., Farina, V., 2006. Testosterone induces neuroprotection from oxidative stress. Effects on catalase activity and 3-nitro-L-tyrosine incorporation into alpha-tubulin in a mouse neuroblastoma cell line. Archives italiennes de biologie 144, 63-73.

Contreras, L., Drago, I., Zampese, E., Pozzan, T., 2010. Mitochondria: The calcium connection. Biochimica et Biophysica Acta (BBA) - Bioenergetics 1797, 607-618.

Devine, M.J., Kittler, J.T., 2018. Mitochondria at the neuronal presynapse in health and disease. Nature reviews Neuroscience 19, 63-80.

Duchen, M.R., 2000. Mitochondria and calcium: from cell signalling to cell death. The Journal of Physiology 529, 57-68.

Fanaei, H., Karimian, S.M., Sadeghipour, H.R., Hassanzade, G., Kasaeian, A., Attari, F., Khayat, S., Ramezani, V., Javadimehr, M., 2014. Testosterone enhances functional recovery after stroke through promotion of antioxidant defenses, BDNF levels and neurogenesis in male rats. Brain research 1558, 74-83.

Figueira, T.R., Melo, D.R., Vercesi, A.E., Castilho, R.F., 2012. Safranine as a fluorescent probe for the evaluation of mitochondrial membrane potential in isolated organelles and permeabilized cells. Methods in molecular biology (Clifton, NJ) 810, 103-117.

Frankenfeld, S.P., Oliveira, L.P., Ortenzi, V.H., Rego-Monteiro, I.C.C., Chaves, E.A., Ferreira, A.C., Leitão, A.C., Carvalho, D.P., Fortunato, R.S., 2014. The Anabolic Androgenic Steroid Nandrolone Decanoate Disrupts Redox Homeostasis in Liver, Heart and Kidney of Male Wistar Rats. PLOS ONE 9, e102699.

Frye, C.A., Seliga, A.M., 2001. Testosterone increases analgesia, anxiolysis, and cognitive performance of male rats. Cognitive, affective & behavioral neuroscience 1, 371-381.

Geinisman, Y., Berry, R.W., Disterhoft, J.F., Power, J.M., Van der Zee, E.A., 2001. Associative learning elicits the formation of multiple-synapse boutons. The Journal of neuroscience : the official journal of the Society for Neuroscience 21, 5568-5573.

Gnaiger, E., 2014. Mitochondrial pathways and respiratory control. An introduction to OXPHOS analysis. . OROBOROS MiPNet Publications, Innsbruck, pp. 80.
Gottlieb, E., Armour, S.M., Harris, M.H., Thompson, C.B., 2003. Mitochondrial membrane potential regulates matrix configuration and cytochrome c release during apoptosis. Cell death and differentiation 10, 709-717.
Gouchie, C., Kimura, D., 1991. The relationship between testosterone levels and cognitive ability patterns. Psychoneuroendocrinology 16, 323-334.
Goudsmit, E., Van de Poll, N.E., Swaab, D.F., 1990. Testosterone fails to reverse spatial memory decline in aged rats and impairs retention in young and middle-aged animals. Behavioral and neural biology 53, 6-20.
Gouras, G.K., Xu, H., Gross, R.S., Greenfield, J.P., Hai, B., Wang, R., Greengard, P., 2000. Testosterone reduces neuronal secretion of Alzheimer's beta-amyloid peptides. Proceedings of the National Academy of Sciences of the United States of America 97, 1202-1205.
Gruenewald, D.A., Matsumoto, A.M., 2003. Testosterone supplementation therapy for older men: potential benefits and risks. Journal of the American Geriatrics Society 51, 101-115; discussion 115.
Gurer, B., Kertmen, H., Kasim, E., Yilmaz, E.R., Kanat, B.H., Sargon, M.F., Arikok, A.T., Erguder, B.I., Sekerci, Z., 2015. Neuroprotective effects of testosterone on ischemia/reperfusion injury of the rabbit spinal cord. Injury 46, 240-248.
Hansen, M.B., Nielsen, S.E., Berg, K., 1989. Re-examination and further development of a precise and rapid dye method for measuring cell growth/cell kill. Journal of immunological methods 119, 203-210.
Hioki, T., Suzuki, S., Morimoto, M., Masaki, T., Tozawa, R., Morita, S., Horiguchi, T., 2014. Brain testosterone deficiency leads to down-regulation of mitochondrial gene expression in rat hippocampus accompanied by a decline in peroxisome proliferator-activated receptor-gamma coactivator 1alpha expression. Journal of molecular neuroscience : MN 52, 531-537.
Isgor, C., Sengelaub, D.R., 2003. Effects of neonatal gonadal steroids on adult CA3 pyramidal neuron dendritic morphology and spatial memory in rats. Journal of neurobiology 55, 179-190.
Kalinine, E., Zimmer, E.R., Zenki, K.C., Kalinine, I., Kazlauckas, V., Haas, C.B., Hansel, G., Zimmer, A.R., Souza, D.O., Muller, A.P., Portela, L.V., 2014. Nandrolone-induced aggressive behavior is associated with alterations in extracellular glutamate homeostasis in mice. Hormones and behavior 66, 383-392.
Kanayama, G., Pope, H.G., 2018. History and epidemiology of anabolic androgens in athletes and non-athletes. Molecular and cellular endocrinology 464, 4-13.
Kasai, H., Matsuzaki, M., Noguchi, J., Yasumatsu, N., Nakahara, H., 2003. Structure-stability-function relationships of dendritic spines. Trends in neurosciences 26, 360-368.
Kaufman, M.J., Janes, A.C., Hudson, J.I., Brennan, B.P., Kanayama, G., Kerrigan, A.R., Jensen, J.E., Pope, H.G., Jr., 2015. Brain and cognition abnormalities in long-term anabolic-androgenic steroid users. Drug and alcohol dependence 152, 47-56.
Lin, M.T., Beal, M.F., 2006. Mitochondrial dysfunction and oxidative stress in neurodegenerative diseases. Nature 443, 787-795.

Lustig, C., Snyder, A.Z., Bhakta, M., O'Brien, K.C., McAvoy, M., Raichle, M.E., Morris, J.C., Buckner, R.L., 2003. Functional deactivations: Change with age and dementia of the Alzheimer type. Proceedings of the National Academy of Sciences 100, 14504-14509.
Ma, F., Liu, D., 2015. 17beta-trenbolone, an anabolic-androgenic steroid as well as an environmental hormone, contributes to neurodegeneration. Toxicology and applied pharmacology 282, 68-76.
MacAskill, A.F., Atkin, T.A., Kittler, J.T., 2010. Mitochondrial trafficking and the provision of energy and calcium buffering at excitatory synapses. The European journal of neuroscience 32, 231-240.
Magnusson, K., Hanell, A., Bazov, I., Clausen, F., Zhou, Q., Nyberg, F., 2009. Nandrolone decanoate administration elevates hippocampal prodynorphin mRNA expression and impairs Morris water maze performance in male rats. Neuroscience letters 467, 189-193.
Martinez-Sanchis, S., Salvador, A., Moya-Albiol, L., Gonzalez-Bono, E., Simon, V.M., 1998. Effects of chronic treatment with testosterone propionate on aggression and hormonal levels in intact male mice. Psychoneuroendocrinology 23, 275-293.
Midzak, A.S., Chen, H., Papadopoulos, V., Zirkin, B.R., 2009. Leydig cell aging and the mechanisms of reduced testosterone synthesis. Molecular and Cellular Endocrinology 299, 23-31.
Muller, A.P., Gnoatto, J., Moreira, J.D., Zimmer, E.R., Haas, C.B., Lulhier, F., Perry, M.L., Souza, D.O., Torres-Aleman, I., Portela, L.V., 2011. Exercise increases insulin signaling in the hippocampus: physiological effects and pharmacological impact of intracerebroventricular insulin administration in mice. Hippocampus 21, 1082-1092.
Muller, A.P., Haas, C.B., Camacho-Pereira, J., Brochier, A.W., Gnoatto, J., Zimmer, E.R., de Souza, D.O., Galina, A., Portela, L.V., 2013. Insulin prevents mitochondrial generation of H(2)O(2) in rat brain. Experimental neurology 247, 66-72.
Nicholls, D.G., 2003. Bioenergetics and transmitter release in the isolated nerve terminal. Neurochemical research 28, 1433-1441.
Nicholls, D.G., 2010. Stochastic aspects of transmitter release and bioenergetic dysfunction in isolated nerve terminals. Biochemical Society transactions 38, 457-459.
Novaes Gomes, F.G., Fernandes, J., Vannucci Campos, D., Cassilhas, R.C., Viana, G.M., D'Almeida, V., de Moraes Rego, M.K., Buainain, P.I., Cavalheiro, E.A., Arida, R.M., 2014. The beneficial effects of strength exercise on hippocampal cell proliferation and apoptotic signaling is impaired by anabolic androgenic steroids. Psychoneuroendocrinology 50, 106-117.
Nunez-Figueredo, Y., Pardo-Andreu, G.L., Ramirez-Sanchez, J., Delgado-Hernandez, R., Ochoa-Rodriguez, E., Verdecia-Reyes, Y., Naal, Z., Muller, A.P., Portela, L.V., Souza, D.O., 2014. Antioxidant effects of JM-20 on rat brain mitochondria and synaptosomes: mitoprotection against Ca(2)(+)-induced mitochondrial impairment. Brain research bulletin 109, 68-76.
Oettinghaus, B., Schulz, J.M., Restelli, L.M., Licci, M., Savoia, C., Schmidt, A., Schmitt, K., Grimm, A., More, L., Hench, J., Tolnay, M., Eckert, A., D'Adamo, P., Franken, P., Ishihara, N., Mihara, K., Bischofberger, J., Scorrano, L., Frank, S., 2016. Synaptic

dysfunction, memory deficits and hippocampal atrophy due to ablation of mitochondrial fission in adult forebrain neurons. Cell death and differentiation 23, 18-28.
Phillis, B.D., Abeywardena, M.Y., Adams, M.J., Kennedy, J.A., Irvine, R.J., 2007. Nandrolone potentiates arrhythmogenic effects of cardiac ischemia in the rat. Toxicological sciences : an official journal of the Society of Toxicology 99, 605-611.
Pieretti, S., Mastriota, M., Tucci, P., Battaglia, G., Trabace, L., Nicoletti, F., Scaccianoce, S., 2013. Brain nerve growth factor unbalance induced by anabolic androgenic steroids in rats. Medicine and science in sports and exercise 45, 29-35.
Pope, H.G., Jr., Wood, R.I., Rogol, A., Nyberg, F., Bowers, L., Bhasin, S., 2014. Adverse health consequences of performance-enhancing drugs: an Endocrine Society scientific statement. Endocrine reviews 35, 341-375.
Portela, L.V., Brochier, A.W., Haas, C.B., de Carvalho, A.K., Gnoato, J.A., Zimmer, E.R., Kalinine, E., Pellerin, L., Muller, A.P., 2016. Hyperpalatable Diet and Physical Exercise Modulate the Expression of the Glial Monocarboxylate Transporters MCT1 and 4. Molecular neurobiology.
Pozzi, R., Fernandes, K.R., de Moura, C.F., Ferrari, R.A., Fernandes, K.P., Renno, A.C., Ribeiro, D.A., 2013. Nandrolone decanoate induces genetic damage in multiple organs of rats. Archives of environmental contamination and toxicology 64, 514-518.
Sims, N.R., 1990. Rapid isolation of metabolically active mitochondria from rat brain and subregions using Percoll density gradient centrifugation. Journal of neurochemistry 55, 698-707.
Sims, N.R., Anderson, M.F., 2008. Isolation of mitochondria from rat brain using Percoll density gradient centrifugation. Nature protocols 3, 1228-1239.
Spritzer, M.D., Daviau, E.D., Coneeny, M.K., Engelman, S.M., Prince, W.T., Rodriguez-Wisdom, K.N., 2011. Effects of testosterone on spatial learning and memory in adult male rats. Hormones and behavior 59, 484-496.
Stauch, K.L., Purnell, P.R., Fox, H.S., 2014. Quantitative proteomics of synaptic and nonsynaptic mitochondria: insights for synaptic mitochondrial vulnerability. Journal of proteome research 13, 2620-2636.
Sundaram, K., Kumar, N., Monder, C., Bardin, C.W., 1995. Different patterns of metabolism determine the relative anabolic activity of 19-norandrogens. The Journal of steroid biochemistry and molecular biology 53, 253-257.
Tan, W., Colombini, M., 2007. VDAC closure increases calcium ion flux. Biochimica et Biophysica Acta (BBA) - Biomembranes 1768, 2510-2515.
Toro-Urrego, N., Garcia-Segura, L.M., Echeverria, V., Barreto, G.E., 2016. Testosterone Protects Mitochondrial Function and Regulates Neuroglobin Expression in Astrocytic Cells Exposed to Glucose Deprivation. Frontiers in aging neuroscience 8, 152-152.
Vazquez-Pereyra, F., Rivas-Arancibia, S., Loaeza-Del Castillo, A., Schneider-Rivas, S., 1995. Modulation of short term and long term memory by steroid sexual hormones. Life sciences 56, Pl255-260.
Volgyi, K., Gulyassy, P., Haden, K., Kis, V., Badics, K., Kekesi, K.A., Simor, A., Gyorffy, B., Toth, E.A., Lubec, G., Juhasz, G., Dobolyi, A., 2015. Synaptic mitochondria: a brain mitochondria cluster with a specific proteome. Journal of proteomics 120, 142-157.

Wang, X., Stocco, D.M., 2005. The decline in testosterone biosynthesis during male aging: A consequence of multiple alterations. Molecular and Cellular Endocrinology 238, 1-7.
Westlye, L.T., Kaufmann, T., Alnaes, D., Hullstein, I.R., Bjornebekk, A., 2017. Brain connectivity aberrations in anabolic-androgenic steroid users. NeuroImage Clinical 13, 62-69.
Yarana, C., Sanit, J., Chattipakorn, N., Chattipakorn, S., 2012. Synaptic and nonsynaptic mitochondria demonstrate a different degree of calcium-induced mitochondrial dysfunction. Life sciences 90, 808-814.
Zhang, G.L., Wang, W., Kang, Y.X., Xue, Y., Yang, H., Zhou, C.M., Shi, G.M., 2013. Chronic testosterone propionate supplement could activated the Nrf2-ARE pathway in the brain and ameliorated the behaviors of aged rats. Behavioural brain research 252, 388-395.

**Figure captions**

**Figure 1. Supraphysiological doses of anabolic-androgen steroids affects synaptic and extrasynaptic mitochondrial calcium handling.** The swelling (A and B synaptic and extrasynaptic, respectively) and percentage of variation (C and D synaptic and extrasynaptic, respectively) stimulated by the mitochondrial substrates (pyruvate, malate, glutamate, succinate, and ADP; PMGSA). In synaptosomes, both AAS increased $Ca^{2+}$ influx and efflux ($Na^{+}$ dependent) (C and D). In extrasynaptic mitochondria NAND increased the $Ca^{2+}$ influx.* Denotes significant difference compared to VEH; # Indicates significant difference between NAND and TEST (One-Way ANOVA, *Post-hoc* Tukey, $p<0.05$).

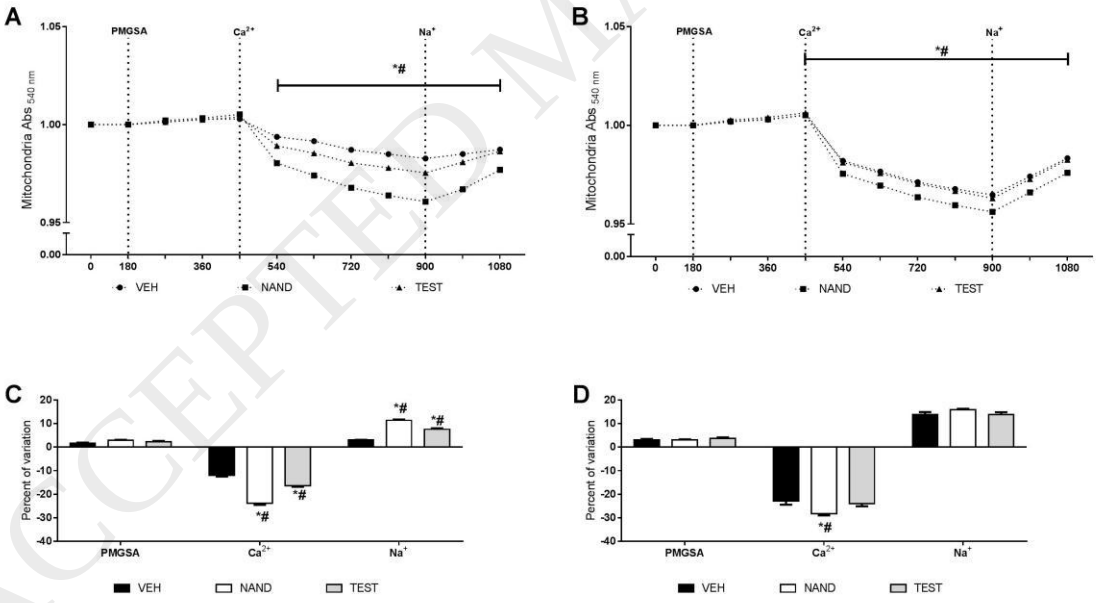


**Figure 2. Anabolic-androgen steroids differentially influence mitochondrial membrane potential (ΔΨm) generation and dissipation.** In synaptosomes (A) and

Extrasynaptic mitochondria (B), NAND effects caused alterations in fluorescence (increased ΔΨm) compared to VEH and TEST in several coupling states. This implicates in impaired ΔΨm formation and dissipation, as demonstrated by delta values in synaptosomes (C) and Extrasynaptic mitochondria (D). * Denotes significant difference compared to VEH; # Indicates significant difference between NAND and TEST (One-Way ANOVA, *Post-hoc* Tukey, $p<0.05$).

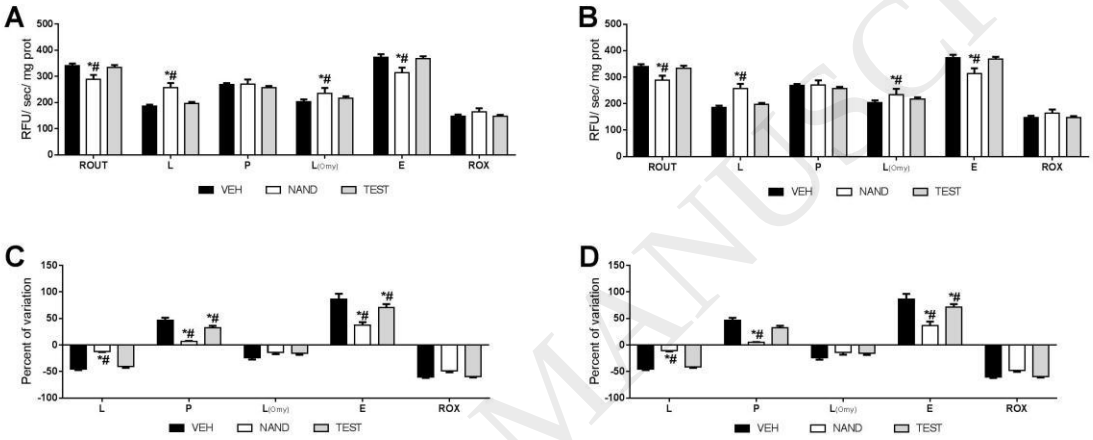


**Figure 3. Exposure to anabolic-androgen steroids mediate synaptic oxygen consumption in different mitochondrial states.** Synaptic mitochondria OCR was increased in the E state by TEST (A). AAS do not cause differences in OxPhos Coupling Efficiency (B), but TEST increased Reserve Respiratory Capacity (C). In extrasynaptic mitochondria, NAND decreased OCR (E) only in the OxPhos state (P) when compared to VEH. AAS do not alter specific mitochondrial functional parameters like OxPhos Coupling Efficiency (F), Reserve Respiratory Capacity (G). In both synaptosomes and extrasynaptic mitochondria (D and H), dehydrogenases activity was decreased by NAND.

* Denotes significant difference compared to VEH; # Indicates significant difference between NAND and TEST (One-Way ANOVA, *Post-hoc* Tukey, p<0.05).

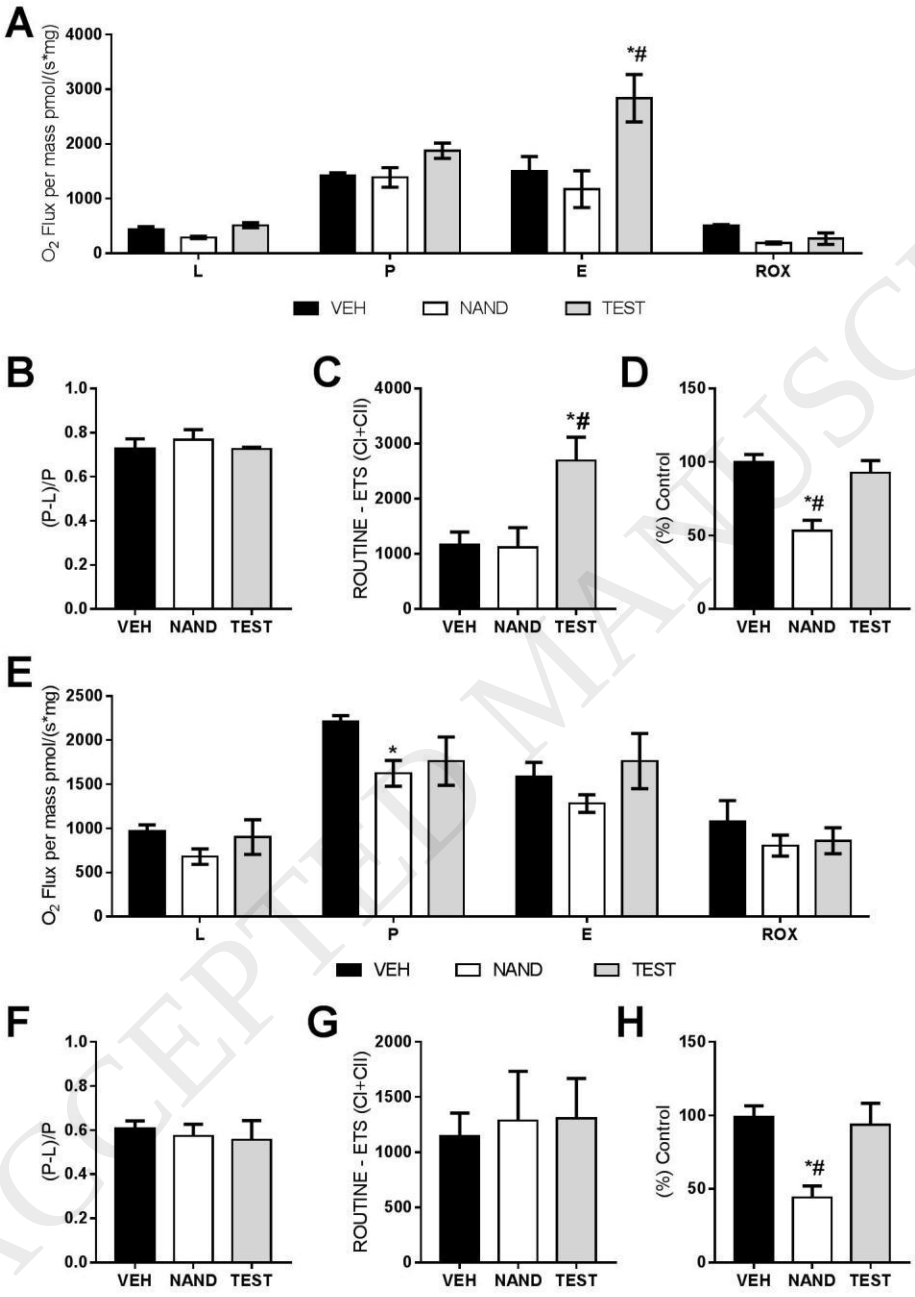

**Figure 4. Nandrolone increases synaptic and extrasynaptic mitochondrial $H_2O_2$ production.** In both synaptosomes (A) and extrasynaptic mitochondria (B), $H_2O_2$ production was increased by NAND compared to both VEH and TEST. * Denotes significant difference compared to VEH; # Indicates significant difference between NAND and TEST (One-Way ANOVA, *Post-hoc* Tukey, $p<0.05$).

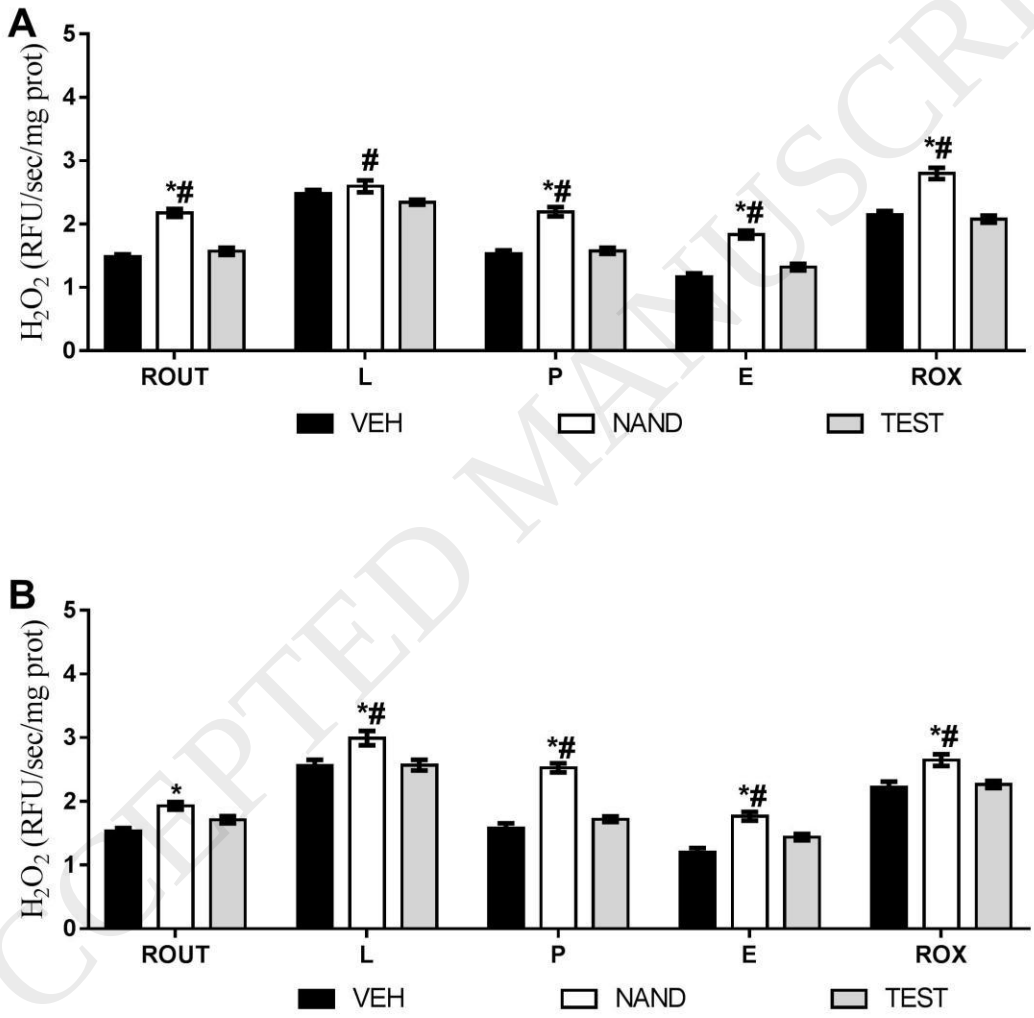


**Figure 5. Nandrolone increases Tau phosphorylation.** Phosphorylated Tau (Ser396) to Tau ratio was increased by NAND compared to both VEH and TEST in cortex (A), but

not hippocampus (B). * Denotes significant difference compared to VEH; # Indicates significant difference between NAND and TEST (One-Way ANOVA, *Post-hoc* Tukey, $p<0.05$).

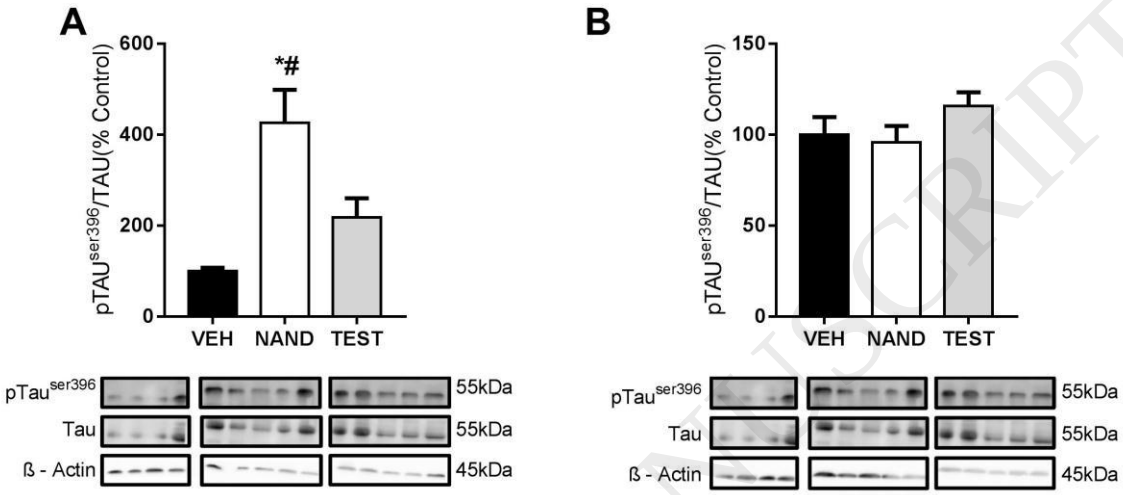

**Capítulo III:** *Testosterone administration after traumatic brain injury reduces mitochondrial dysfunction and neurodegeneration.*

No capitulo III apresentamos o artigo aceito para publicação no periódico "*Journal of Neurotrauma*" em 2019.

O conjunto de resultados obtidos nos capítulos I e II reforçaram o potencial terapêutico da testosterona para intervenção no TCE, devido a modulação positiva na função mitocondrial.

Nesse estudo, camundongos foram submetidos ao TCE severo e tratados por 10 dias com testosterona. Avaliamos a homeostase do cálcio, bioenergética mitocondrial, parâmetros redox e indicadores moleculares de neurodegeneração em amostras de córtex do hemisfério ipsilateral. O TCE aumentou a captação de cálcio e apresentou extrusão de cálcio prejudicada por meio do NCLX e a testosterona preveniu esse efeito. A redução no efluxo de cálcio induzida por TCE foi associada à deterioração da dinâmica do potencial da membrana mitocondrial e à diminuição da eficiência de acoplamento da síntese de ATP mitocondrial. Além disso, foi observado aumento na produção de peróxido de hidrogênio pós-TCE, mas não no imunoconteúdo da proteína SOD2. A administração de testosterona reduziu significativamente essas alterações. Em nível molecular, a testosterona preveniu o aumento da fragmentação de tau e também fosforilação da proteína Tau na serina 396, além do aumento da clivagem de espectrina alfa por ativação de Calpaína-2. Adicionalmente, a testosterona diminuiu tanto a ativação de Caspase-3 quanto a relação Bax / BCL-2, sugerindo uma regulação negativa de sinais apoptóticos mitocondriais. Realizando uma análise com banco de dados de genes (STRING) obtivemos dois agrupamentos de genes / proteínas distintas reguladas positivamente e regulados negativamente, interconectados por meio do SOD2.

Portanto, a administração de testosterona após um TCE severo melhorou a extrusão de cálcio através do trocador de NCLX e a função mitocondrial, reduzindo a expressão excessiva de fatores moleculares associados com a neurodegeneração. Sugerimos assim, que a testosterona tem potencial terapêutico no TCE.

Journal of Neurotrauma

DOI: 10.1089/neu.2018.6266


# Testosterone administration after traumatic brain injury reduces mitochondrial dysfunction and neurodegeneration

Randhall B Carteri, *MSc*,[1] Afonso Kopczynski,[1] Marcelo Salimen Rodolphi *MSc*,[1] Nathan Ryzewski Strogulski, *MSc*,[1] Mônia Sartor,[1] Marceli Feldmann,[1] Marco Antonio De Bastiani, *MSc,* Clovis Milton Duval Wannmacher, *PhD*,[2] Itiane Diehl de Franceschi, *PhD*,[2] Gisele Hansel, *PhD*,[3] Douglas H. Smith[3,] *MD*, Luis Valmor Portela, *PhD*[1*]

[1] Laboratório de Neurotrauma e Biomarcadores - Departamento de Bioquímica, Programa de Pós Graduação em Bioquímica, ICBS, Universidade Federal do Rio Grande do Sul - UFRGS, Porto Alegre, RS, Brasil.

[2] Departmento de Bioquímica, Programa de Posgraduação em Bioquímica, ICBS, Universidade Federal do Rio Grande do Sul - UFRGS, Porto Alegre, RS, Brazil.

[3] Penn Center for Brain Injury and Repair and Department of Neurosurgery, Perelman School of Medicine, University of Pennsylvania, Philadelphia, PA, USA.

**Correspondence:**

* Dr. Luis V. Portela,

Department of Biochemistry,

ICBS, UFRGS. Rua Ramiro Barcelos, 2600 anexo

90035-003, Porto Alegre, RS, Brazil.

Tel: 55 51 33085558; Fax: 55 51 33085544;

E-mail: roskaportela@gmail.com

**Running title:** Testosterone and mitochondrial function after TBI

**Table of contents title:** Testosterone impedes bioenergetics deficits and reduces neurodegeneration after TBI.

Journal of Neurotrauma
Testosterone administration after traumatic brain injury reduces mitochondrial dysfunction and neurodegeneration (DOI: 10.1089/neu.2018.6266)
This paper has been peer-reviewed and accepted for publication, but has yet to undergo copyediting and proof correction. The final published version may differ from this proof.

**Complete address**

**Luis Valmor Portela, *PhD** (Corresponding author)**

Departamento de Bioquímica, ICBS, UFRGS

Rua Ramiro Barcelos 2600, anexo

Bairro Santana, Porto Alegre, RS

Phone: 55 51 33085557

Fax: 55 51 33085540

roskaportela@gmail.com

**Randhall B Carteri, *MSc*,**

Departamento de Bioquímica, ICBS, UFRGS

Rua Ramiro Barcelos 2600, anexo

Bairro Santana, Porto Alegre, RS

Phone: 55 51 33085557

Fax: 55 51 33085540

rcarteri@outlook.com

**Afonso Kopczynski,**

Departamento de Bioquímica, ICBS, UFRGS

Rua Ramiro Barcelos 2600, anexo

Bairro Santana, Porto Alegre, RS

Phone: 55 51 33085557

Fax: 55 51 33085540

afonsokcarvalho@gmail.com

**Marcelo Salimen Rodolphi *MSc*,**

Departamento de Bioquímica, ICBS, UFRGS

Rua Ramiro Barcelos 2600, anexo

Bairro Santana, Porto Alegre, RS

Phone: 55 51 33085557

Fax: 55 51 33085540

marcsalimen@gmail.com

**Nathan Ryzewski Strogulski, *MSc*,**

Departamento de Bioquímica, ICBS, UFRGS

Rua Ramiro Barcelos 2600, anexo

Bairro Santana, Porto Alegre, RS

Phone: 55 51 33085557

Fax: 55 51 33085540

n.strogulski@gmail.com



Journal of Neurotrauma
Testosterone administration after traumatic brain injury reduces mitochondrial dysfunction and neurodegeneration (DOI: 10.1089/neu.2018.6266)
This paper has been peer-reviewed and accepted for publication, but has yet to undergo copyediting and proof correction. The final published version may differ from this proof.

Journal of Neurotrauma
Testosterone administration after traumatic brain injury reduces mitochondrial dysfunction and neurodegeneration (DOI: 10.1089/neu.2018.6266)
This paper has been peer-reviewed and accepted for publication, but has yet to undergo copyediting and proof correction. The final published version may differ from this proof.

**Mônia Sartor,**

Departamento de Bioquímica, ICBS, UFRGS

Rua Ramiro Barcelos 2600, anexo

Bairro Santana, Porto Alegre, RS

Phone: 55 51 33085557

Fax: 55 51 33085540

monia_sartor@hotmail.com

**Marceli Feldmann,**

Departamento de Bioquímica, ICBS, UFRGS

Rua Ramiro Barcelos 2600, anexo

Bairro Santana, Porto Alegre, RS

Phone: 55 51 33085557

Fax: 55 51 33085540

marcelifeldmann@hotmail.com

**Marco Antonio De Bastiani, *MSc,***

Departamento de Bioquímica, ICBS, UFRGS

Rua Ramiro Barcelos 2600, anexo

Bairro Santana, Porto Alegre, RS

Phone: 55 51 33085557

Fax: 55 51 33085540

tyrev@hotmail.com

**Clovis Milton Duval Wannmacher, *PhD*,**

Departamento de Bioquímica, ICBS, UFRGS

Rua Ramiro Barcelos 2600, anexo

Bairro Santana, Porto Alegre, RS

Phone: 55 51 33085557

Fax: 55 51 33085540

clovisdw@ufrgs.br

**Itiane Diehl de Franceschi, *PhD*,**

Departamento de Bioquímica, ICBS, UFRGS

Rua Ramiro Barcelos 2600, anexo

Bairro Santana, Porto Alegre, RS

Phone: 55 51 33085557

Fax: 55 51 33085540

itidiehl@yahoo.com.br

**Gisele Hansel, *PhD*,**

Penn Center for Brain Injury and Repair and Department of Neurosurgery, Perelman School of Medicine, University of Pennsylvania.



Journal of Neurotrauma
Testosterone administration after traumatic brain injury reduces mitochondrial dysfunction and neurodegeneration (DOI: 10.1089/neu.2018.6266)
This paper has been peer-reviewed and accepted for publication, but has yet to undergo copyediting and proof correction. The final published version may differ from this proof.

Penn Center for Brain Injury and Repair and Department of Neurosurgery,

Perelman School of Medicine, University of Pennsylvania,

105 Hayden Hall, 3320 Smith Walk, Philadelphia, PA, USA.

Zip code: 19104-6316

Tel. +1 215-8980881

Fax. +1 215-5733808

gihansel@gmail.com

**Douglas H. Smith*** ***MD*****,**

Penn Center for Brain Injury and Repair and Department of Neurosurgery,

Perelman School of Medicine, University of Pennsylvania,

105 Hayden Hall, 3320 Smith Walk, Philadelphia, PA, USA.

Zip code: 19104-6316

Tel. +1 215-8980881

Fax. +1 215-5733808

smithdou@mail.med.upenn.edu



Journal of Neurotrauma
Testosterone administration after traumatic brain injury reduces mitochondrial dysfunction and neurodegeneration (DOI: 10.1089/neu.2018.6266)
This paper has been peer-reviewed and accepted for publication, but has yet to undergo copyediting and proof correction. The final published version may differ from this proof.

Journal of Neurotrauma
Testosterone administration after traumatic brain injury reduces mitochondrial dysfunction and neurodegeneration (DOI: 10.1089/neu.2018.6266)
This paper has been peer-reviewed and accepted for publication, but has yet to undergo copyediting and proof correction. The final published version may differ from this proof.

## ABSTRACT

Traumatic brain injury (TBI) increases $Ca^{2+}$ influx into neurons and desynchronizes mitochondrial function leading to energy depletion and apoptosis. This process may be influenced by brain testosterone (TS) levels, which are known to decrease after TBI. We hypothesized that a TS based therapy could preserve mitochondrial neuroenergetics after TBI, thereby reducing neurodegeneration. C57BL/6J mice were submitted to sham treatment or severe parasagittal CCI and were subcutaneously injected with either vehicle (VEH-SHAM and VEH-CCI) or testosterone cypionate (15 mg/kg, TS-CCI) for 10 days. Cortical tissue homogenates ipsilateral to injury were used for neurochemical analysis. The VEH-CCI group displayed an increased $Ca^{2+}$-induced mitochondrial swelling after the addition of metabolic substrates (PMGSA). The addition of $Na^{+}$ stimulated mitochondrial $Ca^{2+}$ extrusion through $Na^{+}/Ca^{2+}/Li^{+}$ exchanger (NCLX) in VEH-SHAM and TS-CCI, but not in the VEH-CCI group. Reduction in $Ca^{2+}$ efflux post-injury was associated with impaired mitochondrial membrane potential formation/dissipation, and decreased mitochondrial ATP-synthase coupling efficiency. Corroborating evidence of mitochondrial uncoupling was observed with an increase in $H_2O_2$ production post-injury, but not in SOD2 protein levels. TS administration significantly reduced these neuroenergetic alterations. At molecular level, TS prevented the increase in $pTau^{Ser396}$ and alpha-Spectrin fragmentation by the $Ca^{2+}$dependent Calpain-2 activation, and decreased both Caspase-3 activation and Bax/BCL-2 ratio, which suggests a downregulation of mitochondrial apoptotic signals. STRING database provided two distinct gene/protein clusters “upregulated and downregulated” interconnected through SOD2. Therefore, TS administration after a severe CCI improves the mitochondrial $Ca^{2+}$extrusion through NCLX exchanger and ATP synthesis efficiency, ultimately downregulating the overexpression of molecular drivers of neurodegeneration.

**Keywords: Traumatic brain injury, testosterone, mitochondria, neuroenergetics, neurodegeneration.**

Journal of Neurotrauma
Testosterone administration after traumatic brain injury reduces mitochondrial dysfunction and neurodegeneration (DOI: 10.1089/neu.2018.6266)
This paper has been peer-reviewed and accepted for publication, but has yet to undergo copyediting and proof correction. The final published version may differ from this proof.

## INTRODUCTION

Now recognized as a major health disorder, traumatic brain injury (TBI) commonly results in persisting neurological dysfunction.[1-2] The initial pathophysiological changes resulting from primary mechanical damage can trigger secondary deleterious effects, including progressive neurodegeneration.[3] However, the cellular and molecular mechanisms involved in these progressive changes are poorly understood.[4-5] Nonetheless, it has been suggested that persisting metabolic dysfunction may underlie some of the pathological features of chronic TBI.

In experimental TBI, mitochondrial dysfunction has commonly been described as a source of cellular metabolic crisis.[6-7] This is thought to reflect, in part, pathological increases in intracellular calcium concentrations, which in turn is sequestered by the mitochondria. However, this buffering of calcium comes at a cost of a decreased capacity of mitochondria to generate ATP. The resultant hypometabolism may desynchronize cell function concomitant with a rise in reactive oxygen species.[8-9] With increases in calcium exceeding the capacity of mitochondrial sequestration, proteases such as calpain are activated, causing chemical destruction of the cytoskeleton, which can ultimately lead to cell death.[10]

The entrance of $Ca^{2+}$ in the mitochondrial matrix is mediated through the mitochondrial calcium uniporter (MCU), which imports $Ca^{2+}$across the inner membrane partially, thereby dissipating the mitochondrial membrane potential ($\Delta\Psi_m$). In contrast, the mitochondrial sodium–calcium-lithium exchanger (NCLX), balances $Ca^{2+}$ influx by extruding one $Ca^{2+}$ ion in exchange for three sodium ions ($Na^{+}$).[11] Further, the NCLX is proposed to be responsible for mitochondrial $Ca^{2+}$ extrusion in excitable cells like neurons. Thus, it has been proposed that TBI primes neurons to die owing the confluence of mitochondrial dysfunction and subsequent degenerative processes.[12] Indeed, there has been substantial interest in pharmacologically targeting deleterious pathways in mitochondria after TBI. [9-13-14]

Testosterone (TS) is a gonadal hormone that improves brain glucose metabolism, synaptic plasticity,[15] antioxidant defenses, neurogenesis and cell survival after different *in vitro* and *in vivo* injury models[16] via reductions of pro-apoptotic stimuli.[17] In contrast,

Journal of Neurotrauma
Testosterone administration after traumatic brain injury reduces mitochondrial dysfunction and neurodegeneration (DOI: 10.1089/neu.2018.6266)
This paper has been peer-reviewed and accepted for publication, but has yet to undergo copyediting and proof correction. The final published version may differ from this proof.

decreased TS levels in castrated rats caused perturbations in the hippocampal mitochondrial genes involved in the electron transport system, biogenesis, and oxidative metabolism. However, these processes were recovered soon after the androgen replacement therapy was initiated. Hence, at least in part, the benefits of TS therapy on the brain likely involves direct effects on mitochondrial function.[18] Noteworthy, mice brain TS levels inversely correlate with edema formation and neurological deficits after TBI.[19] Additionally, adult TBI patients are susceptible to acute perturbations in the pituitary function, namely post-traumatic hypopituitarism,[20-21] leading to hypogonadotropic hypogonadism and deficiency in the TS levels. Furthermore, total TS levels were significantly lower in the acute phase of severe TBI compared with mild and moderate TBI.[22] These observations suggest potential benefits of TS therapy after TBI in different aspects of neural cells physiology, including increased neuroenergetic efficiency coupled with a downregulation of apoptotic signals.

Here, a rodent model of severe TBI was used to explore effects of testosterone therapy after injury in context with mitochondria function.

## MATERIAL AND METHODS

### *Animals and treatment protocol*

Ninety-days-old C57BL/6J male mice were obtained from Foundation for Health Science Research (FEPPS, Porto Alegre/RS, Brazil). A total of thirty animals (4-5 per cage) were placed into a controlled temperature room (22ºC $\pm$ 1) under a 12h light/12h dark cycle (lights on at 7 a.m.) and had free access to food and water. The treatment consisted of a daily injection of an equal volume (50 uL) of corn oil (vehicle groups, VEH-SHAM and VEH-CCI; 10 animals per each group) or testosterone cypionate (15 mg/kg; based on previously published work[23]; (Sigma-pharma®, TS-CCI group; 10 animals per group), between 2 p.m. to 3 p.m for 10 days after the head trauma. Subsequently, animals were euthanized and the ipsilateral cortex surrounding the impact injury was dissected for neurochemical analysis. After CCI, animals were randomly assigned to both TS or VEH groups by two trained researchers. The treatment started twenty-four hours after the CCI injury. See the experimental design in Figure 1. All experiments were in agreement with

the Committee on the Care and Use of Experimental Animal Resources, UFRGS, Brazil number 22436.

*Controlled Cortical Impact protocol (CCI)*

To cause TBI, mice were placed in the stereotaxic (Kopf Instruments, Tujunga, CA) with a heating bed (37 ± 1$^{o}$C) and maintained with anesthesia inhalation (2.5 % isoflurane) in a mixture of $N_2$ and $O_2$ (2:1) during the entire surgical procedure. A 4 mm diameter craniotomy was made in the central part of the left parietal bone to perform the CCI injury using an equipment Benchmark stereotaxic impactor, myNeuroLab®, Leica, St. Louis, MO, USA. The injury was induced by a piston of 3.0 mm diameter on the exposed surface of the intact dura mater. Other lesion parameters were fully adjusted in the equipment, as follows: impact velocity of 5.7 m / s; impact duration was 100 ms, and 2 mm of depth penetration. Soon after injury, the area of the craniotomy was isolated with a concave lamella bonded with dental cement, and the scalp was sutured. After the surgical procedure, anesthesia was discontinued and the animals were placed in a heated box to maintain normal body temperature and were monitored for 2 h post-injury.[24]

*Modified Neurological Severity Score*

The evaluation of CCI-induced neurological impairment was performed by two independent single-blinded trained researchers, 24 h after CCI injury using a modified Neurological Severity Score (mNSS). The TS and vehicle administration was initiated after the mNSS test. The previously described 10-point scale[25] was modified to a 6-point scale, assessing functional neurological status of mice based on the presence of reflexes and the ability to perform motor and behavioral tasks, evaluated with the following behavioral composite: a) Exit square; b) Seeking behavior; c) Straight walk; d) Startle reflex; e) Beam balancing; and f) Round stick balancing. One point is awarded for failing to perform a task; thus, a normal, uninjured mouse scores 0.

*Preparation of ipsilateral cortex homogenates*

The whole ipsilateral cortex of mice were collected 10 days after CCI and then homogenized in a specific buffer (320 mM sucrose, 1mM EDTA, pH 7.4).[26]using a pre-



Journal of Neurotrauma
Testosterone administration after traumatic brain injury reduces mitochondrial dysfunction and neurodegeneration (DOI: 10.1089/neu.2018.6266)
This paper has been peer-reviewed and accepted for publication, but has yet to undergo copyediting and proof correction. The final published version may differ from this proof.

cooled glass potter with 10 to 15 strokes. Following a centrifugation step of 1350 *x*g for 3 min at 4 °C, the resulting mitochondria-enriched homogenates in the supernatant, were aliquoted and used for respirometry, calcium handling, mitochondrial membrane potential, and hydrogen peroxide analysis. These assays were performed all simultaneously by the researchers according to their methodological skills, in a time-frame of 10 minutes from euthanasia and start of the analysis, or sample processing for MTT assay. The samples were frozen at − 80 °C for protein quantification and further oxidative stress parameters and western blotting assays. The Pierce™ BCA Protein Assay Kit (Catalog number: 23225) was used for quantification of protein contents of the homogenized samples. The assay was performed according to the manufacturer's instructions. Measurements were performed in triplicates (coefficient of variation between duplicates was < 3 %) and corrected for the absorbance measured in the homogenization buffer only.

*Mitochondrial calcium handling*

To assess mitochondrial calcium buffering capacity, namely calcium influx and efflux, we measured the absorbance spectrophotometrically at 540 nm (Spectra Max M5, Molecular Devices). Mitochondria maintain the fluxes of ions across the inner membrane tightly controlled. This is particularly important because the dual physiological and detrimental roles of $Ca^{2+}$ in the mitochondrial matrix.[11] Ipsilateral cortex homogenates (50 uL) obtained from 10-day-old treated mice were added to standard swelling incubation medium (100 mM KCl, 50 mM Sucrose, 10 mM HEPES and 5 mM $KH_2PO4$) and the basal mitochondrial absorbance was monitored during 3 min in microplates. Mitochondrial substrates, 3.5 mM pyruvate, 4.5 mM malate, 4.5 mM glutamate, 1.2 mM succinate (PMGSA) and 100 uM of adenosine diphosphate (ADP) were added to energize mitochondria and support ATP synthesis. Thus, the absorbance coupled with oxidative phosphorylation was monitored during 5 min. Afterward, calcium ($Ca^{2+}$, 20 mM) was added to induce large-amplitude swelling driven by the colloid osmotic force of $Ca^{2+}$ influx at proteins localized in the mitochondrial matrix. The decrease in the absorbance caused by the $Ca^{2+}$ influx was monitored for 10 min. After calcium-induced mitochondrial swelling, we accessed mitochondrial $Ca^{2+}$ efflux as an indicator of shrinkage. Then, $Na^{+}$ (30 mM) was added to the medium and the increase in the absorbance was monitored for additional 10

Journal of Neurotrauma
Testosterone administration after traumatic brain injury reduces mitochondrial dysfunction and neurodegeneration (DOI: 10.1089/neu.2018.6266)
This paper has been peer-reviewed and accepted for publication, but has yet to undergo copyediting and proof correction. The final published version may differ from this proof.

min. For a mitochondrial enriched suspension, the swelling and shrinkage causes a decrease and increase in the absorbance respectively, which are both discernible even to the naked eye.[27] Finally, we normalized all results for protein content. Also, we used the baseline $Ca^{2+}$ from each group to standardize their own data, and calculated the percentage of variation in the absorbance (540 nm) after the addition of substrates (PMGSA) relative to basal; after addition of $Ca^{2+}$ relative to (PMGSA); and after addition of $Na^{+}$ relative to $Ca^{2+}$.

*Mitochondrial Membrane Potential ($\Delta\Psi_m$)*

The ΔΨm was measured 10 days after CCI through the fluorescence signal emitted by the cationic dye, safranin-O. Ipsilateral cortex homogenates were incubated in the respiration buffer used for the respirometry protocol, additionally supplemented with 10 μM safranin-*O*. The fluorescence was detected with an excitation wavelength of 495 nm and an emission wavelength of 586 nm (Spectra Max M5, Molecular Devices). An increased the fluorescence units mirror decreased $\Delta\Psi_m$ whereas decreased fluorescence units indicate increased $\Delta\Psi_m$. Baseline $\Delta\Psi_m$ was measured without addition of substrates and inhibitors in the incubation medium.

Further, PMGS and ADP (2.5 mM) were incubated to modulate the activity of mitochondrial respiratory complex I, II and V, and consequently ΔΨm. Increased ADP utilization after the addition of PMGS mirrors increased oxygen consumption coupled with ATP synthesis by the F0F1- ATP synthase (respiratory Complex V) along with decreased $\Delta\Psi_m$. Addition of the proton ionophore Carbonyl cyanide 4-trifluoromethoxy-phenylhydrazone (FCCP 1 μM), a chemical uncoupler, trigger decrease in the $\Delta\Psi_m$ and oxidative phosphorylation while stimulates the maximal mitochondrial oxygen consumption. The addition of Sodium azide (NaN6; 20 mM), an inhibitor of mitochondrial respiratory complex IV (cytochrome oxidase), was used to decrease ATP synthesis and disrupt mitochondrial membrane potential. Moreover, we used the data achieved through the manipulation of mitochondrial respiratory rates with the components PMGS, ADP, FCCP and AZ to calculate the percentage of change in the $\Delta\Psi_m$. Each component has a percentage of variation relative to the previous one. For instance, PMGS is relative to the

baseline, and ADP is relative to the PMGS. Data are reported as arbitrary fluorescence units (AFUs) and were normalized to protein content.[28]

*Mitochondrial respiratory protocol*

The ipsilateral cortex of mice was dissected 10 days after CCI and then homogenized in a specific buffer (320 mM sucrose, 1mM EDTA, 0.25 mM dithiothreitol, pH 7.4). Oxygen consumption measurements were performed using a standard respiration buffer (100 mM KCI, 75 mM mannitol, 25 mM sucrose, 5 mM phosphate, 0.05 mM EDTA, and 10 mM Tris-HC1, pH 7.4). Oxygen consumption per tissue mass was measured using the high-resolution Oxygraph-2k system and recorded real-time using DatLab software (Oroboros, Innsbruck, Austria). The results were normalized to the protein content. The experiments were performed at 37°C in a 2-ml chamber, with a modified multi-substrate titration protocol as previously described in detail elsewhere.[26]

Following 5 minutes for establishing routine respiration values, the multi-substrate titration protocol started. The protocol consisted of sequential addition of pyruvate, malate, and glutamate (PMG; 10, 10, and 20 mM, respectively) to obtain State IV respiration; Sub sequentially, adenosine diphosphate (ADP, 2.5 mM) was titrated to obtain OxPHOS capacity of Complex I-Linked substrates (State III); Maximal OxPHOS capacity (StateIII) was obtained with the addition of Succinate (S, 10 mM) in saturating ADP concentrations and non-mitochondrial respiration (ROX) after cyanide (KCN, 5 mM).

Respiratory fluxes were corrected automatically for instrumental background by DatLab taking into account oxygen consumption of the oxygen sensor and oxygen diffusion out of or into the oxygraph chamber measured at experimental conditions in incubation medium without biological sample. ROX was extracted from all of the above-mentioned states and tissue-mass specific oxygen fluxes were compared in different substrate and coupling states.

We calculated flux control factors (FCF), which express the change of flux in a single step of the SUIT protocol, normalized for the high flux as a specific reference state. The respiratory control ratio (RCR = P/L) was obtained in the CI-linked substrate state. For statistical analysis RCR was transformed to its respective FCF, which is the OXPHOS



Journal of Neurotrauma
Testosterone administration after traumatic brain injury reduces mitochondrial dysfunction and neurodegeneration (DOI: 10.1089/neu.2018.6266)
This paper has been peer-reviewed and accepted for publication, but has yet to undergo copyediting and proof correction. The final published version may differ from this proof.

Journal of Neurotrauma
Testosterone administration after traumatic brain injury reduces mitochondrial dysfunction and neurodegeneration (DOI: 10.1089/neu.2018.6266)
This paper has been peer-reviewed and accepted for publication, but has yet to undergo copyediting and proof correction. The final published version may differ from this proof.

coupling efficiency calculated as (P-L)/P = 1-L/P. The FCF for the CII-linked substrate stimulating STATE III respiration (succinate effect) was calculated as 1 – CI/CI&II, determined in the OXPHOS state in the protocol.[26-29] This analysis informs the influence of Complex II on the respiromety of other oxidative complexes. Since RCR ranges from 1.0 to infinity, we calculated the oxidative phosphorylation coupling efficiency, which has boundaries from 0.0 to 1.0 and is directly related to classic RCR (State III/State IV).

*Mitochondrial $H_2O_2$ production and oxidative stress markers*

The pattern of mitochondrial production of hydrogen peroxide ($H_2O_2$) under the modulation of TS was assessed in the ipsilateral cortex homogenates 10 days after CCI through the Amplex Red oxidation method. The same substrates, uncoupler and inhibitors used in the respirometry protocol were incubated sequentially in the respiration buffer supplemented with 10 µM Amplex Red and 2 units/mL horseradish peroxidase to assess $H_2O_2$ generation. The baseline $H_2O_2$ level was measured without the presence of substrate in the incubation medium. Also, PMGS was used as the substrate to stimulate mitochondrial respiration, ADP to analyze the functional capacity of mitochondria to produce ATP, and the proton ionophore FCCP (Carbonyl cyanide 4-trifluoromethoxy-phenylhydrazone, a reversible inhibitor of mitochondrial oxidative phosphorylation) to estimate the maximal mitochondrial electron transport system capacity. Sodium Azide was used to assess non-mitochondrial $H_2O_2$ production (ROX). Fluorescence was monitored at excitation (563 nm) and emission (587 nm) wavelengths with a Spectra Max M5 microplate reader (Molecular Devices, USA).[28]

Moreover, at 10 days following CCI we measured the activity of enzymes involved in the $H_2O_2$ production (Superoxide dismutase - SOD) and degradation (glutathione peroxidase – GPx); the expression levels of the mitochondrial enzyme manganese superoxide dismutase (MnSOD) and total ROS production, altogether here designated as oxidative stress biomarkers. The measurements were performed, as follows:

*a. 2’7’-Dihydro-dichlorofluorescein (DCFH) Oxidation Assay*

The measure of global reactive oxygen species (ROS) production in the ipsilateral cortex homogenates was performed using reduced 2'7'-dihydro-dichlorofluorescein

Journal of Neurotrauma
Testosterone administration after traumatic brain injury reduces mitochondrial dysfunction and neurodegeneration (DOI: 10.1089/neu.2018.6266)
This paper has been peer-reviewed and accepted for publication, but has yet to undergo copyediting and proof correction. The final published version may differ from this proof.

diacetate (DCF-DA). Samples were incubated for 30 min at 37 ºC in the dark with 20 mM sodium phosphate, 140 mM KCl buffer pH 7.4 and 100 µM reduced 2'7'-Dichlorofluorescein diacetate ($H_2$DCF-DA) solution in a 96 wells plate. The $H_2$DCF-DA is enzymatically hydrolyzed by intracellular esterases and $H_2$DCF formed is oxidized by ROS being the DCF fluorescence (480 and 535 nm) proportional to the amount of ROS formed. The calibration curve was performed with standard DCF (0.25–10 µM), and the levels of reactive species were expressed as nmol of DCF formed per mg of protein.[30]

*b. Superoxide Dismutase (SOD) Activity Assay*

SOD activity in the ipsilateral cortex homogenates was determined based on the capacity of pyrogallol to autoxidize, a process highly dependent on superoxide radical.[31] The inhibition of autoxidation of this compound occurs in the presence of SOD, whose activity can be indirectly assayed spectrophotometrically at 420 nm. A calibration curve was performed with purified SOD as standard. A 50 % inhibition of pyrogallol autoxidation is defined as one unit of SOD, and the specific activity was expressed as SOD units per mg of protein. The expression level of MnSOD was analyzed through western blotting (see the session below).

*c. Glutathione Peroxidase (GPx) Assay*

GPx activity in the ipsilateral cortex homogenates was measured using tert-butylhydroperoxide as substrate.[32] The enzyme activity was determined by monitoring the nicotinamide adenosine dinucleotide phosphate (NADPH) disappearance at 340 nm. The medium contain 100 mM potassium phosphate, 1 mM ethylenediaminetetraacetic acid buffer pH 7.7, 0.4 mM azide, 2 mM glutathione reduced, 0.15 U/mL glutathione reductase, 0.1 mM NADPH, 0.5 mM tert-butyl-hydroperoxide, and supernatant sample. One GPx unit is defined as 1 µmol of NADPH consumed per minute. The specific activity was expressed as micromole of NADPH consumed per minute per mg of protein.

*Western blotting*

The Ipsilateral cortex of mice was dissected 10 days after CCI and then homogenized in a buffer solution (EDTA 2 mM, protease and phosphatase inhibitor

Journal of Neurotrauma
Testosterone administration after traumatic brain injury reduces mitochondrial dysfunction and neurodegeneration (DOI: 10.1089/neu.2018.6266)
This paper has been peer-reviewed and accepted for publication, but has yet to undergo copyediting and proof correction. The final published version may differ from this proof.

cocktails I and II (Sigma, St. Louis, USA) 0.001 %, Tris HCl 50 mM, (pH 7,4), glycerol 10 % and Triton X-100 1 %) and centrifuged (1300 g/ 3 min). Supernatant was collected and diluted in an appropriated sample buffer. Samples of 20 µg of protein (n=6-8 per group) were separated by electrophoresis on a 10% or 12% polyacrylamide gel and electrotransferred to PVDF membranes (Amersham, GE Healthcare, Little Chalfont, UK) as previously reported.[33] Primary antibodies against Alpha-Spectrin (Millipore®, GER; 1:1000; ref. MAB1622), Calpain-2 (Cell Signalling®, USA; 1:1000; ref. 2539), Anti-Bax (ABCAM®, USA; 1:1000; ref. ab7977), anti-BCL-2 (ABCAM®, USA; 1:1000; ref. ab7973); Anti-MnSOD (ABCAM®, USA; 1:1000; ref. ab13533); Anti-Tau phospho-S396 (ABCAM®, USA; 1:1000; ref. ab109390); Anti-Tau antibody (ABCAM®, USA; 1:1000; ref. ab32057); Caspase-3 (8G10) (Cell Signalling®, USA; 1:1000; ref. 9665) Cleaved Caspase-3 (Cell Signalling®, USA; 1:1000; ref. 9664). All procedures were conducted according to specific antibody manufacturer's instruction. Primary antibodies were incubated overnight followed by 2 h incubation with horseradish peroxidase-conjugated anti-rabbit or anti-mouse IgG (1:5000) (GE, Little Chalfont, UK) secondary antibodies. Membranes were incubated with Amersham ECL Western Blotting Detection Reagent (GE Healthcare Life Sciences, Little Chalfont, UK) for 5 min and the immunodetection was made by chemoluminescence using Image Quant LAS 4000 (GE, Little Chalfont, UK). The protein expression was quantified using Image J® software (Rockville, USA). The values of optic density were expressed as % of control.

*Cell viability assay*

Cell viability assay was performed 10 days after CCI through the colorimetric [3(4,5-dimethylthiazol-2- yl)- 2,5-diphenyl tetrazolium bromide] (MTT, Sigma) method.[34] Cell homogenates were incubated with 0.5 mg/ml of MTT, at 37°C during 45 min. The formazan product generated during the incubation was solubilized in dimethyl sulfoxide and measured at 560 and 630 nm. The results were expressed as the percentage of control.

*Protein-Protein Interaction Network and Differential Expression Analysis*

Functional interplay between proteins can often be inferred from genomic associations between the genes that encode them. The Search Tool for the Retrieval of

Interacting Genes/Proteins (STRING) is a relational biological database and web source (https://string-db.org/) used to store known and predicted protein-protein interactions. The database utilizes an interaction scoring system computed by combining the probabilities from different evidence channels and corrected for the probability of randomly observing and interaction. Input queries are associated using this scoring system and a graphical network representation can be generated to demonstrate their pairwise interactions. Network representations may provide insights of functional protein interactions (direct and indirect), which facilitate the analysis of modularity in biological processes.[35] The protein-protein interaction (PPI) network between the genes, Sdha and Sdhb (subunits of mitochondrial complex II-succinate dehydrogenase); Atp5d, Atp5a1 and Atp5c1 (subunits of mitochondrial complex V-ATP synthase), and SOD2 (manganese superoxide dismutase-2); Bcl2 (B-Cell Lynphoma 2) and Bax (Bcl-2-like protein 4); Casp3 (Caspase-3) and Capn2 (Calpain-2); Mapt (microtubules associated protein Tau), was constructed using STRINGdb package (STRING version 10).[36] The network association topology obtained then was used to map transcriptomic analyses results with RedeR package.[37]

Based on the experimental molecular and functional results obtained, we searched gene expression data in TBI studies similar to ours, i.e. adult male mice strain C57BL/6, submitted to a single severe CCI injury in the dura matter, ipsilateral brain cortex samples analysis, and the endpoint for the neurochemical analysis close to 10 days after the CCI. We found one study, which partially matched these criteria using adult male mice C57BL/6, submitted to severe CCI, and brain ipsilateral cortex gene expression profiling at day 3 after CCI.[38] Expression data was obtained from Gene Expression Omnibus (GEO) using GEOquery package[39] under the identification GSE58485.[38] Using this dataset, differentially expressed genes of TBI versus Control were obtained using the limma package.[40]

*Statistical Analysis*

Results were calculated and expressed as the mean ± S.E.M. To analyze the differences between groups, we used one-way analysis of variance (ANOVA) followed by a

post-hoc Tukey test; or Kruskal-Wallis test when necessary. All procedures were performed using GraphPad Prism 6.0 software. The differences were considered statistically significant at $p < 0.05$.

## Results

### *Neurological Scores is impaired after CCI*

As expected, we found higher neurological scores (mNSS) in the CCI group relative to SHAM implying in functional impairment of sensory-motor, spatial orientation, reflex, balance and explorative behavior 24 h after the injury (data not shown).

### *Testosterone attenuated the calcium overload into mitochondria after CCI*

Physiologically, there are small fluctuations in the intramitochondrial $Ca^{2+}$ levels and even large transitory increments have low impact to cells integrity. While calcium is an essential signaling molecule, persistent high calcium levels result in overactivaction of $Ca^{2+}$ dependent processes and mitochondrial calcium swelling. This mechanism has been considered the root for subsequent $\Delta\Psi_m$ depolarization, decreased ATP synthesis and increased apoptotic signals observed in neurodegenerative disorders.[11] We found similar mitochondrial $Ca^{2+}$ influx after the energization with PMGSA, implying that all groups were able to respond to a pulse of $Ca^{2+}$ (Figure 2A and B).

However, after the subsequent addition of $Na^+$ to the incubation medium in order to stimulate mitochondrial $Ca^{2+}$ extrusion, the mitochondria swelling of VEH-CCI group remained elevated, indicating a persistent permanence of $Ca^{2+}$ inside mitochondria. In contrast, VEH-SHAM and TS-CCI groups displayed an increase in absorbance, which illustrates a normal mitochondrial $Ca^{2+}$ extrusion in the exchange with $Na^+$ (Figure 2A and B). Taken together, these results indicate that CCI induced an increased mitochondrial $Ca^{2+}$ swelling and deficient NCLX ($Na^+$-dependent) $Ca^{2+}$ shrinkage. Remarkably, TS administration improved the $Na^+$-dependent control of $Ca^{2+}$ levels within the mitochondria matrix in the TS-CCI group, implying it mediates NCLX function (Figure 2A). Also, the percentage of variation in the Ca2+ swelling due to the addition of $Na^+$ was negative for CCI in relation to the other groups, which particularly confirmed that in spite of normal



Journal of Neurotrauma
Testosterone administration after traumatic brain injury reduces mitochondrial dysfunction and neurodegeneration (DOI: 10.1089/neu.2018.6266)
This paper has been peer-reviewed and accepted for publication, but has yet to undergo copyediting and proof correction. The final published version may differ from this proof.

uptake; the $Ca^{2+}$ ions did not transit b (Figure 2B) back from the mitochondrial matrix to the cytosol.

***Testosterone prevented the rupture of mitochondrial membrane potential ($\Delta\Psi_m$) dynamics after CCI***

The entry of $Ca^{2+}$ into the matrix brings together a positive charge thereby generating a depolarizing current that partially dissipates the $\Delta\Psi_m$.[11] As mentioned, the $\Delta\Psi_m$ was measured through the fluorescence signal emitted by safranin-*O* after mitochondria from cortex homogenates had been energized and subsequently manipulated. The decrease in dye concentration in the medium parallels with the accumulation of the dye inside the mitochondria, which results in fluorescence quenching.[41] We showed that the $\Delta\Psi_m$ of VEH-CCI was significantly elevated at baseline and after the addition of FCCP when compared to other groups. Also, the addition of the metabolic substrates (PMGS) increased the $\Delta\Psi_m$ in VEH-CCI relative to other groups while an inhibitor of ATP synthase complex (AZ) completely dissipates $\Delta\Psi_m$ in all groups. Remarkably, TS administration after CCI was able to rescue the $\Delta\Psi_m$ to levels of the control group at baseline, as well as after PMGS and FCCP. After the addition of ADP subsequent to PMGS there was no apparent significant difference in the $\Delta\Psi_m$ between groups (Figure 3A and B). However, it can be noticed that ADP was added subsequent to PMGS (meaning PMGS+ADP) then the comparison of $\Delta\Psi_m$ between PMGS *vs* PMGS plus ADP shows that the VEH-CCI group does not respond to the stimulation whereas SHAM-VEH and TS-CCI groups had a decrease in the $\Delta\Psi_m$ of approximately 100%. Through the additional analysis of the percentage of variation, we confirmed the changes of $\Delta\Psi_m$ in the VEH-CCI group in response to ADP (Figure 3B).

Moreover, the percentage of variation in the $\Delta\Psi_m$ between baseline and PMGS; PMGS and ADP; ADP and FCCP; and FCCP and AZ confirmed that independent of the mitochondrial target explored here, the VEH-CCI group does not effectively generated and dissipated $\Delta\Psi_m$ as did TS-CCI and VEH-SHAM groups (Figure 3B). These detectable alterations in the $\Delta\Psi_m$ may exert negative impact for the formation of proton gradient coupled with ATP synthesis (OxPhos). Actually, when ADP was added to the incubation



Journal of Neurotrauma
Testosterone administration after traumatic brain injury reduces mitochondrial dysfunction and neurodegeneration (DOI: 10.1089/neu.2018.6266)
This paper has been peer-reviewed and accepted for publication, but has yet to undergo copyediting and proof correction. The final published version may differ from this proof.

medium the VEH-CCI group displayed decreased OxPhos capacity (see Figure 4C). Importantly, the percentage of variation in the $\Psi_m$ between VEH-SHAM and TS-CCI groups was not significantly different, which highlights that TS mediated effects on $Ca^{2+}$ swelling also benefits $\Delta\Psi_m$.

***Testosterone prevented the decrease in the OxPhos Coupling Efficiency after CCI***

It has long been recognized that $\Delta\psi_m$ is a critical parameter associated with the cellular capacity to generate ATP by oxidative phosphorylation. Indeed, the $\Delta\psi_m$ is the main component of the proton motive force generated beneath inner membrane during the electron transference through the mitochondrial respiratory complexes.[41] Given that neuroenergetics deficits are commonly associated with memory problems and neurodegeneration we additionally tested whether the alterations in the $\Delta\psi_m$ affect mitochondrial bioenergetics after CCI. Assessment of mitochondrial oxygen consumption was performed in the ipsilateral cortex homogenates. Different mitochondrial respiration states are shown in Figure 4. The representative standard SUIT protocol applied in the present study is illustrated by a VEH-SHAM sample (Figure 4A). The OCR level in the State III was significantly decreased in the VEH-CCI compared to the other groups (Figure 4B). Also, mitochondrial succinate effect and OxPhos Coupling Efficiency was also significantly impaired 10 days after CCI (Figure 4C). Testosterone supplementation prevented the decrease in the OCR, OxPhos Coupling efficiency, and the decrease in succinate effect (Figure 4D). These functional alterations confirm that $Ca^{2+}$ overload impairs $\Delta\psi_m$ and neuroenergetics efficiency, and suggests that brain oxygen consumption in response to metabolic substrates is partially diverted from ATP synthesis to production of ROS after CCI.

***Testosterone attenuated mitochondrial hydrogen peroxide production following CCI***

The mitochondrial oxidation of energy substrates coupled with electron transport system is considered the main site of ROS production including the $H_2O_2$. Here, the baseline $H_2O_2$ level 10 days after CCI was increased in the VEH-CCI compared to other groups (Figure 5A). The addition of the mitochondrial substrates (PMGS and ADP), an uncoupler (FCCP), and a complex VI inhibitor (AZ) evoked a significant increase in the



Journal of Neurotrauma
Testosterone administration after traumatic brain injury reduces mitochondrial dysfunction and neurodegeneration (DOI: 10.1089/neu.2018.6266)
This paper has been peer-reviewed and accepted for publication, but has yet to undergo copyediting and proof correction. The final published version may differ from this proof.

production of $H_2O_2$ by VEH-CCI and TS-CCI groups in relation to VEH-SHAM. However, TS administration after CCI (TS-CCI) caused a significant lower increment in the $H_2O_2$ level when compared to VEH-CCI, implying that testosterone attenuated mitochondrial mechanisms implicated in the rise of $H_2O_2$ levels (Figure 5A and B). Likewise, TS decreased the total ROS levels in mice submitted to CCI, which replicates the regulatory role observed for $H_2O_2$ (Figure 5B). No significant differences were found between groups concerning the enzymatic activity of SOD and GPx (Figure 5C and D, respectively). However, the protein expression level of mitochondrial superoxide dismutase (MnSOD) decreased significantly in the VEH-CCI relative to VEH-SHAM group. Remarkably, 10 days of TS administration after CCI significantly heightened the expression of MnSOD (Figure 5E), which highlights this protein as a molecular target of TS. Given that persistent increase in the $H_2O_2$ levels may cause cell damage, we further explored the mechanistic impact on biomarkers of apoptotic neurodegeneration.

***Testosterone attenuated the expression of molecular biomarkers of neurodegeneration after CCI***

The TBI induces a particular deformation in the neuronal morphology mirrored by axonal rupture and formation of varicosities.[10-42] Also, after TBI neurons displayed an abnormal aggregation of proteins, and increased phosphorylation and degradation of cytoskeletal proteins like Tau and alpha-Spectrin. These abnormalities are consistently associated with neurodegeneration. Here, we displayed increased immunocontent of $pTau^{Ser396}$ /total Tau in VEH-CCI compared to VEH-SHAM and TS-CCI (Figure 6A). Further, the Tau cleavage estimated by the ratio between total Tau (56 kDa)/ Tau fragment (17 kDa) showed an increase in the Tau fragmentation after CCI (Figure 6B). The expression levels of the calcium-activated proteolytic enzyme Calpain-2 was significantly increased in VEH-CCI group compared to other groups (Figure 6C). In addition, the axonal protein alpha-Spectrin (240 kDa), which is abnormally targeted by Calpain-2 thereby generating cleaved products (150/145 kDa), was measured to estimate the neuronal damage (Figure 6D). As expected, we found decreased alfa-Spectrin 240/150 ratio in the VEH-CCI group compared to other groups implying increased protein degradation.

Journal of Neurotrauma
Testosterone administration after traumatic brain injury reduces mitochondrial dysfunction and neurodegeneration (DOI: 10.1089/neu.2018.6266)
This paper has been peer-reviewed and accepted for publication, but has yet to undergo copyediting and proof correction. The final published version may differ from this proof.

The relative increase in the protein Bax/BCL-2 ratio denotes the abundance of mitochondrial intrinsic apoptotic signals in VEH-CCI group (Figure 6E). Moreover, an increased ratio of cleaved Caspase-3/total Caspase-3 reinforces the heightened proteolytic and apoptotic activities after CCI (Figure 6F). As expected, there was significant decreased cell viability in VEH-CCI compared to VEH-SHAM and TS-CCI groups (Figure 6G). Remarkably, 10 days of TS administration after CCI prevented the increase in the molecular effectors of neurodegeneration to date; Tau hyperphosphorylation and fragmentation, Calpain-2 linked with alpha-Spectrin degradation, Bax/BCL-2 ratio, and cleaved Caspase-3/total Caspase-3. Therefore, the aforementioned preserved mitochondrial $Ca^{2+}$ homeostasis and energy efficiency mediated by TS parallel with decreased apoptotic signals.

***Protein-protein interactions***

The resultant protein-protein interaction (PPI) network shows 11 genes/proteins in the nodes and association scores in the edges widths. The PPI network between the genes Sdha and Sdhb (subunits of mitochondrial complex II-succinate dehydrogenase), Atp5d, Atp5a1 and Atp5c1 (subunits of mitochondrial complex V-ATP synthase), Sod2 (manganese superoxide dismutase-2), Bcl2 and Bax; Casp3 (Caspase-3) and Capn2 (Calpain-2); Mapt (microtubules associated protein Tau) highlights two distinct clusters denoting CCI-induced signature: The right side cluster contains genes linked with mitochondrial bioenergetics and the left side cluster contains genes related to apoptotic neurodegeneration. After investigating the expression profile of these genes using the GSE58485 study, we can observe that the mitochondrial bioenergetics cluster is downregulated in CCI (blue), whereas the apoptosis cluster is upregulated in CCI (red) compared to the control group. Also, the two clusters interact functionally through mitochondrial superoxide dismutase (Sod2) gene, thus they are influencing each other in terms of cell physiology (Figure 7).

**DISCUSSION**

In the present study, TS administration after TBI was found to preserve crucial mitochondrial function linked with energy production. Efficacious effects included, maintaining $Ca^{2+}$ homeostasis, membrane potential, the influence of succinate on global

oxidative complexes respirometry, and OxPhos coupling. Collectively, these actions prevented alterations associated with neurodegeneration. These results suggest that TS treatment maintained aspects of mitochondrial function that promote ATP synthesis, thereby maintaining cell survival after severe injury.

It has been well established that pituitary and gonadal hormone levels are often decreased in the brain and plasma after a TBI. This occurs across the acute setting and persists in long-term survival, typically in association with neurological dysfunction. [19-22] Accordingly, TS supplementation after severe TBI appears to be an attractive strategy to reverse persisting neurogenetic deficiencies and reduce neurodegeneration, albeit there are few studies addressing pharmacokinetics and pharmacodymics characteristcs of this drug after TBI, which could provide a better background for dose choices and time regimens.[7-8-43-44]

In a normal cell environment, a transitory increase in the $Ca^{2+}$ levels within mitochondrial matrix is a key activator of ATP synthesis and other $Ca^{2+}$ sensitive processes; whereas a persistent $Ca^{2+}$ elevation can disturb ATP synthesis and promote apoptotic signaling.[7-9] Interestingly, reports have shown that in the acute phase after TBI, brain mitochondria import $Na^{+}$ and $Ca^{2+}$ via NCLX in a putative reverse mode, which then contributes with increased neuronal death.[45-47] The current data provide the first evidence that TS treatment addresses this pathological NCLX function after TBI, although the downstream effect on ATP synthesis was not elucidated.[47] While it is not well established if mitochondrial swelling is a strictly inner-membrane phenomenon, it should be taken into consideration that $Ca^{2+}$ induced mitochondrial swelling and subsequent cell death require an increase in the $Ca^{2+}$ influx or alternatively, a decrease in the inner membrane calcium efflux.[48] Given that $Ca^{2+}$ mediates a variety of neurotoxic secondary events after TBI, the current study addressed potential mechanisms.[46-48] In particular, it was found that TBI impaired $Na^{+}$-stimulated $Ca^{2+}$ efflux through the NCLX, which appears to account for persisting increases in $Ca^{2+}$ concentrations inside the mitochondria. Notably, in the injured mice receiving TS treatment, the NCLX was responsive to $Na^{+}$ and extruded $Ca^{2+}$, which potentially contributed to preserving the mitochondrial energy efficiency.

Journal of Neurotrauma
Testosterone administration after traumatic brain injury reduces mitochondrial dysfunction and neurodegeneration (DOI: 10.1089/neu.2018.6266)
This paper has been peer-reviewed and accepted for publication, but has yet to undergo copyediting and proof correction. The final published version may differ from this proof.

Changes in oxidative metabolism like the $\Delta\psi_m$, and activity of ETS complexes behave in response to $Ca^{2+}$ also appeared to play an important role in post-TBI pathophysiology. $Ca^{2+}$ influx results in a net positive charge in the matrix, leading to alterations in the net charge across the mitochondrial internal membrane and a change in $\Delta\psi_m$ depolarization. However, there remains debate regarding if or how the NCLX exerts influence on $\Delta\psi_m$.[45] In particular, it has been challenging to determine potential contribution of other mitochondrial ionic transporters that can also influence the $Na^+$ and $Ca^{2+}$ gradients.[49]

In normal respiring mitochondria, the $\Delta\Psi_m$ is primarily achieved by pumping protons from the matrix to intermembrane space through some ETS complexes. This is synchronized with the proton motive force driven ATP synthesis by the F0F1-ATP synthase. Given the functional proximity between electrochemical properties of the mitochondrial internal membrane and ATP synthesis, the present study examined the effect of challenging mitochondria in a respiratory protocol. Based on this approach, functional aspects of oxidative phosphorylation, such as substrate uptake and oxidation, F0F1-ATP synthase activity, ubiquinone and cytochrome C pool size and specific electron transport complexes activities can be evaluated using the RCR (respiratory control ratio), which is a respiratory index of the degree of metabolic coupling between ETS and oxidative phosphorylation.[26-29]

Recently, Hill et al.[50] showed that isolated mitochondria from the ipsilateral cortex three days after TBI, present a deficient metabolism, which was followed by a recovery at day 5 after injury. The authors hypothesized that by 5 days post-injury, no dysfunctional mitochondria remain in the injured brain.[50] In contrast to the present study, a previous report demonstrated responses of mitochondria to treatments with substrates and inhibitors after TBI appeared to be dependent on the localization of mitochondria at synaptic and non-synaptic sites[51] The different findings may reflect the use of homogenates from ipsilateral cortex enriched in mitochondria for the respirometry protocol in the present study. The results identify prolonged dysfunctions in the Complex V (F0F1-ATP Synthase) 10 days after TBI. As global metabolic consequences, the oxygen consumption rate (OCR) by mitochondria in the State III is not efficiently coupled with ATP

synthesis (OxPhos), implying that at least in part, the oxygen consumption is not appropriately coupled with ATP production. In contrast with these findings, other recent studies have shown significant differences in the State IV between Sham and CCI groups up to 5 days after CCI likely due differences related to the gradient preparation and tissue collection.[50-51]

An uncontrolled mitochondrial metabolic uncoupling is a key mechanism leading to ROS production in brain pathologies, including TBI.[8-12-51] When mitochondria dysfunction persists, the mitochondria themselves begin to consume ATP, burn energy of nutrients as heat, swell upon $Ca^{2+}$ overload. This leads to production of deleterious compounds, such as ROS that directly attack and damage mitochondria as well as other cellular structures.[12-50-52] The present results demonstrate that after severe TBI, mitochondrial $H_2O_2$ production remained elevated across the entire respiratory protocol, and that TS supplementation attenuated the $H_2O_2$ overproduction. Similarly, TS supplementation attenuated total ROS (superoxide anion, hydroxyl radicals, lipid hydroperoxides, and $H_2O_2$ levels), confirming that increased $H_2O_2$ quantitatively impacts the global pro-oxidative status. Demonstrations that high ROS levels induce oxidative damage to the components of neural cell membranes and mitochondria have often been seen in TBI studies and, together with $Ca^{2+}$ overload, may represent to mitochondrial dysfunction as a deleterious feed-forward cycle.[12-52] This is supported by the study by Hill et al.,[48] which demonstrated that the time course of the mitochondrial respiratory alterations in the cortex and hippocampus after CCI in the rat, runs in parallel with the evolution of oxidative damage to mitochondria and cellular proteins.[50]

The current data also demonstrate that in addition to decreased Succinate levels and ATP synthesis induced by TBI, the elevation of $H_2O_2$ represents a direct manifestation of prolonged mitochondrial dysfunction, which apparently has the $Ca^{2+}$ overload as the main trigger. As an antidote of oxidative damage, endogenous ROS-detoxifying systems (enzymatic and non-enzymatic) in mitochondria remove excessive ROS. In the present study, total superoxide dismutase (SOD) and glutathione peroxidase (GPx) activities were found to be not affected by TS treatment post-injury despite elevated total ROS and $H_2O_2$.



Journal of Neurotrauma
Testosterone administration after traumatic brain injury reduces mitochondrial dysfunction and neurodegeneration (DOI: 10.1089/neu.2018.6266)
This paper has been peer-reviewed and accepted for publication, but has yet to undergo copyediting and proof correction. The final published version may differ from this proof.

Journal of Neurotrauma
Testosterone administration after traumatic brain injury reduces mitochondrial dysfunction and neurodegeneration (DOI: 10.1089/neu.2018.6266)


At the protein level, mitochondrial MnSOD immunocontent was decreased after injury in the present study, but overexpressed in the TS-CCI group, indicating transcriptional and/or post-translational influences. Remarkably, mitochondrial-associated oxidative stress can initiate stimulation or induction of the antioxidant gene SOD2, whose protein has enhancing cell survival properties. In the present study, it was found that the MnSOD immunocontent and $H_2O_2$ levels displayed opposite profiles. This is somewhat unexpected because the enzyme converts superoxide anion to $H_2O_2$, in turn, which is neutralized mainly by the GPx activity. Likewise, in a previous study, CCI study in mice showed that even in the presence of increased lipid peroxidation (by 4-HNE) the gene expression of CuSOD (cytosolic) and MnSOD (mitochondrial) in the cortex and hippocampus did not vary over the course of 1-week, although the transcription factor of antioxidant response elements (Nrf2-ARE) was overexpressed.[53] Therefore, the long-term increase in $H_2O_2$ levels observed after TBI in the present study appear to be most related to the effects of persistently increased $Ca^{2+}$ levels on mitochondria metabolism, or alternatively by the electron reductive force direct on superoxide anion, rather than by SOD expression.[54]

A particular structural aspect of TBI that is associated with progressive neurodegeneration is the axonal pathology leading to the destabilization of microtubules associated proteins, axonal accumulation of neurotoxic proteins, and degradation of neuronal cytoskeletal proteins mainly by $Ca^{2+}$ dependent proteases.[10-42] For instance, hyperphosphorylated Tau protein aggregates within neurites and neuronal cell bodies are present after TBI, the degree of which correlates with progressive neuronal dysfunction, functional decline, and behavioral changes, observed in both in humans and rodents. [3-42-55]

Elevated cytosolic $Ca^{2+}$ after TBI increase the activity of protein kinases involved in the aberrant phosphorylation of Tau, as well as trigger the proteolysis of the cytoskeletal protein alpha-Spectrin by Calpain-2. Also, excessive intramitochondrial $Ca^{2+}$ concentrations stimulate permeability transition pore formation and Cytochrome C release, which in turn raises Caspase-3 proteolytic activity.[12] Although both Calpain-2 and Caspase-3 are able to cleave alpha-Spectrin in 150 kDa fragments, it has been demonstrated that at a short-time window after TBI the breakdown by Calpain-2 overcome Caspase-3.[56-57]

Journal of Neurotrauma
Testosterone administration after traumatic brain injury reduces mitochondrial dysfunction and neurodegeneration (DOI: 10.1089/neu.2018.6266)
This paper has been peer-reviewed and accepted for publication, but has yet to undergo copyediting and proof correction. The final published version may differ from this proof.

In the present study, it was found that TS treatment post-TBI prevented the overexpression of pTau$^{Ser396}$, Calpain-2 and cleaved Caspase-3 ratio after CCI. This was accompanied by decreased Tau fragmentation (55/17 kDa) and alpha-Spectrin fragmentation (150 kDa). In both humans and rodents, the levels of alpha-Spectrin in serum and brain tissue have been found to increase after TBI and remain elevated from 12 h to 6 days before decreasing to basal levels.[56-58] Intriguingly, in a rodent TBI model of axonal injury, prolonged Calpain activation (4 to 14 days) correlated with subsequent cell death.[59] Accordingly, TS administered for 10 days post-TBI in the present study appears to have protected neurons that would have otherwise degenerated due to secondary pathological cascades.

Furthermore, the activation of Caspase-3 by cleavage also culminates in degradation of cytoskeletal proteins, and together with energy impairment and exacerbated ROS production, it has been linked with mitochondrial dysfunction and apoptosis. Here, a predominance of the expression of pro-apoptotic protein Bax relative to anti-apoptotic protein Bcl-2 was observed after TBI, which was attenuated by TS treatment. The resulting increase in cell viability in the TS-treated animals suggests an increase of mitochondrial survival helped prevent apoptosis.[60]

This study also allowed for the development of an association network to examine the effect of severe TBI in the mouse on the expression of various genes and proteins using the STRING database.[61] Therefore, we acquired a high-throughput transcriptional dataset (GSE58485) with similar methodological characteristics to our CCI protocol and evaluated differential expression patterns of key molecular players driving the secondary pathology. From the relatively small STRING interaction query used in the present study, two distinct clusters were observed, illustrating a mechanistic integration between mitochondrial bioenergetics failure and increments of apoptotic signaling. Within the bioenergetics cluster, the subunits of ATP synthase, succinate dehydrogenase, and Sod2 are highly connected. Remarkably, Sod2 is an important regulator of superoxide levels originated from the oxidative metabolism, thus the association with mitochondria cluster could be expected, reassuring the biological validity of this network. Also, Sod2 serve as the bridge

between the two clusters and is highly connected with Casp3 and Bcl2, genes associated with apoptotic neurodegeneration.

Overall, it was found that short-term TS supplementation after a severe TBI preserved normal mitochondrial $Ca^{2+}$ management and energy efficiency, thereby, preventing cell death via apoptosis. In particular, modulation of mitochondrial NCLX activity by TS was found to play a central role in this cell preservation. Accordingly, the current data highlights the importance of maintaining normal TS levels after TBI, which appears to specifically address post-injury mitochondria dysfunction.

**KNOWLEDGEMENTS**

The authors would like to thank to the Center for Brain Injury & Repair, University of Pennsylvania (CBIR-UPENN) for the technical and scientific support; and to the Brazilian scientific agencies/programs INNT-CNPq #465346, CNPq # 401645/2012-6, CAPES, FAPERGS-Pronex, FAPERGS-PPSUS # 03/2017 and support from the US National Institute of Neurological Disorders and Stroke of the National Institutes of Health under award numbers R01NS092398, R01NS094003 and R01NS038104.

**AUTHOR DISCLOSURE STATEMENT**

No competing financial interests exist.



Journal of Neurotrauma
Testosterone administration after traumatic brain injury reduces mitochondrial dysfunction and neurodegeneration (DOI: 10.1089/neu.2018.6266)
This paper has been peer-reviewed and accepted for publication, but has yet to undergo copyediting and proof correction. The final published version may differ from this proof.

**REFERENCES**

1. Meaney DF, Morrison B, Dale Bass C. The mechanics of traumatic brain injury: a review of what we know and what we need to know for reducing its societal burden. Journal of biomechanical engineering. 2014;136(2):021008.

2. Rosenfeld JV, Maas AI, Bragge P, Morganti-Kossmann MC, Manley GT, Gruen RL. Early management of severe traumatic brain injury. Lancet. 2012;380(9847):1088-98.

3. Blennow K, Hardy J, Zetterberg H. The neuropathology and neurobiology of traumatic brain injury. Neuron. 2012;76(5):886-99.

4. Johnson VE, Weber MT, Xiao R, Cullen DK, Meaney DF, Stewart W, et al. Mechanical disruption of the blood–brain barrier following experimental concussion. Acta neuropathologica. 2018;135(5):711-26.

5. Meng Q, Zhuang Y, Ying Z, Agrawal R, Yang X, Gomez-Pinilla F. Traumatic Brain Injury Induces Genome-Wide Transcriptomic, Methylomic, and Network Perturbations in Brain and Blood Predicting Neurological Disorders. EBioMedicine. 2017;16:184-94.

6. Gilmer LK, Roberts KN, Joy K, Sullivan PG, Scheff SW. Early mitochondrial dysfunction after cortical contusion injury. Journal of neurotrauma. 2009;26(8):1271-80.

7. Hiebert JB, Shen Q, Thimmesch AR, Pierce JD. Traumatic brain injury and mitochondrial dysfunction. The American journal of the medical sciences. 2015;350(2): 132-8.

8. Pandya JD, Nukala VN, Sullivan PG. Concentration dependent effect of calcium on brain mitochondrial bioenergetics and oxidative stress parameters. Front Neuroenergetics. 2013;5:10.

9. Vekaria HJ, Talley Watts L, Lin AL, Sullivan PG. Targeting mitochondrial dysfunction in CNS injury using Methylene Blue; still a magic bullet? Neurochemistry international. 2017;109:117-25.

Journal of Neurotrauma
Testosterone administration after traumatic brain injury reduces mitochondrial dysfunction and neurodegeneration (DOI: 10.1089/neu.2018.6266)
This paper has been peer-reviewed and accepted for publication, but has yet to undergo copyediting and proof correction. The final published version may differ from this proof.

10. Johnson VE, Stewart W, Weber MT, Cullen DK, Siman R, Smith DH. SNTF immunostaining reveals previously undetected axonal pathology in traumatic brain injury. Acta neuropathologica. 2016;131(1):115-35.

11. Jafri MS, Kumar R. Modeling Mitochondrial Function and Its Role in Disease. Progress in molecular biology and translational science. 2014;123:103-25.

12. Ji J, Tyurina YY, Tang M, Feng W, Stolz DB, Clark RS, et al. Mitochondrial injury after mechanical stretch of cortical neurons in vitro: biomarkers of apoptosis and selective peroxidation of anionic phospholipids. Journal of neurotrauma. 2012;29(5):776-88.

13. Gajavelli S, Sinha VK, Mazzeo AT, Spurlock MS, Lee SW, Ahmed AI, et al. Evidence to support mitochondrial neuroprotection, in severe traumatic brain injury. Journal of bioenergetics and biomembranes. 2015;47(1-2):133-48.

14. Cheng G, Kong RH, Zhang LM, Zhang JN. Mitochondria in traumatic brain injury and mitochondrial-targeted multipotential therapeutic strategies. British journal of pharmacology. 2012;167(4):699-719.

15. Hatanaka Y, Hojo Y, Mukai H, Murakami G, Komatsuzaki Y, Kim J, et al. Rapid increase of spines by dihydrotestosterone and testosterone in hippocampal neurons: Dependence on synaptic androgen receptor and kinase networks. Brain research. 2015;1621:121-32.

16. Fanaei H, Karimian SM, Sadeghipour HR, Hassanzade G, Kasaeian A, Attari F, et al. Testosterone enhances functional recovery after stroke through promotion of antioxidant defenses, BDNF levels and neurogenesis in male rats. Brain research. 2014;1558:74-83.

17. Gurer B, Kertmen H, Kasim E, Yilmaz ER, Kanat BH, Sargon MF, et al. Neuroprotective effects of testosterone on ischemia/reperfusion injury of the rabbit spinal cord. Injury. 2015;46(2):240-8.

18. Hioki T, Suzuki S, Morimoto M, Masaki T, Tozawa R, Morita S, et al. Brain testosterone deficiency leads to down-regulation of mitochondrial gene expression in rat hippocampus accompanied by a decline in peroxisome proliferator-activated receptor-

gamma coactivator 1alpha expression. Journal of molecular neuroscience : MN. 2014;52(4):531-7.

19. Lopez-Rodriguez AB, Acaz-Fonseca E, Spezzano R, Giatti S, Caruso D, Viveros MP, et al. Profiling Neuroactive Steroid Levels After Traumatic Brain Injury in Male Mice. Endocrinology. 2016;157(10):3983-93.

20. Bavisetty S, Bavisetty S, McArthur DL, Dusick JR, Wang C, Cohan P, et al. Chronic hypopituitarism after traumatic brain injury: risk assessment and relationship to outcome. Neurosurgery. 2008;62(5):1080-93; discussion 93-4.

21. Tanriverdi F, Senyurek H, Unluhizarci K, Selcuklu A, Casanueva FF, Kelestimur F. High risk of hypopituitarism after traumatic brain injury: a prospective investigation of anterior pituitary function in the acute phase and 12 months after trauma. The Journal of clinical endocrinology and metabolism. 2006;91(6):2105-11.

22. Tölli A, Borg J, Bellander BM, Johansson F, Höybye C. Pituitary function within the first year after traumatic brain injury or subarachnoid haemorrhage. Journal of endocrinological investigation. 2017;40(2):193-205.

23. Martinez-Sanchis S, Salvador A, Moya-Albiol L, Gonzalez-Bono E, Simon VM. Effects of chronic treatment with testosterone propionate on aggression and hormonal levels in intact male mice. Psychoneuroendocrinology. 1998;23(3):275-93.

24. Smith DH, Soares HD, Pierce JS, Perlman KG, Saatman KE, Meaney DF, et al. A model of parasagittal controlled cortical impact in the mouse: cognitive and histopathologic effects. Journal of neurotrauma. 1995;12(2):169-78.

25. Albert-Weissenberger C, Varrallyay C, Raslan F, Kleinschnitz C, Siren AL. An experimental protocol for mimicking pathomechanisms of traumatic brain injury in mice. Experimental & translational stroke medicine. 2012;4:1.

26. Gnaiger E. Mitochondrial pathways and respiratory control. An introduction to OXPHOS analysis. 4th ed. Innsbruck: OROBOROS MiPNet Publications; 2014.



Journal of Neurotrauma
Testosterone administration after traumatic brain injury reduces mitochondrial dysfunction and neurodegeneration (DOI: 10.1089/neu.2018.6266)
This paper has been peer-reviewed and accepted for publication, but has yet to undergo copyediting and proof correction. The final published version may differ from this proof.

27. Luongo TS, Lambert JP, Gross P, Nwokedi M, Lombardi AA, Shanmughapriya S, et al. The mitochondrial Na(+)/Ca(2+) exchanger is essential for Ca(2+) homeostasis and viability. Nature. 2017;545(7652):93-7.

28. Portela LV, Brochier AW, Haas CB, de Carvalho AK, Gnoato JA, Zimmer ER, et al. Hyperpalatable Diet and Physical Exercise Modulate the Expression of the Glial Monocarboxylate Transporters MCT1 and 4. Molecular neurobiology. 2017;54(8):5807-14.

29. Burtscher J, Zangrandi L, Schwarzer C, Gnaiger E. Differences in mitochondrial function in homogenated samples from healthy and epileptic specific brain tissues revealed by high-resolution respirometry. Mitochondrion. 2015;25:104-12.

30. LeBel CP, Ischiropoulos H, Bondy SC. Evaluation of the probe 2',7'-dichlorofluorescin as an indicator of reactive oxygen species formation and oxidative stress. Chemical research in toxicology. 1992;5(2):227-31.

31. Marklund S. Pyrogallol autoxidation. Boca Raton: CRC Press Inc.; 1985.

32. Wendel A. Glutathione peroxidase. Methods in enzymology. 77: Academic Press; 1981. p. 325-33.

33. Muller AP, Gnoatto J, Moreira JD, Zimmer ER, Haas CB, Lulhier F, et al. Exercise increases insulin signaling in the hippocampus: physiological effects and pharmacological impact of intracerebroventricular insulin administration in mice. Hippocampus. 2011; 21(10):1082-92.

34. Hansen MB, Nielsen SE, Berg K. Re-examination and further development of a precise and rapid dye method for measuring cell growth/cell kill. Journal of immunological methods. 1989;119(2):203-10.

35. Szklarczyk D, Morris JH, Cook H, Kuhn M, Wyder S, Simonovic M, et al. The STRING database in 2017: quality-controlled protein-protein association networks, made broadly accessible. Nucleic acids research. 2017;45(D1):D362-D8.



Journal of Neurotrauma
Testosterone administration after traumatic brain injury reduces mitochondrial dysfunction and neurodegeneration (DOI: 10.1089/neu.2018.6266)
This paper has been peer-reviewed and accepted for publication, but has yet to undergo copyediting and proof correction. The final published version may differ from this proof.

36. Franceschini A, Szklarczyk D, Frankild S, Kuhn M, Simonovic M, Roth A, et al. STRING v9.1: protein-protein interaction networks, with increased coverage and integration. Nucleic acids research. 2013;41(Database issue):D808-15.

37. Castro MA, Wang X, Fletcher MN, Meyer KB, Markowetz F. RedeR: R/Bioconductor package for representing modular structures, nested networks and multiple levels of hierarchical associations. Genome biology. 2012;13(4):R29.

38. Israelsson C, Kylberg A, Bengtsson H, Hillered L, Ebendal T. Interacting Chemokine Signals Regulate Dendritic Cells in Acute Brain Injury. PLoS ONE. 2014;9(8):e104754.

39. Davis S, Meltzer PS. GEOquery: a bridge between the Gene Expression Omnibus (GEO) and BioConductor. Bioinformatics (Oxford, England). 2007;23(14):1846-7.

40. Ritchie ME, Phipson B, Wu D, Hu Y, Law CW, Shi W, et al. limma powers differential expression analyses for RNA-sequencing and microarray studies. Nucleic acids research. 2015;43(7):e47.

41. Figueira TR, Melo DR, Vercesi AE, Castilho RF. Safranine as a fluorescent probe for the evaluation of mitochondrial membrane potential in isolated organelles and permeabilized cells. Methods in molecular biology (Clifton, NJ). 2012;810:103-17.

42. Johnson VE, Stewart W, Smith DH. Axonal pathology in traumatic brain injury. Experimental neurology. 2013;246:35-43.

43. Perez-Pinzon MA, Stetler RA, Fiskum G. Novel mitochondrial targets for neuroprotection. Journal of cerebral blood flow and metabolism : official journal of the International Society of Cerebral Blood Flow and Metabolism. 2012;32(7):1362-76.

44. DeWitt DS, Hawkins BE, Dixon CE, Kochanek PM, Armstead W, Bass CR, et al. Pre-Clinical Testing of Therapies for Traumatic Brain Injury. Journal of neurotrauma. 2018;35(23):2737-54.

45. Boyman L, Williams GS, Khananshvili D, Sekler I, Lederer WJ. NCLX: the mitochondrial sodium calcium exchanger. Journal of molecular and cellular cardiology. 2013;59:205-13.

46. Kim B, Matsuoka S. Cytoplasmic Na+-dependent modulation of mitochondrial Ca2+ via electrogenic mitochondrial Na+-Ca2+ exchange. J Physiol. 2008;586(6):1683-97.

47. Zhao X, Gorin FA, Berman RF, Lyeth BG. Differential hippocampal protection when blocking intracellular sodium and calcium entry during traumatic brain injury in rats. Journal of neurotrauma. 2008;25(10):1195-205.

48. Giorgi C, Agnoletto C, Bononi A, Bonora M, De Marchi E, Marchi S, et al. Mitochondrial calcium homeostasis as potential target for mitochondrial medicine. Mitochondrion. 2012;12(1):77-85.

49. Jiang D, Zhao L, Clapham DE. Genome-wide RNAi screen identifies Letm1 as a mitochondrial Ca2+/H+ antiporter. Science (New York, NY). 2009;326(5949):144-7.

50. Hill RL, Singh IN, Wang JA, Hall ED. Time courses of post-injury mitochondrial oxidative damage and respiratory dysfunction and neuronal cytoskeletal degradation in a rat model of focal traumatic brain injury. Neurochemistry international. 2017;111:45-56.

51. Kulbe JR, Hill RL, Singh IN, Wang JA, Hall ED. Synaptic Mitochondria Sustain More Damage than Non-Synaptic Mitochondria after Traumatic Brain Injury and Are Protected by Cyclosporine A. Journal of neurotrauma. 2017;34(7):1291-301.

52. Ji J, Kline AE, Amoscato A, Arias AS, Sparvero LJ, Tyurin VA, et al. Global lipidomics identifies cardiolipin oxidation as a mitochondrial target for redox therapy of acute brain injury. Nature neuroscience. 2012;15(10):1407-13.

53. Miller DM, Wang JA, Buchanan AK, Hall ED. Temporal and spatial dynamics of nrf2-antioxidant response elements mediated gene targets in cortex and hippocampus after controlled cortical impact traumatic brain injury in mice. Journal of neurotrauma. 2014;31(13):1194-201.

54. Gardner R, Salvador A, Moradas-Ferreira P. Why does SOD overexpression sometimes enhance, sometimes decrease, hydrogen peroxide production? A minimalist explanation. Free Radic Biol Med. 2002;32(12):1351-7.



Journal of Neurotrauma
Testosterone administration after traumatic brain injury reduces mitochondrial dysfunction and neurodegeneration (DOI: 10.1089/neu.2018.6266)
This paper has been peer-reviewed and accepted for publication, but has yet to undergo copyediting and proof correction. The final published version may differ from this proof.

55. Shahim P, Tegner Y, Wilson DH, Randall J, Skillback T, Pazooki D, et al. Blood biomarkers for brain injury in concussed professional ice hockey players. JAMA neurology. 2014;71(6):684-92.

56. Miller DM, Singh IN, Wang JA, Hall ED. Nrf2-ARE activator carnosic acid decreases mitochondrial dysfunction, oxidative damage and neuronal cytoskeletal degradation following traumatic brain injury in mice. Experimental neurology. 2015;264:103-10.

57. Zhang Z, Larner SF, Liu MC, Zheng W, Hayes RL, Wang KK. Multiple alphaII-spectrin breakdown products distinguish calpain and caspase dominated necrotic and apoptotic cell death pathways. Apoptosis : an international journal on programmed cell death. 2009;14(11):1289-98.

58. Siman R, Shahim P, Tegner Y, Blennow K, Zetterberg H, Smith DH. Serum SNTF Increases in Concussed Professional Ice Hockey Players and Relates to the Severity of Postconcussion Symptoms. Journal of neurotrauma. 2015;32(17):1294-300.

59. Saatman KE, Abai B, Grosvenor A, Vorwerk CK, Smith DH, Meaney DF. Traumatic axonal injury results in biphasic calpain activation and retrograde transport impairment in mice. Journal of cerebral blood flow and metabolism : official journal of the International Society of Cerebral Blood Flow and Metabolism. 2003;23(1):34-42.

60. Toro-Urrego N, Garcia-Segura LM, Echeverria V, Barreto GE. Testosterone Protects Mitochondrial Function and Regulates Neuroglobin Expression in Astrocytic Cells Exposed to Glucose Deprivation. Frontiers in aging neuroscience. 2016;8:152-.

61. de la Fuente A. From 'differential expression' to 'differential networking' - identification of dysfunctional regulatory networks in diseases. Trends in genetics : TIG. 2010;26(7):326-33.



Journal of Neurotrauma
Testosterone administration after traumatic brain injury reduces mitochondrial dysfunction and neurodegeneration (DOI: 10.1089/neu.2018.6266)
This paper has been peer-reviewed and accepted for publication, but has yet to undergo copyediting and proof correction. The final published version may differ from this proof.

**FIGURE LEGENDS**

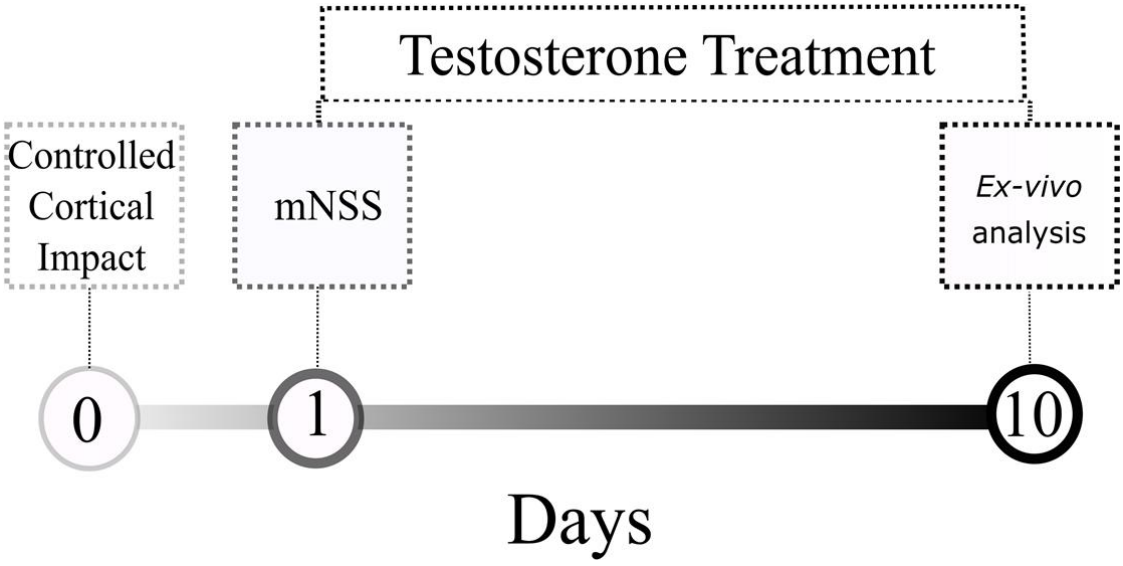


**Figure 1.** Experimental Design. Anesthetized mice were submitted to a single parasagittal severe controlled cortical impact (CCI) injury. Twenty-four hours later they were submitted to modified Neurological Severity Score evaluation (mNSS), and soon afterwards animals were injected with testosterone (TS) or vehicle (oil) for 10 days (n=10, per group).



Journal of Neurotrauma
Testosterone administration after traumatic brain injury reduces mitochondrial dysfunction and neurodegeneration (DOI: 10.1089/neu.2018.6266)
This paper has been peer-reviewed and accepted for publication, but has yet to undergo copyediting and proof correction. The final published version may differ from this proof.

Journal of Neurotrauma
Testosterone administration after traumatic brain injury reduces mitochondrial dysfunction and neurodegeneration (DOI: 10.1089/neu.2018.6266)
This paper has been peer-reviewed and accepted for publication, but has yet to undergo copyediting and proof correction. The final published version may differ from this proof.

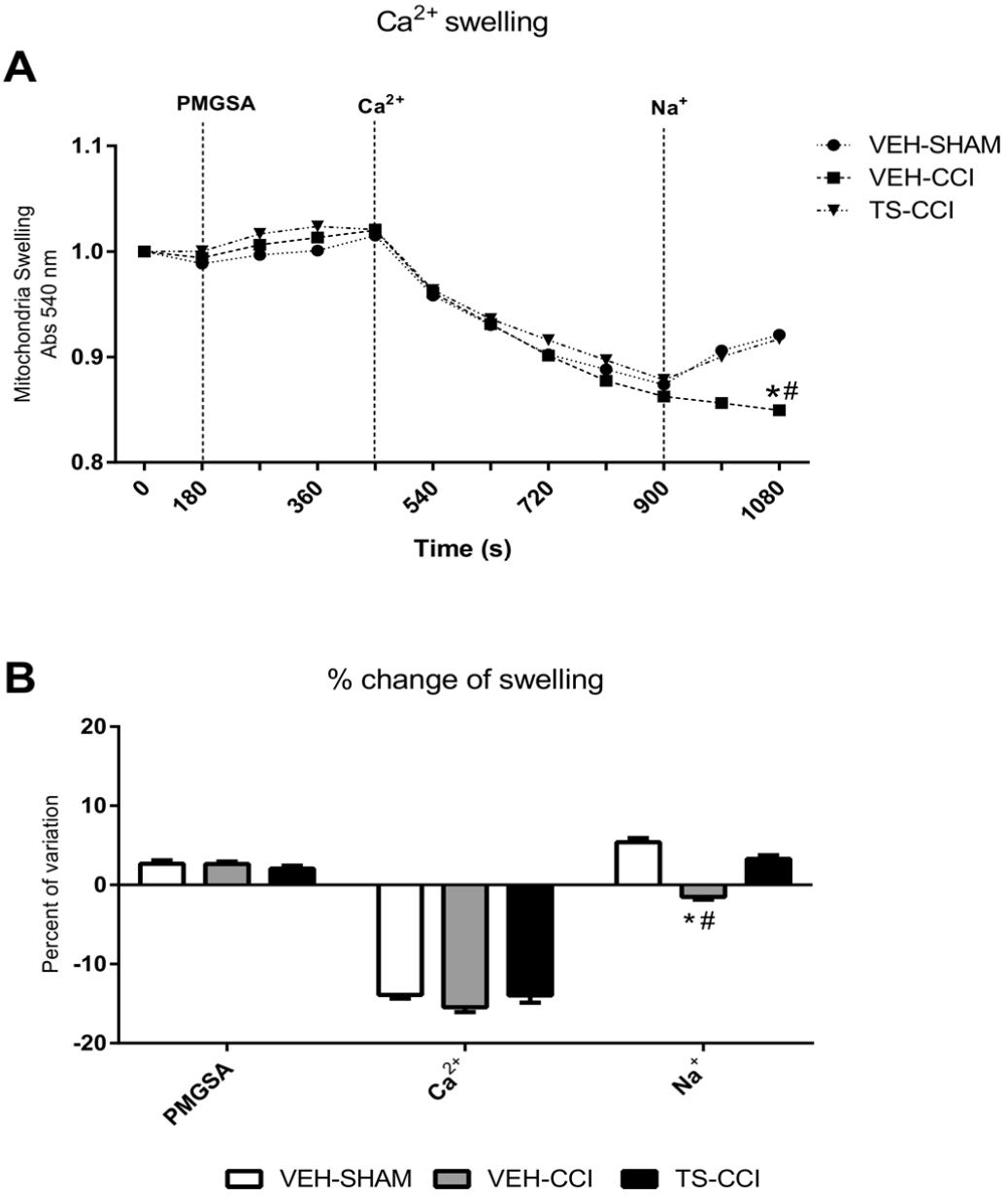


**Figure 2.** Testosterone mediates mitochondrial calcium extrusion by the $Na^+$ dependent channel (NCLX) after CCI. The mitochondrial $Ca^{2+}$ swelling (that is, decrease absorbance at 540 nm) stimulated by the metabolic substrates pyruvate, malate, glutamate, succinate, and ADP (PMGSA) was similar between groups. Stimulation of $Ca^{2+}$ extrusion (that is, increase absorbance at 540 nm) through the NCLX channel after addition of $Na^+$ was impaired in the VEH-CCI group (A and B). Testosterone (TS) administration partially

recovered the capacity of mitochondria to extrude $Ca^{2+}$ from the matrix (A and B) (n= 6-8, per group). * Denotes significant difference compared to VEH-SHAM; # Indicates significant difference compared to TS-CCI.



Journal of Neurotrauma
Testosterone administration after traumatic brain injury reduces mitochondrial dysfunction and neurodegeneration (DOI: 10.1089/neu.2018.6266)
This paper has been peer-reviewed and accepted for publication, but has yet to undergo copyediting and proof correction. The final published version may differ from this proof.

Journal of Neurotrauma
Testosterone administration after traumatic brain injury reduces mitochondrial dysfunction and neurodegeneration (DOI: 10.1089/neu.2018.6266)
This paper has been peer-reviewed and accepted for publication, but has yet to undergo copyediting and proof correction. The final published version may differ from this proof.

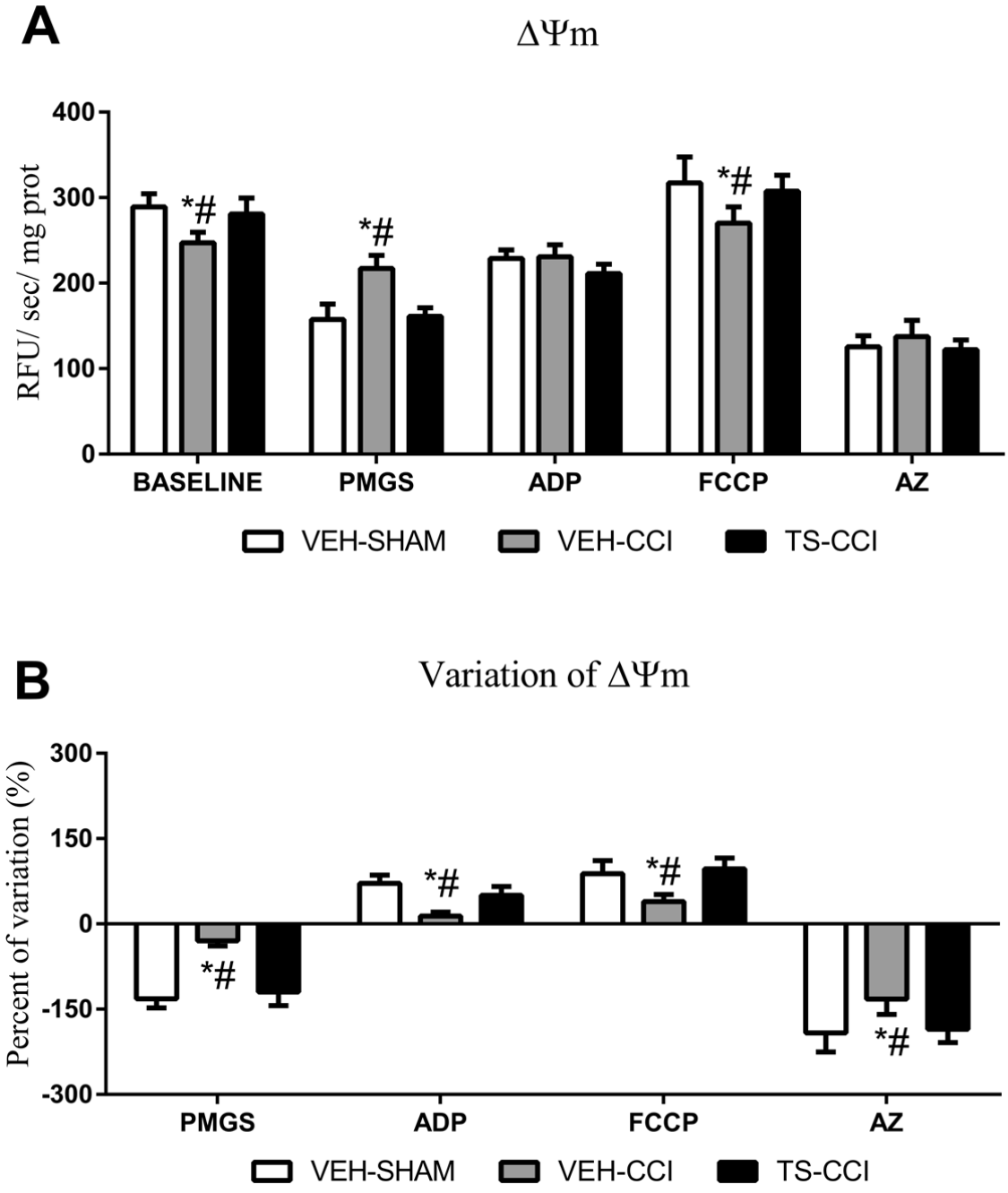


**Figure 3.** Testosterone sustained the dynamics (generation and dissipation) of mitochondrial membrane potential (ΔΨm). The fluorescent dye *safranin*-O is incorporated within the mitochondria of the ipsilateral cortex homogenates then decreasing the fluorescent signal of the medium. The ΔΨm of the VEH-CCI was significantly different from VEH-SHAM and TS-CCI groups at baseline, after addition of the metabolic substrates PMGS, and the uncoupler FCCP. The percentage of variation (B) in the ΔΨm between

baseline and PMGS; PMGS and ADP; ADP and FCCP; and FCCP and AZ confirmed that the VEH-CCI group does not effectively generate and dissipate ΔΨm as did TS-CCI and VEH-SHAM groups (n= 6-8, per group). *Indicates significant difference compared to VEH-SHAM; # Indicates significant difference compared to TS-CCI.



Journal of Neurotrauma
Testosterone administration after traumatic brain injury reduces mitochondrial dysfunction and neurodegeneration (DOI: 10.1089/neu.2018.6266)
This paper has been peer-reviewed and accepted for publication, but has yet to undergo copyediting and proof correction. The final published version may differ from this proof.

Journal of Neurotrauma
Testosterone administration after traumatic brain injury reduces mitochondrial dysfunction and neurodegeneration (DOI: 10.1089/neu.2018.6266)



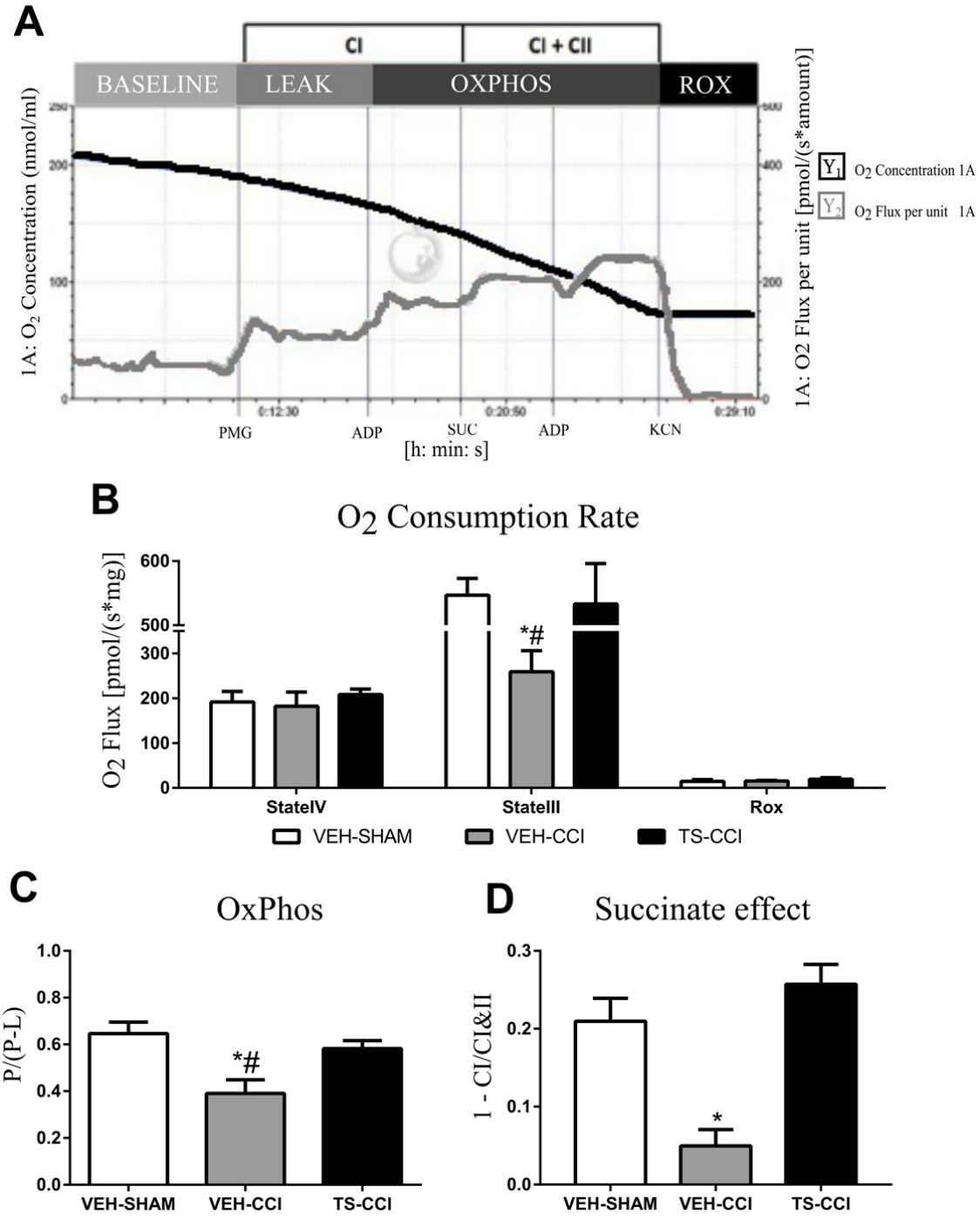


**Figure 4.** Oxygen consumption in different mitochondrial states 10 days after CCI. The representative standard SUIT protocol of VEH-SHAM mice illustrates the profile of oxygen consumption by an ipsilateral cortex homogenate after the addition of pyruvate, malate, and glutamate (PMG), adenosine diphosphate (ADP), Succinate (Suc), FCCP and KCN (A); Oxygen consumption rate at different mitochondrial states (B); Oxphos coupling efficiency

(C) and Succinate effect (D) were significantly decreased after CCI. Testosterone (TS) administration attenuated the mitochondrial bioenergetics dysfunction after CCI (B, C, and D) (n= 6-8, per group). *Indicates significant difference compared to VEH-SHAM; # Indicates significant difference compared to TS-CCI.

Journal of Neurotrauma
Testosterone administration after traumatic brain injury reduces mitochondrial dysfunction and neurodegeneration (DOI: 10.1089/neu.2018.6266)
This paper has been peer-reviewed and accepted for publication, but has yet to undergo copyediting and proof correction. The final published version may differ from this proof.

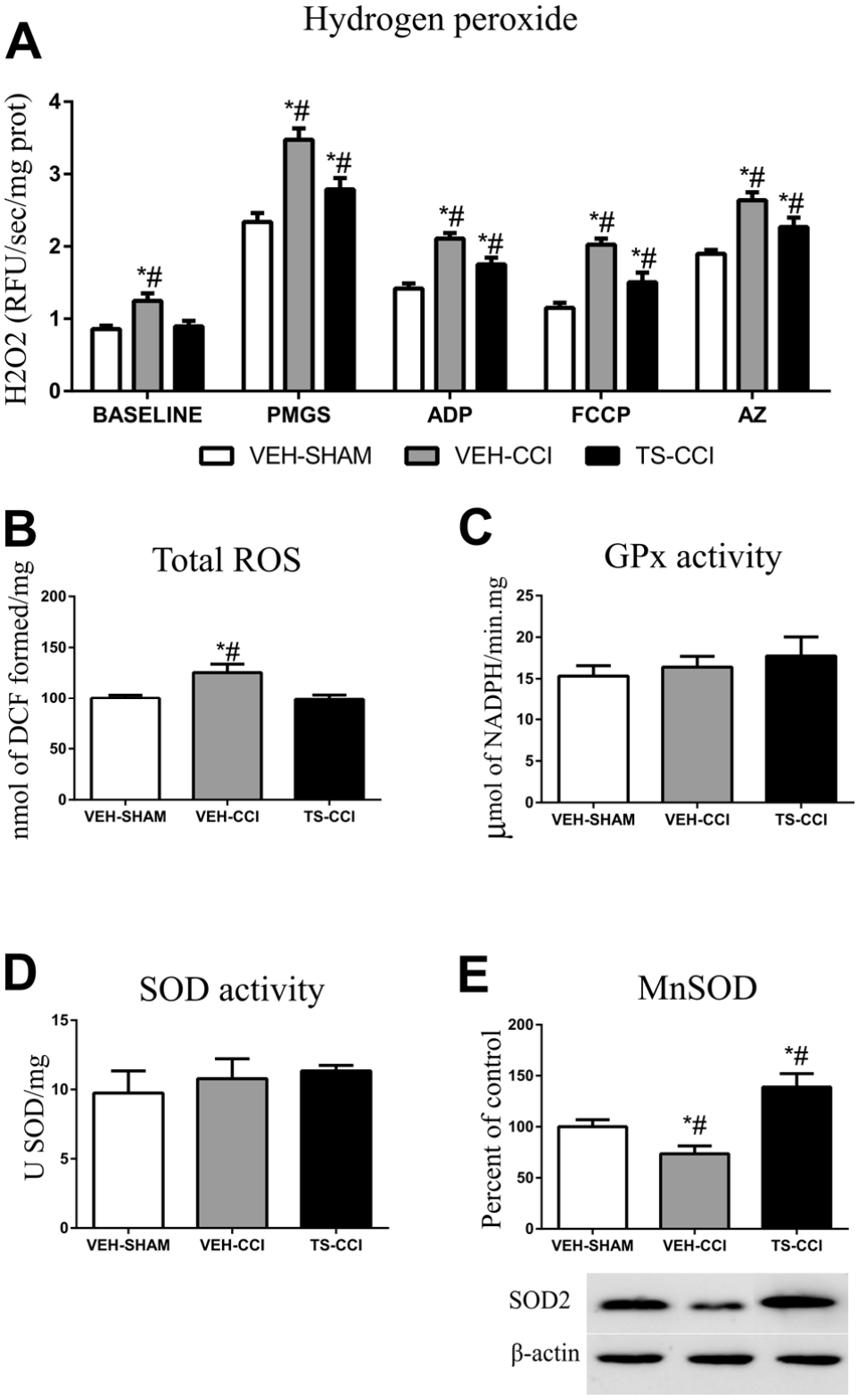


**Figure 5.** Mitochondrial hydrogen peroxide ($H_2O_2$) production and oxidative stress parameters after CCI. The $H_2O_2$ levels in the ipsilateral cortex at baseline and after the

addition of substrates (PMGS and ADP), uncoupler (FCCP) and ATP synthase inhibitor (AZ) are shown after CCI (A). Testosterone administration for 10 days after CCI significantly decreased the $H_2O_2$ levels after CCI (n= 6-8, per group). *Denotes significant difference compared to VEH-SHAM; # Indicates significant difference when compared to TS-CCI.



Journal of Neurotrauma
Testosterone administration after traumatic brain injury reduces mitochondrial dysfunction and neurodegeneration (DOI: 10.1089/neu.2018.6266)
This paper has been peer-reviewed and accepted for publication, but has yet to undergo copyediting and proof correction. The final published version may differ from this proof.

Journal of Neurotrauma
Testosterone administration after traumatic brain injury reduces mitochondrial dysfunction and neurodegeneration (DOI: 10.1089/neu.2018.6266)



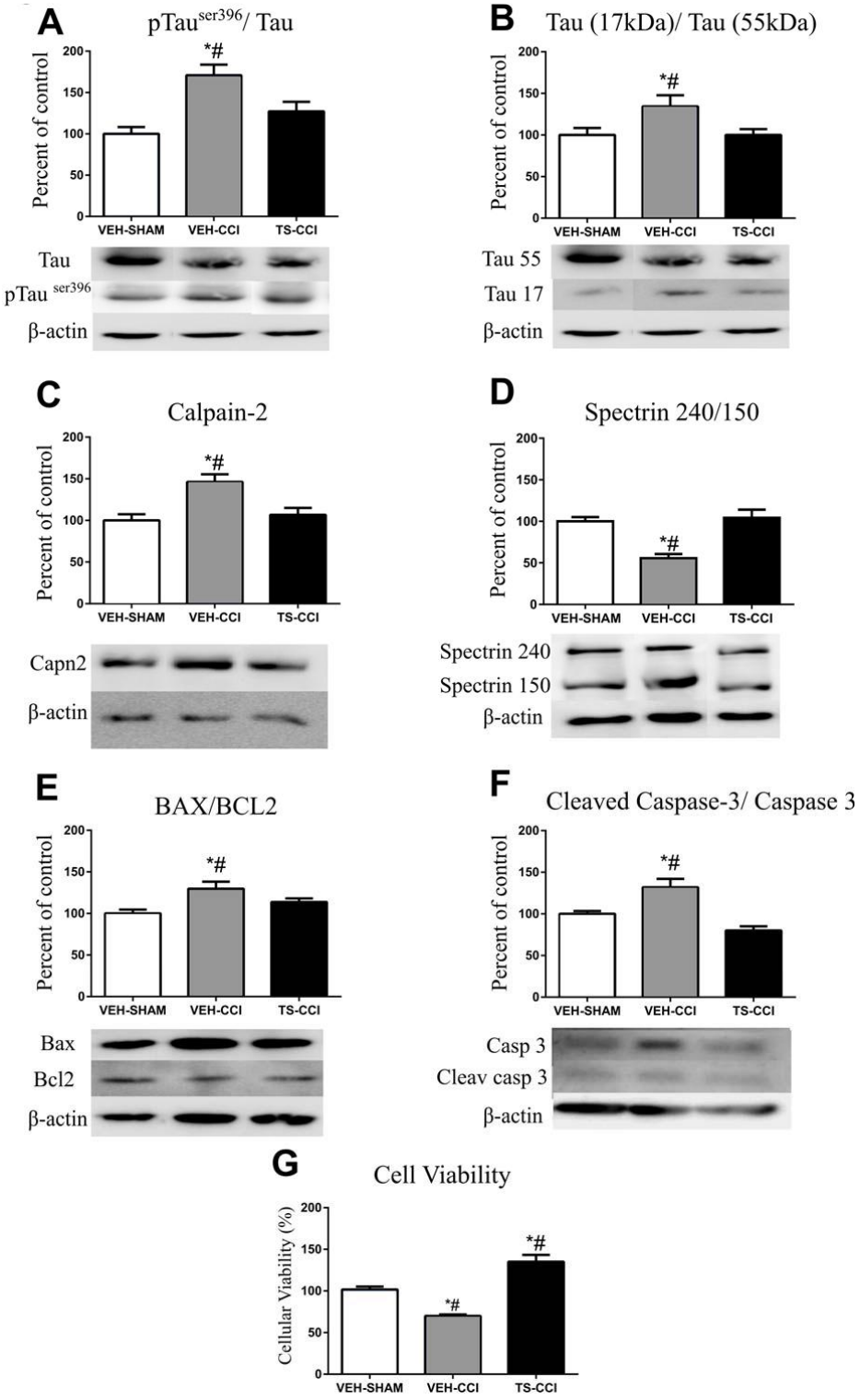


**Figure 6.** Testosterone attenuates molecular effectors of neurodegeneration after a severe CCI. A CCI event significantly altered the protein expression levels of Tau phosphorylated at Ser396 (A) and stimulated Tau protein fragmentation (B). Further, increase in the

immunocontent of Calpain-2 (C) and fragmentation of its substrate alfa-Spectrin (D) suggests an exacerbated calcium-activated protease activity. The expression of apoptotic effectors Bax/Bcl2 (E) and cleaved caspase-3 (F) were increased in the ipsilateral cortex after CCI, followed by decreased cell viability (G). Testosterone (TS) administration attenuated the expression levels of the mentioned effectors of neurodegeneration (A, B, C, D, and F) (n= 6, per group). *Indicates significant difference compared to VEH-SHAM. # Indicates significant difference compared to TS-CCI.



Journal of Neurotrauma
Testosterone administration after traumatic brain injury reduces mitochondrial dysfunction and neurodegeneration (DOI: 10.1089/neu.2018.6266)
This paper has been peer-reviewed and accepted for publication, but has yet to undergo copyediting and proof correction. The final published version may differ from this proof.

Journal of Neurotrauma
Testosterone administration after traumatic brain injury reduces mitochondrial dysfunction and neurodegeneration (DOI: 10.1089/neu.2018.6266)
This paper has been peer-reviewed and accepted for publication, but has yet to undergo copyediting and proof correction. The final published version may differ from this proof.

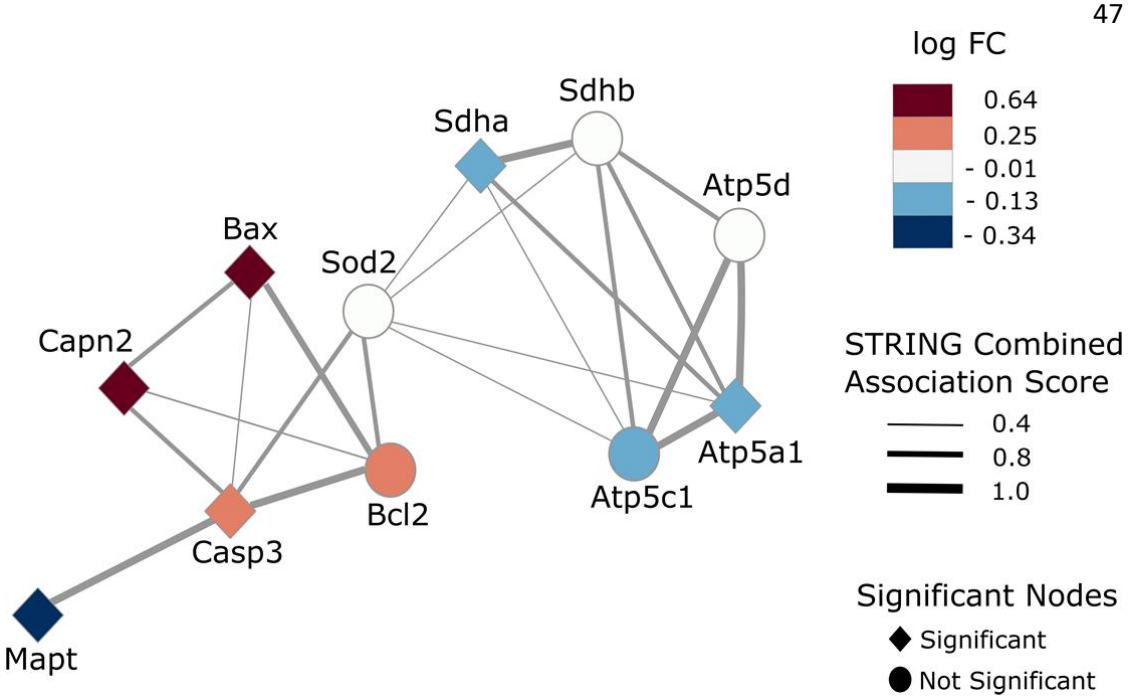


**Figure 7.** Protein-Protein Interaction (PPI) Network Representation of Differential Expression Analysis. GEO dataset GSE58485 was used to compare CCI versus Control samples, and STRING was employed to obtain known association between 11 genes/proteins of interest showed in the nodes and association scores in the edges widths. The results from the differential expression analysis of these genes were mapped over the PPI network topology. Protein-protein interactions (PPI) network between the genes Sdha and Sdhb (subunits of mitochondrial complex II-succinate dehydrogenase), Atp5d, Atp5a1 and Atp5c1 (subunits of mitochondrial complex V-ATP synthase), Sod2 (manganese superoxide dismutase-2), Bcl2 and Bax; Casp3 (Caspase-3) and Capn2 (Calpain-2); Mapt (microtubules associated protein Tau) highlight two distinct clusters: The right side cluster contains genes linked with mitochondrial bioenergetics and the left side cluster contains genes related to apoptotic neurodegeneration. After investigating the expression profile of these genes using GSE58485 study, we observed that the mitochondrial bioenergetics cluster is downregulated in CCI (blue), whereas the apoptosis cluster is upregulated in CCI (red) compared to the control. Also, the two clusters interact functionally through mitochondrial superoxide dismutase (Sod2) gene, thus they are influencing each other in terms of cell physiology.

**Capítulo IV:** *Exercise combined with anabolic steroids in a mice model of repetitive sports-related traumatic brain injury.*

No capitulo IV apresentamos o artigo submetido ao periódico "*Neuroscience Letters*".

Comumente, atletas utilizam abusam de diferentes esteroides em combinação visando o desempenho esportivo[1], e também estão expostos a riscos de TCE repetidos (concussão relacionada ao esporte). Cronicamente, a concussão relacionada ao esporte na prática esportiva pode resultar em encefalopatia traumática crônica (ETC).

Essa condição tem recebido atenção crescente da literatura e da mídia em geral[2]. Entretanto, não encontramos na literatura atual um modelo específico para investigação da concussão relacionada ao esporte em roedores. Mais especificamente, nenhum estudo considerou o exercício crônico como uma variável dos desfechos associados ao TCE.

O modelo proposto nesta tese prejudicou parâmetros funcionais mitocondriais e induziu a astrogliose reativa, bem como aumentou os marcadores de neurodegeneração no córtex e no hipocampo.

Além disso, investigamos as consequências do uso de diferentes esteroides combinados nas respostas metabólicas associadas ao desenvolvimento de CTE. Surpreendentemente, o uso concomitante de uma combinação de EAA atenuou danos mitocondriais e níveis de marcadores de neurodegeneração, embora sem efeitos benéficos sobre a astrogliose. Dadas as limitações experimentais, o estudo é um passo importante na tentativa de padronizar um modelo de concussão relacionada ao esporte em camundongos, o que tem importância significativa para o desenvolvimento de estratégias para entender os mecanismos que governam o dano cerebral em atletas.

1. Dados obtidos da World Anti-Doping Agency (WADA).
2. Filme estadunidense de 2015, Concussion (No Brasil, "Um Homem entre Gigantes").

Elsevier Editorial System(tm) for
Neuroscience Letters

Manuscript Draft

Manuscript Number:

Title: Exercise combined with anabolic steroids in a mice model of repetitive sports-related traumatic brain injury

Article Type: Research paper

Keywords: Sports concussion, repeated head trauma, mitochondria, exercise, anabolic androgenic steroids.

Corresponding Author: Dr. Luis V. Portela, Ph.D.

Corresponding Author's Institution: Federal University of Rio Grande do Sul

First Author: Randhall B Carteri, Ph.D.

Order of Authors: Randhall B Carteri, Ph.D.; Afonso Kopzcynski; Catiane B Alves, M.Sc; Marcus V Lara; Wesley Cotta; Marcelo S Rodolphi, M.Sc; Nathan R Strogulski, M.Sc; Chárist on A Dal Belo, Ph.D.; Lucia H Vinadé, Ph.D.; Lisiane O Porciuncula, Ph.D.; Luis V. Portela, Ph.D.

Abstract: Athletes engaged in contact sports often use performance enhancing drugs like anabolic androgenic steroids (AAS) and are at an increased risk of repetitive mild traumatic brain injury (TBI), a trigger for mitochondrial malfunction. We aimed to investigate the neuroenergetic consequences of repeated mild TBI in exercised mice concomitantly administered with an AAS cocktail. Groups were allocated as exercise without head injury (SHAM), exercise plus repetitive head injury (SRC), and exercise plus SRC, testosterone and nandrolone (AAS). Sixty-day old mice (CF1) of all groups had free access to running wheel for 35 days, and were investigated for maximal exercise performance on a treadmill (at days 35, 40 and 45). Immediately after, mice were submitted to closed controlled cortical impact with parameters adjusted to simulate concussion. After injury protocols animals rested for 48 h. Synaptossomes isolated from the whole brain were used for neurochemical and respirometry analysis. The mitochondrial ATP synthesis (OxPhos), H2O2 production, membrane potential (ΔΨm), Ca2+ efflux was significantly impaired by SRC and prevented in AAS mice. There was increased reactive gliosis in the dentate gyrus of hippocampus of SRC and AAS mice. Also, cleaved spectrin (120/240) and pTauSer396, well-known markers of axonal degeneration, were increased in the hippocampus of SRC and AAS mice. In conclusion, SRC and AAS groups showed increased hippocampal neurodegeneration, whereas AAS attenuated mitochondrial dysfunction. The experimental protocol proposed here is a step towards the establishment of an integrative model to study SRC in mice.

Suggested Reviewers: Nancy J Berman
Department of Anatomy and Cell Biology,, University of Kansas Medical Center
NBERMAN@kumc.edu
She is an expert in cell biology.

Henrik Zetterberg Ph.D.
Department of Psychiatry and Neurochemistry,, University of Gothenburg,
h.zetterberg@ucl.ac.uk
He is an expert in biomarkers of neurodegeneration in TBI.

Robert Siman Ph.D.
Professor, Department of Neurosurgery, Center for Brain Injury and Repair, Perelman School, University of Pennsylvania
siman@mail.med.upenn.edu
He is a world expert in biomarkers in TBI.

Cheryl L Wellington Ph.D.
Department of Pathology and Laboratory Medicine, University of British Columbia
wcheryl@mail.ubc.ca
She is an world expert in concussive models

William P Meehan III Ph.D.
The Micheli Center for Sports Injury Prevention
William.meehan@childrens.harvard.edu
He is a renowned researcher in concussion

David Meaney
Department of Bioengineering,, University of Pennsylvania
dmeaney@seas.upenn.edu
He is a world expert in mitochondria dysfunction after TBI and in TBI models

Rebakah Mannix
Division of Emergency Medicine, Boston Children’s Hospital
Rebekah.Mannix@childrens.harvard.edu
She is world expert in concussion in the clinical settings

Gary Fiskum
Department of Anesthesiology, University of Maryland School of Medicine
gfisk001@umaryland.edu
He is a world expert in TBI

**UNIVERSIDADE FEDERAL DO RIO GRANDE DO SUL**
**INSTITUTO DE CIÊNCIAS BÁSICAS DA SAÚDE**
**DEPARTAMENTO DE BIOQUÍMICA**
**PROGRAMA DE PÓS-GRADUAÇÃO EM CB: BIOQUÍMICA**
**ppgbioq@ufrgs.br**

**Porto Alegre, May 21st, 2019**

**Dr. Stephen G. Waxman**

Editor-in-Chief of Neuroscience Letters
Yale University School of Medicine,
New Haven, Connecticut, USA

Dear Dr. Waxman,

I am sending enclosed our manuscript entitled *"***Exercise combined with anabolic steroids in a mice model of repetitive sports-related traumatic brain injury**" by Carteri et al. to be considered for publication in the Neuroscience Letters. In this work, we propose a mice model of sport-related concussion, which combined two variables that are usually neglected in concussive models that is, the previously engagement of animals in exercise training and the abuse of enhancing performance drugs. As endpoints, we build a panel of parameters driving mitochondrial neuroenergetics and measured molecular markers associated with neurodegeneration after traumatic brain injury.

I hope this manuscript reach the standard necessary to be accepted for publication in this journal.

Yours sincerely,

**Prof. Dr. Luis Valmor Portela**

Department of Biochemistry, ICBS
Universidade Federal do Rio Grande do Sul
Rua Ramiro Barcelos 2600 Anexo
CEP 90.035-003, Porto Alegre, Rio Grande do Sul, Brazil
Email: roskaportela@gmail.com
Tel/Fax: +55 51 3308 5557.

## Highlights

- A mice model of sports-related concussion (SRC) is proposed;
- The SRC in exercised mice replicates findings of athlete's brain
- Impaired synaptic mitocondrial function, increased astrogliosis and axonal markers was evidenced;
- Exercise and anabolic androgenic steroids cocktail partially attenuated SRC-related outcomes

# Exercise combined with anabolic steroids in a mice model of repetitive sports-related traumatic brain injury

Randhall B. Carteri[1], Afonso Kopzcynski[1], Catiane B. Alves[2], Marcus V.S. Lara[2], Wesley Cotta[1], Marcelo S. Rodolphi[1], Nathan R. Strogulski[1], Cháristo A. Dal Belo[3], Lucia H. Vinadé [3], Lisiane O. Porciuncula [2], Luis V. Portela[1*].

[1] Laboratório de Neurotrauma e Biomarcadores - Departamento de Bioquímica, Programa de Pós-Graduação em Bioquímica, ICBS, Universidade Federal do Rio Grande do Sul - UFRGS, Porto Alegre, RS, Brazil.

[2] Laboratório de Estudos sobre o Sistema Purinérgico - Departamento de Bioquímica, Programa de Pós-Graduação em Bioquímica, ICBS, Universidade Federal do Rio Grande do Sul - UFRGS, Porto Alegre, RS, Brazil.

[3] Laboratório de Neurobiologia e Toxinologia (LANETOX) - Universidade Federal do Pampa - UNIPAMPA, São Gabriel, RS, Brazil.

*** Corresponding author:**

**Dr. Luis Valmor Portela**

Departamento de Bioquímica, ICBS

Universidade Federal do Rio Grande do Sul-UFRGS

Rua Ramiro Barcelos 2600, anexo

CEP 90035003

Porto Alegre, RS

Brasil

Tel. +55 51 33085557

Email. Roskaportela@gmail.com

**Abstract**

Athletes engaged in contact sports often use performance enhancing drugs like anabolic androgenic steroids (AAS) and are at an increased risk of repetitive mild traumatic brain injury (TBI), a trigger for mitochondrial malfunction. We aimed to investigate the neuroenergetic consequences of repeated mild TBI in exercised mice concomitantly administered with an AAS cocktail. Groups were allocated as exercise without head injury (SHAM), exercise plus repetitive head injury (SRC), and exercise plus SRC, testosterone and nandrolone (AAS). Sixty-day old mice (CF1) of all groups had free access to running wheel for 35 days, and were investigated for maximal exercise performance on a treadmill (at days 35, 40 and 45). Immediately after, mice were submitted to closed controlled cortical impact with parameters adjusted to simulate concussion. After injury protocols animals rested for 48 h. Synaptossomes isolated from the whole brain were used for neurochemical and respirometry analysis. The mitochondrial ATP synthesis (OxPhos), $H_2O_2$ production, membrane potential ($\Delta\Psi m$), $Ca^{2+}$ efflux was significantly impaired by SRC and prevented in AAS mice. There was increased reactive gliosis in the dentate gyrus of hippocampus of SRC and AAS mice. Also, cleaved spectrin (120/240) and $pTau^{Ser396}$, well-known markers of axonal degeneration, were increased in the hippocampus of SRC and AAS mice. In conclusion, SRC and AAS groups showed increased hippocampal neurodegeneration, whereas AAS

attenuated mitochondrial dysfunction. The experimental protocol proposed here is a step towards the establishment of an integrative model to study SRC in mice.

**Keywords:** Sports concussion, repeated head trauma, mitochondria, exercise, anabolic androgenic steroids.

**Declarations of interest:** none

**Author's contribution:**

Randhall Carteri: Study design, animal treatments and surgery, respirometry assays, data analysis, figures layout and manuscript writing.

Afonso Kopzcinski: Animal surgery, neurochemical assays, data analysis and figures layout.

Catiane Alves: Immunohistochemistry assays and data analysis.

Marcus Lara: Immunohistochemistry assays and data analysis.

Wesley Cotta: Animal surgery, Western blot, data analysis and figures layout.

Marcelo Rodolphi: Neurochemical assays and data analysis.

Nathan Strogulski: behavioral experiments, spectrophotometry assays and data analysis.

Chárist on Dal Belo: physical exercise testing and data analysis.

Lucia Helena Vinadé: physical exercise testing and data analysis.

Lisiane Porciuncula: results discussions and data analysis

Luis V Portela: study design, data analysis, and manuscript writing.

## 1. Introduction

The repeatedly imposed biomechanical forces in sports related-concussion (SRC) translate into diffuse damage to the brain [1]. Actually, professional athletes engaged in contact / collision sports are at an increased risk of suffering repetitive mild traumatic brain injury (TBI), which pathophysiological mechanisms still need scrutiny [2]. Nonetheless, post-mortem neuropathological findings have led to the identification of a brain disorder commonly seen in American football players namely chronic traumatic encephalopathy (CTE), characterized by the neuronal loss, diffuse axonal injury and hyperphosphorylation of cytoskeletal Tau protein, a hallmark of neurodegeneration [3-5]. It is well established in animal models of moderate and severe TBI that impaired intracellular $Ca^{2+}$ homeostasis and mitochondrial bioenergetics dysfunctions contributes to propagate neurodegeneration overtime whereas the comprehension of the pathological mechanisms after repetitive brain trauma is still limited [6-8] . Along with neurons, the astrocytes are also injured by TBI ultimately displaying a reactive morphology (astrogliosis), changing their metabolic pattern and increasing the expression of proteins like GFAP and S100B that once release to extracellular fluids are considered biomarkers of brain injury including TBI [9-12]. These astrocytic modifications may have the properties of supporting neuronal survival or designate cells to die; however, it has been difficult to find a definitive astrocytic cellular signature for each of these outcomes [13-15].

A particular aspect associated with SRC is the intrinsic characteristics of the affected subjects. Athletes are under exhaustive routine of physical exercise training and psychological pressure, and as consequence, they should maintain their body in the upper

limit of physiological functions [16, 17], hence, is not uncommon they abuse of performance-enhancing drugs hoping to gain a competitive edge. Some athletes take high doses of anabolic androgenic steroids (AAS), individually or combined [18, 19], to increase muscle mass and improve oxidative metabolism in spite of the general health risks reported in peripheral organs but little explored into the brain. Also, the athlete's exercise training program *per se* is a variable able to mediate increase mitochondrial biogenesis and positive metabolic adaptations to skeletal muscle and brain [20, 21]. However, when cocktails of AAS and repetitive mild TBI are combined in highly exercise trained individuals the brain mitochondrial bioenergetics machinery might display unpredictable metabolic responses.

Up to now, there are still gaps to be filled regarding neuroenergetic mechanisms behind the secondary damage associated with repetitive mild TBI. Even in the clinical settings it has been difficult to establish precise clinicopathological correlates of CTE pathology due to premorbid and morbidity factors affecting the individuals [4]. Considering these issues it seems relevant to further explore models of repeated mild TBI translating the neurometabolic changes that follow SRC [22]. Yet, to our knowledge, few animal models have combined variables that mimic athletes' environmental challenges that ultimately might lead to unique brain metabolic signatures likely reflecting the role of mitochondria on the fate of cell death and survival [4, 22, 23].

We aimed to investigate the neuroenergetic consequences of repeated mild TBI in exercised mice concomitantly administered with an AAS cocktail.

## 2. Methods

## 2.1. Animals and treatment protocol

Male 90 days old CF1 mice (n = 40 and n = 6-11 per group) were obtained from (CREAL, Porto Alegre/RS, Brazil). Animals (4-5 per cage) were placed into a controlled temperature room (22ºC ± 1) under a 12 h light/12h dark cycle (lights on at 7 a.m.) and had free access to food, water and an exercise running wheel. For exercise testing purposes, a non-exercised (naïve) group was allocated to a cage with a fixed running wheel. After 15 days of exercise adaptation [24], AAS administration was initiated and animals were maintained with free access to the running wheel. The groups were allocated as SHAM (without head injury), SRC (submitted to repetitive head injury) and AAS (submitted to repetitive head injury and administered with testosterone plus nandrolone). All experimental groups (SHAM, SRC and AAS) performed physical exercise through the free access in the running wheel. The treatment consisted of a daily subcutaneous injection of corn oil (SHAM and SRC groups), or a cocktail of nandrolone decanoate (7.5 mg/kg, Organon®) plus testosterone cypionate (7.5 mg/kg, Sigma Pharma) in the AAS group [25, 26]. After additional twenty days of exercise, the groups SRC and AAS were submitted to three closed CCI (E1, E2 and E3) separated by 5 days/each. The AAS and vehicle administration was paused for 48 h after each SRC protocol. See Figure 1E for details. All experiments were in agreement with the Committee on the Care and Use of Experimental Animal Resources, UFRGS, Brazil number 22436.

## 2.2. Sports-Related Concussion protocol

In the days of SRC protocol, mice were previously allocated on an individual sealed electrical treadmill; with shock bars with adjustable voltage (set at 3.0 mA) placed close to the rear paws. Prior to the test procedures, animals were familiarized to the treadmill using 5 min exposures per day for three days, with a fixed speed of 16 m/min with shock bars on. The maximum exercise capacity protocol was performed in stages with crescent speed as follows: at starting stage the speed of 8 m/min for 3 min, followed by increments of 4 m/min every three minutes until reaching the maximum speed of 40 m/min. The test was terminated if the mouse remained in the shock area for 5 seconds, or if the test lasted 36 min with the mouse running at 40 m/min [27]. Immediately after exercise, animals of SRC and AAS groups were anesthetized with isoflurane inhalation and rapidly placed in the stereotaxic (Kopf Instruments, Tujunga, CA) with a heating bed (37 ± 1 $^{o}$C). The hair was removed and TBI was performed using an Benchmark stereotaxic impactor, myNeuroLab®, Leica, St. Louis, MO, USA. Animals were placed in the central area of the stereotaxic (without ear bars fixation) with the head above a thin layer of aluminum paper (See Figure 1 A-D for details). The closed head injury was induced by a piston of 5.0 mm diameter directing the impact to the midline between ears and eyes (See Figure 1 A-D for details). Other lesion parameters were fully adjusted in the equipment, as follows: impact velocity of 5.7 m / s; impact duration was 100 ms, and 5.0 mm of depth penetration. Soon after injury animals were placed in a heated box to maintain normal body temperature and were monitored for 24 h post-injury when no pharmacological treatment was performed [28]. Animals returned to protocol of exercise, drug and oil administration 48 h after injury. A total of 3 mild TBIs were performed (E1,

E2 and E3). SHAM animals were anesthetized without suffer impact to the head. Animals had two-days resting followed by exercise monitoring.

2.3. Synaptosomes isolation

Animal's whole brain was rapidly removed and homogenized in 500 μL of isolation buffer (320 mM sucrose, 10 mM Tris, 0,1% BSA, pH 7.4). Synaptosome-enriched bands were obtained following a discontinuous Percoll® (GE Healthcare, Little Chalfont, UK) gradient protocol [29, 30], then resuspended in a sucrose and Tris buffer (320 mM sucrose, 10mM Tris, pH 7.4) and immediately used for the respirometry, hydrogen peroxide assays , mitochondrial membrane potential ($\Delta\Psi m$) and $Ca^{2+}$ handling (*n* = 6-8 per group). Aliquots of the samples were used for protein quantification using Pierce™ BCA Protein Assay Kit (Catalog number: 23225).

2.4. High Resolution Respirometry Respiratory protocol

Oxygen consumption rate (OCR) measurements were performed at 37°C using Oxygraph-2k system with DatLab software (Oroboros Instruments, Innsbruck, Austria) and normalized to the protein content. Synaptosomes aliquots were incubated in a 2-ml chamber with standard respiration buffer (100 mM KCI, 75 mM mannitol, 25 mM sucrose, 5 mM phosphate, 0.05 mM EDTA, and 10 mM Tris-HC1, pH 7.4) [8, 31]

Routine (R) OCR was measured after 5 min to estabilization. Leak respiration (L) was obtained with titration of pyruvate, malate, glutamate and Succinate (PMGS; 10, 10, 20 and 10 mM, respectively); Maximal capacity of oxidative phosphorylation (OxPHOS; P) was obtained after titration of Adenosine diphosphate (ADP, 2.5 mM). Finally,

Residual oxygen consumption (ROX) was measured after both antimycin-A and cyanide (AA, 2 mM and KCN, 5 mM). We calculated the biochemical OXPHOS coupling efficiency (P-L)/P and reserve respiratory capacity (RRC) relative to maximal OxPhos activity (RRC; P - R) [8].

### 2.5. Mitochondrial $H_2O_2$ production

Mitochondrial production of hydrogen peroxide ($H_2O_2$) was assessed with the AmplexRed® (Invitrogen, Paisley, UK) hydrogen peroxide assay kit in isolated synaptosomes (n=8 per group) incubated in respiration buffer supplemented with 10 µM Amplex Red and 2 units/mL horseradish peroxidase to assess $H_2O_2$ generation. The same substrates and inhibitors used for respirometry were incubated sequentially. Fluorescence was monitored at excitation (563 nm) and emission (587 nm) wavelengths with a Spectra Max M5 microplate reader (Molecular Devices, USA) [32, 33]. Data are expressed as RFU/sec/mg protein.

### 2.6. Mitochondrial Membrane Potential (ΔΨm)

The ΔΨm was measured by using the fluorescence signal of the cationic dye, Safranin-O. Isolated synaptosomes were incubated in the respiration buffer used in the respirometry protocol supplemented with 10 µM safranin-O. The same substrates, and inhibitors used for respirometry were incubated sequentially, but included Oligomycin (Oligo, 2 µg/ml) to inhibit ATP-Synthase activity ($L_{omy}$) and the protonophore Carbonyl cyanide-4-(trifluoromethoxy)phenylhydrazone FCCP) to induce uncoupling (E) and dissipate ΔΨm before antimycin-A and cyanide. Fluorescence was detected with an

excitation wavelength of 495 nm and an emission wavelength of 586 nm (Spectra Max M5, Molecular Devices). Data are reported as arbitrary fluorescence units (AFUs) [33].

2.7. Mitochondrial calcium handling

Mitochondrial calcium influx and efflux was obtained measuring spectrophotometrical absorbance at 540 nm (Spectra Max M5, Molecular Devices). Synaptosomes were added to standard swelling incubation medium (100 mM KCl, 50 mM Sucrose, 10 mM HEPES and 5 mM $KH_2PO^4$) and basal mitochondrial absorbance was monitored during 3 min. Mitochondrial substrates were added to support ATP production (3.5 mM pyruvate, 4.5 mM malate, 4.5 mM glutamate, 1.2 mM succinate and 100 uM ADP) and the mitochondrial absorbance during coupled oxidative phosphorylation (PMGSA) was monitored during 5 min. Subsequently, 10 mM $Ca^{2+}$ was added to induce swelling due to influx into the mitochondrial matrix ($Ca^{2+}$). Mitochondrial calcium efflux through the sodium–calcium-lithium exchanger (NCLX), was monitored (10 min) after addition of 25 mM $Na^+$. A decrease and increase in absorbance indicates swelling and shrinkage, respectively [8]. The results are expressed as absorbance in 540 nm.

2.8. Immunohistochemistry

For immunohistochemistry, mice were perfused with phosphate-buffered saline (PBS, pH:7.4), and brains were removed from the skull and post-fixed with 4% paraformaldehyde (from Sigma Aldrich, São Paulo/Brazil) solution at 4 °C for 24 h. After this period, the brain was then placed in 30% sucrose solution containing 0.02 % of

azide at 4°C, until the brains are properly sectioned by vibratome (Leica Biosystems, Mannheim, Wetzlar, Germany). Coronal slices and serial 30μm thick vibratome sections of left hemispheric brain (except cerebellum) were made, mounted on slides coated with 10 % (3-Aminopropyl) triethoxysilane) (from Sigma Aldrich, São Paulo/Brazil) and dried at room temperature overnight. The slices were then stored in boxes of microscope slides at -20 ° C until the day of the experiment.

For immunofluorescence, slices were submitted to heat-induced antigen retrieval (66°C) in oven for laboratory, with antigen retrieval solution (10 mM citric acid, pH:6.0) for 15 min. After removal from the oven, slices were placed to cool in room temperature for 20 min and washed in PBS (pH:7.4) for 3×5 min. Subsequently, slices were permeabilized with a solution containing PBS (pH:7.4) and 1 %Triton X-100 for 15 min, following blockage with a solution containing 5 % goat serum (Sigma Aldrich), PBS (pH:7.4) and 0.3 %Triton X-100 for 1 h at room temperature and then incubated with rabbit anti-glial fibrillary acidic protein (GFAP) (1:200, Dako) at 4 °C for 48 h, in a humid chamber. After rinsing five times in PBS (pH:7.4), sections were incubated with anti-rabbit secondary antibody conjugated to Alexa Fluor 488 fluorescent dye for GFAP (1:100; Invitrogen, Biogen Porto Alegre/RS, Brazil), in PBS for 2 h at room temperature. After staining, sections were washed in PBS (for 3×5 min), counterstained with 0.001% DAPI (Invitrogen) for 15 min, and rinsed again. Coverslips were mounted using a fluorescence mounting medium (Dako, São Paulo/Brazil) [34]. For immunohistochemical analyses, all lighting conditions and magnifications were kept constant. All images were acquired using a fluorescence Nikon microscope with NIS Elements AR 2.30 software. The Tiff images (1372 ×1024 pixels) were captured at an objective lens magnification of

20×. The fluorescence intensities were quantified using the NIH ImageJ software, using the setup calibration information of the NIS Elements AR 2.30 software of 0.322 µm/pixel for the objective 20x. Data is reported as mean fluorescence intensity, calculated as percent of SHAM group (considered 100 %).

2.9. Western blotting

Left hemisphere cortex and hippocampi of mice were dissected and then homogenized in a buffer solution (EDTA 2 mM, protease and phosphatase inhibitor cocktails I and II (Sigma, St. Louis, USA) 0.001 %, Tris HCl 50 mM, (pH 7.4), glycerol 10 % and Triton X-100 1 %) and centrifuged (1300 g/ 3 min). Supernatant was collected and diluted in an appropriated sample buffer. Samples of 20 µg of protein (n=6-8 per group) were separated by electrophoresis on a 10% or 12% polyacrylamide gel and electrotransferred to PVDF membranes (Amersham, GE Healthcare, Little Chalfont, UK) as previously reported.[24] Primary antibodies against Alpha-Spectrin (Millipore®, GER; 1:1000; ref. MAB1622); Anti-Tau phospho-S396 (ABCAM®, USA; 1:1000; ref. ab109390); Anti-Tau antibody (ABCAM®, USA; 1:1000; ref. ab32057). All procedures were conducted according to specific antibody manufacturer's instruction. Primary antibodies were incubated overnight followed by 2 h incubation with horseradish peroxidase-conjugated anti-rabbit or anti-mouse IgG (1:5000) (GE, Little Chalfont, UK) secondary antibodies [8]. Membranes were incubated with Amersham ECL Western Blotting Detection Reagent (GE Healthcare Life Sciences, Little Chalfont, UK) for 5 min and the immunodetection was made by chemoluminescence using Image Quant LAS

4000 (GE, Little Chalfont, UK). Protein expression was quantified using Image J® software (Rockville, USA). The values of optic density were expressed as % of control.

2.10. Statistical Analysis

Results were calculated and expressed as mean ± S.E.M. Data normality was assessed with Shapiro-Wilk test. Differences between groups were assessed using one-way analysis of variance (ANOVA) followed by Tukey's post-hoc test. All procedures were performed using GraphPad Prism 6.0 software. Differences were considered statistically significant at $p < 0.05$.

## 3. Results

3.1. Effects of SR-TBI and AAS on exercise performance test and

All exercised groups (SHAM, SRC and AAS) displayed increased maximum exercise capacity compared to naïve group in the E1, E2 and E3 days (Figure 1F; Two-way Anova ($F(3.34)=9.146$; $p< 0.0001$).

3.2. Impaired synaptosomal mitochondria bioenergetics after SRC is partially prevented by AAS

Oxygen consumption rates (OCR) in synaptosomes (Figure 2A) were not different in R, L and ROX states. There was a significant decrease OCR in P state ($F_{(2.\ 20)} = 6.2$, $p<0.008$) of SRC group compared to both SHAM and AAS groups (Mean diff=21.91 and 48.8). OxPhos coupling efficiency was not different between groups (Figure 2B).

There was decreased RRC in SRC group compared to Sham and AAS (Figure 2C; $F_{(2.\ 20)}$ = 6.012, p<0.009). Moreover, ANOVA comparisons showed significant increase in $H_2O_2$ levels at baseline in SRC group (Figure 2D; $F_{(2.\ 20)}$ = 17.12, p<0.0001).

The addition of PMGS (L state) induced significantly elevated $H_2O_2$ production in SRC compared to SHAM and AAS ($F_{(2.20)}$=15.6, $p$ = 0.0002). Addition of ADP (P state) yielded significantly higher $H_2O_2$ production only in SRC compared to SHAM ($F_{(2.20)}$=9.85, $p$ = 0.0011) while no differences were observed comparing AAS to SHAM or CCI. Strikingly, AAS prevented SRC-induced increased hydrogen peroxide production in different mitochondrial coupling states.

3.3. Mitochondrial membrane potential ($\Delta\Psi_m$) dynamics and calcium buffering was impaired after SRC but prevented by AAS co-administration

Impaired dynamics of $\Delta\psi_m$ is a mechanism of mitochondrial dysfunction and increased $H_2O_2$ production [35]. Evaluation of $\Delta\psi_m$ in synaptosomes showed no significant differences in the L state. There were significant group differences for P, $L_{omy}$ and E states ($F_{(2.20)}$=18.09, p<0.0001), ($F_{(2.20)}$=14.62, p<0.0001) and ($F_{(2.20)}$=9.67, p<0.0011) (Figure 3A).

Aiming to determine mitochondrial calcium handling responses (influx/efflux) to metabolic challenges, we evaluated swelling and shrinkage. There were significant differences between groups following PMGSA and $Ca^{2+}$ addition (Figure 3B). The specific variations in $Ca^{2+}$ efflux capacity stimulated by $Na^{+}$ was significant different between groups (Figure 3B, $F_{(2.20)}$ = 78.56, p<0.0001). Uptake was impaired in both SRC and AAS compared to SHAM, with a significant difference between SRC and AAS ($p$ <

0.001 for all comparisons). Taken together, these results indicate that exposure to AAS partially preserved mitochondrial $\Delta\psi_m$ dynamics, and resulted in a less detrimental effect on $Ca^{2+}$ uptake in and efflux in synaptic mitochondria even after SRC.

3.4. Increased astrogliosis induced by SRC in hippocampus

Immunohistochemistry for glial fibrillary acidic protein (GFAP) in the dentate gyrus (DG) of hippocampi showed increased astrogliosis in SRC and AAS (Figure 4A). There was no statistical differences in the Granular Layer; however, in the molecular layer (Figure 4C, $F_{(2.9)} = 84.37$, $p = 0.0001$), a significant difference was found in SRC and AAS compared to SHAM. Analysis of polymorphic layer (D) indicated a significant difference only when comparing AAS to SHAM (Figure 4D, $F_{(2.9)}= 5.271$, $p = 0.0305$).

3.5. Increased molecular biomarkers of axonal neurodegeneration in SRC

Abnormal degradation of cytoskeletal proteins like alpha-Spectrin and phosphorylation of Tau is a consistent feature following TBI associated with neurodegeneration. We displayed increased cleavage of alpha-Spectrin (240 kDa) in SRC and AAS compared to SHAM, as demonstrated by the immunocontent of 120/240 kDa fragments in the cortex (Figure 5A, $F_{(2.20)} = 4.52$, $p<0.0240$). In the hippocampus, alpha-Spectrin cleavage in SRC and AAS groups were significant different when compared to SHAM (Figure 5B, $F_{(2.20)} = 30.92$, $p<0.0001$).

Since we found increased astrogliosis in the hippocampi we further evaluated Tau phosphorylation as indicated by the ratio of $pTau^{Ser396}$. The SRC and AAS groups were different from SHAM group (Figure 5C, $F_{(2.20)}=19.66$, $p<0.001$). Therefore, the

aforementioned mitochondrial dysfunction and astrogliosis induced by SRC parallel with increased activation of calcium dependent proteases and markers of neurodegeneration. Although the AAS cocktail sustained mitochondrial function, it was not able to prevent astrogliosis or neurodegeneration.

## 4. Discussion

Here we showed that the association of physical exercise and AAS administration is neuroprotective against the mitochondrial dysfunctions in a mice model of SRC, however it was not neuroprotective against neuronal cytoskeletal abnormalities. This multi-intervention protocol was designed to mimic the environmental of SRC in athletes, that often comprises intense exercise training, use of enhancing performance drugs and repeated mild TBI, followed by post-concussive pauses.

It is currently accepted that repeated concussions can result in cumulative damage leading to long-term neuropsychiatric symptoms and increased concentration of biomarkers related to neurodegenerative disorders [3, 36]. Although many studies have investigated the effects of repeated TBI in rodents, currently few models combined the effect of exercise, whereas here the exercise in the running wheel was determined as fixed variable in our protocol [7, 37, 38]. Additionally, the high incidence of AAS abuse for professional athletes has raised considerable health concerns as well as it is not known whether these hormones could accelerate or delay secondary biochemical mechanisms associated with SRC [18, 39]. With this in mind, we aimed to develop a reliable, low-cost animal model to investigate mitochondria-related outcomes after repeated TBI in mice and evaluate the consequences of supraphysiological doses of the two most used AAS in

sports (testosterone plus nandrolone) [40, 41]. Also, we used five-day intervals between injuries to allow the course of neurodegenerative mechanisms, and 2-days exercise resting to simulate a period of "recovery and return to sports practice", which is an alternative to the current literature submitting mice to repeated mild TBI spaced by 24 h interval [39]. Here, we showed that the disturbances in components involved in the mitochondrial neuroenergetics machinery after SRC is not associated with increased axonal markers of neurodegeneration.

It has been shown that physical exercise up regulates several neuroprotective mechanisms associated with neuroplasticity [21, 41], such as increased antioxidant defenses, improved biogenesis, and function of neuronal mitochondria [22, 32, 33]. However, these exercise-induced adaptations may have unpredictable effects when neural cells are submitted to metabolic challenges as occurs in SRC [42]. Actually, kainate-induced injury model was more neurotoxic to previously exercised animals than for the sedentary ones, and also, intracerebroventricular streptozotocin administration in free running wheel exercised mice exacerbates memory deficits [32, 43]. However, findings in experimental models of TBI have given support to the relevance of exercise as both therapeutic [44, 45] and prophylactic [38, 46, 47] strategy; though we raised concerns particularly regarding the plethora of professional requirements that put pressure into athletes physiology and lifestyle and, in some circumstances, it may act on opposite to the expected benefits in the mitochondrial neuroenergetic adaptations. Concerns also exist regarding the time-window for athletes be engaged in exercise programs following a TBI, [48, 49]. Thus, it is still necessary to provide a mechanistic basis to recommend an

appropriate time for re-exposition to physical activity after concussive injury otherwise it could exacerbate neurological symptoms and the damage to neural cells [42].

Similar to athletes in the upper limit of physiological capacity, exercised mice showed increased performance in the physical exhaustion test regardless AAS, which confirms the absence of motor impairments and overall metabolic adaptations achieved by the running wheel protocol. However, when overtrained mice were further challenged by repetitive mild TBIs mitochondria displayed characteristics of dysfunction. Therefore, the commonly reported impairment in mitochondrial bioenergetics after TBI [6-8] was confirmed by our findings, since OCR and RRC were decreased by SRC, meanwhile the AAS cocktail was partially mitoprotective. The present results indicates that SRC causes uncoupling of oxygen consumption rate (OCR) with ATP synthesis, which are accessory substrates to divert oxygen to ROS production, as demonstrated here by the increased $H_2O_2$ production [8]. These alterations can be explained at least partially by the impaired $\Delta\Psi_m$ formation/dissipation, alongside with persistent $Ca^{2+}$ load into mitochondria due to deficient neuronal $Na^{+}$dependent $Ca^{2+}$ efflux. Altogether, these components may work as substrates for progressive neurodegeneration often reported in TBI studies [8, 50, 51]. Based on the effects of AAS cocktail, it was not possible to sustain the premise that even a partial sustainment of mitochondrial ATP production, $Ca^{2+}$ homeostasis and membrane potential may halt SRC-associated neurodegeneration [8, 23].

Repeated TBI-induced diffused astrocyte deformation leading to reactive astrogliosis conceptually characterized by up regulation of GFAP [10, 12, 15, 52]. We found that SRC and AAS increased astrogliosis in the dentate gyrus. Considering the pivotal function of astrocytes and the importance of hippocampus in brain connectivity,

this response may conceptually exert a profound impact in memory processing following SRC [10, 13, 53] albeit we did not addressed this issue. Therefore, it remains to be determined how these responses are related to long-term neurological outcomes following injury, since it is reportedly that astrogliosis is involved in both neuroprotection and neurodegeneration [10, 13-15, 54]. Also, it was recently demonstrated that an AAS cocktail administered in cycles for seven weeks prior to TBI exacerbated microgliosis, and axonal degeneration but not caused behavioral deficits seven-days post-injury [39].

It has been shown that mild TBI induced progressive axonal pathology is characterized by aberrant phosphorylation of Tau and proteolysis of the cytoskeletal protein alpha-Spectrin by $Ca^{2+}$ dependent proteases [36, 55] In both humans and rodents, alpha-Spectrin levels increase after head injury, paralleling with increased Tau phosphorylation and aggregation, which correlates with progressive neuronal dysfunction, and behavioral changes [36, 56]. Here, our proposed model of SRC augmented both molecular markers of axonal degeneration, as it has been reported in post-mortem brain of athletes. Remarkably, AAS beneficial effects to mitochondrial function were not associated with lower magnitude of astrogliosis or axonal neurodegeneration. Although, in the present study the animals were trained throughout the course of protocol, which approximates our model with SRC environment, we cannot establish further relations of the neurobiochemical variables with long-term outcomes, which stands as a future challenge.

In conclusion, we developed a mice model of SRC, which combined exercise and use of enhancing performance drugs. We found alterations in key elements associated

with mitochondrial function in SRC mice, like ATP synthesis, $Ca^{2+}$ efflux and increased $H_2O_2$ production. Both SRC and AAS groups showed increased hippocampal neurodegeneration, tough AAS attenuated mitochondrial dysfunction caused by the repetitive head injury. The experimental protocol proposed here is a step towards the establishment of an integrative model to study SRC in mice.

**Acknowledgements**

This work was supported by the Brazilian grants of Conselho Nacional de Desenvolvimento Científico e Tecnológico (CNPq) #426796/2016-0 and 141100/2013-3, CNPq-Instituto Nacional de Neurociência Translacional-INNT #465346/2014-6, FAPERGS/PRONEX#16/2551-0000499-4 and also by the Conselho de Aperfeiçoamento de Pessoal de Nível Superior (CAPES) #1663.

## 5. References

[1] Z. Yang, P. Wang, D. Morgan, D. Lin, J. Pan, F. Lin, K.H. Strang, T.M. Selig, P.D. Perez, M. Febo, B. Chang, R. Rubenstein, K.K.W. Wang, Temporal MRI characterization, neurobiochemical and neurobehavioral changes in a mouse repetitive concussive head injury model, Scientific Reports 5 (2015) 11178.

[2] R. Mannix, W.P. Meehan Iii, A. Pascual-Leone, Sports-related concussions — media, science and policy, Nature Reviews Neurology 12 (2016) 486.

[3] A.C. McKee, R.A. Stern, C.J. Nowinski, T.D. Stein, V.E. Alvarez, D.H. Daneshvar, H.-S. Lee, S.M. Wojtowicz, G. Hall, C.M. Baugh, D.O. Riley, C.A. Kubilus, K.A. Cormier, M.A. Jacobs, B.R. Martin, C.R. Abraham, T. Ikezu, R.R. Reichard, B.L. Wolozin, A.E. Budson, L.E. Goldstein, N.W. Kowall, R.C. Cantu, The spectrum of disease in chronic traumatic encephalopathy, Brain : a journal of neurology 136 (2013) 43-64.

[4] D.H. Smith, V.E. Johnson, J.Q. Trojanowski, W. Stewart, Chronic traumatic encephalopathy — confusion and controversies, Nature Reviews Neurology (2019).

[5] J.R. Kulbe, E.D. Hall, Chronic traumatic encephalopathy-integration of canonical traumatic brain injury secondary injury mechanisms with tau pathology, Prog Neurobiol 158 (2017) 15-44.
[6] R.L. Hill, I.N. Singh, J.A. Wang, E.D. Hall, Time courses of post-injury mitochondrial oxidative damage and respiratory dysfunction and neuronal cytoskeletal degradation in a rat model of focal traumatic brain injury, Neurochem Int 111 (2017) 45-56.
[7] W.B. Hubbard, B. Joseph, M. Spry, H.J. Vekaria, K.E. Saatman, P.G. Sullivan, Acute Mitochondrial Impairment Underlies Prolonged Cellular Dysfunction after Repeated Mild Traumatic Brain Injuries, J Neurotrauma (2018).
[8] R.B. Carteri, A. Kopczynski, M.S. Rodolphi, N.R. Strogulski, M. Sartor, M. Feldmann, M.A. De Bastiani, C.M. Duval Wannmacher, I.D. de Franceschi, G. Hansel, D.H. Smith, L.V. Portela, Testosterone Administration after Traumatic Brain Injury Reduces Mitochondrial Dysfunction and Neurodegeneration, Journal of neurotrauma (2019).
[9] M.A. Stefani, R. Modkovski, G. Hansel, E.R. Zimmer, A. Kopczynski, A.P. Muller, N.R. Strogulski, M.S. Rodolphi, R.K. Carteri, A.P. Schmidt, J.P. Oses, D.H. Smith, L.V. Portela, Elevated glutamate and lactate predict brain death after severe head trauma, Ann Clin Transl Neurol 4 (2017) 392-402.
[10] J.E. Burda, A.M. Bernstein, M.V. Sofroniew, Astrocyte roles in traumatic brain injury, Experimental neurology 275 (2016) 305-315.
[11] A.E. Bohmer, J.P. Oses, A.P. Schmidt, C.S. Peron, C.L. Krebs, P.P. Oppitz, T.T. D'Avila, D.O. Souza, L.V. Portela, M.A. Stefani, Neuron-specific enolase, S100B, and glial fibrillary acidic protein levels as outcome predictors in patients with severe traumatic brain injury, Neurosurgery 68 (2011) 1624-1630; discussion 1630-1621.
[12] H. Zetterberg, D.H. Smith, K. Blennow, Biomarkers of mild traumatic brain injury in cerebrospinal fluid and blood, Nat Rev Neurol 9 (2013) 201-210.
[13] M.V. Sofroniew, H.V. Vinters, Astrocytes: biology and pathology, Acta neuropathologica 119 (2010) 7-35.
[14] L.J. Van Eldik, M.S. Wainwright, The Janus face of glial-derived S100B: beneficial and detrimental functions in the brain, Restorative neurology and neuroscience 21 (2003) 97-108.
[15] M. Brenner, Role of GFAP in CNS injuries, Neuroscience letters 565 (2014) 7-13.
[16] J. Jakeman, S. Adamson, J. Babraj, Extremely short duration high-intensity training substantially improves endurance performance in triathletes, Applied physiology, nutrition, and metabolism = Physiologie appliquee, nutrition et metabolisme 37 (2012) 976-981.
[17] M. Gerber, R. Brand, F. Antoniewicz, S. Isoard-Gautheur, H. Gustafsson, R. Bianchi, F. Colledge, D.J. Madigan, S. Brand, S. Ludyga, Implicit and explicit attitudes towards sport among young elite athletes with high versus low burnout symptoms, Journal of Sports Sciences (2019) 1-8.
[18] P. Simon, E.W. Neuberger, G. Wang, Y.P. Pitsiladis, Antidoping Science: Important Lessons From the Medical Sciences, Curr Sports Med Rep 17 (2018) 326-331.

[19] A.D. Fraser, Doping control from a global and national perspective, Therapeutic drug monitoring 26 (2004) 171-174.
[20] S. Dandanell, A.K. Meinild-Lundby, A.B. Andersen, P.F. Lang, L. Oberholzer, S. Keiser, P. Robach, S. Larsen, B.R. Ronnestad, C. Lundby, Determinants of maximal whole-body fat oxidation in elite cross-country skiers: Role of skeletal muscle mitochondria, Scandinavian journal of medicine & science in sports 28 (2018) 2494-2504.
[21] S. Camandola, M.P. Mattson, Brain metabolism in health, aging, and neurodegeneration, The EMBO journal 36 (2017) 1474-1492.
[22] H. Bolouri, H. Zetterberg, Frontiers in Neuroengineering
Animal Models for Concussion: Molecular and Cognitive Assessments-Relevance to Sport and Military Concussions. In: F.H. Kobeissy (Ed.), Brain Neurotrauma: Molecular, Neuropsychological, and Rehabilitation Aspects, CRC Press/Taylor & Francis.
(c) 2015 by Taylor & Francis Group, LLC., Boca Raton (FL), 2015.
[23] G. Cheng, R.-h. Kong, L.-m. Zhang, J.-n. Zhang, Mitochondria in traumatic brain injury and mitochondrial-targeted multipotential therapeutic strategies, British Journal of Pharmacology 167 (2012) 699-719.
[24] A.P. Muller, J. Gnoatto, J.D. Moreira, E.R. Zimmer, C.B. Haas, F. Lulhier, M.L. Perry, D.O. Souza, I. Torres-Aleman, L.V. Portela, Exercise increases insulin signaling in the hippocampus: physiological effects and pharmacological impact of intracerebroventricular insulin administration in mice, Hippocampus 21 (2011) 1082-1092.
[25] K.R. Bonson, R.G. Johnson, D. Fiorella, R.A. Rabin, J.C. Winter, Serotonergic control of androgen-induced dominance, Pharmacol Biochem Behav 49 (1994) 313-322.
[26] E. Kalinine, E.R. Zimmer, K.C. Zenki, I. Kalinine, V. Kazlauckas, C.B. Haas, G. Hansel, A.R. Zimmer, D.O. Souza, A.P. Muller, L.V. Portela, Nandrolone-induced aggressive behavior is associated with alterations in extracellular glutamate homeostasis in mice, Hormones and behavior 66 (2014) 383-392.
[27] S. Marcaletti, C. Thomas, J.N. Feige, Exercise Performance Tests in Mice, Curr Protoc Mouse Biol 1 (2011) 141-154.
[28] D.H. Smith, H.D. Soares, J.S. Pierce, K.G. Perlman, K.E. Saatman, D.F. Meaney, C.E. Dixon, T.K. McIntosh, A model of parasagittal controlled cortical impact in the mouse: cognitive and histopathologic effects, Journal of neurotrauma 12 (1995) 169-178.
[29] N.R. Sims, Rapid isolation of metabolically active mitochondria from rat brain and subregions using Percoll density gradient centrifugation, Journal of neurochemistry 55 (1990) 698-707.
[30] N.R. Sims, M.F. Anderson, Isolation of mitochondria from rat brain using Percoll density gradient centrifugation, Nature protocols 3 (2008) 1228-1239.
[31] E. Gnaiger, Mitochondrial pathways and respiratory control. An introduction to OXPHOS analysis. , OROBOROS MiPNet Publications, Innsbruck, 2014, 80 pp.

[32] A.P. Muller, E.R. Zimmer, E. Kalinine, C.B. Haas, J.P. Oses, A. Martimbianco de Assis, A. Galina, D.O. Souza, L.V. Portela, Physical exercise exacerbates memory deficits induced by intracerebroventricular STZ but improves insulin regulation of H(2)O(2) production in mice synaptosomes, J Alzheimers Dis 30 (2012) 889-898.
[33] L.V. Portela, A.W. Brochier, C.B. Haas, A.K. de Carvalho, J.A. Gnoato, E.R. Zimmer, E. Kalinine, L. Pellerin, A.P. Muller, Hyperpalatable Diet and Physical Exercise Modulate the Expression of the Glial Monocarboxylate Transporters MCT1 and 4, Mol Neurobiol (2016).
[34] V.R. Torrez, E.R. Zimmer, E. Kalinine, C.B. Haas, K.C. Zenki, A.P. Muller, D.O. Souza, L.V. Portela, Memantine mediates astrocytic activity in response to excitotoxicity induced by PP2A inhibition, Neuroscience letters 696 (2019) 179-183.
[35] T.R. Figueira, D.R. Melo, A.E. Vercesi, R.F. Castilho, Safranine as a fluorescent probe for the evaluation of mitochondrial membrane potential in isolated organelles and permeabilized cells, Methods in molecular biology (Clifton, N.J.) 810 (2012) 103-117.
[36] V.E. Johnson, W. Stewart, D.H. Smith, Axonal pathology in traumatic brain injury, Experimental neurology 246 (2013) 35-43.
[37] M.G. Clark, K., Sport-Related Traumatic Brain Injury. In: G.G. Laskowitz D (Ed.), Translational Research in Traumatic Brain Injury, CRC Press/Taylor and Francis Group, Boca Raton (FL), 2016.
[38] J.M. Taylor, M.H. Montgomery, E.J. Gregory, N.E. Berman, Exercise preconditioning improves traumatic brain injury outcomes, Brain Res 1622 (2015) 414-429.
[39] D.R. Namjoshi, W.H. Cheng, M. Carr, K.M. Martens, S. Zareyan, A. Wilkinson, K.A. McInnes, P.A. Cripton, C.L. Wellington, Chronic Exposure to Androgenic-Anabolic Steroids Exacerbates Axonal Injury and Microgliosis in the CHIMERA Mouse Model of Repetitive Concussion, PLoS One 11 (2016) e0146540.
[40] J.G. Oberlander, L.P. Henderson, The Sturm und Drang of anabolic steroid use: angst, anxiety, and aggression, Trends Neurosci 35 (2012) 382-392.
[41] S.A. Neeper, F. Gomez-Pinilla, J. Choi, C. Cotman, Exercise and brain neurotrophins, Nature 373 (1995) 109.
[42] G.S. Griesbach, Exercise after traumatic brain injury: is it a double-edged sword?, Pm r 3 (2011) S64-72.
[43] M. Ramsden, N.C. Berchtold, J. Patrick Kesslak, C.W. Cotman, C.J. Pike, Exercise increases the vulnerability of rat hippocampal neurons to kainate lesion, Brain research 971 (2003) 239-244.
[44] D.H. Kim, I.G. Ko, B.K. Kim, T.W. Kim, S.E. Kim, M.S. Shin, C.J. Kim, H. Kim, K.M. Kim, S.S. Baek, Treadmill exercise inhibits traumatic brain injury-induced hippocampal apoptosis, Physiol Behav 101 (2010) 660-665.
[45] I.G. Ko, S.E. Kim, L. Hwang, J.J. Jin, C.J. Kim, B.K. Kim, H. Kim, Late starting treadmill exercise improves spatial leaning ability through suppressing CREP/BDNF/TrkB signaling pathway following traumatic brain injury in rats, J Exerc Rehabil 14 (2018) 327-334.

[46] F. da Silva Fiorin, A.P. de Oliveira Ferreira, L.R. Ribeiro, L.F. Silva, M.R. de Castro, L.R. da Silva, M.E. da Silveira, Jr., A.P. Zemolin, F. Dobrachinski, S. Marchesan de Oliveira, J.L. Franco, F.A. Soares, A.F. Furian, M.S. Oliveira, M.R. Fighera, L.F. Freire Royes, The Impact of Previous Physical Training on Redox Signaling after Traumatic Brain Injury in Rats: A Behavioral and Neurochemical Approach, Journal of neurotrauma 33 (2016) 1317-1330.
[47] M.R.T. de Castro, A.P.O. Ferreira, G.L. Busanello, L.R.H. da Silva, M.E.P. da Silveira Junior, F.D.S. Fiorin, G. Arrifano, M.E. Crespo-Lopez, R.P. Barcelos, M.J. Cuevas, G. Bresciani, Previous physical exercise alters the hepatic profile of oxidative-inflammatory status and limits the secondary brain damage induced by severe traumatic brain injury in rats, 595 (2017) 6023-6044.
[48] G.S. Griesbach, F. Gomez-Pinilla, D.A. Hovda, Time window for voluntary exercise-induced increases in hippocampal neuroplasticity molecules after traumatic brain injury is severity dependent, J Neurotrauma 24 (2007) 1161-1171.
[49] J.L. Humm, D.A. Kozlowski, D.C. James, J.E. Gotts, T. Schallert, Use-dependent exacerbation of brain damage occurs during an early post-lesion vulnerable period, Brain Res 783 (1998) 286-292.
[50] I.S. Balan, A.J. Saladino, B. Aarabi, R.J. Castellani, C. Wade, D.M. Stein, H.M. Eisenberg, H.H. Chen, G. Fiskum, Cellular Alterations in Human Traumatic Brain Injury: Changes in Mitochondrial Morphology Reflect Regional Levels of Injury Severity, Journal of Neurotrauma 30 (2013) 367-381.
[51] J. Ji, Y.Y. Tyurina, M. Tang, W. Feng, D.B. Stolz, R.S. Clark, D.F. Meaney, P.M. Kochanek, V.E. Kagan, H. Bayir, Mitochondrial injury after mechanical stretch of cortical neurons in vitro: biomarkers of apoptosis and selective peroxidation of anionic phospholipids, Journal of neurotrauma 29 (2012) 776-788.
[52] P. Shahim, Y. Tegner, N. Marklund, K. Hoglund, E. Portelius, D.L. Brody, K. Blennow, H. Zetterberg, Astroglial activation and altered amyloid metabolism in human repetitive concussion, Neurology 88 (2017) 1400-1407.
[53] A. Adamsky, I. Goshen, Astrocytes in Memory Function: Pioneering Findings and Future Directions, Neuroscience 370 (2018) 14-26.
[54] I.P. Karve, J.M. Taylor, P.J. Crack, The contribution of astrocytes and microglia to traumatic brain injury, British journal of pharmacology 173 (2016) 692-702.
[55] V.E. Johnson, W. Stewart, M.T. Weber, D.K. Cullen, R. Siman, D.H. Smith, SNTF immunostaining reveals previously undetected axonal pathology in traumatic brain injury, Acta neuropathologica 131 (2016) 115-135.
[56] R. Siman, P. Shahim, Y. Tegner, K. Blennow, H. Zetterberg, D.H. Smith, Serum SNTF Increases in Concussed Professional Ice Hockey Players and Relates to the Severity of Postconcussion Symptoms, J Neurotrauma 32 (2015) 1294-1300.

**Figure legends**

**Figure 1. Sports-related concussion protocol and experimental design.** The SRC protocol was performed using an impactor attached to stereotaxic device (A) placed at 90$^{o}$ in the midline between eyes and ears (B, C and D). Mice were gently placed in a cushioned support, with the head placed above a thin layer of paper (HS), allowing full head movement after the impact. Experimental design (E), and physical exercise capacity test performed before the impact (F). All groups performing voluntary exercise in the running wheel demonstrated improved performance when challenged in a treadmill protocol (n = 8 - 10 per group). * indicates significant differences of naïve compared to all other groups. SRC, sports-related concussion; S = Start of treatment; E1, E2 and E3 = SRC protocols; Timeline (A) = Neurochemical assays.

**Figure 2. Physical exercise plus anabolic androgen steroids (AAS) attenuated impaired mitochondrial metabolism after the sports-related concussion protocol.** Synaptossomal OCR (A) of SRC group did not respond similarly to other groups after the addition of ADP as substrate for ATP synthesis (P). The interventions did not affect OxPhos Coupling Efficiency (B). SRC caused decrease in the Reserve Respiratory Capacity (C). The mitochondrial $H_2O_2$ production (D) was increased in SRC group in routine (ROUT), and after the addition of substrates PMGS (L) and ADP (P). The groups SHAM, SRC, and AAS performed physical exercise during the course of the experimental protocol (approximately 45 days) (n = 6 - 8 per group). * Denotes significant difference compared to SHAM; # Indicates significant difference between

SRC and AAS. AAS, testosterone plus nandrolone; SRC, Sports-related concussion; OCR, Oxygen consumption rate.

**Figure 3. Anabolic androgenic steroids (AAS) sustained mitochondrial membrane potential (ΔΨm) and calcium efflux after the sports-related concussion protocol.** The SRC protocol altered the ΔΨm in sinaptossomes after the addition of PMGS+ADP (P), PMGS+ADP+ olygomicin ($L_{omy}$), and the uncoupler FCCP (E). The AAS partially sustained the ΔΨm (A). Both SRC and AAS showed impaired $Na^{+}$-dependent mitochondrial $Ca^{2+}$ efflux after being energized with metabolic substrates (Pyruvate, Malate, Glutamate and Succinate, plus ADP), as demonstrated by the changes in absorbance at 540 nm after $Ca^{2+}$ (swelling) and Na+ (shrinkage) loading (B). The groups SHAM, SRC, and AAS performed physical exercise during the course of the experimental protocol (approximately 45 days) (n = 6 - 8 per group). *Denotes significant difference compared to SHAM; #Indicates significant difference between SRC and AAS. AAS, testosterone plus nandrolone; SRC, Sports-related concussion.

**Figure 4. Increased astrogliosis in hippocampus induced by the sports-related concussion protocol.** Immunohistochemistry for glial fibrillary acidic protein (GFAP) in the subregions of Dentate gyrus (DG) (A) showed increased astrogliosis, without statistical significance in the Granular Layer (B). A significant increment was found in the Molecular Layer of SRC and AAS groups (C); and in the Polymorphic layer of the AAS group (D) (n = 4 per group). *Denotes significant difference compared to SHAM.

All images were captured at a magnification of 20×. AAS, testosterone plus nandrolone; SRC, Sports-related concussion.

**Figure 5. Increased markers of axonal damage following the sports-related concussion protocol.** Increased neuronal cytoskeletal damage was induced by SRC as indicated by the cleavage of alpha-spectrin into fragments (240 to 120 kDa ratio) in cortex (A) and hippocampus (B). The increased phosphorylation of Tau at $Ser^{396}$ in the hippocampus was evident in the SRC and AAS groups (n = 6 per group). *Denotes significant difference compared to SHAM. AAS, testosterone plus nandrolone; SRC, Sports-related concussion.

**Figure 1**

**Click here to download high resolution image**

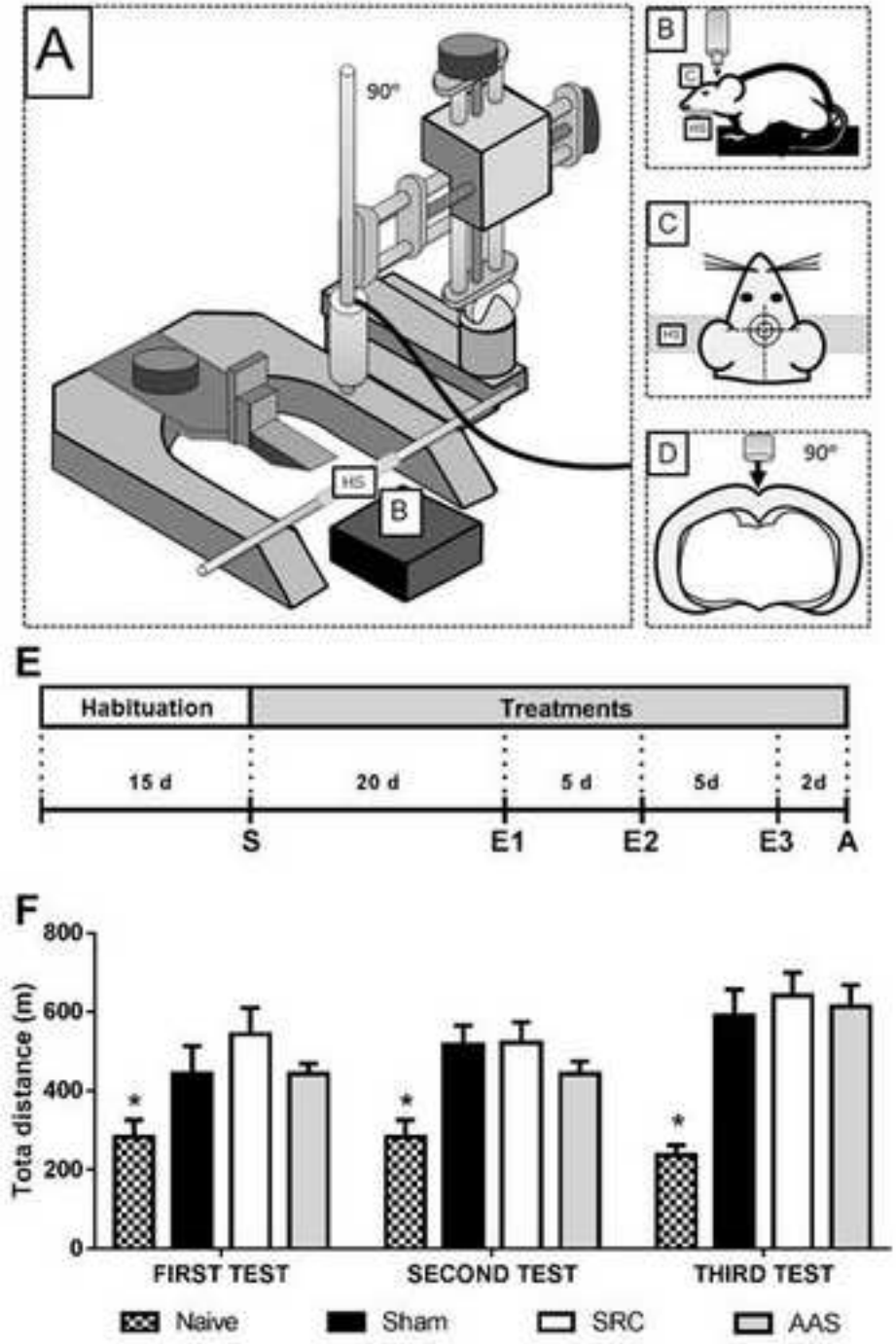

**Figure 2**

Click here to download high resolution image

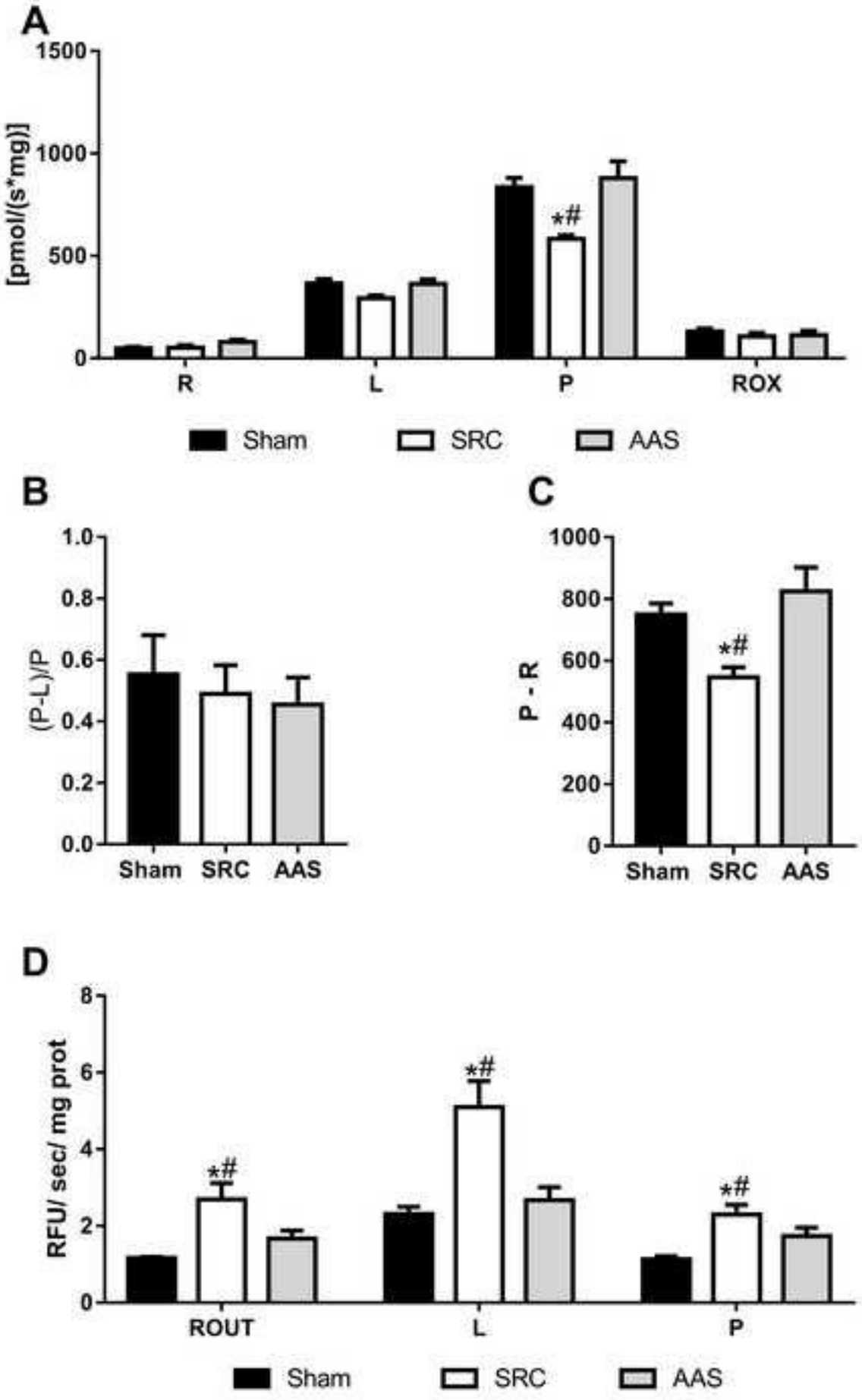

**Figure 3**

Click here to download high resolution image

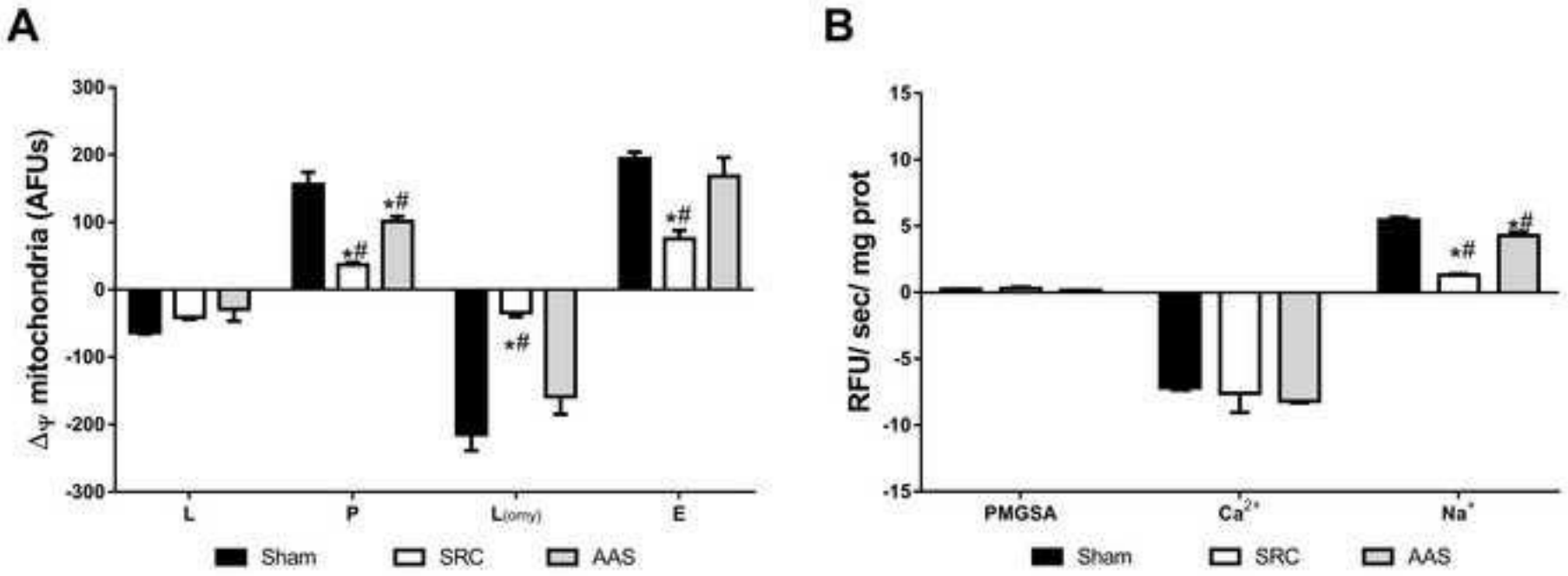

Figure 4

Click here to download high resolution image

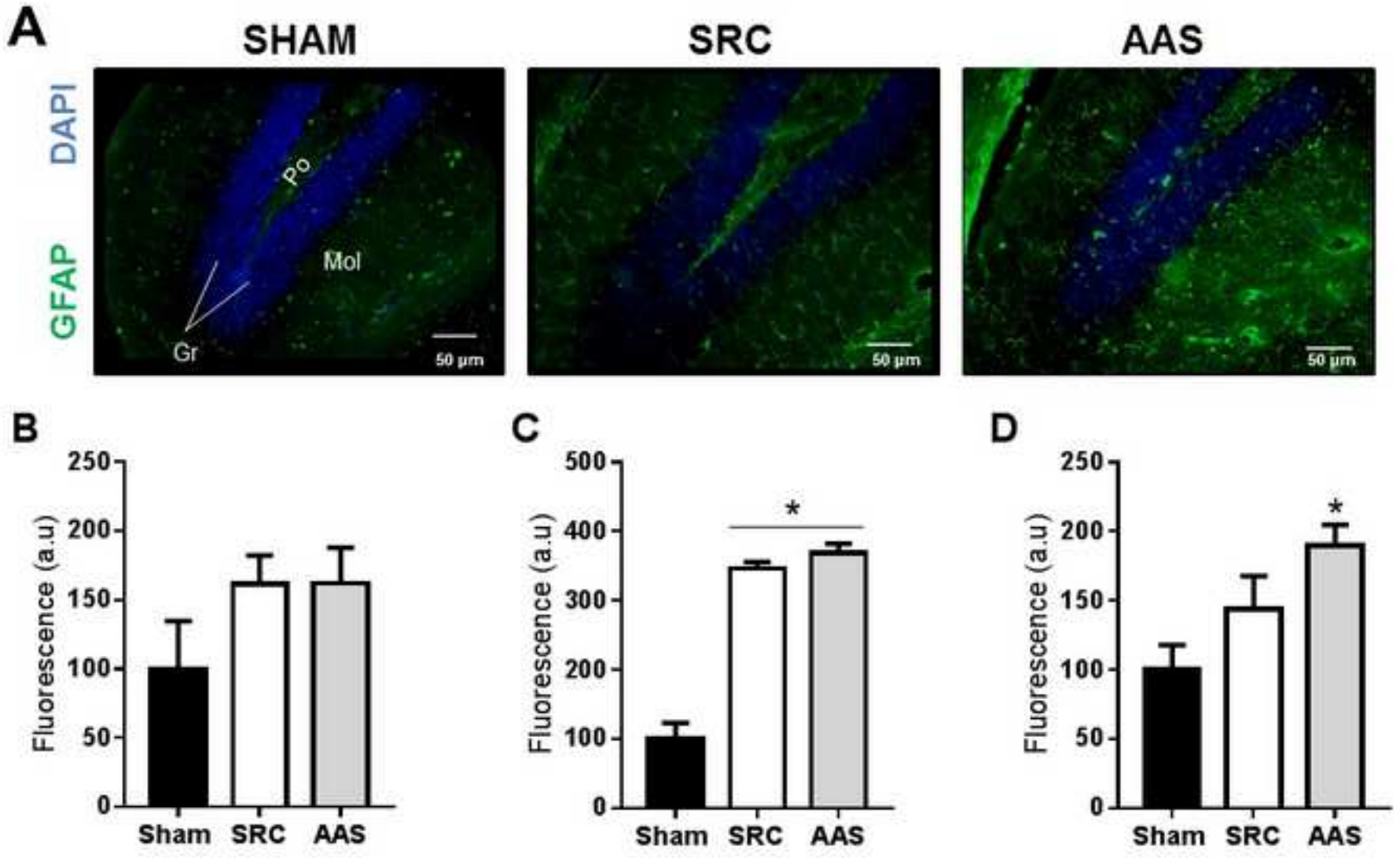

**Figure 5**

Click here to download high resolution image

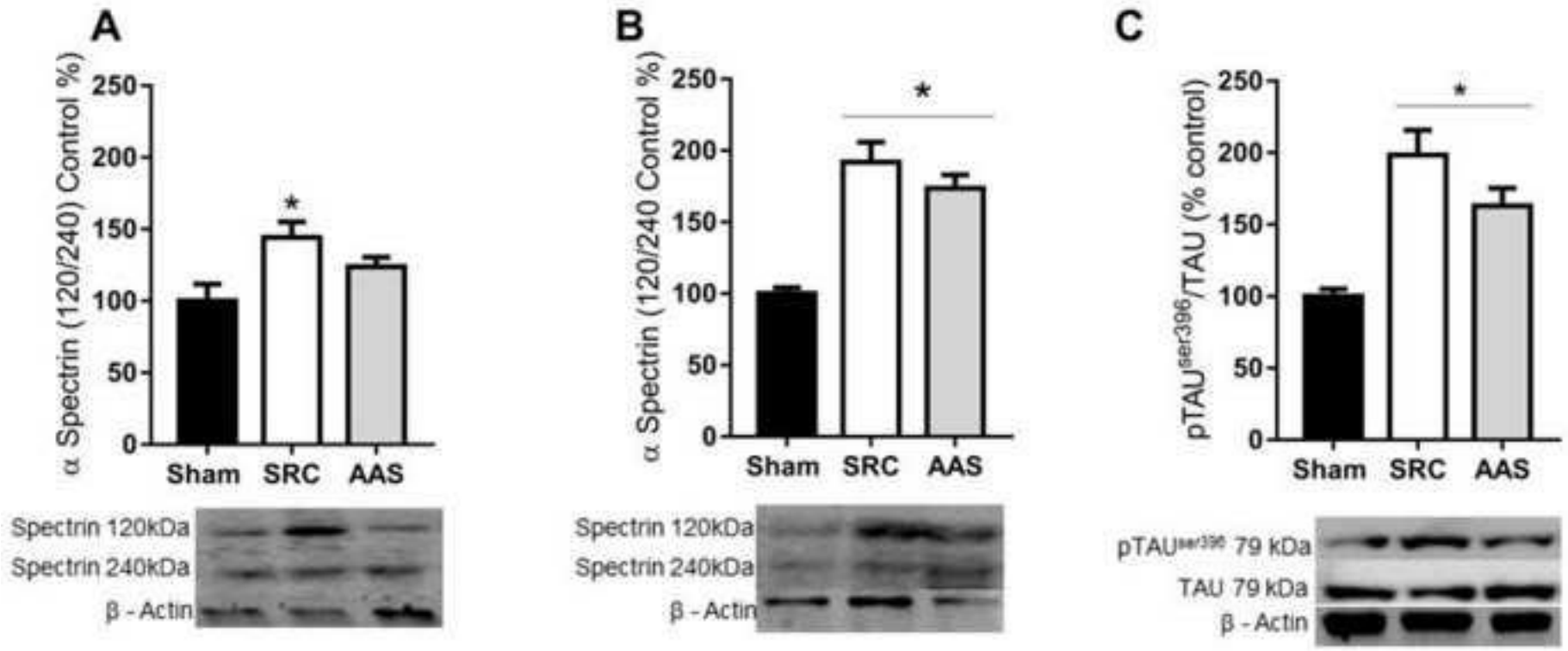

**Capítulo V:** *Mitochondrial preconditioning through different volumes of exercise improves outcomes of traumatic brain injury.*

No capitulo V apresentamos um artigo em preparação para submissão ao periódico "*Journal of Neurotrauma*".

O exercício físico é uma estratégia reconhecida por proporcionar benefícios globais à saúde, resultando também em neuroproteção devido ao aumento de mecanismos tróficos e reserva cognitiva. A prescrição de exercícios físicos para a saúde envolve uma série de variáveis, entre elas o volume (quantidade de exercício em um determinado período de tempo). Entretanto, ainda não é reconhecido se diferentes volumes de exercício promovem níveis distintos de pré-condicionamento e neuroproteção após o TCE. Assim pretendemos entender do ponto de vista neuroenergético e comportamental, se um volume maior de exercício físico promove adaptações cerebrais mais efetivas para a neuroprotecao após um TCE grave do que um volume menor de exercício físico. Anedoticamente, seria como perguntar se um indivíduo que pratica exercícios diariamente e sofre um TCE grave teria os mesmos desfechos que um individuo que realiza um volume menor de exercício (por exemplo, três vezes na semana).

Portanto, nesse estudo investigamos os efeitos profiláticos de diferentes volumes de exercício físico no TCE grave. Demonstramos que o exercício promove maior sobrevida e atenua os danos mitocondriais, modulação das cascatas apoptóticas e neurotróficas, resultando na prevenção do comprometimento da memória espacial após TCE grave. Nossos resultados indicaram que tanto o alto quanto o baixo volume de exercícios voluntários evitaram o comprometimento mitocondrial e de memória. Assim, enfatizamos a importância do exercício físico na função mitocondrial, beneficiando diferentes desfechos do TCE.

# Mitochondrial preconditioning through different volumes of exercise improves outcomes of traumatic brain injury

Afonso Kopczynski, [1] Marcelo Salimen Rodolphi *MSc*, [1] Nathan Ryzewski Strogulski, *MSc*, [1] Jean Pierre Oses, *PhD*,[1] Marco Antônio De Bastiani, *PhD* [2] Luis Valmor Portela, *PhD,*[1] Douglas H. Smith, *MD*,[3] Randhall B Carteri, *PhD*,[1]

[1] Laboratório de Neurotrauma e Biomarcadores - Departamento de Bioquímica, Programa de Pós-Graduação em Bioquímica, ICBS, Universidade Federal do Rio Grande do Sul - UFRGS, Porto Alegre, RS, Brasil.

[2] Departmento de Bioquímica, Programa de Posgraduação em Bioquímica, ICBS, Universidade Federal do Rio Grande do Sul - UFRGS, Porto Alegre, RS, Brazil.

[3] Penn Center for Brain Injury and Repair and Department of Neurosurgery, Perelman School of Medicine, University of Pennsylvania, Philadelphia, PA, USA.

**Correspondence:**

* Randhall B. Carteri,
Department of Biochemistry,
ICBS, UFRGS. Rua Ramiro Barcelos, 2600 anexo
90035-003, Porto Alegre, RS, Brazil.
Tel: 55 51 33085558; Fax: 55 51 33085544;
E-mail: rcarteri@outlook.com

**Running title:** Exercise and mitochondrial preconditioning in TBI

**Table of contents title:** Exercise promotes mitochondrial preconditioning and promotes neuronal survival after TBI.

**Complete address**

**Randhall B Carteri, *PhD*, [*] (Corresponding author)**

Departamento de Bioquímica, ICBS, UFRGS

Rua Ramiro Barcelos 2600, anexo

Bairro Santana, Porto Alegre, RS

Phone: 55 51 33085557

Fax: 55 51 33085540

rcarteri@outlook.com

**Afonso Kopczynski,**

Departamento de Bioquímica, ICBS, UFRGS

Rua Ramiro Barcelos 2600, anexo

Bairro Santana, Porto Alegre, RS

Phone: 55 51 33085557

Fax: 55 51 33085540

afonsokcarvalho@gmail.com

**Marcelo Salimen Rodolphi *MSc*,**

Departamento de Bioquímica, ICBS, UFRGS

Rua Ramiro Barcelos 2600, anexo

Bairro Santana, Porto Alegre, RS

Phone: 55 51 33085557

Fax: 55 51 33085540

marcsalimen@gmail.com

**Nathan Ryzewski Strogulski, *MSc*,**

Departamento de Bioquímica, ICBS, UFRGS

Rua Ramiro Barcelos 2600, anexo

Bairro Santana, Porto Alegre, RS

Phone: 55 51 33085557

Fax: 55 51 33085540

n.strogulski@gmail.com

**Jean Pierre Oses,**

Departamento de Bioquímica, ICBS, UFRGS

Rua Ramiro Barcelos 2600, anexo

Bairro Santana, Porto Alegre, RS

Phone: 55 51 33085557

Fax: 55 51 33085540

Jean.pierre.oses@gmail.com

**Marco Antônio De Bastiani**

Departamento de Bioquímica, ICBS, UFRGS

Rua Ramiro Barcelos 2600, anexo

Bairro Santana, Porto Alegre, RS

Phone: 55 51 33085557

Fax: 55 51 33085540

tyrev@hotmail.com

**Luis Valmor Portela, *PhD***

Departamento de Bioquímica, ICBS, UFRGS

Rua Ramiro Barcelos 2600, anexo

Bairro Santana, Porto Alegre, RS

Phone: 55 51 33085557

Fax: 55 51 33085540

roskaportela@gmail.com

**Douglas H. Smith, MD,**

Penn Center for Brain Injury and Repair and Department of Neurosurgery,

Perelman School of Medicine, University of Pennsylvania,

105 Hayden Hall, 3320 Smith Walk, Philadelphia, PA, USA.

Zip code: 19104-6316

Tel. +1 215-8980881

Fax. +1 215-5733808

smithdou@mail.med.upenn.edu

**ABSTRACT**

Neuronal preconditioning is a recognized prophylactic strategy in detrimental brain conditions in Traumatic Brain Injury (TBI). Impaired mitochondrial neuroenergetics is a key secondary mechanism influencing short- and long-term neurological outcomes after TBI. In addition, physical exercise is an effective strategy of neuronal preconditioning, increasing transcriptional factors like cAMP response element-binding protein (CREB), which increases the expression of brain derived neurotrophic factor (BDNF), a key mediator of the synaptic plasticity, mitochondrial biogenesis, bioenergetic mechanisms and memory formation. Here we investigated whether distinct exercise volumes in mice induce precondiotioning to long-term outcomes of severe TBI. CF1 male mice were randomized to Sedentary (SED); Low-volume (LV) and high-volume (HV) exercise groups. After thirty days of training, animals underwent randomization to SHAM or TBI induction, resulting in six groups: SED, LV, HV (SHAM) and SED TBI, LV-TBI and HV-TBI. Different exercise volumes increased survival rate after TBI, preventing mitochondrial function deficits indicated by oxygen consumption in different coupling states, oxidative phosphorilation coupling efficiency, membrane potential dynamics and hydrogen peroxide production. Further, exercise training avoided TBI-induced Tau-hyperphosphorylation and improved BDNF-CREB signaling culminating in preserved cognitive function. In summary, different volumes of exercise exert neuronal preconditioning in the hippocampus, modulating mitochondrial bioenergetics response and neurotrophic signaling leading to preserved memory function up to 30 days after a single severe TBI.

**Keywords: Exercise, Traumatic brain injury, mitochondria, neuroenergetics, neurotrophic signals,**

## INTRODUCTION

Neuronal preconditioning is a recognized prophylactic strategy in detrimental brain conditions, such as Traumatic Brain Injury (TBI).[1] In physiological conditions, the brain has the highest energy demand relative to other organs, thus not surprisingly the capacity of brain mitochondria to work as a synchronizer of metabolic pathways may exerts a deterministic role in the cell fate for survival or neurodegeneration.[2] Yet, the impairment in the synchronization of mitochondrial neuroenergetics is a key secondary mechanism influencing short- and long-term neurological outcomes after TBI.

Beyond being highly specialized in support energy to cells mitochondria further integrate a variety of mechanisms involved in the neural cell homeostasis such as the reactive oxygen species (ROS) production, and antiapoptotic signaling.[3] [4] Remarkably, the regulation of these mitochondrial-associated functions are compromised after TBI in a time profile that follows bioenergetics deficits coupled with ROS production and cognitive decline.[2]

Physical exercise effectively enable neuronal preconditioning, thus increasing transcriptional factors like cAMP response element-binding protein (CREB), which increases the expression of brain derived neurotrophic factor (BDNF), a key mediator of the synaptic plasticity, mitochondrial biogenesis, bioenergetic mechanisms and memory formation.[5] [6] [7] [8] Therefore, physical exercise, provides settings of molecular and cellular benefits that may yield preventive reserves against neurodegenerative disorders

and cognitive decline. [9, 10] Whereas the knowledge of these functional adaptations has provided the background necessary to propose physical exercise as a preventive intervention, the interrogation about dose-response relationship between prior exercise volume and modulation of secondary mechanisms of TBI needs to be responded.

In highly exercised individuals, the increased volume is mandatory to achieve better physical performance, thus it can be expected they reach a high threshold of neuroenenergetic and neurotrophic preconditioning due to the positive effects of exercise on the brain [11]. Yet, it is unknown whether subjects that are eventually engaged in lower volume of exercise achieve necessary brain adaptations to enable preventive neuroprotection against the consequences of a head injury. Since volume is an important variable to exercise prescription, it is imperative to determine how it affects the magnitude of underlying neurotrophic signaling and neuroenergetic mechanisms.[8] Also, it is not known whether exercise volume mediating these outcomes may exert neuroprotection and preserve cognitive function after TBI.

Here we investigated whether distinct exercise volumes in mice induce mitochondrial neuroenergetics and neurotrophic precondiotioning, which might serve as neuroprotective reserve against TBI. The results showed that different exercise volumes in a voluntary running wheel improved neurometabolic and neurological outcomes after a severe TBI in mice.

## MATERIAL AND METHODS

### *Animals and treatment protocols*

Ninety-days-old CF1 male mice were obtained from CREAL (CREAL, Porto Alegre/RS, Brazil). A total of 4 animals per cage (38 cm × 32 cm × 16 cm acrylic box with sawdust) couple with a running wheel were placed into a controlled room temperature (22ºC ± 1) under a 12h light/12h dark cycle (lights on at 7 a.m.) and had free access to food and water. All animals were randomly assigned before the exercise preconditioning protocol, which consisted of 15 days of exercise habituation followed by 15 days of exercise training. The animals were grouped as Sendentary (SED; the running wheel was locked); Low-volume (LV; alternate 2 days' free running wheel and 2days locked running wheel) and high-volume (HV, freely running wheel every day) exercise. After thirty days of training, animals underwent a second randomization to SHAM or TBI induction, resulting in the groups: SED, LV, HV (SHAM groups) and SED TBI, LV-TBI and HV-TBI (TBI groups). See the experimental design in the Figure 1A.

All experiments were in agreement with the Committee on the Care and Use of Experimental Animal Resources, UFRGS, Brazil number (#22436).

*Controlled Cortical Impact protocol (CCI)*

After 30 days' protocol, a severe TBI was performed placing mice in the stereotaxic (Kopf Instruments, Tujunga, CA) with a heating bed (37 ± 1$^{o}$C) maintained with anesthesia inhalation (2.5 % isoflurane) in a mixture of $N_2$ and $O_2$ (2:1). A 4 mm diameter craniotomy was performed in the central part of the left parietal bone followed by CCI injury induced by the Benchmark stereotaxic impactor (myNeuroLab®, Leica, St. Louis, MO, USA). The head injury was performed with a piston of 3.0 mm diameter (adjusted to impact velocity of 5.7 m / s; impact duration was 100 ms, and 2 mm of depth

penetration) on the exposed surface of dura mater. After injury, craniotomy area was isolated using a concave lamella bonded with dental cement and sutured. Following recover from anesthesia the animals were placed in a heated box and were monitored up to 4 h post-injury.[12] After recovery animals were submitted to behavioral tests and finally euthanized to dissect ipsilateral hippocampus, which was used for neurochemical analysis (See the protocol time line, Figure 1A).

*Open Field Test*

Open field (OF) behavioral test was used to access (n = 10 per group) spontaneous locomotor activity 48 h and 72 h post CCI (Figure 1A). The experiments were conducted in a sound-attenuated room under low-intensity light. The apparatus consists of a square acrylic boxes (50 × 50 × 50 cm) that were positioned on the floor where mice were randomly placed into individually. The locomotor activity and exploratory profile was recorded with a video camera for 10 min. The analysis was performed using a specific software (Any-maze, Stoelting, Woods Dale, IL).[13]

*Morris Water Maze*

The Morris Water Maze was used to assess spatial memory as described elsewhere.[14] Twenty-four days after CCI animals (n = 10 per group) were submitted to a flag-test, and after 24 h they were trained daily in a four-trial MWM to find a hidden platform; followed by one-day probe testing without the platform. The time spent in the target quadrant was measured. The analysis was performed using a specific software (Any-maze, Stoelting, Woods Dale, IL).[14]

*Preparation of ipsilateral cortex homogenates*

Whole ipsilateral hippocampal tissue of mice were collected 30 days after CCI (Figure 1A) and then homogenized in a specific buffer (320 mM sucrose, 1mM EDTA, pH 7.4), [15] using a pre-cooled glass potter with 10 to 15 strokes. After centrifugation (1350 *x*g for 3 min at 4 °C), we obtained a mitochondria enriched homogenates that were aliquoted and used for respirometry, membrane potential and hydrogen peroxide analysis. These analyses were performed simultaneously by different researchers, in a time-window of 10 minutes from euthanasia and start of analysis. The samples were also used for protein quantification (Pierce™ BCA Protein Assay Kit Catalog number: 23225) and immunoblotting.

*Mitochondrial respiratory protocol*

Ipsilateral hippocampal oxygen consumption rates (OCR) were obtained at 37°C using the high-resolution Oxygraph-2k system and recorded real-time using DatLab software (Oroboros, Innsbruck, Austria) in standard buffer (100 mM KCI, 75 mM mannitol, 25 mM sucrose, 5 mM phosphate, 0.05 mM EDTA, and 10 mM Tris-HC1, pH 7.4). Routine OCR was recorded for 5 min (ROUT), followed by the sequential titration of pyruvate, malate, glutamate and succinate (PMGS; 10, 10, 20 and 10 mM, respectively) to obtain Leak OCR (L). Sub sequentially, adenosine diphosphate (ADP, 2.5 mM) was titrated to obtain Maximal OxPHOS capacity (P); Oligomycin was then titatred to obtain $L_{omy}$ OCR and maximal eletron transport capacity (E) was obtained following titration of the proton ionophore Carbonyl cyanide 4-trifluoromethoxy-

phenylhydrazone (FCCP 1 μM). Non-mitochondrial respiration (ROX) after the inhibition of complex I, III and IV with rotenone, antimicyn-A and cyanide (ROT, AA and KCN, 2, 2.5 and 5 mM, respectively). Following correction of obtained OCR for ROX tissue-mass specific oxygen fluxes in different substrate and coupling states were compared.[15] Further we calculated the biochemical coupling efficiency ( $(P-L_{omy})/P$) for mitochondrial functioning, limitation of OXPHOS capacity by the capacity of the phosphorylation system (excess E-P factor; (E-P)/E) and capacity reserve (E-Routine), and Leak Control ratio (L/E) to measure the proton leakage of the system.[15, 16]

*Mitochondrial Membrane Potential ($\Delta\Psi_m$)*

The ΔΨm was obtained from the fluorescence signal (excitation wavelength of 495 nm and emission wavelength of 586 nm) of ipsilateral hippocampal samples incubated in the respiration buffer supplemented with 10 μM safranin-*O* (Spectra Max M5, Molecular Devices). Increased the fluorescence units mirror decreased $\Delta\Psi_m$ whereas decreased fluorescence units indicate increased $\Delta\Psi_m$. The incubation without substrates represents the baseline $\Delta\Psi_m$. Substrates for complex I, II (PMGS) and V (ADP), uncoupling with FCCP (1 μM) and inhibition of complex IV, were used to modulate ΔΨm dynamic responses. Moreover, fluorescence units of each coupling state were used to calculate the relative percentage of change in $\Delta\Psi_m$. Data are expressed as arbitrary fluorescence units (AFUs) and were normalized to protein content. [17]

*Mitochondrial $H_2O_2$ production*

Mitochondrial production of hydrogen peroxide ($H_2O_2$) of ipsilateral hippocampi was assessed in samples incubated in the respiration buffer supplemented with 10 μM Amplex Red and 2 units/mL horseradish peroxidase, in different mitochondrial coupling states. Baseline $H_2O_2$ level was measured without the presence of substrates in the incubation medium. Using the same substrates and inhibitors indicated in respirometry, L, P and Lomy coupling states were induced to assess $H_2O_2$ production. Fluorescence was monitored at excitation (563 nm) and emission (587 nm) wavelengths with a Spectra Max M5 microplate reader (Molecular Devices, USA).[17]

*Western blotting*

The Ipsilateral hippocampi samples (20 μg of protein; n=6-8 per group) were prepared as described elsewhere to perform electrophoresis using polyacrylamide gel and PVDF membranes as detailed elsewhere.[14] (Amersham, GE Healthcare, Little Chalfont, UK).[14] Primary antibodies against Anti-Tau phospho-S396 (ABCAM®, USA; 1:1000; ref. ab109390); Anti-Tau antibody (ABCAM®, USA; 1:1000; ref. ab32057); Caspase-3 (8G10) (Cell Signalling®, USA; 1:1000; ref. 9665) Cleaved Caspase-3 (Cell Signalling®, USA; 1:1000; ref. 9664). All procedures were conducted according to specific antibody manufacturer's instruction. Primary antibodies were incubated overnight followed by 2 h incubation with horseradish peroxidase-conjugated anti-rabbit or anti-mouse IgG (1:5000) (GE, Little Chalfont, UK) secondary antibodies. Membranes were incubated with Amersham ECL Western Blotting Detection Reagent (GE Healthcare Life Sciences, Little Chalfont, UK) for 5 min and the immunodetection was made by chemoluminescence using Image Quant LAS 4000 (GE, Little Chalfont,

UK). The protein expression was quantified using Image J® software (Rockville, USA). The values of optic density were expressed as % of control.

*Statistical Analysis*

To calculate survival proportions, we used the product limit (Kaplan-Meier) method;[18] Results were calculated and expressed as the mean ± S.E.M. To analyze differences between groups, we used two-way analysis of variance (ANOVA) followed by a post-hoc Tukey test. All procedures were performed using GraphPad Prism 7.0 software. The differences were considered statistically significant at $p < 0.05$.

## RESULTS

### *Different exercise volumes increased survival rate after TBI*

Exercised groups ran a total of 35.000 +/- mts in the wheel in the first 15 days' habituation phase. There was a significant difference in total distance ran between LV and HV ($p<0.0001$, Figure 1C) at the end of exercise protocol. After TBI, both exercised groups showed increased survival when compared to TBI group. This setting of results indicates that the exercise protocols achieve different volumes of training, but they equally protect mice to evolve to death after a severe TBI (Figure 1D).

### *Different exercise volumes did not change locomotor and exploratory profile after TBI*

The open field test performed at 48 h after TBI showed no significant differences between groups in the distance traveled (m) across 10 min evaluation and in the time

spent in peripheral and center zones (48 h, Figure 2A and C). At 72 h after TBI there was no significant differences in the distance traveled across 10 min and in the time in both zones (Figure 2B and D). The slight decrease in locomotor activity at 72 h suggest that mice were already habituated in the arena. Also, the total distance traveled at 48 h and 72 h (Figure 2E and F, respectively) were not different between groups implying in absence of locomotor or exploratory deficits.

***Exercise preconditioning and mitochondrial bioenergetics after TBI***

Hippocampal OCR in different coupling states is showed in Figure 3A, where TBI significantly impaired the oxygen consumption after addition of ADP (P) and FCCP (ETS) relative to other groups ($p< 0.01$, Figure 3 A). The biochemical coupling efficiency indicates that exercise (LV and HV) improved the efficiency of ATP synthesis when compared to SED group ($p< 0.0009$Figure, Figure 3 B). TBI significantly decreased the coupling efficiency ($p< 0.0001$, Figure 3B), which can be attributed to decreased limitation of OXPHOS capacity by the yield of the phosphorylation system (Figure 3C) and to the lower reserve capacity (Figure 3 D). Actually, this is further confirmed by the increased Leak control ratio, which conceptually indicates and increased uncoupling between ETS and OxPHOS (Figure 3 E). Remarkably, independent on volume (LV TBI and HV TBI) exercise preconditioning similarly prevented alterations in mitochondrial respiratory states.

To further explore potential mechanisms leading to increased proton leakage and impaired coupling of ATP synthesis, we assessed $\Delta\psi_m$ responsiveness to metabolic substrates, an inhibitor of oxidative complex V and uncoupler (FCCP). The percentage of

variation in the $\Delta\Psi_m$ between baseline and ADP; ADP and Oligomycim; Oligomycim and FCCP; and FCCP and ROX confirmed that independent of the mitochondrial target explored here, TBI impairs the effective generation and dissipation of $\Delta\Psi_m$. Exercise volume alone did not alter the $\Delta\Psi_m$ relative to SED. However, regardless volume (LV and HV) exercise was able to sustain the membrane potential dynamics when the brain was submitted to a neuroenergetic challenge caused by TBI ($p< 0.0001$; Figure 3F). These detectable alterations in the $\Delta\Psi_m$ caused by TBI explains the lower responsiveness in OCR, and the reduced coupling between ETS and OxPhos. These changes are in line with the observed increased Leak Ratio, and hypothetically might indicate a partial diversion of oxygen to ROS production induced by TBI.

We found that LV and HV exercise *per se* decreased the $H_2O_2$ relative to SED, after the addition of metabolic substrates (PMGS) to complex I and II and the oligomycin, an inhibitor of FoF1-ATP synthase. Moreover, $H_2O_2$ levels were significantly increased by TBI in all coupling states ($p<0.001$, Figure 3G), and both LV and HV exercise protocols attenuated the mitochondrial production of $H_2O_2$ after PMGS, ADP, and oligomycin. Given the dual importance of $H_2O_2$ levels as mediator of cell damage and as signaling molecule with trophic properties, we further explored whether neuroenergetics deficit and $H_2O_2$ impact molecular signals of neurodegeneration and survival.

***Prior exercise training avoids Tau-hyperphosphorylation and improved neurotrophic signaling after TBI***

Exercise *per se* did not significantly altered $pTau^{Ser396}$ levels relative to SED. Also, there was an increase in the immunocontent of $pTau^{Ser396}$ / Tau, a classical pathophysiological finding in TBI and hallmark of neurodegeneration in brain disorders (Figure 4A). Remarkably, exercise prevented this elevation independent of training volume. However, we found no differences between groups in the immunocontent of cytochrome C (Figure 4B). Moreover, neurotrophic factors play a pivotal role in brain neuroplasticity and neurometabolic support, which could determine the neurological outcomes after TBI. Here, we found that different exercise volumes increased similarly the phosphorylation of CREB at ser133 and pro-BDNF/BDNF ratio (Figure 4C and D). However, TBI decreased $pCREB^{ser133}$ and pro-BDNF/BDNF ratio. Regardless volume, exercise prevented the decreased neurotrophic signaling in TBI mice (Figure 4C and C). Given the benefits of exercise preconditioning on neurotrophic factors levels one can expect a positive modulation on memory processing after TBI.

***Exercise preconditioning prevented cognitive impairment after TBI.***

All animals performed equally the flag test indicating no apparent visual damage due to TBI (Figure 5A). In the learning phase of spatial memory, the TBI group spent more time searching the hidden platform as evidenced throughout training days 1 and 4, and both exercise protocols were able to prevent this deficit (Figure 5B). In the probe test the mice engaged in HV of exercise displayed a significant better performance relative to other groups ($p<0.0001$ SED and $p< 0.0139$ LV), though LV also improved the time in the target zone relative to SED ($p<0.005$) (Figure 5C). Also, TBI spent less time in the target quadrant relative to other groups, and both LV-TBI and HV-TBI showed no

significant impairment (Figure 5 C) relative to non TBI groups. No differences in average speed were observed between groups (Figure 5 D). Taken together, these results confirm the beneficial effects of exercise on spatial memory and highlights its prophylatic importance against the neurological deficits after TBI.

## DISCUSSION

In the present study, LV and HV of exercise preconditioning resulted in preserved mitochondrial function and sustained levels of neurotrophic factors, culminating in improved memory outcomes thirty-days following severe TBI. The beneficial effects of exercise on mitochondria and neurotrophic signals were independent of total volume performed throughout the exercise protocols. Taken together, our results support that mitochondrial modulation is a crucial component of the exercise-induced neuronal preconditioning and highlights its relevance as a prophylactic strategy against the secondary mechanisms that rise after TBI.

Impaired ATP synthesis by mitochondria is a key component of TBI pathology, which was confirmed in this study. [19] [20]. Here, TBI caused long-term desynchronization between the $\Delta\Psi m$ dynamics and activity of ETS complexes, resulting in proton motive force driven to $H_2O_2$ production rather to ATP synthesis by FoF1-ATP synthase. The exacerbated levels of $H_2O_2$ may damage proteins from mitochondrial membranes resulting in a less effective bioenergetics, and increase probability to intrinsic apoptotic signaling. Total mitochondrial citochrome c, an indicator of apoptosis was not altered by exercise or TBI, albeit an assay of mitochondrial citochrome c release, provide more feasible perspective of proapototic activity.[21] It has long been recognized that

Δψm is a critical parameter associated with the cellular capacity to generate ATP by oxidative phosphorylation and also it importance to ROS generation.[22] Further, sedentary mice showed elevated $H_2O_2$ production across the entire respiratory protocol, and beyond, TBI exacerbated this response. Exercise, regardless of volume or TBI, attenuated $H_2O_2$ production in mice. Since elevated ROS levels damages structural components of the neural cells, this redox preconditioning by exercise seems of vital importance in the long-term consequences of TBI. [23, 24] [19] Taken together, we evidenced that different volumes of exercise induce benefits to mitochondrial function, which are sustained even 30 d after a severe TBI.

Appropriate synaptic function and plasticity rely on preserved mitochondria function.[25] Impaired synaptic plasticity of hippocampal neurons has been extensively demonstrated following TBI, commonly associated with decreased brain-derived neurotrophic factor (BDNF) levels.[26] [27] Accordingly, BDNF is a central effector of exercise-induced synaptic plasticity in mature neurons,[28] which could be upregulated by phosphorylation of CREB at Ser133, regulating neuronal survival and cognitive outcomes.[29] Strikingly, CREB activation and the resulting BDNF expression remained decreased up to 30 days after head injury, whereas exercise preconditioning regardless of volume prevented these effects. Whereas the up regulation of neurotrophic factors is a key component of exercise benefits in TBI, our results suggests that even lower volume of exercise exerts a positive effect to TBI, which reinforce that even performing lower volumes of exercise may help to conceptualize that “lower could be more”. Alongside decrease in neurotrophic factors, markedly structural damage is a hallmark of TBI, intimately connected to the degree of neurodegeneration.[30, 31] Tau, is a microtubule

associated protein which aggregates upon phosphorylation, and is commonly seen increased within the brain after TBI in humans and rodents. Here, exercise preconditioning prevented Tau hyperphosphorylation, which could be directly associated with the prevention of TBI-induced axonal degeneration. [30, 32, 33]

Moreover, the improved mitochondrial function, increased neurotrophic signals and decreased $H_2O_2$ and Tau phosphorylation were associated with the improvement in the learning and memory performance in the spatial memory paradigm of MWM. Even though improved cognition and neurogenesis being a classical benefit associated with exercise,[34] [35] here we further showed that both LV and HV may exerted similar effects. In addition, exercise prevented long-term cognitive deficits induced by severe TBI up to 30 d after injury, regardless of volume. Therefore, the present results combined reinforces the axiomatic concept of exercise-induced neuroprotection in TBI.

In summary, different volumes of exercise exert neuronal preconditioning in the hippocampus, modulating mitochondrial bioenergetics response and neurotrophic factors leading to preserved memory function up to 30 days after a single severe TBI. Therefore, these results highlight the prophylactic importance of performing regular physical exercise to neuronal health, which could be determinant of favorable neurological outcome even after a severe TBI.

**KNOWLEDGEMENTS**

The authors would like to thank the Brazilian scientific agencies/programs INNT-CNPq #465346, CNPq # 401645/2012-6, CAPES, FAPERGS-Pronex, FAPERGS-PPSUS # 03/2017.

## AUTHOR DISCLOSURE STATEMENT

No competing financial interests exist.

## REFERENCES


1. Yokobori, S., et al., *Preconditioning for traumatic brain injury.* Transl Stroke Res, 2013. **4**(1): p. 25-39.
2. Meaney, D.F., B. Morrison, and C. Dale Bass, *The mechanics of traumatic brain injury: a review of what we know and what we need to know for reducing its societal burden.* J Biomech Eng, 2014. **136**(2): p. 021008.
3. Correia, S.C., et al., *Mitochondrial preconditioning: a potential neuroprotective strategy.* Frontiers in aging neuroscience, 2010. **2**: p. 138.
4. Correia, S.C., et al., *Mitochondria: the missing link between preconditioning and neuroprotection.* Journal of Alzheimer's disease : JAD, 2010. **20 Suppl 2**(Suppl 2): p. S475-S485.
5. Mota, B.C., et al., *Exercise pre-conditioning reduces brain inflammation and protects against toxicity induced by traumatic brain injury: behavioral and neurochemical approach.* Neurotox Res, 2012. **21**(2): p. 175-84.
6. Chio, C.C., et al., *Exercise attenuates neurological deficits by stimulating a critical HSP70/NF-kappaB/IL-6/synapsin I axis in traumatic brain injury rats.* 2017. **14**(1): p. 90.
7. Zhao, Z., et al., *Voluntary Exercise Preconditioning Activates Multiple Antiapoptotic Mechanisms and Improves Neurological Recovery after Experimental Traumatic Brain Injury.* J Neurotrauma, 2015. **32**(17): p. 1347-60.
8. Chen, F., et al., *Mitochondria Are Critical for BDNF-Mediated Synaptic and Vascular Plasticity of Hippocampus following Repeated Electroconvulsive Seizures.* Int J Neuropsychopharmacol, 2018. **21**(3): p. 291-304.
9. Mandolesi, L., et al., *Effects of Physical Exercise on Cognitive Functioning and Wellbeing: Biological and Psychological Benefits.* Frontiers in psychology, 2018. **9**: p. 509-509.
10. Sanders, L.M.J., et al., *Dose-response relationship between exercise and cognitive function in older adults with and without cognitive impairment: A systematic review and meta-analysis.* 2019. **14**(1): p. e0210036.
11. Garber, C.E., et al., *American College of Sports Medicine position stand. Quantity and quality of exercise for developing and maintaining cardiorespiratory, musculoskeletal, and neuromotor fitness in apparently healthy adults: guidance for prescribing exercise.* Med Sci Sports Exerc, 2011. **43**(7): p. 1334-59.
12. Smith, D.H., et al., *A model of parasagittal controlled cortical impact in the mouse: cognitive and histopathologic effects.* J Neurotrauma, 1995. **12**(2): p. 169-78.

13. Kalinine, E., et al., *Nandrolone-induced aggressive behavior is associated with alterations in extracellular glutamate homeostasis in mice.* Horm Behav, 2014. **66**(2): p. 383-92.
14. Muller, A.P., et al., *Exercise increases insulin signaling in the hippocampus: physiological effects and pharmacological impact of intracerebroventricular insulin administration in mice.* Hippocampus, 2011. **21**(10): p. 1082-92.
15. Gnaiger, E., *Mitochondrial pathways and respiratory control. An introduction to OXPHOS analysis*. 4th ed. 2014, Innsbruck: OROBOROS MiPNet Publications.
16. Burtscher, J., et al., *Differences in mitochondrial function in homogenated samples from healthy and epileptic specific brain tissues revealed by high-resolution respirometry.* Mitochondrion, 2015. **25**: p. 104-12.
17. Portela, L.V., et al., *Hyperpalatable Diet and Physical Exercise Modulate the Expression of the Glial Monocarboxylate Transporters MCT1 and 4.* Mol Neurobiol, 2017. **54**(8): p. 5807-5814.
18. Machin, D., Y.B. Cheung, and M. Parmar, *Survival Analysis: A Practical Approach*. 2006: Wiley.
19. Hill, R.L., et al., *Time courses of post-injury mitochondrial oxidative damage and respiratory dysfunction and neuronal cytoskeletal degradation in a rat model of focal traumatic brain injury.* Neurochem Int, 2017. **111**: p. 45-56.
20. Kulbe, J.R., et al., *Synaptic Mitochondria Sustain More Damage than Non-Synaptic Mitochondria after Traumatic Brain Injury and Are Protected by Cyclosporine A.* Journal of Neurotrauma, 2017. **34**(7): p. 1291-1301.
21. Robertson, C.L., M. Saraswati, and G. Fiskum, *Mitochondrial dysfunction early after traumatic brain injury in immature rats.* Journal of Neurochemistry, 2007. **101**(5): p. 1248-1257.
22. Figueira, T.R., et al., *Safranine as a fluorescent probe for the evaluation of mitochondrial membrane potential in isolated organelles and permeabilized cells.* Methods Mol Biol, 2012. **810**: p. 103-17.
23. Ji, J., et al., *Global lipidomics identifies cardiolipin oxidation as a mitochondrial target for redox therapy of acute brain injury.* Nature neuroscience, 2012. **15**(10): p. 1407-1413.
24. Ji, J., et al., *Mitochondrial injury after mechanical stretch of cortical neurons in vitro: biomarkers of apoptosis and selective peroxidation of anionic phospholipids.* J Neurotrauma, 2012. **29**(5): p. 776-88.
25. Cheng, A., Y. Hou, and M.P. Mattson, *Mitochondria and neuroplasticity.* ASN neuro, 2010. **2**(5): p. e00045-e00045.
26. Griesbach, G.S., D.A. Hovda, and F. Gomez-Pinilla, *Exercise-induced improvement in cognitive performance after traumatic brain injury in rats is dependent on BDNF activation.* Brain Res, 2009. **1288**: p. 105-15.
27. Chou, W., et al., *Exercise Rehabilitation Attenuates Cognitive Deficits in Rats with Traumatic Brain Injury by Stimulating the Cerebral HSP20/BDNF/TrkB Signalling Axis.* 2018. **55**(11): p. 8602-8611.
28. Vaynman, S., Z. Ying, and F. Gomez-Pinilla, *Hippocampal BDNF mediates the efficacy of exercise on synaptic plasticity and cognition.* Eur J Neurosci, 2004. **20**(10): p. 2580-90.

29. Lonze, B.E. and D.D. Ginty, *Function and regulation of CREB family transcription factors in the nervous system.* Neuron, 2002. **35**(4): p. 605-23.
30. Johnson, V.E., W. Stewart, and D.H. Smith, *Axonal pathology in traumatic brain injury.* Exp Neurol, 2013. **246**: p. 35-43.
31. Johnson, V.E., et al., *SNTF immunostaining reveals previously undetected axonal pathology in traumatic brain injury.* Acta Neuropathol, 2016. **131**(1): p. 115-35.
32. Blennow, K., J. Hardy, and H. Zetterberg, *The neuropathology and neurobiology of traumatic brain injury.* Neuron, 2012. **76**(5): p. 886-99.
33. Shahim, P., et al., *Blood biomarkers for brain injury in concussed professional ice hockey players.* JAMA Neurol, 2014. **71**(6): p. 684-92.
34. Suijo, K., et al., *Resistance exercise enhances cognitive function in mouse.* Int J Sports Med, 2013. **34**(4): p. 368-75.
35. Cotman, C.W. and N.C. Berchtold, *Exercise: a behavioral intervention to enhance brain health and plasticity.* Trends Neurosci, 2002. **25**(6): p. 295-301.

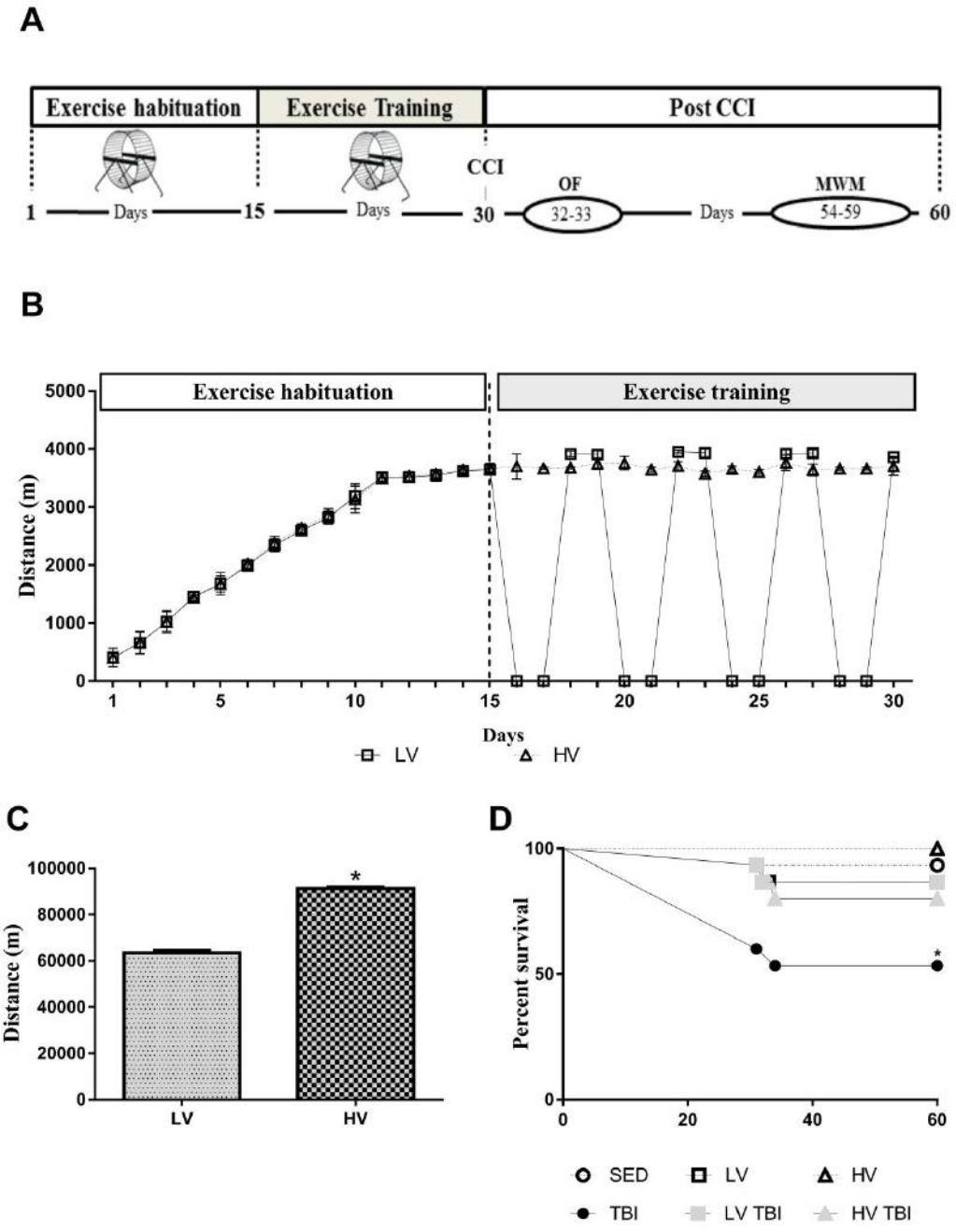


**Figure 1. Exercise precondioning strategy characterization and survival rate.** Experimental design (A). Animals initially had 15 days' period of freely exercise habituation in the running wheel; afterwards animals were submitted to exercise training phase constitute of additional 15 days of freely continuous exercise (HV, High volume; running wheel unlocked) or to intermittent exercise (LV, Low volume; alternate 2 days running wheel locked or unlocked) (B). Total distance run in the habituation plus

exercise training phases (C); Decreased survival rate after a single severe CCI (D). Abbreviations: Sedentary (SED); Open field (OF); Morris water maze (MWM), Controlled cortical impact (TBI); Low volume TBI (LV TBI); High volume TBI (HV TBI). * Denotes significant difference between groups.

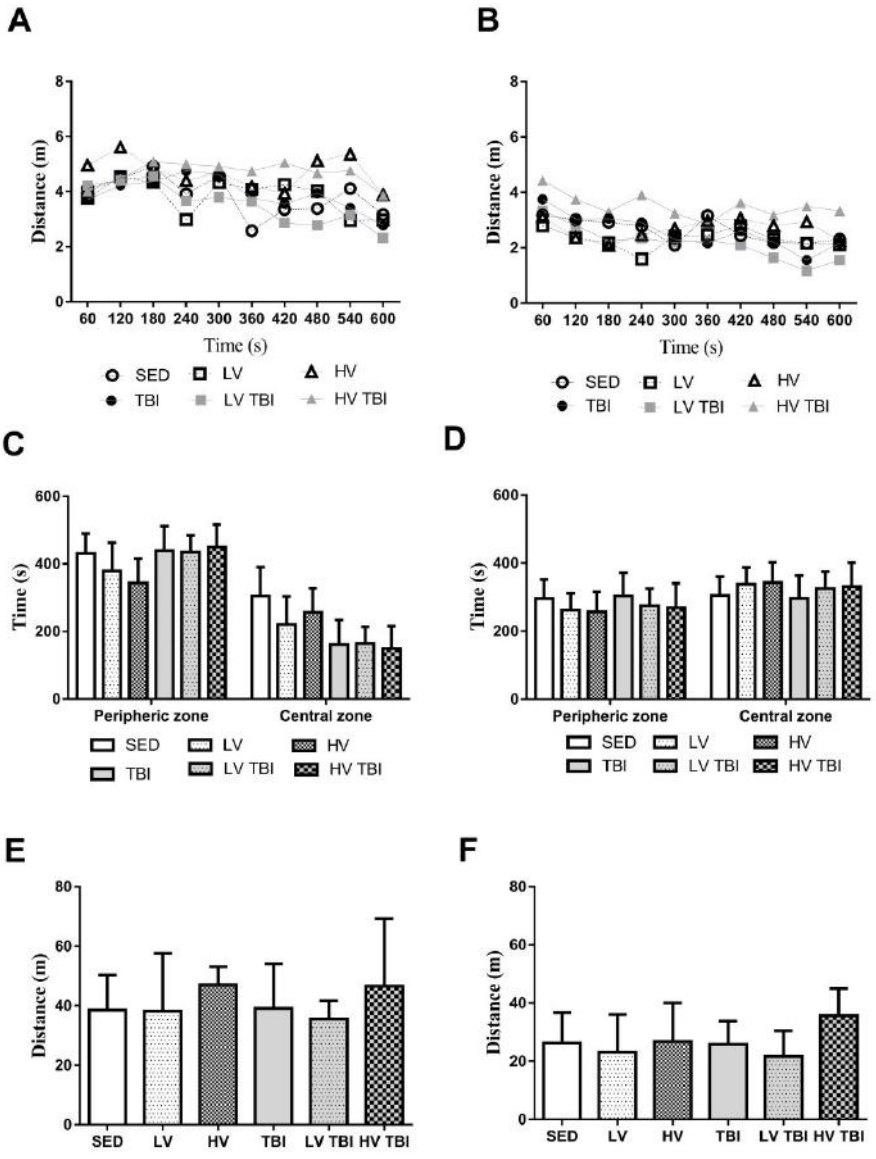


**Figure 2. Open field test parameters in mice engaged in different volumes of exercise training in the running wheel.** After thirty days of low volume (LV) or high volume (HV) exercise, the locomotor across 10 min, total distance traveled and the time spent in the center and periphery zones (exploratory profile) was measured at 48 h (A, C

and E) and 72 h (B, D and F) after TBI. There was no difference between groups. Abbreviations: Sedentary (SED); Open field (OF); Controlled cortical impact (TBI); Low volume TBI (LV TBI); High volume TBI (HV TBI).

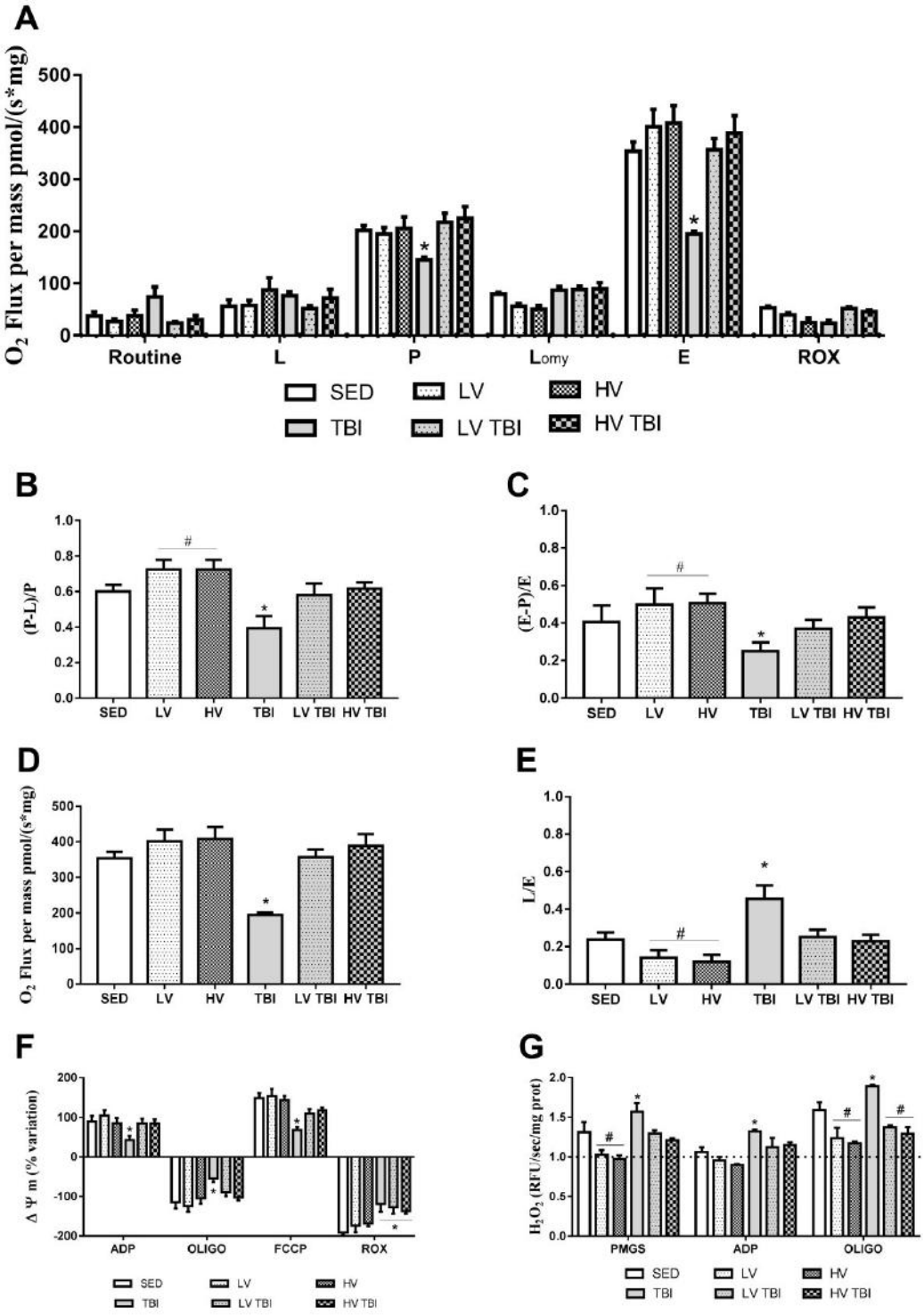

**Figure 3. Mitochondrial bioenergetic parameters.** Oxygen consumption rate (OCR) was accessed after titration of different mitochondrial substrates, uncuppler and inhibitors (A). Mitochondrial biochemical efficiency was used to indicate mitochondrial OXPHOS functioning (B) and the excess E-P factor (C) and mitochondrial reserve capacity (D) were used to evaluate the ETS capacity. Further evaluations of leak control ratio (E) was used to indicate ETS proton leak; the percent of $\Delta\psi_m$ variation (F) as indicator of dynamics after challenges; and mitochondrial $H_2O_2$ production (G) as a signature of this of mitochondrial bioenergetics abnormalities. Abbreviations: Sedentary (SED); Open field (OF); Morris water maze (MWM), Controlled cortical impact (TBI); Low volume TBI (LV TBI); High volume TBI (HV TBI). * Denotes significant difference comparing to all groups. # Denotes significant difference comparing to SED.

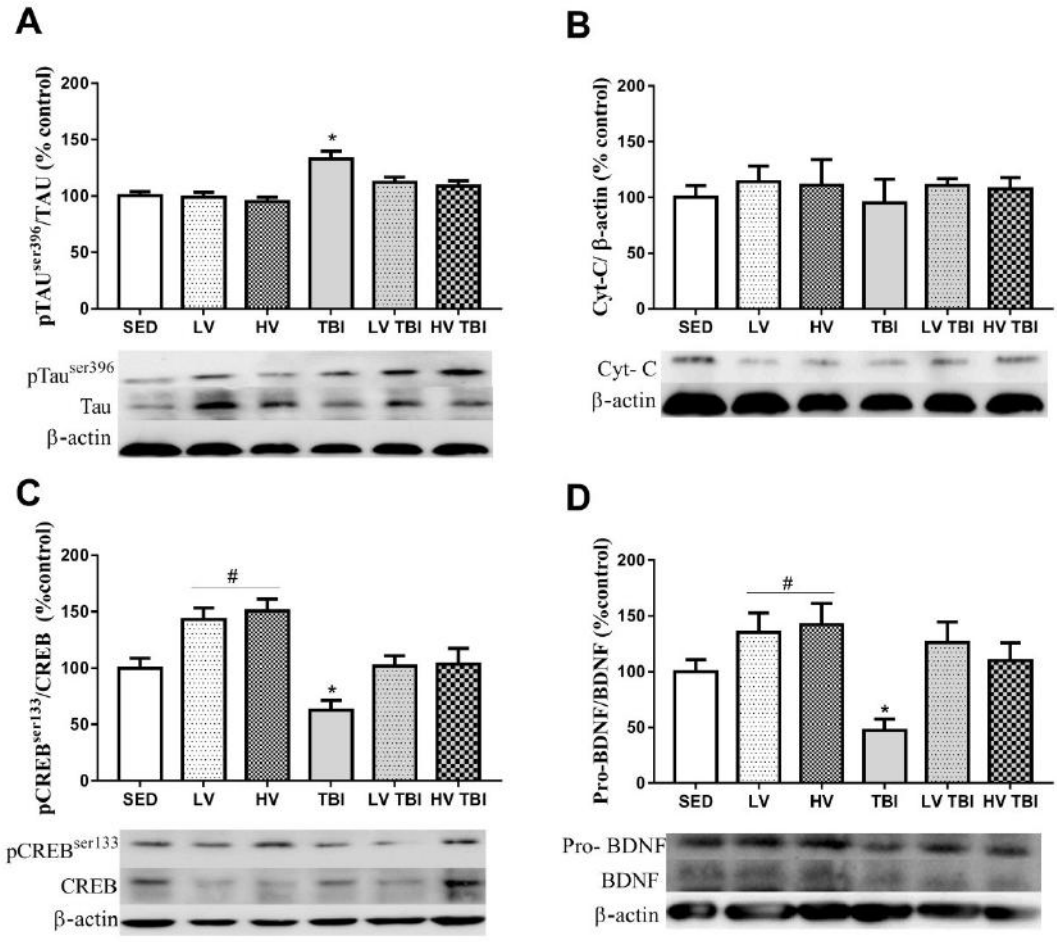

**Figure 4. Exercise preconditioning effects on molecular biomarkers.** Hippocampal pTau$^{Ser396}$ levels increased after TBI (A). No differences in cytochrome C levels between groups was observed (B). Increased pCREB$^{ser133}$ and pro-BDNF/BDNF ratio by physical exercise (C and D), and in contrast, decreased by TBI (C and D). * Denotes significant difference comparing to all groups. # Denotes significant difference comparing to SED.

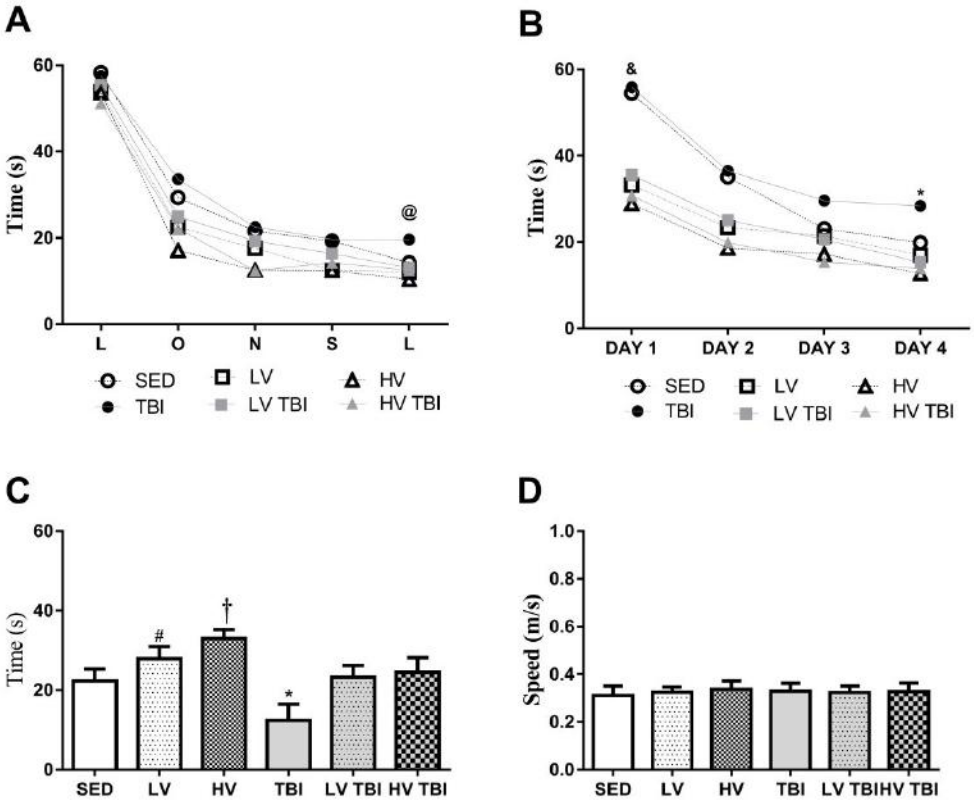


**Figure 5. Effects of exercise volumes and severe traumatic brain injury on spatial memory paradigm of Morris water maze.** In the flag test all groups learned to find the platform (A). In the acquisition TBI group spent more time searching for the platform than other groups (B). In the test phase without the platform, the exercised HV group spent more time in the quadrant zone than LV and SED. TBI decreased the time in the quadrant zone, and LV and HV TBI prevented this memory deficit (C). The

swimming speed was similar between groups (D). *† Denotes significant difference comparing to all groups. & Denotes significant difference comparing to exercise groups. @ Denotes significant difference comparing to first trial. # Denotes difference compared to SED.

**Capítulo VI:** *Mitochondrial modulation induced by intermittent fasting improves metabolic connectivity and bioenergetics synchronization after traumatic brain injury.*

No capitulo VI apresentamos um artigo em preparação para submissão.

Sabendo que o traumatismo cranioencefálico (TCE) está associado a um metabolismo cerebral prejudicado e que o jejum intermitente (IF) é uma abordagem dietética reconhecida por causar reprogramação metabólica cerebral, investigamos o potencial profilático de uma estratégia de IF em camundongos para restringir os déficits neuroenergéticos e cognitivos que se seguem ao TCE grave. Nesse trabalho, diferentes abordagens metodológicas foram aplicadas para desvendar a reprogramação da neuroenergética cerebral em razão do IF.

Nossos resultados demonstram que cinco dias após a lesão, o TCE induziu comprometimento da captação de glicose e conectividade metabólica, efeito que foi prevenido pelo IF. Além disso, o IF preveniu a disfunção mitocondrial, detrimento na homeostase de cálcio e no potencial da membrana mitocondrial induzidas pelo TCE. Ainda, a produção aumentada de peróxido de hidrogênio mitocondrial induzida por TCE foi atenuada por IF, culminando em viabilidade celular preservada. Esses defeitos metabólicos foram refletidos no comprometimento da memória espacial induzido pelo TCE que foi prevenido pelo IF.

Dessa forma, IF modulou mecanismos associados à progressão da lesão após TCE grave, prevenindo o comprometimento mitocondrial e cognitivo, melhorando a conectividade metabólica. Esses resultados expandem a literatura e fornecem novas evidências funcionais e moleculares fortalecendo os benefícios profiláticos ao cérebro, particularmente após um TCE grave.

**FULL TITLE:** *Mitochondrial modulation induced by intermittent fasting improves metabolic connectivity and bioenergetics synchronization after traumatic brain injury.*

Randhall B Carteri, *MSc*,[1] Afonso Kopzynski,[1] Lizia N Menegassi,[1] Nathan R Strogulski, *MSc*,[1] Marcelo S Rodolphi *MSc*,[1] Samuel Greggio,[2] Gianina T Venturin,[2] Jaderson Costa da Costa,[2] Debora G Souza *PhD,*[3] Gisele Hansel *PhD,*[1] Franciele Rohden *PhD*,[3] Marco A de Bastiani *MSc*,[4] Douglas H Smith, *PhD*[5] & Luis Valmor Portela, *PhD*[1*]

[1] Laboratory of Neurotrauma and Biomarkers - Department of Biochemistry, Graduate Program in Biochemistry, ICBS, Federal University of Rio Grande do Sul - UFRGS, Porto Alegre, Brazil.

[3] Brain Institute of Rio Grande do Sul (BraIns), Pontifical Catholic University of Rio Grande do Sul (PUCRS), Porto Alegre, Brazil

[3] Department of Biochemistry, Graduate Program in Biochemistry, ICBS, Federal University of Rio Grande do Sul - UFRGS, Porto Alegre, Brazil.

[4] Cell Biochemistry Laboratory - Department of Biochemistry, Graduate Program in Biochemistry, ICBS, Federal University of Rio Grande do Sul - UFRGS, Porto Alegre, Brazil.

[5] Penn Center for Brain Injury and Repair and Department of Neurosurgery, Perelman School of Medicine, University of Pennsylvania, Philadelphia, PA, USA.

**Correspondence:**

* Dr. Luis V. Portela,
Department of Biochemistry,
ICBS, UFRGS. Rua Ramiro Barcelos, 2600 anexo
90035-003, Porto Alegre, RS, Brazil.
Tel: 55 51 33085558; Fax: 55 51 33085544;
E-mail: roskaportela@gmail.com

***Abstract***

Traumatic Brain Injury (TBI) is associated with impaired brain metabolism culminating in neurodegeneration through mitochondria–associated mechanisms. Intermittent Fasting (IF) is a recognized dietary approach, which cause brain metabolic reprograming thereby improving function by mechanisms that requires an integral mitochondrial functioning. Therefore, the potential of IF as a preconditioning strategy relative to severe TBI remains to be explored regarding mitochondrial bioenergetics and cognitive function. Here, we show that prior IF in mice sustains mitochondrial neuroenergetics activity and metabolic connections between brain areas thereby avoiding memory deficits after severe TBI.

## INTRODUCTION

Currently established as a paramount worldwide health concern, traumatic brain injury (TBI) faces uprising scientific attention.[1, 2] TBI pathophysiological abnormalities progress beyond the primary insult (developed out of the impact force acting on the brain tissue), outcropping an abstruse secondary insult constituting of the amalgamation of deleterious mitochondria-associated mechanisms,[3-5] linked to impaired calcium ($Ca^{2+}$) homeostasis,[6] increased degradation of structural proteins,[7, 8] and apoptotic neurodegeneration.[6, 9] Therefore, mitochondria becomes a key candidate targeted in strategies aiming to ensure favorable cellular and neurological outcomes after TBI, [1, 10, 11] where a variety of pharmacological interventions have repeatedly failed. Regardless TBI, intermittent fasting (IF) has demonstrated to cause brain metabolic reprograming[12],[13] directly influencing glucose and ketone bodies cycling namely "Intermittent metabolic switching" (IMS),[14] and improving the mitochondrial responsiveness to substrates and brain resilience to insults.[15, 16] Accordingly, rodents maintained on IF exhibit increased neuronal resistance to insults including epileptic seizures and stroke.[17, 18] In a rodent model, a 24 h fasting prior to moderate TBI promoted neuroprotection; however when the fasting period was prolonged to 48 h there were no apparent benefits.[19] These results interrogate which is the feasible time-window necessary to achieve central benefits induced by dietary restriction strategies like IF.

While the high energy consumption rates is an important aspect driven normal neuronal communication,[20] the hypometabolism in specific brain areas after TBI[21] has been intimately linked with neuropsychological symptoms and long-term neurodegeneration.[22],[23, 24] Such TBI associated pathologies may arise from impaired physical and/or metabolic connectivity between neurons, nearby or distant to each other. Positron emission tomography with [$^{18}$F]-fluorodeoxyglucose (FDG-PET) is an established tool measuring in vivo cerebral metabolic rate of glucose (CMRglc),[25] interpreted as the coupling between synaptic transmission and local glucose consumption.[26] Additionally, FDG-PET can provide an integrative analysis of whole brain metabolism, namely metabolic connectivity (MC), through the correlation of the

glucose uptake values among different brain anatomical regions of interest (ROI). The magnitude of the correlation implies in the existence of functional association.[27] Since TBI induces secondary alterations linked with mitochondrial dysfunction particularly in structures associated with memory processing, we challenged this organelle with a IF preconditioning protocol to counterbalance neuroenergetic deficits and the loss of synaptic connectivity.

Notwithstanding the improvement in understanding the pathological process of TBI, developing preconditioning strategies in TBI is an utmost challenge to health professionals. From a translational point of view, IF seems attractive because of the easiness and low cost of its application as well as the reported benefits in both rodents and human clinical trials. [28],[29] Therefore, given the potential to promote synaptic strength and metabolic reserve, we hypothesized that an IF prophylactic strategy in mice might restrain the neuroenergetic deficits and metabolic connectivity that follows severe TBI.

## RESULTS

### *Intermittent fasting promotes metabolic shift without changes in body mass*

Based on the concept of IMS, we implied 10 cycles of 24-hour intervals of food deprivation followed by 24-hour ad libitum food access (IF),[30] as a prophylactic strategy to reduce metabolic impairment after TBI. As expected, the IF protocol here implied induced IMS, while no significant detectable changes in body mass. Total ketones were increased in the IF group (Figure 1A; mean diff. vs SHAM: 0.032; $p$ <0.0001 and mean diff. vs CCI: 0.031; $p$ <0.0001) and decreased levels of blood glucose (Figure 1 B; mean diff. vs SHAM = -40.63; $p$=0.0174 and mean diff. vs CCI = -40.63; $p$=0.0174) measured 2 h after a fasting day. When total ketones (Figure 1A; vs SHAM: $p$ <0.743 and vs CCI: $p$ <0.998) and blood glucose (Figure 1B; vs SHAM: $p$ <0.153 and vs CCI: $p$ <0.807) were assessed after an ad-libitum day, no differences were observed. When total ketones and blood glucose were assessed after an ad-libitum day and before CCI injury, no differences were observed among groups (figure 1C; $p$ = 0.720, $F$ = 0.333 and D; $p$ = 0.561, F = 0.591, respectively). Body mass was accessed in five different

time-points before; and 24, 48, 72 and 120 h after CCI. Body mass was not different among groups before or after CCI (Figure 1E). The food consumption 48 h before CCI increased in IF group. However, no difference was observed in total food consumption at 24 h before and after CCI (Figure 1F). Therefore, IF promoted the substrates shift and did not influenced body mass, as in agreement with recent literature evaluating weight loss after up to 30 days of IF in comparison to normal diet regimen.[31]

***Intermittent fasting partially prevents the rupture of brain metabolic connectivity after CCI***

Glucose hypometabolism is known to occur after a TBI event.[32, 33] Therefore, we used FDG-PET to estimate the glucose uptake in specific regions of interest (ROI) (Figure 2 A-G). There was decreased FDG uptake in the whole brain 5 days after CCI, and in the regions comprising the synaptosomes preparations (cortex, hippocampi, hypothalamus and cerebellum) as well as in other ROI investigated (see supplementary Table 1). The IF strategy was able to attenuate this effect. Further, we evaluated brain metabolic connectivity through a correlation network and hierarchical clustering of glucose uptake values across all regions evaluated (Figure 2 H-J). It was observed that CCI triggered a distinct association profile and correlation strength compared to control. Indeed, the highly connected functional metabolism displayed by the normal brain was shifted to a brain metabolically poorly correlated and lowly connected due to a severe CCI. Surprisingly, the IF strategy before CCI was able to recover the metabolic integration and association strengths post-injury.

***Intermittent fasting preserves synaptic and mitochondrial integrity after CCI***

Qualitative analysis of Transmission electron microscopy (Figure 3) shows intact SHAM mitochondria (Figure 3 A-D), with defined external and internal membranes as well as mitochondrial cristae (red arrows). Mitochondrial integrity was comprised in CCI (Figure 3 E-H), where damaged mitochondria with membrane ruptures form herniation, a structural characteristic of mitochondrial dysfunction, albeit it is unspecific regarding function. The IF strategy prevented this abnormalities (Figure 3 I-L), as illustrated by the integrity of mitochondria cristae (red arrow), as well as the external and internal

membranes. Synaptic clefts of SHAM (Figure 3 B and C) marked by the presence of synaptic density, abundance of vesicles in the pre-synaptic membrane and the connection of the post-synaptic membrane to its active zone presenting an electron-dense mark. While there are still observable presynaptic membranes loaded with vesicles in CCI (Figure 3 F and G), vesicle is dispersed without binding to a post-synaptic membrane (yellow stars). Even when it forms the synaptic cleft, there is no synaptic density (red arrow). Remarkably, IF also preserved synaptic integrity (Figure 3 I and J), and it can be observed two synaptic connections, the pre-synaptic membranes having many vesicles and making intimate contact with the post-synaptic membrane. Also, there are electron-dense marked synaptic clefts.

***Intermittent fasting prevents the impairment in mitochondrial calcium efflux through NCLX channel after CCI***

The observed loss of integrity of synapses may parallel with disrupted calcium homeostasis impacting mitochondrial function and cell integrity.[34] Therefore, we evaluated $Ca^{2+}$ influx and efflux in mitochondrial synaptosomes. The mitochondria absorbance at 540 nm was not significant different between groups before and after addition of mitochondrial substrates (PMGSA) (Figure 4A). Mitochondria from all groups were able to respond to a challenge of $Ca^{2+}$ after the energization with PMGSA (Figure 4A); however, mitochondrial swelling was higher in the CCI group, as demonstrated by the percentage of variation (Figure 4A and B). Additionally, after the addition of $Na^{+}$ to stimulate mitochondrial $Ca^{2+}$ efflux, the CCI group showed reduced functional capacity of NCLX channel to extruded the high $Ca^{2+}$ levels. In contrast, SHAM and IF groups displayed an increase in absorbance, which illustrates mitochondrial shrinkage due to $Ca^{2+}$ efflux in exchange with $Na^{+}$ (Figure 4A and B). Taken together, these results indicate that CCI induced increased mitochondrial swelling and deficient NCLX ($Na^{+}$-dependent) calcium efflux. Remarkably, IF improved NCLX function leading to almost normal extrusion of $Ca^{2+}$ in exchange with $Na^{+}$.

***Intermittent fasting prevents the rupture of mitochondrial membrane potential ($\Delta\Psi_m$) dynamics after CCI***

The $\Delta\Psi_m$ measured with fluorescence signal emitted by safranin-*O* in synaptosomes is showed in Figure 4C and D. The decrease in dye concentration in the medium parallel with the accumulation of the dye inside the mitochondria, which results in fluorescence quenching.[35] In the Routine state, were respiration is sustained by endogenous substrates, CCI showed a significant decreased fluorescence (Figure 4C; SHAM vs CCI: mean diff. = -27.7; $p$ <0.0001; CCI vs IF mean diff. = 28; $p$ <0.0001 and IF vs SHAM: $p$ = 0.9987). In $L_{(PMG)}$, CCI showed a significant decreased fluorescence compared to SHAM (Figure 4C; SHAM vs CCI: mean diff. = -17,3; $p$ = 0.0217; CCI vs IF $p$ = 0.3017 and IF vs SHAM: $p$ = 0.4508), while the percentage of variation was not different among groups, which implies in no impairment in the polarization of the mitochondrial inner membrane (elevated $\Delta\Psi_{m,}$ Figure 4D). At this point, ADP was added to activate OxPhos and this is associated with a decrease in $\Delta\Psi_m$ (increase in fluorescence in $P_{(CI)}$) (Figure 4C). This occurs due to protons being shuttled back to the matrix through the FoF1-ATP synthase thereby triggering phosphorylation of ADP to ATP. There is a concomitant increase in the OCR via decreased constraining effect of the proton gradient on electron transport. In this respiratory state, the $\Delta\Psi_m$ of CCI was significantly decreased compared to both SHAM and IF groups (Figure 4C; SHAM vs CCI: mean diff. = -35.1; $p$ <0.0001; CCI vs IF mean diff. = 35.17*;* $p$ < 0.0001 and IF vs SHAM: $p$ > 0.9999). The IF showed a significantly higher variation in $\Delta\Psi_m$ compared to both SHAM and CCI groups (Figure 4D; SHAM vs CCI: $p$ = 0.0898; IF vs SHAM $p$ = 0.3774 and IF vs CCI $p$ = 0.0032). In saturating concentrations of ADP, CI and CII – linked substrates generated a significant increase in fluorescence due to decreased $\Delta\Psi_m$ ($P_{(CI+CII)}$) in the CCI relative to other groups, and the same pattern was observed for the percent of variation (Figures 4 C and D). After Complex I inhibition by Rotenone ($P_{(CII)}$), $\Delta\Psi_m$ decreased, generating a significantly smaller variation in the CCI group. No differences observed in the ROX state, when cyanide (KCN) was added to inhibit Complex IV.

***Intermittent fasting prevents mitochondrial bioenergetics dysfunction after CCI***

Given that decreased $\Delta\Psi_m$ is often coupled with neuroenergetic deficits following TBI we further explored whether IF promotes sustained mitochondrial bioenergetics in response to substrates following CCI. Firstly, phosphate consumption in synaptosomes

were found decreased in CCI compared to both SHAM and IF (4E). We used a defined protocol of mitochondrial oxygen consumption rate (OCR) assessment performed with ipsilateral hemisphere preparations of synaptosomes (Figure 4 F). Intermittent fasting prevented the decrease in OCR induced by CCI in all phosphorylating states (Figure 4F), which is reflected by preserved OxPhos Coupling efficiency (Figure 4 G; SHAM vs CCI: mean diff. = -0.171; $p$ = 0.0062; IF vs SHAM: mean diff. = 0.019; $p$ = 0.932 and IF vs CCI: mean diff. = 0.031; $p$<0.0001). Reserve Respiratory capacity in CCI also presented decreased response (Figure 4 H; SHAM vs CCI: mean diff. = -614; $p$ = 0.0017; IF vs SHAM: mean diff. = 238.9; $p$ = 0.367 and IF vs CCI: mean diff. = 852.9; $p$ = 0.0002). No significant differences was observed relative to how CI-linked and CII-linked oxidation of substrates influenced total OCR in the phosphorylating state as indicated by both, the succinate effect and rotenone effect (Supplemental Figure 3 C and D; $p$ = 0.967, $F$ = 0.326 and $p$ = 0.879, F = 0.129, respectively). These functional alterations confirmed that CCI impact oxidative phosphorylation up to 5 days after CCI and that IF mitochondrial preconditioning was beneficial against energy deficits caused by severe TBI. [36, 37] In addition, there results suggesting that brain oxygen consumption in response TBI could be partially diverted from ATP synthesis to production of ROS after CCI.

***Intermittent fasting attenuates hydrogen peroxide production preserves cell viability following CCI***

Under metabolic stress, increased intracellular ionic charges (e.g. $Ca^{2+}$) may cause the collapse of the mitochondrial buffering capacity, $\Delta\psi_m$, proton gradient driven ATP synthesis. Mitochondrial oxidation of energy substrates coupled with electron transport system is a key site of ROS production, including $H_2O_2$. Conceptually, exacerbated uncoupling of the electron transport system associated with decreased antioxidant defenses implies in a presence of detrimental ROS production. Here, baseline $H_2O_2$ levels 5 days following injury were increased in CCI compared to SHAM, while IF was not significant different compared to CCI nor SHAM (Figure 4 I). Addition of the CI-linked mitochondrial substrates ($L_{(PMG)}$) significantly increased $H_2O_2$ production in the CCI

group. While no differences where observed between groups with the addition of ADP ($P_{(CI)}$), in the respiratory state $P_{(CI+CII)}$ there was higher mitochondrial $H_2O_2$ production in CCI compared to both SHAM and IF. After inhibition of CI and complex VI, $H_2O_2$ production was higher in both CCI and IF groups compared to SHAM. Remarkably, IF attenuated the increased $H_2O_2$ production in different mitochondrial respiration states (Figure 4I). Given that mitochondrial bioenergetics dysfunction and $H_2O_2$ levels may impact cell survival, we further explored cell viability (Figure 4 J). Remarkably, CCI decreased cell viability, and IF prevented this effect (SHAM vs CCI: $p$ <0.0001; IF vs SHAM $p$ = 0.1847 and IF vs CCI $p$ = 0.0004). Therefore, the aforementioned preserved $\Delta\psi_m$, $Ca^{2+}$ efflux capability, and mitochondrial bioenergetics, linked with decreased $H_2O_2$ production mediated by IF parallel with sustained cell viability 5 days after CCI.

***Intermittent fasting attenuates spatial memory deficits five days after CCI***

The MWM task is a robust method to evaluate learning and memory deficits in mice submitted to brain trauma. During the acquisition (training) phase of MWM, the SHAM group showed a significant decrease in the time to find the hidden platform when compared to other groups (Figure 5A). In the first training day, SHAM group was different from both CCI and IF. Analyzing the sub sequential training days, SHAM group remained different when compared to CCI and IF, albeit CCI and IF were also statistically different, indicating attenuated learning deficit in the IF group. The probe trial indicated that CCI spatial memory deficits, since the time in the target zone (Figure 5B) was significantly higher for CCI compared to both SHAM (Mean difference: 13.99; $p$ = 0.0032) and IF (Mean difference: 10.36; $p$ = 0.038) with no significant difference between SHAM and IF (Mean difference: 3.633; $p$ = 0.94). The latency to first entry in the target zone (Figure 5C) was significantly higher in CCI compared to both SHAM (25.54; $p$ = 0.0042) and IF (22.15; $p$ = 0.0114), with no differences between SHAM and IF (3.383; $p$ = 0.8514). The representative tracking plots illustrate the characteristic path performed by a mouse during the probe test (Figure 5D). These results confirms that IF is able to prevent cognitive deficits associated with TBI.

**DISCUSSION**

Although there are robust set of evidences indicating that dietary restriction paradigms exert prophylactic effects against different brain insults, studies addressed to TBI are scarce.[19, 38] Recently, it has been proposed that the benefits associated with IF regimens are related to a "Intermittent metabolic switching"(IMS), which refers to repeating cycles of a metabolic challenges such as dietary restriction and/or exercise, which cause liver glycogen stores depletion and increased circulating ketone levels, followed by a recovery period characterized by eating, resting and sleeping. Based on this concept, we induced IMS to prime brain mitochondrial metabolic adaptations before a severe TBI.

The IF protocol resulted in lack of detectable changes in body mass, which is an agreement with recent literature evaluating weight loss after up to 30 days of IF in comparison to normal diet regimen.[31] Additionally, our IF protocol promoted IMS as indicated by significant differences in total ketones bodies concentration after a fasting day and no differences after *ad libitum* feeding day, albeit the concentrations of total ketones and glucose soon before TBI induction were not different. This implies that beyond the already demonstration of acute fasting as neuroprotective against TBI, the prolonged IF may also provide neuroprotection through the development of neuroenergetic adaptations. [19] Altogether, our findings integrate new components to IMS which may have with potential relevance to TBI neurological outcomes.

Normal brain processes, such as neurotransmission, ionic homeostasis and membrane potentials are metabolically demanding, bolstering the emerging attention to mitochondrial function in the pathogenesis of several brain disorders, including TBI and also the interest in target mitochondria with therapies.[12, 39] Precisely, TBI impairs brain metabolism and glucose uptake, in addition to mitochondrial capability to manage high intracellular $Ca^{2+}$ inputs often accompanied by persistent neuroenergetics deficits, increased ROS production and apoptotic signaling, leading to a progressive neurodegeneration and memory deficits.[32, 33], [7, 8], [6, 9] Impaired synaptic activity reduces mitochondria energy production at synaptic sites, but also astrocyte proliferation and microglial activation seems to be associated with hypometabolism in neurodegeneration process,[40] which is also a hallmark in severe TBI. Recently, the

axiomatic concept relative to FDG-PET representing neuronal glucose consumption specifically at synapses was challenged by Zimmer et al,[41] showing that FDG PET signal is substantially affected by pharmacological activation of the astroglial glutamate transporter GLT-1.[42] Remarkably, brain metabolic connectivity is altered by TBI, [42] which could reflect a combination of altered neuronal and astrocytic activity.[43] Our results apraently support these concepts, as TBI decreased whole brain and region specific glucose uptake and disrupted metabolic connectivity, an effect prevented by IF preconditioning. Mitochondrial bioenergetics in synaptic terminals was preserved by IF and concomitantly reshape metabolic architecture, leading to partial recovery of glucose uptake. Thus, prophylactic IF strengthens the pre-existent synaptic connections and/or pave the way to build new synaptic connections after TBI due to metabolic adaptations yield by IMS.

Here we clearly demonstrated not only the impaired synaptossomal structure (a mirror of synapse) but also mitochondrial structural damage 5 d after CCI. Moreover, the coupling between impaired mitochondrial function, exacerbated ROS production and oxidative damage, is a common feature in TBI.[44] Therefore, we assessed mitochondria calcium handling in a swelling protocol. Mitochondria respond promptly to cytosolic $Ca^{2+}$ oscilations accumulating $Ca^{2+}$ when concentration rises above 0.5 μM. This occurs mainly to the activation of mitochondrial dehydrogenases and the storage of excess $Ca^{2+}$.[45] Owing that the resting free $Ca^{2+}$ concentration ranges between 100–200 nM in cytosol of most cells, free $Ca^{2+}$ in both cytosol and mitochondria can transiently and abruptly increase by a factor of 10–20 in an tightly coordinated process, intimately dependent on the mitochondrial membrane potential.[46, 47] The outer mitochondrial membrane voltage dependent anion channel (VDAC) conducts $Ca^{2+}$ in addition to monovalent ions, controlling $Ca^{2+}$ permeation.[48] As for the inner membrane, $Ca^{2+}$ influx into the matrix is mainly regulated by the mitochondrial calcium uniporter (MCU), positively charging the matrix paralleling with $\Delta\psi_m$ depolarization, while the $Ca^{2+}/Na^{+}/Li^{+}$ exchanger NCLX predominantly controls $Ca^{2+}$ efflux to maintain intramitochondrial homeostasis.[48] Although it is not well established if mitochondrial swelling is a strictly inner-membrane phenomenon,[49] a disturbance in calcium homeostasis is linked to neuronal cell death, via the formation of the permeability

transition pore (PTP), which is opened by excessive $Ca^{2+}$ accumulation inside mitochondria causing mitochondrial swelling.[50] In this context, ATP is a vital component to induce reversal of swelling, as demonstrated by Albert Lester Lehninger in a classic set of experiments.[51] Notably, higher permeability to $Ca^{2+}$ results in protein release and apoptosis, inducing permeability transition pore opening and cell death.[52] Even though a transitory increase in the $Ca^{2+}$ levels within mitochondrial matrix activates ATP synthesis and other $Ca^{2+}$ sensitive processes in normal cell environment, a persistent $Ca^{2+}$ increase exerts detrimental effects, as increased $Ca^{2+}$ levels parallels with the secondary hypometabolism after TBI.[53-55] Our results indicate that calcium influx is potentially exacerbated after TBI, in addition to impairment in calcium efflux. Mitochondrial NCLX channel is voltage dependent and eletrogenic, and in pathological conditions like TBI, it operates in a putative reverse mode.[56-58],[53] Exacerbated $H_2O_2$ production leads to peroxidation of mitochondrial lipid membranes associated with alterations in the mitochondrial $\Delta\Psi_m$ and $Ca^{2+}$ overload. Accordingly, $\Delta\psi_m$ dynamics at day 5 after CCI was significantly impaired relative to other groups, and most importantly, IF group showed similar responses as SHAM group. Disruptions of $\Delta\Psi_m$, paralleling decreased ATP synthesis has been observed in response to many apoptotic stimuli.[59] Precisely, CCI induced persistent mitochondrial dysfunction in the synaptic terminals throughout 5 days after injury, as indicated by several aspects of mitochondrial function, whilst IF prevented these effects. Both impairment in $\Delta\Psi_m$ and $Ca^{2+}$ are intimately associated with membrane structure, and could be the result of a vicious circle associating bioenergetic dysfunction and exacerbated $H_2O_2$ production.[60] After TBI, mitochondrial dysfunction parallels with oxidative damage to mitochondria *per se* and cytoskeletal proteins.[36] This could be partially explained by up-regulation of brain antioxidant responses suppressing oxidative stress induced by dietary restriction. [61, 62] Considering the impairment in mitochondrial ATP production and $\Delta\Psi_m$ combined with the deficient shrinkage in the CCI group, it is plausible to assume that indeed $Ca^{2+}$ overload following TBI precedes decreased cell viability. Strikingly, IF prevented impaired mitochondrial $Ca^{2+}$ homeostasis, which potentially benefits mitochondrial metabolism and overall cells survival.

Mitochondrial bioenergetics, calcium buffering capacity, and structural integrity

are early compromised following TBI injury in rodents. [36, 39, 63] Following the time-course after injury, several mitochondrial functional parameters appear to recover and remain stable at day 7, but no improvements comparable to uninjured animals are observed.[64] Isolated mitochondria from ipsilateral cortex present impaired metabolism three days after TBI and restored function at 5 days after injury.[36] It is plausible that dysfunctional mitochondria are for the most part no longer present in the injured brain 5 days following injury,[36] albeit, density-based gradients often select healthier mitochondrial populations compared to tissue homogenate analysis.[65] Brain mitochondria are heterogeneous, consisting of both synaptic and non-synaptic populations, as isolated synaptic mitochondria consist of pre-synaptic mitochondria located within the synaptosomes, while isolated non-synaptic mitochondria consist of neuronal (axonal, somal, dendritic) and non-neuronal (glial, vascular, etc.) mitochondria.[66, 67] Synaptic mitochondria exhibit increased oxidative damage, decreased bioenergetics and higher vulnerability to calcium imbalance compared to non-synaptic mitochondria.[66, 67] Mitochondrial metabolism after TBI is dependent on the localization of mitochondria in synaptic and non-synaptic sites, as synaptic mitochondria sustain increased damage 24 h following TBI [68]. Appropriate neurotransmission and synaptic plasticity relies on synaptic mitochondrial function, [69] processes that are negatively affected following TBI, [70] where the degree of mitochondrial dysfunction is a decisive factor to subsequent cell death, and functional recovery. [12, 64, 71]

Nevertheless, the effects of IF on brain mitochondrial metabolism are still controversial. It was initially accepted that increased mitochondrial biogenesis and oxygen consumption were induced by IF,[72] albeit this view was heavily challenged. A wide-range of posterior mechanistic-oriented studies using different approaches, suggests that IF does not necessarily increase oxygen consumption *per se*,[73, 74] but leads to an improvement in overall mitochondrial function, through increased in the antioxidant activity/decreased ROS production,[75] increased neurotrophic factors,[76, 77] mitochondrial biogenesis[78] and improved insulin signaling[79] in rodents. The pattern of response to injury is different among specific mitochondrial populations within the brain and coordinated adaptations that can optimize brain metabolism are remarkably complex and are beyond whole-brain basal oxygen consumption. Regardless of the fact

that these improvements are not always detectable in normal (i.e. without the presence of a pathologic disorder) conditions, the combined mechanisms explored in the present study can explain how IF induced mitochondrial improvement leading to sustained functionality when facing an adverse environment caused by TBI, or in other types of brain injury.[80]

The potential benefit of IF on learning and memory performance has been attributed to several metabolic effects.[81, 82] In agreement with this conjecture, we challenged mice in the MWM task and observed that a severe CCI injury imposes spatial learning and memory deficits whereas IF prevented these effects, as indicated by progressive decreases in the latency times with increasing training and the performance in the probe trial similar to sham animals. Several reports indicated enhanced cognitive function and preserved cognitive function after IF paradigms.[83-85] Impairment in brain bioenergetics precedes alterations in behavioral performance, albeit this direct causal relationship is currently strictly correlative.[86] The present results expand current literature indicating a cognitive benefit associated to IF and highlights that its prophylactic benefits are consistent with mitochondrial metabolic reprograming providing trophic support to synaptic connectivity.

## CONCLUSION

In summary, prophylactic intermittent fasting causes metabolic benefits to brain after a severe head injury. Remarkably, IF prevented mitochondrial bioenergetics deficits coupled with improved glucose uptake and synaptic connectivity. Taken together, these findings elucidate new trophic mechanisms mediated by IF, which may contributes to preventing the progressive injury associated with TBI, including memory deficits. These results expand the literature and provide functional and molecular pieces of evidence strengthening the prophylactic benefits of IF to individuals at increased risk of TBI.

## METHODS

### *Animals and treatment protocol*

Male 180 days old C57BL/6J mice obtained from Foundation for Health Science Research (FEPPS, Porto Alegre / RS, Brazil). Animals (4-5 per cage) were placed into a controlled temperature room (22ºC ± 1) under a 12h light/12h dark cycle (lights on at 7 a.m.) and had free access to food and water. Animals were assigned to two different dietary regimens: a normal, ad libitum diet and an alternate-day fasting, where animals had no food access during 24 h and ad libitum food access in the following day. Animals underwent a total of 10 cycles of food restriction and access. Subsequently, 48h after the last fasting day for the AF group, animals were submitted to a severe CCI injury. After CCI, animals were monitored during 5 days and underwent behavioral analysis. On the $5^{th}$ day, animals were euthanized and the ipsilateral hemisphere surrounding the impact injury was dissected for further neurochemical analysis. Body mass was accessed in 5 different time-points before CCI and 24, 48, 72 and 120 h after CCI. Total Ketones and blood glucose were assessed using specific meters and test strips in tail-tip blood samples (FreeStyle Optium Neo and β-Ketone Monitoring System; Abbott, Brazil and On Call® Plus glucose meter; ACON Laboratories, Inc., US, respectively). Blood samples were collected by skilled personnel using the routine tail-tip technique. See the experimental design in the Supplemental figure 01. All experiments were in agreement with the Committee on the Care and Use of Experimental Animal Resources, UFRGS, Brazil number 22436.

*Controlled Cortical Impact protocol (CCI)*

Injury was induced using a benchmark stereotaxic impactor (myNeuroLab®, Leica, St. Louis, MO, USA). Mice maintained in anesthesia (2.5 % isoflurane in a 2:1 mixture of $N_2$ and $O_2$), were placed in the stereotaxic (Kopf Instruments, Tujunga, CA) with a heating bed (37 ± 1 $^{o}$C) and submitted to a 4 mm diameter craniotomy in the center of bregma. Severe injury was induced by a 3.0 mm piston, impact velocity of 5.7 m / s; impact duration was 100 ms, and 2 mm of depth penetration in the exposed dura mater. Immediately after impact, craniotomy area was covered with a concave lamella bonded

with dental cement, and scalp suturation. After these procedures, anesthesia was discontinued and animals were monitored for at least 2 h post-injury.[87]

*microPET-Scan analysis*

Mice were submitted to [$^{18}$F] FDG uptake evaluation using positron emission tomography scans (microPET), performed at the Brain Institute (Porto Alegre, Rio Grande do Sul, Brazil) 5 days after CCI. Prior to scans, animals were fasted overnight, with *ad libitum* access to water. Animals were placed on a controlled temperature environment, and an intraperitoneal injection of 200μL of [$^{18}$F]FDG, with radioactive activity of 240μCi approximately, was made, allowing conscious drug uptake for 40 min. Animals were then anesthetized (Ketamine/Xylasine 90mg/kg and 7.5mg/kg respectively) and microPET-Scans performed. Images were analyzed based on regions of interest previously defined to determine region specific Standard Uptake Values (SUV). [88] Further, SUV were normalized to body mass.

*Metabolic connectivity*

In this analysis, we integrated several parameters in *R statistics software*. Pearson's R correlation were calculated among the SUV of brain regions. Networks were built using the "*RedeR*" package. Further, we performed clustering with both "euclidean distance" and "complete linkage agglomeration method"; using the "*pvclust*" package, "10000 bootstraps" and "seed 123" parameters were set for assessing the uncertainty in hierarchical clustering. Additionally, heatmaps were obtained from the correlation plots. Finally, the networks were built using the "*RedeR*" package.

*Preparation of Ipsilateral hemisphere synaptosomes and tissue homogenates*

Synaptosome-enriched bands were obtained using a discontinuous Percoll® (GE Healthcare, 17-0891-01) gradient centrifugation protocol, [89, 90] and resuspended in a sucrose and Tris buffer (320mM sucrose, 10mM Tris, pH 7.4) for transmission electron

microscopy, respirometry, mitochondrial swelling, mitochondrial membrane potential and hydrogen peroxide analysis. The remaining samples were frozen at − 80 °C for protein quantification (Pierce™ BCA Protein Assay Kit; Catalog number: 23225).

*Transmission electron microscopy*

Isolated synaptosomes were resuspended in 1mL of paraformoldehyde 4% plus 2.5% glutaraldehyde in 0.1M phosphate buffer. Briefly, three 30 min washes were performed with 0.1 M phosphate buffer, following 45 min immersion in 2% osmium tetroxide for post-fixation with three sub sequential 15 min washes with 0.1 M phosphate buffer. Thereafter, samples were dehydrated with acetone gradient (30 to 100%) and bathed for 2 h after mixing with increasing concentrations of EPON resin until a 24h bath with 100% concentration. Inclusion in silicone molds and pure resin was performed at 0 ° C for 72 hours. Finally, ultramicrotomy sections (100nm) were deposited in copper grids and contrasted with 2% uranyl acetate and lead citrate, analyzed by JEOL transmission electron microscopy (JEM1200, Center of Microscopy and Microanalysis - CMM, UFRGS). Magnifications are indicated in the figures.

*Mitochondrial calcium handling*

Mitochondrial calcium buffering capacity was obtained measuring the refractance spectrophotometrically at 540 nm (Spectra Max M5, Molecular Devices) of synaptossomes in added to standard swelling incubation medium (100 mM KCl, 50 mM Sucrose, 10 mM HEPES and 5 mM $KH_2PO_4$) in microplates. Baseline refractance was monitored during 3 min, following addition of 3.5 mM pyruvate, 4.5 mM malate, 4.5 mM glutamate, 1.2 mM succinate and 100 uM ADP (PMGSA) to obtain the refractance associated with oxidative phosphorylation, monitored during 5 min.

Afterward, calcium ($Ca^{2+}$, 20 mM) was added to induce large-amplitude swelling driven by the colloid osmotic force of $Ca^{2+}$ influx at proteins localized in the mitochondrial matrix, and refractance was monitored for 10 min. Finally, mitochondrial shrinkage related to $Ca^{2+}$ efflux was induced by addition of $Na^{+}$ (30 mM) were

refractance was monitored for additional 10 min. For a mitochondrial enriched suspension, the swelling and shrinkage causes a decrease and increase in the absorbance respectively, which are both discernible even to the naked eye.[91] Finally, we normalized all results for protein content and calculated the percentage of variation in the mitochondrial refractance after the addition of substrates PMGSA relative to basal; after addition of $Ca^{2+}$ relative to PMGSA; and after addition of $Na^{+}$ relative to $Ca^{2+}$.

*Mitochondrial Membrane Potential ($\Delta\Psi_m$)*

The $\Delta\Psi_m$ was measured in synaptosomes 5 days after CCI through the fluorescence signal detected with excitation wavelength of 495 nm and an emission wavelength of 586 nm (Spectra Max M5, Molecular Devices) emitted by the *safranin-O* cationic dye normalized to protein content. Samples were incubated in the respiration buffer used for the respirometry supplemented with 10 μM *safranin-O*. Baseline $\Delta\Psi_m$ (ROUTINE) was measured without addition of substrates and inhibitors in the incubation medium, followed by sequential addition of substrates used in respirometry (see below) to obtain the following coupling states: $L_{PMG}$ (PMG 2.5 mM), $P_{CI}$ (ADP 2.5mM); $P_{CI+CII}$ (S 2mM); $P_{CII}$ (Rot 2mM) and ROX (KCN 2.5mM). In addition these values were used calculate the percentage of change in the $\Delta\Psi_m$ relative to the previous coupling state.[92]

*Mitochondrial respiratory protocol*

Synaptosomal oxygen consumption rates were measured at 37°C using a standard respiration buffer (100 mM KCI, 75 mM mannitol, 25 mM sucrose, 5 mM phosphate, 0.05 mM EDTA, and 10 mM Tris-HC1, pH 7.4) in Oxygraph-2k system and recorded real-time using DatLab software (Oroboros, Innsbruck, Austria). Oxygen consumption per tissue mass was obtained in different coupling states with a modified multi-substrate titration protocol as previously described in detail elsewhere.[93]

Briefly, following 5 minutes for establishing ROUTINE respiration values, titration protocol started with sequential addition of pyruvate, malate, and glutamate (PMG; 10, 10, and 20 mM, respectively) to obtain Leak ($L_{PMG}$) respiration. Sub

sequentially, adenosine diphosphate (ADP, 2.5 mM) was titrated to obtain OxPHOS capacity of Complex I-Linked substrates ($P_{CI}$). Maximal CI and CII-Linked OxPHOS capacity was obtained with addition of Succinate (S, 10 mM) in saturating ADP concentrations ($P_{CI+CII}$). Complex II specific capacity ($P_{CII}$) was obtained with Rotenone (ROT, 2.0mM) and non-mitochondrial respiration (ROX) after cyanide (KCN, 5 mM). ROX was extracted from all of the above-mentioned states and Tissue-mass specific oxygen fluxes were normalized to the protein content.

We calculated Flux control factors (FCF), which express the change of flux in a single step of the SUIT protocol, normalized for the high flux as a specific reference state. Respiratory control ratio ($RCR = P/L$) was obtained in the CI-linked substrate state. For statistical analysis RCR was transformed to its respective FCF (OXPHOS coupling efficiency: $P_{CI}$-$L_{CI}/P_{CI} = 1$-$L_{CI}/P_{CI}$). We calculated CI stimulating CII respiration (Rotenone effect: $1 - P_{CII}/P_{CI+CII}$) and CII stimulating Maximal OCR (Succinate effect: $1 - P_{CI}/P_{CI+CII}$). Finally, Reserve Respiratory Capacity was assessed in the OxPHOS state as (ROUTINE - Maximal OxPHOS capacity).[93, 94]

*Mitochondrial $H_2O_2$ production*

Mitochondrial hydrogen peroxide ($H_2O_2$) production in different coupling states of was assessed in synaptosomes in the respirometry buffer supplemented with 10 μM Amplex Red and 2 units / mL horseradish peroxidase. The same sequence and amount of substrates used for $\Delta\Psi_m$ analyses were used. Fluorescence was monitored at excitation (563 nm) and emission (587 nm) wavelengths with a Spectra Max M5 microplate reader (Molecular Devices, USA).[92]

*Cell viability assay*

Cell viability assay was performed 5 days after CCI through the colorimetric [3(4,5-dimethylthiazol-2- yl)- 2,5-diphenyl tetrazolium bromide] (MTT, Sigma) method.[95] Synaptosomes were incubated with 0.5 mg/ml of MTT, at 37°C during 45 min. The formazan product generated during the incubation was solubilized in dimethyl

sulfoxide and measured at 560 and 630 nm. The results were expressed as percentage of control.

*Morris Water Maze task*

We additionally investigated the cognitive function of animals using a spatial memory paradigm. [96, 97] Animals (n=10 per group) were challenged in the Morris Water Maze task (MWM). The apparatus was a black, circular pool (110 cm diameter) with water at 21 ± 1 °C. Mice underwent four daily training trials during 4 days, aiming to find a hidden black platform submerged in a fixed place of the tank. If the animal failed to find the platform in 60 s, it was manually placed on the platform and allowed to rest for 20 s. Trials were separated by at least 10 min to avoid hypothermia. The result is the average of four trials per animal/day/group, used as an indicator of learning. The second phase of the MWM task, namely test phase (1 day), is an indicator of memory retention. Test phase was performed without the submerged platform 24 h after the 4 days training, measuring the time spent in the target quadrant. Videos were obtained and analyzed using the N-Maze program.[97]

*Statistical Analysis*

Results were calculated and expressed as the mean ± S.E.M. To analyze the differences between groups, we used one-way analysis of variance (ANOVA) followed by a post-hoc Tukey test; or Kruskal-Wallis test when necessary. All procedures were performed using GraphPad Prism 6.0 software. The differences were considered statistically significant at $p < 0.05$.

**REFERENCES**


1. Blennow, K., J. Hardy, and H. Zetterberg, *The neuropathology and neurobiology of traumatic brain injury.* Neuron, 2012. **76**(5): p. 886-99.
2. Rosenfeld, J.V., et al., *Early management of severe traumatic brain injury.* Lancet, 2012. **380**(9847): p. 1088-98.
3. Roozenbeek, B., A.I. Maas, and D.K. Menon, *Changing patterns in the epidemiology of traumatic brain injury.* Nat Rev Neurol, 2013. **9**(4): p. 231-6.
4. Dash, P.K., et al., *Biomarkers for the diagnosis, prognosis, and evaluation of treatment efficacy for traumatic brain injury.* Neurotherapeutics, 2010. **7**(1): p. 100-14.
5. Cheng, G., et al., *Mitochondria in traumatic brain injury and mitochondrial-targeted multipotential therapeutic strategies.* British journal of pharmacology, 2012. **167**(4): p. 699-719.
6. Hemphill, M.A., et al., *Traumatic brain injury and the neuronal microenvironment: a potential role for neuropathological mechanotransduction.* Neuron, 2015. **85**(6): p. 1177-92.
7. Johnson, V.E., et al., *SNTF Immunostaining Reveals Previously Undetected Axonal Pathology in Traumatic Brain Injury.* Acta neuropathologica, 2016. **131**(1): p. 115-135.
8. Johnson, V.E., W. Stewart, and D.H. Smith, *Axonal pathology in traumatic brain injury.* Exp Neurol, 2013. **246**: p. 35-43.
9. Zetterberg, H., D.H. Smith, and K. Blennow, *Biomarkers of mild traumatic brain injury in cerebrospinal fluid and blood.* Nat Rev Neurol, 2013. **9**(4): p. 201-10.
10. Schon, E.A. and S. Przedborski, *Mitochondria: the next (neurode)generation.* Neuron, 2011. **70**(6): p. 1033-1053.
11. Gajavelli, S., et al., *Evidence to support mitochondrial neuroprotection, in severe traumatic brain injury.* Journal of Bioenergetics and Biomembranes, 2015. **47**(1): p. 133-148.
12. Hiebert, J.B., et al., *Traumatic brain injury and mitochondrial dysfunction.* Am J Med Sci, 2015. **350**(2): p. 132-8.
13. Pani, G., *Neuroprotective effects of dietary restriction: Evidence and mechanisms.* Seminars in Cell & Developmental Biology, 2015. **40**: p. 106-114.
14. Mattson, M.P., et al., *Intermittent metabolic switching, neuroplasticity and brain health.* Nat Rev Neurosci, 2018. **19**(2): p. 63-80.
15. Amigo, I., et al., *Caloric restriction increases brain mitochondrial calcium retention capacity and protects against excitotoxicity.* Aging Cell, 2017. **16**(1): p. 73-81.
16. López-Lluch, G., et al., *Calorie restriction induces mitochondrial biogenesis and bioenergetic efficiency.* Proceedings of the National Academy of Sciences of the United States of America, 2006. **103**(6): p. 1768.
17. Anson, R.M., et al., *Intermittent fasting dissociates beneficial effects of dietary restriction on glucose metabolism and neuronal resistance to injury from calorie intake.* Proc Natl Acad Sci U S A, 2003. **100**(10): p. 6216-20.

18. Goodrick, C.L., et al., *Effects of intermittent feeding upon body weight and lifespan in inbred mice: interaction of genotype and age.* Mech Ageing Dev, 1990. **55**(1): p. 69-87.
19. Davis, L.M., et al., *Fasting is neuroprotective following traumatic brain injury.* J Neurosci Res, 2008. **86**(8): p. 1812-22.
20. Hyder, F., D.L. Rothman, and M.R. Bennett, *Cortical energy demands of signaling and nonsignaling components in brain are conserved across mammalian species and activity levels.* Proc Natl Acad Sci U S A, 2013. **110**(9): p. 3549-54.
21. Nakashima, T., et al., *Focal brain glucose hypometabolism in patients with neuropsychologic deficits after diffuse axonal injury.* AJNR Am J Neuroradiol, 2007. **28**(2): p. 236-42.
22. Shiga, T., et al., *Loss of neuronal integrity: a cause of hypometabolism in patients with traumatic brain injury without MRI abnormality in the chronic stage.* Eur J Nucl Med Mol Imaging, 2006. **33**(7): p. 817-22.
23. Daulatzai, M.A., *Cerebral hypoperfusion and glucose hypometabolism: Key pathophysiological modulators promote neurodegeneration, cognitive impairment, and Alzheimer's disease.* J Neurosci Res, 2017. **95**(4): p. 943-972.
24. Scholl, M., et al., *Early astrocytosis in autosomal dominant Alzheimer's disease measured in vivo by multi-tracer positron emission tomography.* Sci Rep, 2015. **5**: p. 16404.
25. Phelps, M.E., et al., *Tomographic measurement of local cerebral glucose metabolic rate in humans with (F-18)2-fluoro-2-deoxy-D-glucose: validation of method.* Ann Neurol, 1979. **6**(5): p. 371-88.
26. Magistretti, P.J., *Neuron-glia metabolic coupling and plasticity.* J Exp Biol, 2006. **209**(Pt 12): p. 2304-11.
27. Horwitz, B., R. Duara, and S.I. Rapoport, *Intercorrelations of glucose metabolic rates between brain regions: application to healthy males in a state of reduced sensory input.* J Cereb Blood Flow Metab, 1984. **4**(4): p. 484-99.
28. Selman, C., *Dietary restriction and the pursuit of effective mimetics.* Proc Nutr Soc, 2014. **73**(2): p. 260-70.
29. Tinsley, G.M. and P.M. La Bounty, *Effects of intermittent fasting on body composition and clinical health markers in humans.* Nutr Rev, 2015. **73**(10): p. 661-74.
30. Xie, K., et al., *Every-other-day feeding extends lifespan but fails to delay many symptoms of aging in mice.* Nature Communications, 2017. **8**: p. 155.
31. Gotthardt, J.D., et al., *Intermittent Fasting Promotes Fat Loss With Lean Mass Retention, Increased Hypothalamic Norepinephrine Content, and Increased Neuropeptide Y Gene Expression in Diet-Induced Obese Male Mice.* Endocrinology, 2016. **157**(2): p. 679-691.
32. Mandelkow, E.M. and E. Mandelkow, *Biochemistry and cell biology of tau protein in neurofibrillary degeneration.* Cold Spring Harb Perspect Med, 2012. **2**(7): p. a006247.
33. Vekaria, H.J., et al., *Targeting mitochondrial dysfunction in CNS injury using Methylene Blue; still a magic bullet?* Neurochemistry International, 2017.

34. Jafri, M.S. and R. Kumar, *Modeling Mitochondrial Function and Its Role in Disease.* Progress in molecular biology and translational science, 2014. **123**: p. 103-125.
35. Figueira, T.R., et al., *Safranine as a fluorescent probe for the evaluation of mitochondrial membrane potential in isolated organelles and permeabilized cells.* Methods Mol Biol, 2012. **810**: p. 103-17.
36. Hill, R.L., et al., *Time courses of post-injury mitochondrial oxidative damage and respiratory dysfunction and neuronal cytoskeletal degradation in a rat model of focal traumatic brain injury.* Neurochemistry International, 2017.
37. Kulbe, J.R., et al., *Synaptic Mitochondria Sustain More Damage than Non-Synaptic Mitochondria after Traumatic Brain Injury and Are Protected by Cyclosporine A.* J Neurotrauma, 2017. **34**(7): p. 1291-1301.
38. Rich, N.J., et al., *Chronic caloric restriction reduces tissue damage and improves spatial memory in a rat model of traumatic brain injury.* J Neurosci Res, 2010. **88**(13): p. 2933-9.
39. Gilmer, L.K., et al., *Early mitochondrial dysfunction after cortical contusion injury.* Journal of neurotrauma, 2009. **26**(8): p. 1271-1280.
40. Fan, Z., et al., *Longitudinal influence of microglial activation and amyloid on neuronal function in Alzheimer's disease.* Brain, 2015. **138**(Pt 12): p. 3685-98.
41. Zimmer, E.R., et al., *[(18)F]FDG PET signal is driven by astroglial glutamate transport.* Nature neuroscience, 2017. **20**(3): p. 393-395.
42. Byrnes, K., et al., *FDG-PET imaging in mild traumatic brain injury: a critical review.* Frontiers in Neuroenergetics, 2014. **5**(13).
43. Hadera, M.G., et al., *Modification of Astrocyte Metabolism as an Approach to the Treatment of Epilepsy: Triheptanoin and Acetyl-L-Carnitine.* Neurochem Res, 2016. **41**(1-2): p. 86-95.
44. Hall, E.D., R.A. Vaishnav, and A.G. Mustafa, *Antioxidant therapies for traumatic brain injury.* Neurotherapeutics, 2010. **7**(1): p. 51-61.
45. Nicholls, D.G., *Mitochondrial calcium function and dysfunction in the central nervous system.* Biochimica et Biophysica Acta (BBA) - Bioenergetics, 2009. **1787**(11): p. 1416-1424.
46. Gunter, T.E. and S.-S. Sheu, *Characteristics and possible functions of mitochondrial Ca2+ transport mechanisms.* Biochimica et Biophysica Acta (BBA) - Bioenergetics, 2009. **1787**(11): p. 1291-1308.
47. Gellerich, F.N., et al., *The regulation of OXPHOS by extramitochondrial calcium.* Biochimica et Biophysica Acta (BBA) - Bioenergetics, 2010. **1797**(6): p. 1018-1027.
48. Contreras, L., et al., *Mitochondria: the calcium connection.* Biochim Biophys Acta, 2010. **1797**(6-7): p. 607-18.
49. Giorgi, C., et al., *Mitochondrial calcium homeostasis as potential target for mitochondrial medicine.* Mitochondrion, 2012. **12**(1): p. 77-85.
50. Duchen, M.R., *Mitochondria and calcium: from cell signalling to cell death.* J Physiol, 2000. **529 Pt 1**: p. 57-68.
51. Lehninger, A.L., *Reversal of various types of mitochondrial swelling by adenosine triphosphate.* J Biol Chem, 1959. **234**: p. 2465-71.

52. Tan, W. and M. Colombini, *VDAC closure increases calcium ion flux.* Biochim Biophys Acta, 2007. **1768**(10): p. 2510-5.
53. Zhao, X., et al., *Differential hippocampal protection when blocking intracellular sodium and calcium entry during traumatic brain injury in rats.* J Neurotrauma, 2008. **25**(10): p. 1195-205.
54. Johnson, V.E., et al., *SNTF immunostaining reveals previously undetected axonal pathology in traumatic brain injury.* Acta Neuropathol, 2016. **131**(1): p. 115-35.
55. Wang, Y., et al., *Protection against TBI-Induced Neuronal Death with Post-Treatment with a Selective Calpain-2 Inhibitor in Mice.* J Neurotrauma, 2018. **35**(1): p. 105-117.
56. Kim, B. and S. Matsuoka, *Cytoplasmic Na+-dependent modulation of mitochondrial Ca2+ via electrogenic mitochondrial Na+-Ca2+ exchange.* J Physiol, 2008. **586**(6): p. 1683-97.
57. Smets, I., et al., *Ca<sup>2+</sup> uptake in mitochondria occurs via the reverse action of the Na<sup>+</sup>/Ca<sup>2+</sup> exchanger in metabolically inhibited MDCK cells.* American Journal of Physiology - Renal Physiology, 2004. **286**(4): p. F784-F794.
58. Griffiths, E.J., *Reversal of mitochondrial Na/Ca exchange during metabolic inhibition in rat cardiomyocytes.* FEBS Letters, 1999. **453**(3): p. 400-404.
59. Gottlieb, E., et al., *Mitochondrial membrane potential regulates matrix configuration and cytochrome c release during apoptosis.* Cell Death Differ, 2003. **10**(6): p. 709-17.
60. Gardner, R., A. Salvador, and P. Moradas-Ferreira, *Why does SOD overexpression sometimes enhance, sometimes decrease, hydrogen peroxide production? A minimalist explanation.* Free Radic Biol Med, 2002. **32**(12): p. 1351-7.
61. Li, L., Z. Wang, and Z. Zuo, *Chronic Intermittent Fasting Improves Cognitive Functions and Brain Structures in Mice.* PLoS ONE, 2013. **8**(6): p. e66069.
62. Hyun, D.H., et al., *Calorie restriction up-regulates the plasma membrane redox system in brain cells and suppresses oxidative stress during aging.* Proc Natl Acad Sci U S A, 2006. **103**(52): p. 19908-12.
63. Singh, I.N., et al., *Time course of post-traumatic mitochondrial oxidative damage and dysfunction in a mouse model of focal traumatic brain injury: implications for neuroprotective therapy.* J Cereb Blood Flow Metab, 2006. **26**(11): p. 1407-18.
64. Wang, W.-X., P.G. Sullivan, and J.E. Springer, *Mitochondria and microRNA crosstalk in traumatic brain injury.* Progress in Neuro-Psychopharmacology and Biological Psychiatry, 2017. **73**: p. 104-108.
65. *Use of Fluorescent Reporters to Measure Mitochondrial Membrane Potential and the Mitochondrial Permeability Transition*, in *Drug-Induced Mitochondrial Dysfunction*.
66. Stauch, K.L., P.R. Purnell, and H.S. Fox, *Quantitative proteomics of synaptic and nonsynaptic mitochondria: insights for synaptic mitochondrial vulnerability.* J Proteome Res, 2014. **13**(5): p. 2620-36.

67. Yarana, C., et al., *Synaptic and nonsynaptic mitochondria demonstrate a different degree of calcium-induced mitochondrial dysfunction.* Life Sci, 2012. **90**(19-20): p. 808-14.
68. Kulbe, J.R., et al., *Synaptic Mitochondria Sustain More Damage than Non-Synaptic Mitochondria after Traumatic Brain Injury and Are Protected by Cyclosporine A.* Journal of Neurotrauma, 2017. **34**(7): p. 1291-1301.
69. Cheng, A., Y. Hou, and M.P. Mattson, *Mitochondria and neuroplasticity.* ASN Neuro, 2010. **2**(5): p. e00045.
70. Sullivan, P.G., et al., *Traumatic brain injury alters synaptic homeostasis: implications for impaired mitochondrial and transport function.* J Neurotrauma, 1998. **15**(10): p. 789-98.
71. Lifshitz, J., et al., *Mitochondrial damage and dysfunction in traumatic brain injury.* Mitochondrion, 2004. **4**(5-6): p. 705-13.
72. Nisoli, E., et al., *Calorie restriction promotes mitochondrial biogenesis by inducing the expression of eNOS.* Science, 2005. **310**(5746): p. 314-7.
73. Chausse, B., et al., *Intermittent Fasting Results in Tissue-Specific Changes in Bioenergetics and Redox State.* PLoS ONE, 2015. **10**(3): p. e0120413.
74. Ferguson, M., et al., *Effect of long-term caloric restriction on oxygen consumption and body temperature in two different strains of mice.* Mechanisms of ageing and development, 2007. **128**(10): p. 539-545.
75. Cerqueira, F.M., et al., *Calorie restriction increases cerebral mitochondrial respiratory capacity in a NO•-mediated mechanism: Impact on neuronal survival.* Free Radical Biology and Medicine, 2012. **52**(7): p. 1236-1241.
76. Arumugam, T.V., et al., *Age and energy intake interact to modify cell stress pathways and stroke outcome.* Ann Neurol, 2010. **67**(1): p. 41-52.
77. Duan, W., et al., *Dietary restriction stimulates BDNF production in the brain and thereby protects neurons against excitotoxic injury.* J Mol Neurosci, 2001. **16**(1): p. 1-12.
78. Cassano, P., et al., *Tissue-specific effect of age and caloric restriction diet on mitochondrial DNA content.* Rejuvenation Res, 2006. **9**(2): p. 211-4.
79. Lu, J., et al., *Alternate Day Fasting Impacts the Brain Insulin Signaling Pathway of Young Adult Male C57BL/6 Mice.* Journal of neurochemistry, 2011. **117**(1): p. 154-163.
80. Yu, Z.F. and M.P. Mattson, *Dietary restriction and 2-deoxyglucose administration reduce focal ischemic brain damage and improve behavioral outcome: evidence for a preconditioning mechanism.* J Neurosci Res, 1999. **57**(6): p. 830-9.
81. Mattson, M.P., *Energy Intake and Exercise as Determinants of Brain Health and Vulnerability to Injury and Disease.* Cell metabolism, 2012. **16**(6): p. 706-722.
82. Longo, V.D. and M.P. Mattson, *Fasting: molecular mechanisms and clinical applications.* Cell Metab, 2014. **19**(2): p. 181-92.
83. Halagappa, V.K.M., et al., *Intermittent fasting and caloric restriction ameliorate age-related behavioral deficits in the triple-transgenic mouse model of Alzheimer's disease.* Neurobiology of Disease, 2007. **26**(1): p. 212-220.

84. Singh, R., et al., *Late-onset intermittent fasting dietary restriction as a potential intervention to retard age-associated brain function impairments in male rats.* Age (Dordr), 2012. **34**(4): p. 917-33.
85. Hu, Y. and M. Zhang, *Postoperative intermittent fasting prevents hippocampal oxidative stress and memory deficits in a rat model of chronic cerebral hypoperfusion.* 2018.
86. Watson, W.D., et al., *Impaired cortical mitochondrial function following TBI precedes behavioral changes.* Frontiers in Neuroenergetics, 2013. **5**: p. 12.
87. Smith, D.H., et al., *A model of parasagittal controlled cortical impact in the mouse: cognitive and histopathologic effects.* J Neurotrauma, 1995. **12**(2): p. 169-78.
88. Mirrione, M.M., et al., *A novel approach for imaging brain-behavior relationships in mice reveals unexpected metabolic patterns during seizures in the absence of tissue plasminogen activator.* NeuroImage, 2007. **38**(1): p. 34-42.
89. Sims, N.R., *Rapid isolation of metabolically active mitochondria from rat brain and subregions using Percoll density gradient centrifugation.* J Neurochem, 1990. **55**(2): p. 698-707.
90. Sims, N.R. and M.F. Anderson, *Isolation of mitochondria from rat brain using Percoll density gradient centrifugation.* Nat Protoc, 2008. **3**(7): p. 1228-39.
91. Nunez-Figueredo, Y., et al., *Antioxidant effects of JM-20 on rat brain mitochondria and synaptosomes: mitoprotection against Ca(2)(+)-induced mitochondrial impairment.* Brain Res Bull, 2014. **109**: p. 68-76.
92. Portela, L.V., et al., *Hyperpalatable Diet and Physical Exercise Modulate the Expression of the Glial Monocarboxylate Transporters MCT1 and 4.* Mol Neurobiol, 2016.
93. Gnaiger, E., *Mitochondrial pathways and respiratory control. An introduction to OXPHOS analysis.* . 4th ed, ed. M.P. Network. 2014, Innsbruck: OROBOROS MiPNet Publications. 80.
94. Burtscher, J., et al., *Differences in mitochondrial function in homogenated samples from healthy and epileptic specific brain tissues revealed by high-resolution respirometry.* Mitochondrion, 2015. **25**: p. 104-112.
95. Hansen, M.B., S.E. Nielsen, and K. Berg, *Re-examination and further development of a precise and rapid dye method for measuring cell growth/cell kill.* J Immunol Methods, 1989. **119**(2): p. 203-10.
96. Kalinine, E., et al., *Nandrolone-induced aggressive behavior is associated with alterations in extracellular glutamate homeostasis in mice.* Horm Behav, 2014. **66**(2): p. 383-92.
97. Muller, A.P., et al., *Exercise increases insulin signaling in the hippocampus: physiological effects and pharmacological impact of intracerebroventricular insulin administration in mice.* Hippocampus, 2011. **21**(10): p. 1082-92.

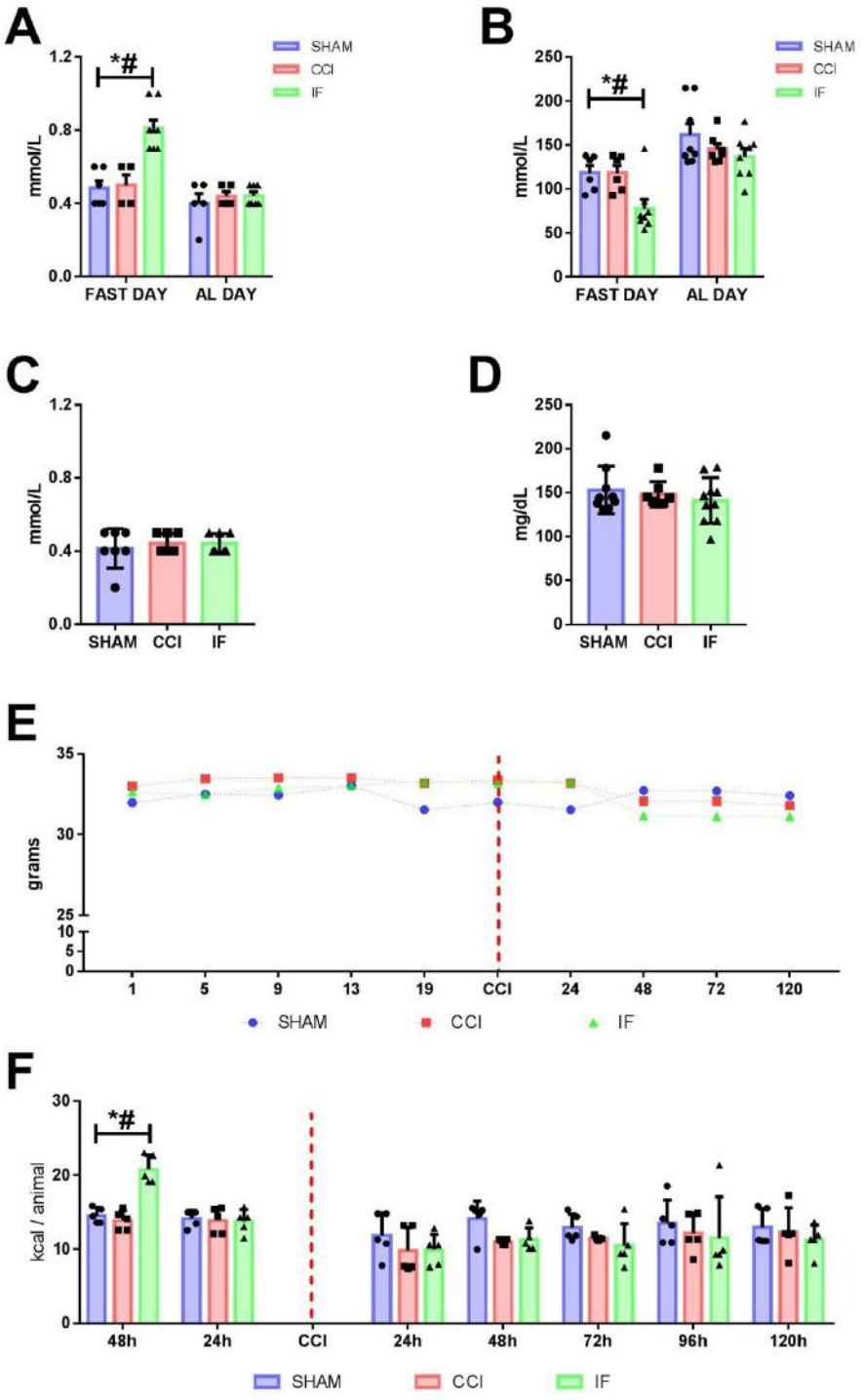


**Figure 01. Total blood ketones bodies and glucose, body mass and food consumption.** Total Ketones and blood glucose concentration after the last fasting day (A; 72 h before CCI); and following ad libitum food access day (B, 48 h before CCI). Total blood ketones and glucose concentrations 24 h before CCI showed no significant differences (C and D). No changes in body mass observed (E). Total food consumed in Kcal/animal (F) increased significantly in intermittent fasting (IF) group 48 h before

CCI, but no differences observed in the subsequent days (n = 7-10). Controlled cortical impact (CCI). *# Significant difference comparing IF to both SHAM and CCI groups.

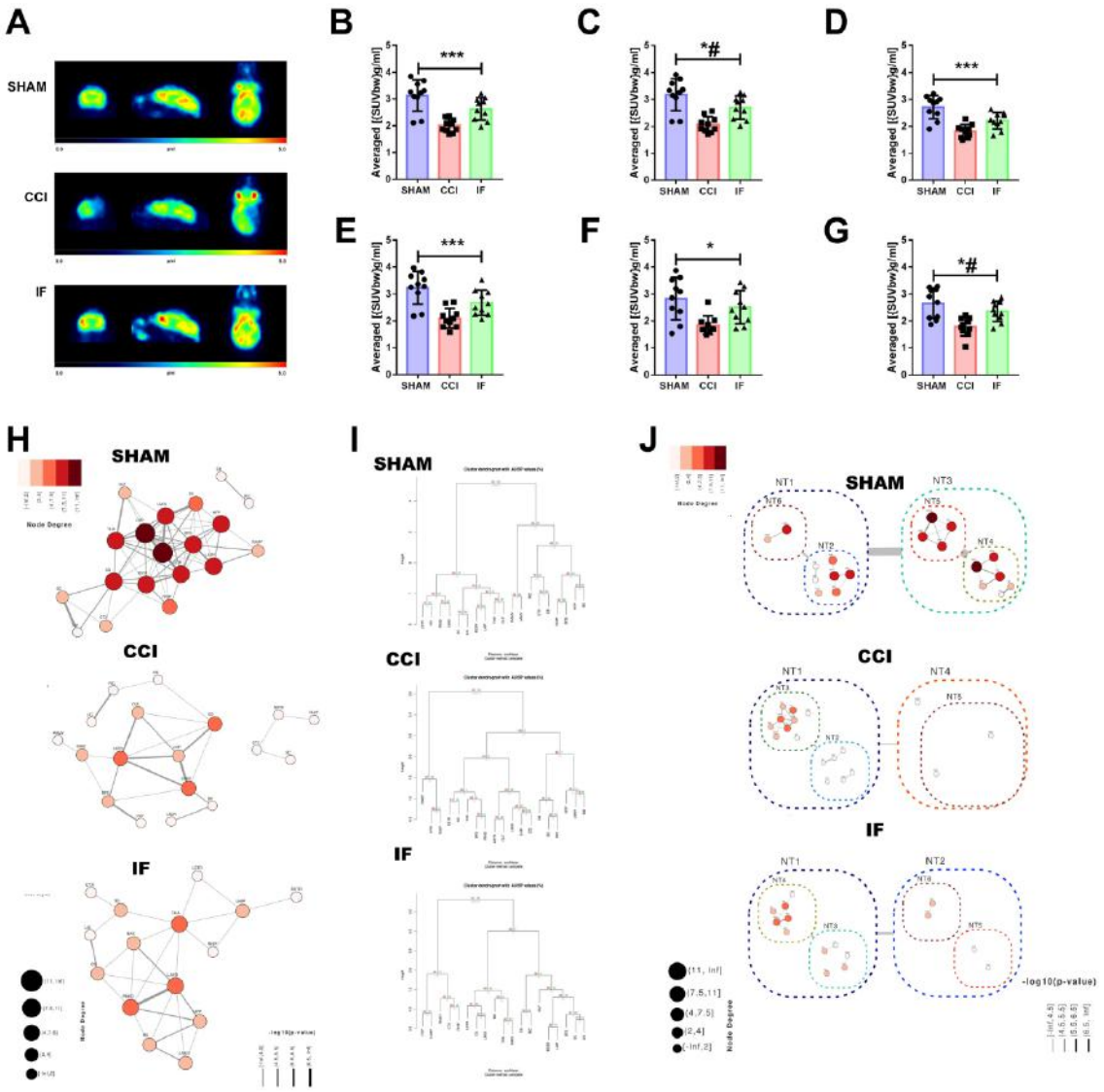


**Figure 02. Prior intermittent fasting (IF) prevents the decrease in glucose uptake and loss of metabolic connectivity induced by CCI.** Regions of interest and average templates of FDG-PET data (A). Decreased glucose uptake 5 days after CCI was evident in the whole brain (B), combined acquisitions of the brain regions of ipsilateral hemisphere used to synaptosomal preparations (C), cortex (D) hippocampi (E) hypothalamus (F) and cerebellum (G) (*n* = 7-10). Brain metabolic connectivity and integration through correlation network and hierarchical clustering based on the FDG uptake values across all regions evaluated (Figure 2 H-J). These analyses showed that CCI triggered a desynchronized profile, characteristic of impaired metabolic

connectivity. Prior IF before CCI prevented the loss of metabolic integration between brain areas and improved association strengths. Controlled cortical impact (CCI).

* Significant difference of CCI compared to SHAM;

*# Significant difference of CCI when compared to both SHAM and IF groups;

*** Significant differences between all group comparisons.

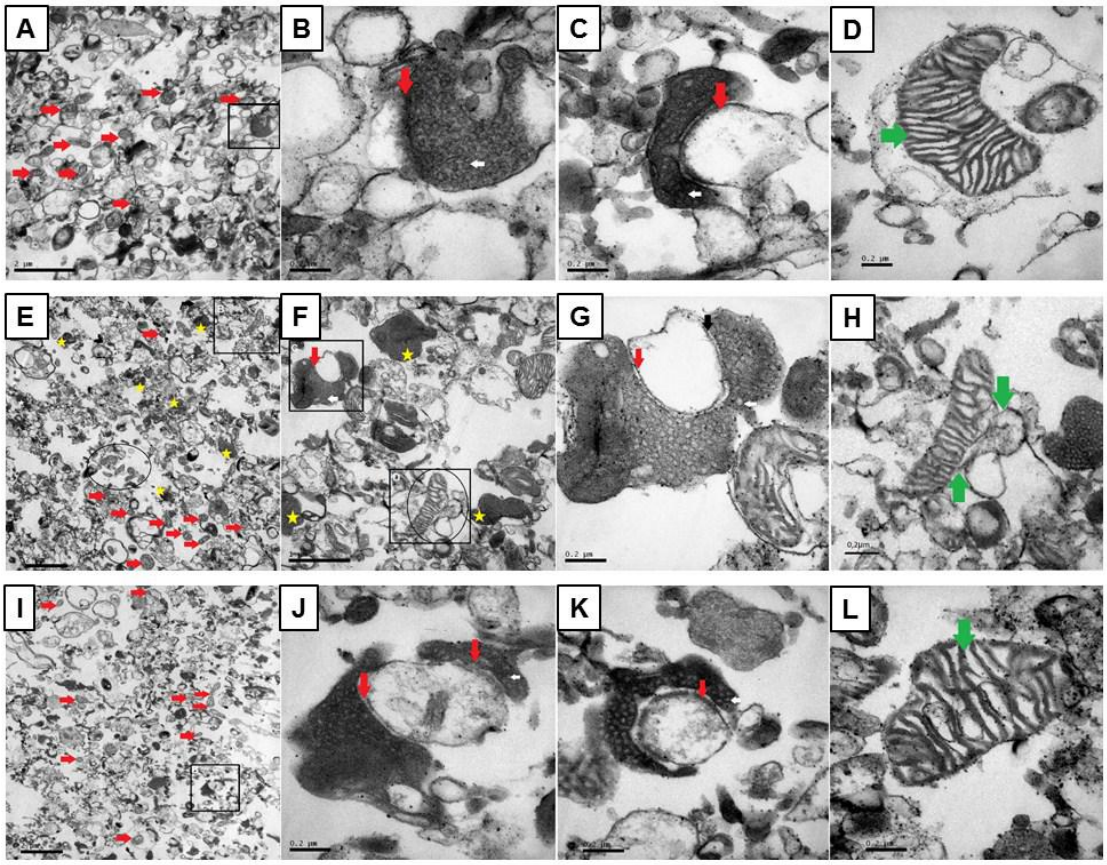


**Figure 03. Intermittent fasting (IF) preserves synaptic and mitochondrial integrity 5 days after CCI.** Representative image of SHAM, CCI and IF (A, E and I; 10,000X) showing an overview of the sample ($n$ = 3). Mitochondria of SHAM (detailed in D) presents clearly defined external and internal membranes with prominence for mitochondrial cristae (red and green arrows, A, B and D). Images from CCI (E) shows many intact mitochondria (red and green arrows, E, F, and H), albeit some mitochondria display membrane ruptures forming herniations (green arrow detailed in H). Remarkably, IF (red arrows, I) predominantly presents intact mitochondria with preserved cristae and outer and inner membranes (green arrow detailed in L). Detailed synaptic clefts indicated that CCI induced damage to pre-synaptic membranes (F and G; red arrows, 100.000X), with visible loose of vesicles, without binding to postsynaptic

clefts (E, F; yellow stars), and absence of synaptic density (F, G; red arrows). Detailed synaptic clefts of both SHAM (B and C; red arrows, 100.000X) and IF (J and K; red arrows, 100.000X) are marked by the presence of normal synaptic density, presenting abundance of vesicles in the pre-synaptic, and the connection of the post-synaptic membrane to its active zone, which is illustrated by an electron-dense mark.

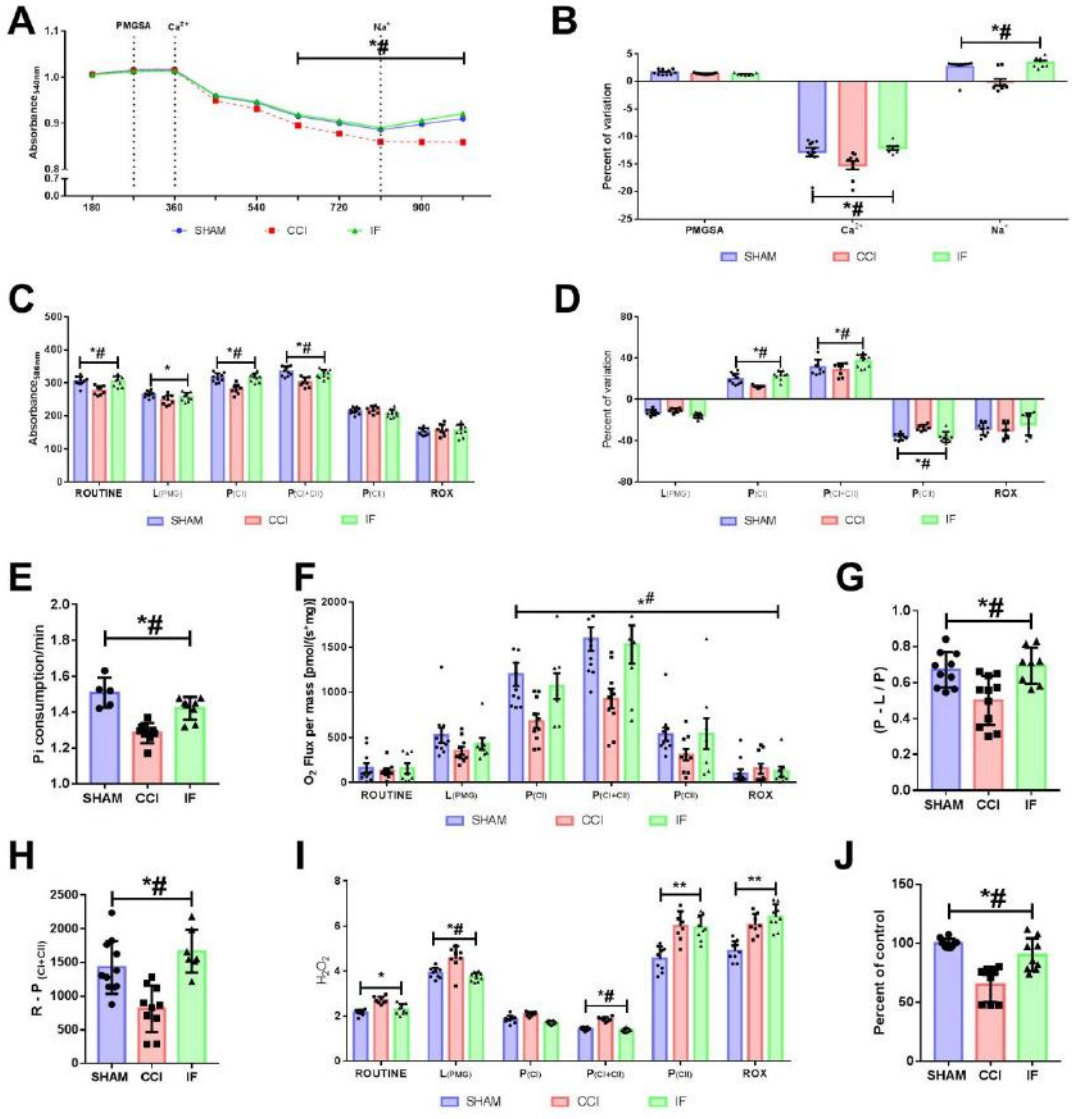


**Figure 04. Intermittent fasting (IF) prevents mitochondrial dysfunction 5 days after CCI.** Mitochondrial $Ca^{2+}$ swelling (A and B) stimulated by a calcium challenge in energized mitochondrial with substrates (pyruvate, malate, glutamate, succinate, and ADP; PMGSA) was significantly elevated in CCI group. Mitochondrial calcium $Ca^{2+}$ extrusion through the $Na^{+}/Ca^{2+}/Li^{+}$ exchanger after addition of $Na^{+}$ was impaired in CCI group (A and B). The fluorescent dye safranin-O incorporated within synaptosomal

mitochondria of the ipsilateral hemisphere then decreasing the fluorescent signal of the medium (C). Mitochondrial membrane potential ($\Delta\Psi_m$) is significantly decreased at Routine in CCI group. The percentage of variation in the $\Delta\Psi_m$ in the transition from $P_{CI}$ to $P_{CI+CII}$ and after CI inhibition ($P_{(CII)}$) confirmed that CCI group does not effectively generates and dissipated $\Delta\Psi_m$ as did SHAM and IF groups (D). Inorganic phosphate consumption by synaptosomes (E) was decreased only CCI. Synaptosomal oxygen consumption rates (OCR) at different mitochondrial states (F) indicated impairment in the phosphorylating states ($P_{(CI)}$, $P_{(CI+II)}$, $P_{(CII)}$) and ROX; in the Oxphos coupling efficiency (G) and Reserve Respiratory Capacity (H) by CCI. IF prevented the impairment in mitochondrial $Ca^{2+}$ efflux, $\Delta\Psi_m$ and bioenergetics after CCI. Also, mitochondrial $H_2O_2$ production (I) in synaptosomes were significantly increased at Routine, $L_{(PMG)}$, $P_{(CI+CII)}$, Rotenone ($P_{(CII)}$) and ROX by CCI. IF significantly decreased $H_2O_2$ production before complex I and IV inhibition. Cell viability (J) was decreased by CCI, which was prevented by IF ($n$ = 7-10). Sequential addition of pyruvate, malate, and glutamate ($L_{PMG}$), adenosine diphosphate (ADP; $P_{CI}$), and succinate (Suc) and ADP ($P_{CI+CII}$), Rotenone ($P_{CII}$) and cyanide (ROX).

* Significant difference when comparing SHAM to CCI.

*# Significant difference between CCI and both SHAM and IF.

** Significant difference between both CCI and IF compared to SHAM.

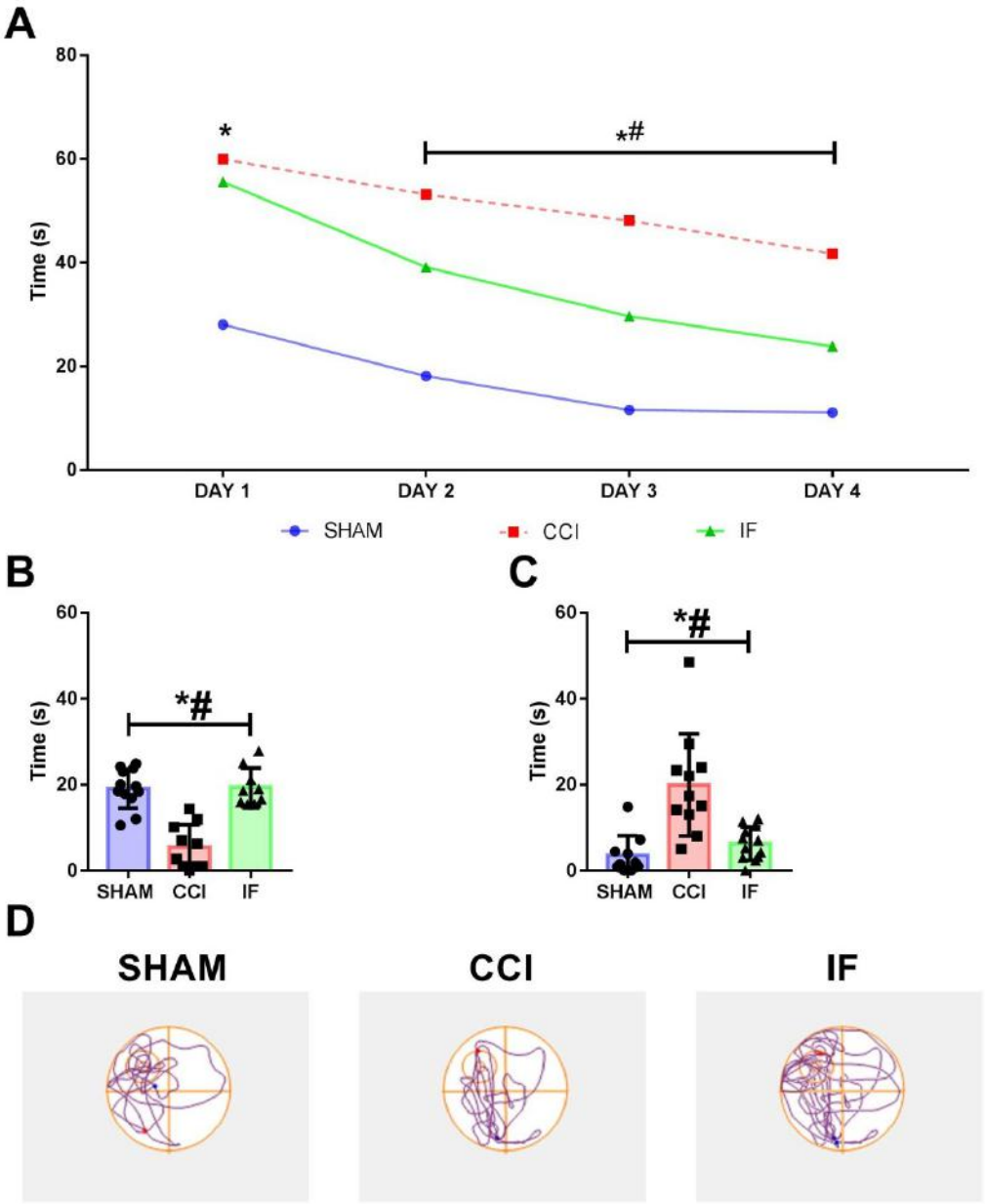


**Figure 05. Spatial memory parameters.** Animals of CCI groups presented impaired learning in the Morris Water Maze task compared to SHAM (A). Animals from CCI spent less time in the target quadrant (B) and showed increased latency to first entry in the target quadrant (C). Impaired learning and retrieval 5 d following CCI was prevented by IF. Representative video tracking from each group (D) shows the path of animals in the test phase of MWM **(***n* = 8-10).

*# Significant difference of CCI and IF compared to SHAM;

*# Significant difference comparing CCI to both SHAM and IF groups.

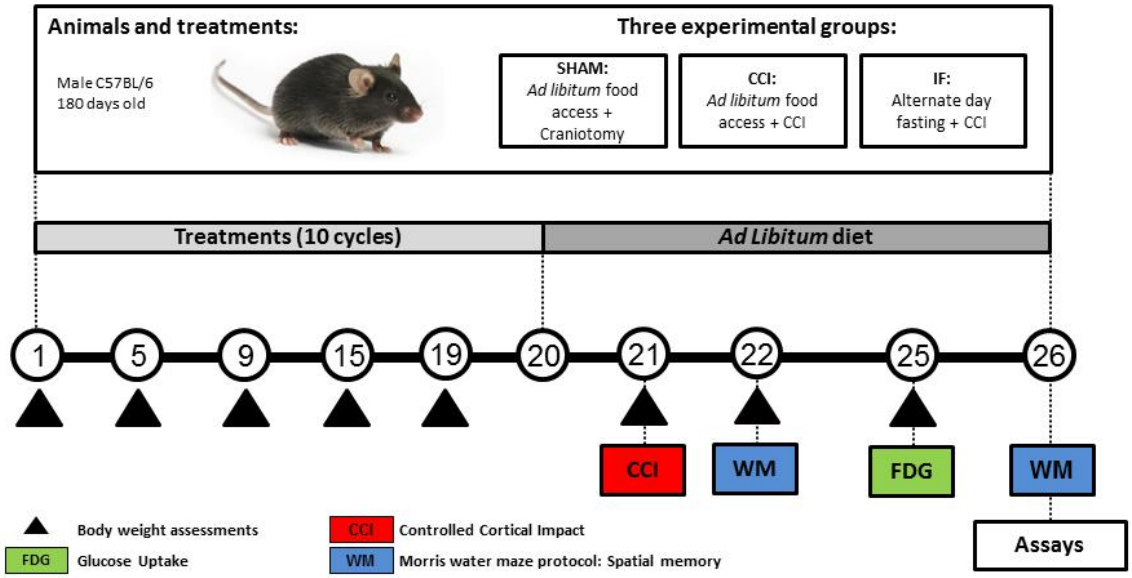


**Supplemental Figure 01.** Study design and protocols. CCI: controlled cortical impact; WMT: Morris Water Maze training; FDG: FDG-PET glucose uptake; WMT: water maze training; WM: Morris Water Maze probe trial.

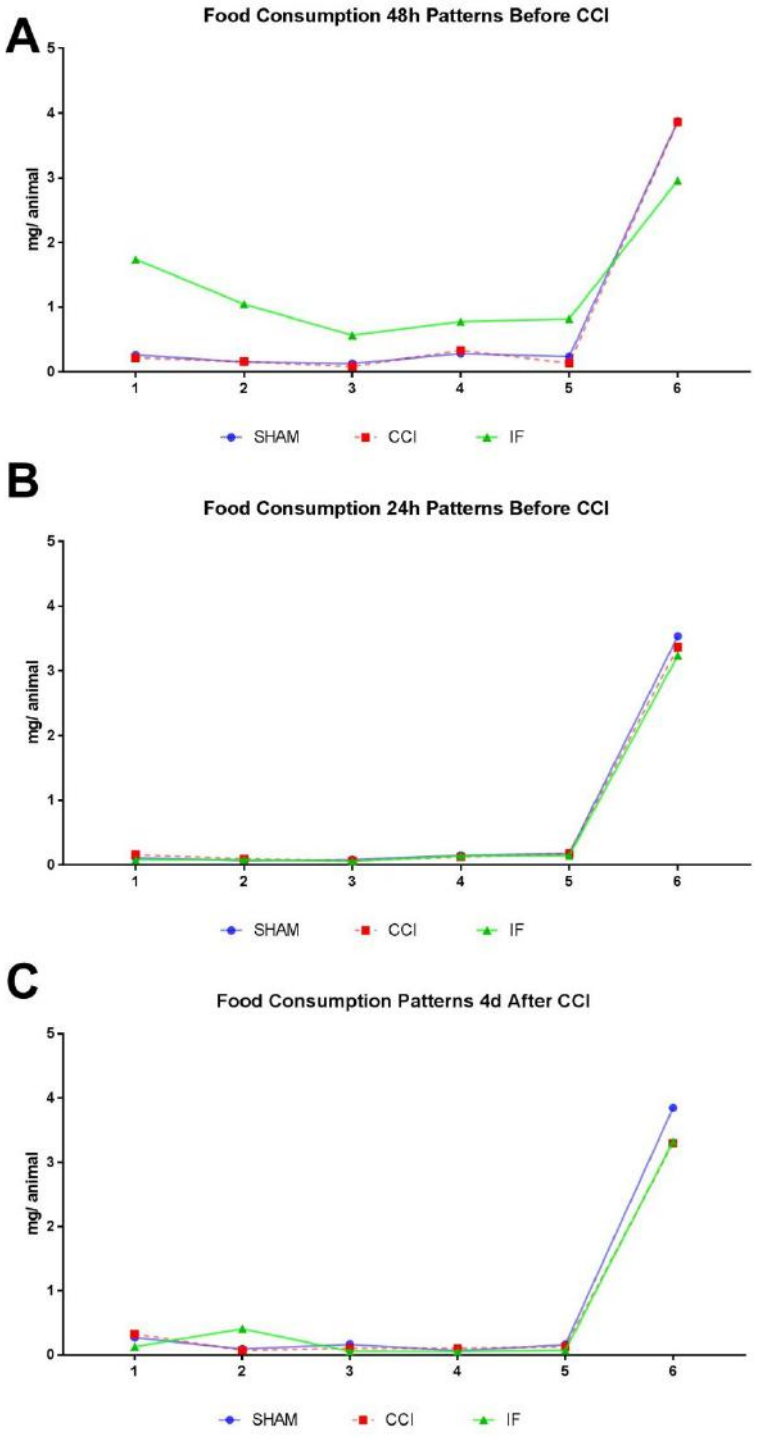


**Supplemental Figure 02.** Food consumption patterns measured in different time points (1 indicates 9 AM, and 6 indicates 7 PM). Mice from intermittent fasting (IF) group consumed significantly more food in the course of 48 h before CCI (A). Following *ad-libitum* dieting, 24 h before CCI (B) and 4 days after CCI (C) animals from all groups showed similar food consumption patterns. *# Denotes significant difference when compared to both SHAM and IF groups. Controlled cortical impact (CCI)

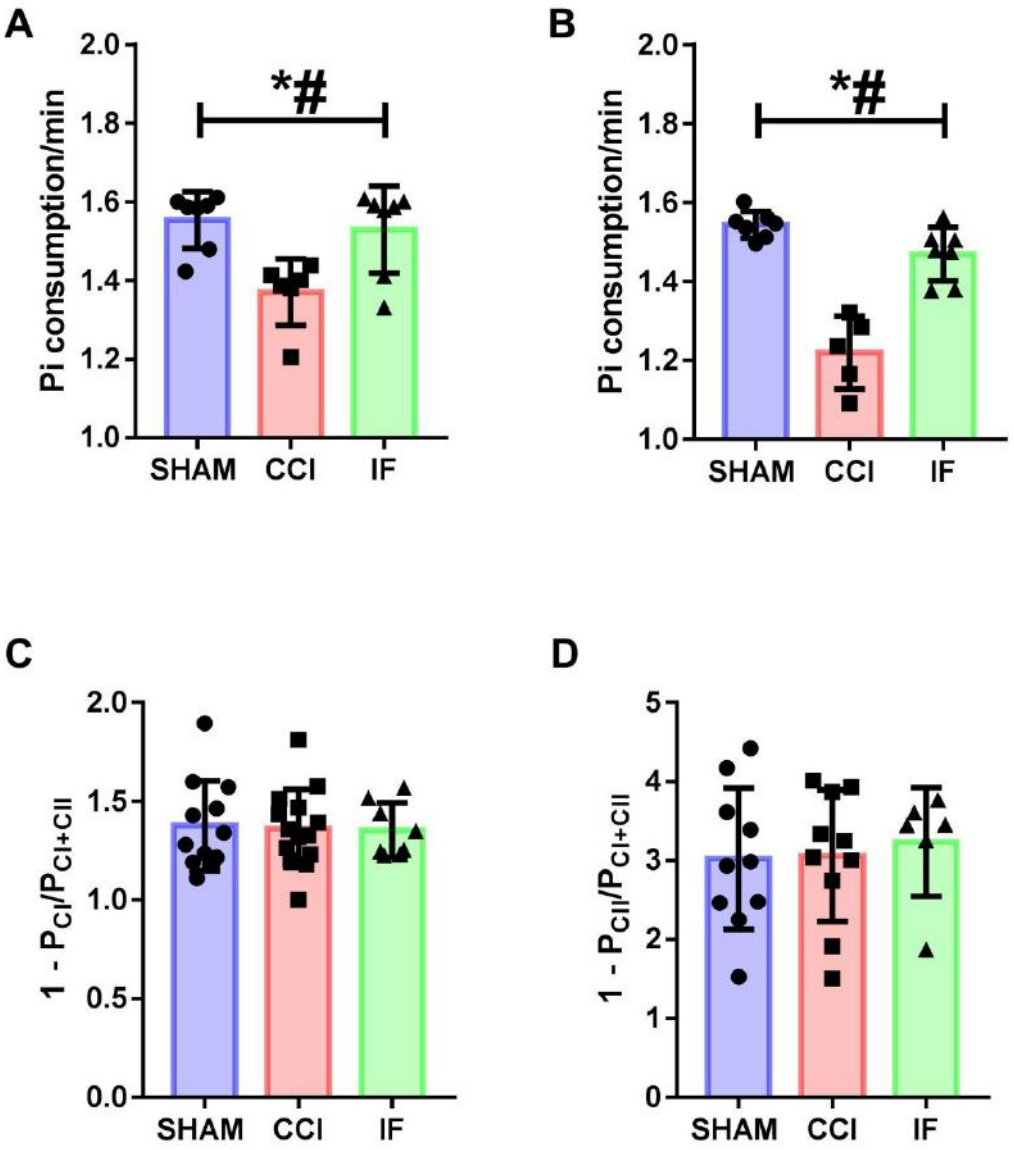


**Supplemental Figure 03.** Additional bioenergetics parameters, showing decreased Pi consumption in cortex (A) and hippocampi (B) homogenates; No significant differences observed in succinate (C) and rotenone (D) effects.

**Supplementary Table 01.** Standard uptake values (SUV) of FDG in the different regions of interest (ROI).

| **Tukey's multiple comparisons test** | **Mean Diff,** | **95,00% CI of diff,** | ***p* Value** |
|---|---|---|---|
| *Contralateral Striatum* | | | |
| CCI vs. SHAM * | -1,313 | -1,849 to -0,7772 | <0,0001 |
| IF vs. SHAM * | -0,6593 | -1,195 to -0,1235 | 0,0111 |
| IF vs. CCI * | 0,6537 | 0,118 to 1,189 | 0,0119 |
| *Ipsilateral Striatum* | | | |
| CCI vs. SHAM * | -1,172 | -1,708 to -0,6363 | <0,0001 |
| IF vs. SHAM | -0,5041 | -1,04 to 0,0316 | 0,0701 |
| IF vs. CCI* | 0,6679 | 0,1322 to 1,204 | 0,0099 |
| *Cortex* | | | |
| CCI vs. SHAM * | -0,8987 | -1,434 to -0,363 | 0,0003 |
| IF vs. SHAM | -0,5056 | -1,041 to 0,03019 | 0,0691 |
| IF vs. CCI | 0,3931 | -0,1426 to 0,9289 | 0,1969 |
| *Contralateral Hippocampus* | | | |
| CCI vs. SHAM * | -1,116 | -1,652 to -0,5805 | <0,0001 |
| IF vs. SHAM * | -0,5983 | -1,134 to -0,06256 | 0,0242 |
| IF vs. CCI | 0,5179 | -0,01785 to 1,054 | 0,0607 |
| *Ipsilateral Hippocampus* | | | |
| CCI vs. SHAM * | -1,136 | -1,672 to -0,6006 | <0,0001 |
| IF vs. SHAM * | -0,5599 | -1,096 to -0,02414 | 0,0381 |
| IF vs. CCI * | 0,5764 | 0,04067 to 1,112 | 0,0314 |
| *Thalamus* | | | |
| CCI vs. SHAM * | -1,321 | -1,856 to -0,7848 | <0,0001 |
| IF vs. SHAM * | -0,6677 | -1,203 to -0,132 | 0,0099 |
| IF vs. CCI * | 0,6528 | 0,1171 to 1,189 | 0,0121 |
| *Cerebellum* | | | |
| CCI vs. SHAM * | -0,8691 | -1,405 to -0,3333 | 0,0005 |
| IF vs. SHAM | -0,2994 | -0,8352 to 0,2363 | 0,3882 |
| IF vs. CCI * | 0,5696 | 0,0339 to 1,105 | 0,0340 |
| *Basal forebrain and septum* | | | |
| CCI vs. SHAM * | -0,8744 | -1,41 to -0,3386 | 0,0004 |
| IF vs. SHAM | -0,2658 | -0,8015 to 0,27 | 0,4741 |
| IF vs. CCI * | 0,6086 | 0,07284 to 1,144 | 0,0213 |
| *Hypothalamus* | | | |

| | | | |
|---|---|---|---|
| CCI vs. SHAM * | -0,9899 | -1,526 to -0,4542 | <0,0001 |
| IF vs. SHAM | -0,3228 | -0,8585 to 0,2129 | 0,3333 |
| IF vs. CCI * | 0,6672 | 0,1314 to 1,203 | 0,0100 |
| | | | |
| *Contralateral Amygdala* | | | |
| CCI vs. SHAM * | -0,8649 | -1,401 to -0,3292 | 0,0005 |
| IF vs. SHAM | -0,2478 | -0,7835 to 0,2879 | 0,5225 |
| IF vs. CCI * | 0,6171 | 0,08136 to 1,153 | 0,0192 |
| | | | |
| *Ipsilateral Amygdala* | | | |
| CCI vs. SHAM * | -0,7091 | -1,245 to -0,1733 | 0,0056 |
| IF vs. SHAM | -0,1772 | -0,7129 to 0,3586 | 0,7172 |
| IF vs. CCI | 0,5319 | -0,003836 to 1,068 | 0,0522 |
| | | | |
| *Brain stem* | | | |
| CCI vs. SHAM * | -1,062 | -1,598 to -0,5262 | <0,0001 |
| IF vs. SHAM | -0,2876 | -0,8234 to 0,2481 | 0,4175 |
| IF vs. CCI * | 0,7743 | 0,2386 to 1,31 | 0,0021 |
| | | | |
| *Superior colliculi* | | | |
| CCI vs. SHAM * | -1,35 | -1,886 to -0,8147 | <0,0001 |
| IF vs. SHAM * | -0,84 | -1,376 to -0,3043 | 0,0007 |
| IF vs. CCI | 0,5104 | -0,02535 to 1,046 | 0,0657 |
| | | | |
| *Olfactory bulb* | | | |
| CCI vs. SHAM * | -0,9205 | -1,456 to -0,3847 | 0,0002 |
| IF vs. SHAM | -0,4667 | -1,002 to 0,06902 | 0,1021 |
| IF vs. CCI | 0,4538 | -0,08199 to 0,9895 | 0,1155 |
| | | | |
| *Contralateral Midbrain* | | | |
| CCI vs. SHAM * | -1,462 | -1,998 to -0,9268 | <0,0001 |
| IF vs. SHAM * | -0,5909 | -1,127 to -0,05514 | 0,0265 |
| IF vs. CCI * | 0,8716 | 0,3359 to 1,407 | 0,0004 |
| | | | |
| *Ipsilateral Midbrain* | | | |
| CCI vs. SHAM | -1,405 | -1,94 to -0,8688 | <0,0001 |
| IF vs. SHAM | -0,5028 | -1,039 to 0,03295 | 0,0711 |
| IF vs. CCI | 0,9018 | 0,366 to 1,437 | 0,0003 |
| | | | |
| *Whole Brain* | | | |
| CCI vs. SHAM * | -1,128 | -1,664 to -0,5923 | <0,0001 |
| IF vs. SHAM | -0,4992 | -1,035 to 0,03651 | 0,0738 |
| IF vs. CCI * | 0,6288 | 0,0931 to 1,165 | 0,0165 |

* Denotes significant differences

# PARTE III

## Discussão

Nesta tese investigamos diferentes estratégias terapêuticas e profiláticas para tentar modular mecanismos secundários que levam a processos neurodegenerativos associados ao TCE, com ênfase na mitocôndria devido ao seu papel integrador na fisiologia celular que vai além do conceito de uma organela responsável pela síntese de ATP para as células. Mesmo que o papel da mitocôndria fosse restrito a fosforilação oxidativa, este aspecto funcional já justificaria o papel determinante destas organelas na sobrevivência e morte dos diferentes tipos celulares, particularmente os mais sensíveis a diminuição da síntese de ATP, como por exemplo, os neurônios. Através de abordagens experimentais, investigamos efeitos sistêmicos de altas doses de EAA, para avançar no entendimento de seus efeitos na atividade dos complexos respiratórios que, em conjunto com outros componentes da maquinaria mitocondrial, influenciam a bioenergética. Além disso, apresentamos um modelo animal que pode auxiliar em investigações de ETC resultantes do TCE associado ao esporte. O conjunto de evidências aqui apresentadas tem potencial translacional e de aplicação direta no TCE pois utilizamos fármacos previamente aprovados pelas agências reguladoras sanitárias dos EUA e Brasil, e estratégias comportamentais de baixo custo de aplicação.

Avaliamos inicialmente, se os EAA induzem alterações no metabolismo mitocondrial do coração e fígado após um tratamento de 19 dias. Essa duração foi escolhida pois trabalhos do nosso grupo evidenciaram aumento de agressividade associado a níveis elevados de glutamato extracelular no cérebro, sendo que o o glutamato poderia ter implicação em mecanismos neurodegenerativos (Kalinine *et al.*, 2014), embora esta última hipótese não foi testada testada nesta publicação prévia.

Em níveis fisiológicos, os EAA podem induzir melhorias no metabolismo energético (Pongkan *et al.*, 2015) devido a suas reconhecidas propriedades tróficas principalmente no tecido muscular esquelético. Entretanto, a administração de doses supra fisiológicas causa aumento na produção de espécies reativas de oxigênio juntamente com dano oxidativo, o que é, conceitualmente, sugestivo de disfunção mitocondrial no nível dos complexos oxidativos da cadeia de transporte de elétrons (Frankenfeld *et al.*, 2014). Vários estudos relatam desequilíbrio redox (aumento de espécies reativas e/ou diminuição das defesas antioxidantes) induzido pelo tratamento com AAS em diferentes órgãos, sugerindo padrões distintos de acordo com a característica da substância investigada. Nossos dados sugerem que, doses supra fisiológicas de NAND, e TS (em menor magnitude) podem comprometer a homeostase

mitocondrial de $Ca^{2+}$, a dinâmica do potencial de membrana mitocondrial e causar perturbações na homeostase redox no coração e fígado. Estes dois EAA são reconhecidamente os mais frequentemente utilizados para fins de estética ou desempenho físico. Também, utilizamos preliminarmente estes dois órgãos porque eles são os mais investigados, e os que apresentam maior magnitude de alterações morfológicas em estudos post-mortem com usuários crônicos de EAA, como atletas profissionais ou recreacionais. Como não detectamos danos histopatológicos evidentes causados pela NAND ou TS, concluímos que o comprometimento de metabolismo energético oxidativo e o desequilíbrio redox, ambos associados a função mitocondrial, precedem os danos estruturais a estes órgãos. Com esse estudo, além de reproduzir achados bioquímicos da literatura como a ruptura de homeostase redox em fígado e coração (Chaves *et al.*, 2006; Vasilaki *et al.*, 2016). Ainda, demonstramos pela primeira vez com o uso de respirometria de alta resolução alterações especificas nos estados respiratórios mitocondriais causados principalmente pela NAND e em menos extensão pela TS. De maneira geral podemos sugerir que a mitocôndria poderia predizer com mais sensibilidade modificações funcionais, pelo menos no fígado e coração. Com isso conseguimos atingir o primeiro objetivo específico proposto: *"(a) Avaliar efeitos periféricos de diferentes EAA no metabolismo mitocondrial"*.

Posteriormente, considerando que o objetivo principal era propor uma terapia para o TCE baseado na modulação da bioenergética mitocondrial por EAA, estendemos as investigações a diferentes populações mitocondriais no sistema nervoso central de camundongos. Para atingir nosso segundo objetivo *"(b) Avaliar efeitos cerebrais de diferentes EAA em populações mitocondriais específicas no sistema nervoso central"*, utilizamos preparações de sinaptossomas, um modelo clássico de isolamento de terminais nervosos, que fornecem um modelo preciso para testar a atividade mitocondrial mimetizando em uma sinapse funcional do cérebro (Nicholls, 2003). Digno de nota, mitocôndrias do sistema nervoso central apresentam características diferenciadas em relação à sua localização (sináptica ou extra-sináptica) que, dependendo dos estímulos, afetam suas funções (Stauch *et al.*, 2014). Aparentemente, mitocôndrias sinápticas exibem maior susceptibilidade ao dano oxidativo e maior vulnerabilidade ao influxo excessivo de cálcio em comparação com mitocôndrias extra sinápticas, o que poderia resultar em diferentes padrões de resposta às doses supra fisiológicas de EAA (Yarana *et al.*, 2012). Nosso estudo destacou que altas doses de NAND causam efeitos neurotóxicos afetando componentes da bioenergética mitocondrial sináptica e extra sináptica, como o influxo de cálcio, potencial de membrana e produção de

$H_2O_2$, uma espécie reativa com potencial neurotóxico. Além disso, a NAND também induziu aumento da fosforilação de proteína Tau no córtex, demonstrando uma maior vulnerabilidade desta área. Embora tenha afetado o influxo de cálcio e a dinâmica do potencial de membrana mitocondrial, a testosterona causou alterações neurometabólicas com menor magnitude sugerindo menor toxicidade, tal como foi demonstrado em coração e fígado. Ambos NAND ou TS não afetaram o desempenho no teste de memória utilizado (*Morris Water Maze*), embora também assumimos que as alterações mitocondriais descritas poderiam representar apenas um estágio inicial de neurotoxicidade induzida por abuso de EAA. Está bem estabelecido que o abuso de EAA pode induzir efeitos psiquiátricos indesejáveis, como alterações de humor, aumento de comportamentos agressivo, ansioso e depressivo, que podem estar mecanisticamente associados à captação prejudicada de glutamato e aumento da atividade do receptor N-metil-D-Aspartato (NMDAr) além de influxo exagerado de cálcio neuronal (Le Greves *et al.*, 1997; Kalinine *et al.*, 2014). O conjunto dos nosso resultados nos levou a uma nova questão: "*Se o prejuízo na bioenergética mitocondrial causado pela NAND, somadas ao aumento previamente descrito da agressividade via ligação do glutamato no receptor NMDA* (Kalinine *et al.*, 2014), *poderiam ser evitados pelo antagonismo do NMDAr?"*. Para obter a resposta, tratamos animais por 5 dias com doses suprafisiológicas (15 mg / kg) de NAND associado ou não com memantina (10 mg /kg) (Laboratório Teuto Brasileiro S.A, Goiás, Brasil), um fármaco bloqueador do canal iônico do receptor NMDA, e avaliamos a memória de reconhecimento, a liberação de glutamato além dos demais parâmetros bioenergéticos e de sinalização celular. Nesse trabalho, realizamos preparações de sinaptossomas de hipocampo, refinando uma técnica clássica da literatura (Sims e Anderson, 2008). Surpreendentemente, os animais apresentaram diminuição da memória de reconhecimento pela NAND, efeito prevenido com tratamento concomitante com memantina. Portanto, demonstramos um mecanismo diretamente alterado pela NAND via NMDA com influencia direta na memória de reconhecimento (este trabalho em sua forma preliminar está no ANEXO I desta tese).

No próximo objetivo proposto: " *(c) Avaliar o potencial terapêutico de EAA no detrimento metabólico após o TCE"* investimos no potencial terapêutico da TS uma vez que ela vem sendo amplamente proposta para estratégias de reposição hormonal para diminuir os impactos das mudanças fisiológicas associadas ao envelhecimento, incluindo a perda cognitiva (Hua *et al.*, 2016). Após o TCE os níveis de hormônios neuroesteroides, hipofisários e gonadais diminuem no cérebro e plasma, sendo correlacionados com

comprometimentos neurológicos (Tanriverdi *et al.*, 2006; Bavisetty *et al.*, 2008; Lopez-Rodriguez *et al.*, 2016; Tölli *et al.*, 2016) Assim, baseado em nosso conjunto inicial de resultados, que demonstrou menor toxidade, investigamos se a TS poderia atenuar o comprometimento neurometabólico decorrente de um TCE grave em camundongos (Baxter *et al.*, 2013). Como havíamos proposto, a TS promoveu benefícios neurometabólicos que podem ser determinantes para os desfechos clínicos neurológicos após o TCE. Evidenciamos que a suplementação de TS após um TCE severo preservou o manuseio mitocondrial de $Ca^{2+}$ e a capacidade de eficiência energética, prevenindo assim a progressão de diferentes vias apoptóticas associadas a neurodegeneração. Este trabalho destaca também, pela primeira vez na literatura a modulação da atividade do NCLX mitocondrial pela TS para a prevenção da neurodegeneração associada ao TCE. Por outro lado, fornecemos evidências funcionais e moleculares para sugerir a TS como uma droga candidata para combater a disfunção mitocondrial e deficiência energética, que são alterações secundarias proeminentes e determinantes de sobrevivência e morte após o TCE grave. Com o avanço no entendimento da modulação de mecanismos bioenergéticos com o tratamento com diferentes EAA e também as investigações da terapia com TS após o TCE puderam não somente expandir a o potencial anabólico e trófico desses fármacos, mas também propor uma perspectiva terapêutica para a testosterona, que já foi proposta recentemente para o tratamento de lesão na coluna espinhal (Gorgey *et al.*, 2017).

Conforme destacado anteriormente na introdução, uma importante lacuna nos estudos envolvendo o TCE é a falta de modelos pré-clinicos para avaliar as consequências de TCE repetido especificamente em atletas, considerando a alta incidência nessa população (Langlois *et al.*, 2006). Considerando os efeitos específicos do exercício físico no sistema nervoso central, é importante considerar esse fator em investigações visando elucidar mecanismos, entender suas interações e propor tratamentos para ETC resultante de concussão relacionada ao esporte. Assim, nosso próximo objetivo foi "*(d) Propor um modelo de TCE repetido em roedores para estudo da concussão relacionada ao esporte"*. Nosso modelo consiste em expor os animais de maneira irrestrita ao exercício físico voluntário, onde após 30 dias (onde os animais já apresentam capacidade física superior a animais sem exercício) iniciamos um protocolo de concussão (PC) simulando uma competição com um protocolo de exaustão em esteira ergométrica seguido imediatamente por um impacto cortical controlado, e 24 h para recuperação. Foram realizados três PC separados por 5 dias. Nosso modelo induziu aumento de fosforilação de proteína Tau e degradação de proteínas de citoesqueleto neuronal

comumente relacionadas com ETC após concussões em atletas (Smith, Douglas H. *et al.*, 2019). O PC também induziu prejuízo na função mitocondrial e dinâmica do potencial de membrana, juntamente com sobrecarga de $Ca^{2+}$ e aumento da produção de $H_2O_2$ além de induzir a reatividade de astrócitos. Além disso, investigamos como EAA combinados (TS+NAND), tal como comumente utilizados no âmbito esportivo (Simon *et al.*, 2018), influenciavam tais respostas. Surpreendentemente, a combinação de EAA utilizada resultou em atenuação do dano mitocondrial e no aumento de marcadores de neurodegeneração, sem benefício na astrogliose induzida pelo PC. Embora inicialmente se tenha descartado uma relação entre esteroides e o dano no TCE (Mills *et al.*, 2012) achados recentes indicam exacerbação de lesão axonal com a utilização de EAA combinados após TCE (Namjoshi *et al.*, 2016). Destacamos assim, que pudemos contribuir para esse tópico de estudo, considerando de extrema relevância a continuidade desse trabalho, visando aprimorar o modelo proposto e também elucidar as relações crônicas de EAA com o dano induzido por TCE e o desenvolvimento de ETC. Nosso modelo é um importante passo para estudar alterações resultantes do TCE repetitivo associado ao esporte. E também, geramos evidências de um possível pré-condicionamento induzido pela combinação de EAA no contexto do TCE associado ao exercício. Considerando as limitações de um modelo em fase precoce, abrimos uma possibilidade de estudos futuros para aprimorar o modelo e também investigar efeitos de pré-condicionamento neuronal associados ao uso de EAA.

O pré-condicionamento neuronal como estratégia profilática no TCE é um tema também abordado ao longo do desenvolvimento dessa tese. Considerando que o exercício é um importante indutor de pré-condicionamento cerebral no TCE (Chio *et al.*, 2017), definimos o próximo objetivo *"(e) Avaliar o potencial de pré-condicionamento pelo exercício físico no TCE grave e investigar a influência do "volume" de exercício na neuroenergética mitocondrial, sinalização apoptótica, sinalização neurotrófica e memória espacial".*

Um dos aspectos mais impactantes desta abordagem foi utilizar diferentes volumes de exercício. Como o volume é a variável mais importante da prescrição de exercício (Garber *et al.*, 2011), e comumente existe uma associação popular indicando que sempre "mais é melhor", nossos resultados são importantes referentes a efeitos benéficos no cérebro. Demonstramos que tanto o baixo quanto alto volume foram capazes de promover adaptações neuroenergéticas e moleculares tróficas que se opuseram aos afeitos do TCE severo. Surpreendentemente, esses efeitos se relacionaram com a manutenção da função cognitiva 30 dias após a lesão. Estes resultados fornecem insumos neurobiológicos para reforçar os

benefícios da atividade física regular para a saúde do cérebro. Levando em conta o caráter preventivo, é possível utilizar estas informações para educar e contribuir para a sociedade sobre a importância de proteger o cérebro através do pré-condicionamento neuronal. Em termos mecanísticos, reforçamos a importância do eixo CREB-BDNF nos efeitos de precondicionamento neuronal induzido pelo exercício e seu papel no TCE, associado também com alterações na função mitocondrial resultando nos desfechos cognitivos encontrados. Novamente, a modulação da função mitocondrial foi um fator envolvido na melhora dos desfechos associados com o TCE. Ainda, mostramos que tanto déficits bioenergéticos quanto cognitivos são mensuráveis até 30 dias após a lesão, indicando também que tanto baixo quanto alto volume de exercício induziram uma proteção de longo-prazo.

Além do exercício, estratégias nutricionais como o jejum intermitente (IF) podem induzir pré-condicionamento neuronal e influenciar os desfechos do TCE (Mattson *et al.*, 2018). Finalmente, nosso último objetivo foi *" (f) Avaliar o potencial de pré-condicionamento do jejum intermitente no TCE grave em desfechos neurometabólicos e cognitivos"*. O modelo utilizado de jejum intermitente exerceu um efeito profilático no TCE grave experimental: Observou-se modulação dos componentes da conectividade metabólica avaliada por FDG-PET e da função mitocondrial preservando a bioenergética cerebral, prevenindo a combinação de déficits neuroenergéticos e neurodegeneração apoptótica. Em uma análise qualitativa preliminar através de microscopia eletrônica, observamos também dano na estrutura sináptica e na estrutura mitocondrial. Notavelmente, o jejum intermitente evitou a disfunção mitocondrial induzida pelo TCE, sustentando a captação de glicose e conectividade metabólica, síntese de ATP mitocondrial, homeostase de $Ca^{2+}$ e potencial de membrana, juntamente com produção atenuada de $H_2O_2$, culminando em função cognitiva preservada. Em conjunto, esses achados elucidam os mecanismos subjacentes modulados pelo jejum intermitente, que podem contribuir para prevenir a lesão progressiva associada ao TCE. Esses resultados fornecem evidências funcionais e moleculares que fortalecem os efeitos benéficos atribuídos do jejum intermitente à saúde geral do cérebro, e seus benefícios profiláticos em injúrias cerebrais como o TCE. Ainda, considerando de forma conjunta os achados do capítulo V e capítulo VI, de modo que o exercício e a estratégia nutricional possibilitaram desfechos melhores após o TCE, sugerimos que a modulação de diferentes mecanismos que se relacionam entre si, explicam os resultados obtidos, conforme ilustrado na **figura 12**.

**Figura 12 – Diferentes mecanismos modulados por exercício físico e jejum intermitente resultam em melhores desfechos após o traumatismo cranioencefálico em roedores.**

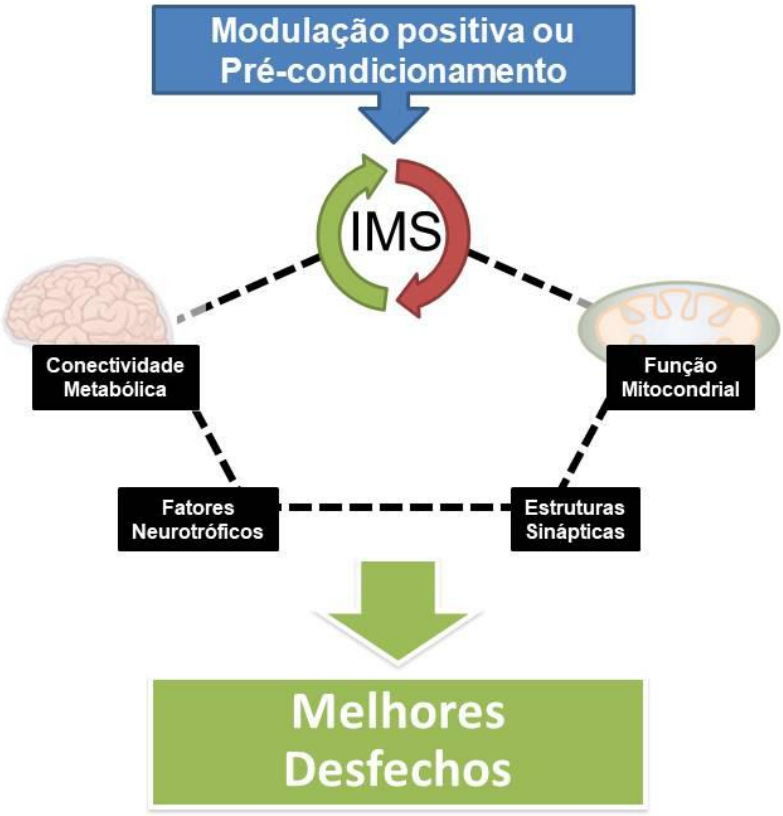


Com base nos achados expostos na presente tese e em mecanismos já descritos, sugerimos que diferentes mecanismos, como a conectividade metabólica cerebral, a função mitocondrial, a indução de fatores neurotróficos, a integralidade das estruturas sinápticas se relacionam entre si, e quando modulados positivamente por diferentes estratégias de pré-condicionamento, resultam em melhores desfechos. Fonte: Adaptado de (Roozenbeek *et al.*, 2013).

## Conclusão

Na presente tese, avançamos no entendimento da modulação bioenergética mitocondrial induzida por diferentes EAA em coração, fígado e cérebro. Além disso, sugerimos a testosterona como um fármaco com potencial adjuvante na farmacoterapia no TCE. Propusemos também um modelo para estudo de ETC associada com TCE no esporte, preenchendo uma importante lacuna na literatura relacionado a deficiência de um modelo que contemplasse o ambiente competitivo do esporte. Finalmente, demonstramos que a modulação do metabolismo mitocondrial por diferentes volumes de exercício voluntário e por jejum intermitente é capaz de promover efeito profilático no TCE severo, preservando componentes vitais para sobrevivência neuronal, como os componentes mitocondriais

envolvidos na bionergeetica. Além de avançar em termos de mecanismos fisiopatológicos, nosso conjunto de resultados têm alto potencial translacional e impacto direto tanto para estratégicas para promoção de saúde, como para compreensão de mecanismos para alvos terapêuticos. Esses resultados expandem a literatura e fornecem evidências funcionais e moleculares da importância da mitocôndria como alvo terapêutico e profilático no TCE grave. Concluímos que diferentes estratégias capazes de modulação do metabolismo mitocondrial têm impacto direto nos desfechos neurometabólicos, moleculares e comportamentais associados ao TCE. Assim, este estudo confirma o papel central da mitocôndria na fisiologia e em processos patológicos associados ao dano secundário do TCE e a sua importância como alvo terapêutico e de estratégias de precondicionamento.

## Referências


ALTMANN, R. **Die Elementarorganismen Und Ihre Beziehungen Zu Den Zellen**. Leipzig: Veit & comp., 1890. 145.

AMIGO, I. et al. Caloric restriction increases brain mitochondrial calcium retention capacity and protects against excitotoxicity. **Aging Cell,** v. 16, n. 1, p. 73-81, Feb 2017. ISSN 1474-9718.

ANSON, R. M. et al. Intermittent fasting dissociates beneficial effects of dietary restriction on glucose metabolism and neuronal resistance to injury from calorie intake. **Proc Natl Acad Sci U S A,** v. 100, n. 10, p. 6216-20, May 13 2003. ISSN 0027-8424 (Print)
0027-8424.

ARABI, Y. M. et al. Permissive underfeeding and intensive insulin therapy in critically ill patients: a randomized controlled trial. **Am J Clin Nutr,** v. 93, n. 3, p. 569-77, Mar 2011. ISSN 0002-9165.

BAVISETTY, S. et al. Chronic hypopituitarism after traumatic brain injury: risk assessment and relationship to outcome. **Neurosurgery,** v. 62, n. 5, p. 1080-93; discussion 1093-4, May 2008. ISSN 0148-396x.

BAXTER, D. et al. Pituitary Dysfunction after Blast Traumatic Brain Injury: The UK BIOSAP Study. **Annals of Neurology**, Oxford, UK**,** v. 74, n. 4, p. 527-536, 09/24
03/08/received
05/08/revised
05/24/accepted 2013. ISSN 0364-5134
1531-8249. Disponível em: < http://www.ncbi.nlm.nih.gov/pmc/articles/PMC4223931/ >.

BENDA, C. Weitere Mitteilungen über die Mitochondria. **Verh Dtsch Physiol Ges:**, p. 376-83, 1898.

BERGINK, E. W. et al. Comparison of the receptor binding properties of nandrolone and testosterone under in vitro and in vivo conditions. **J Steroid Biochem,** v. 22, n. 6, p. 831-6, Jun 1985. ISSN 0022-4731 (Print)
0022-4731.

BILOTTA, F.; ROSA, G. Glycemia management in critical care patients. **World J Diabetes,** v. 3, n. 7, p. 130-4, Jul 15 2012. ISSN 1948-9358.

BLENNOW, K.; HARDY, J.; ZETTERBERG, H. The neuropathology and neurobiology of traumatic brain injury. **Neuron,** v. 76, n. 5, p. 886-99, Dec 6 2012. ISSN 0896-6273.

BOLOURI, H.; ZETTERBERG, H. Frontiers in Neuroengineering
Animal Models for Concussion: Molecular and Cognitive Assessments-Relevance to Sport and Military Concussions. In: KOBEISSY, F. H. (Ed.). **Brain Neurotrauma: Molecular, Neuropsychological, and Rehabilitation Aspects**. Boca Raton (FL): CRC Press/Taylor & Francis
(c) 2015 by Taylor & Francis Group, LLC., 2015.

BOLTON HALL, A. N. et al. Repeated Closed Head Injury in Mice Results in Sustained Motor and Memory Deficits and Chronic Cellular Changes. **PLoS One,** v. 11, n. 7, p. e0159442, 2016. ISSN 1932-6203.

BONDANELLI, M. et al. Anterior pituitary function may predict functional and cognitive outcome in patients with traumatic brain injury undergoing rehabilitation. **J Neurotrauma,** v. 24, n. 11, p. 1687-97, Nov 2007. ISSN 0897-7151 (Print)
0897-7151.

BRAND, M. D.; NICHOLLS, D. G. Assessing mitochondrial dysfunction in cells. **Biochem J,** v. 435, n. 2, p. 297-312, Apr 15 2011. ISSN 0264-6021.

BRASURE, M. et al. AHRQ Comparative Effectiveness Reviews. In: (Ed.). **Multidisciplinary Postacute Rehabilitation for Moderate to Severe Traumatic Brain Injury in Adults**. Rockville (MD): Agency for Healthcare Research and Quality (US), 2012.

BROWN-BORG, H. M.; RAKOCZY, S. Metabolic adaptations to short-term every-other-day feeding in long-living Ames dwarf mice. **Experimental gerontology,** v. 48, n. 9, p. 10.1016/j.exger.2013.06.009, 07/04 2013. ISSN 0531-5565
1873-6815. Disponível em: < http://www.ncbi.nlm.nih.gov/pmc/articles/PMC3816083/ >.

BUSARDO, F. P. et al. The impact of nandrolone decanoate on the central nervous system. **Curr Neuropharmacol,** v. 13, n. 1, p. 122-31, Jan 2015. ISSN 1570-159X (Print)
1570-159x.

CADET, J. L.; KRASNOVA, I. N. Cellular and molecular neurobiology of brain preconditioning. **Molecular neurobiology,** v. 39, n. 1, p. 50-61, 2009. ISSN 0893-7648
1559-1182. Disponível em: < https://www.ncbi.nlm.nih.gov/pubmed/19153843

https://www.ncbi.nlm.nih.gov/pmc/PMC2677026/ >.

CALÌ, T.; OTTOLINI, D.; BRINI, M. Mitochondrial Ca(2+) and neurodegeneration. **Cell calcium,** v. 52, n. 1, p. 73-85, 2012. ISSN 1532-1991
0143-4160. Disponível em: < https://www.ncbi.nlm.nih.gov/pubmed/22608276
https://www.ncbi.nlm.nih.gov/pmc/PMC3396847/ >.

CAMANDOLA, S.; MATTSON, M. P. Brain metabolism in health, aging, and neurodegeneration. **Embo j,** v. 36, n. 11, p. 1474-1492, Jun 1 2017. ISSN 0261-4189.

CARTERI, R. Menopause Progression and Oxidative Stress: Associated Mechanisms and the Importance of Physical Exercise. In: CATALÁ, A. (Ed.). **Lipid Peroxidation: Inhibition, Effects and Mechanisms**. Hauppauge, NY, USA: Nova Science Publishers, Inc., 2016. cap. 15, ISBN 978-1-53610-506-3.

CHAVES, E. A. et al. Nandrolone decanoate impairs exercise-induced cardioprotection: role of antioxidant enzymes. **J Steroid Biochem Mol Biol,** v. 99, n. 4-5, p. 223-30, Jun 2006. ISSN 0960-0760 (Print)
0960-0760.

CHENG, G. et al. Mitochondria in traumatic brain injury and mitochondrial-targeted multipotential therapeutic strategies. **British journal of pharmacology,** v. 167, n. 4, p. 699-719, 2012. ISSN 1476-5381
0007-1188. Disponível em: < https://www.ncbi.nlm.nih.gov/pubmed/23003569
https://www.ncbi.nlm.nih.gov/pmc/PMC3575772/ >.

CHIO, C. C. et al. Exercise attenuates neurological deficits by stimulating a critical HSP70/NF-kappaB/IL-6/synapsin I axis in traumatic brain injury rats. v. 14, n. 1, p. 90, Apr 24 2017. ISSN 1742-2094.

CHISU, V. et al. Testosterone induces neuroprotection from oxidative stress. Effects on catalase activity and 3-nitro-L-tyrosine incorporation into alpha-tubulin in a mouse neuroblastoma cell line. **Arch Ital Biol,** v. 144, n. 2, p. 63-73, May 2006. ISSN 0003-9829 (Print)
0003-9829.

COGLIATI, S.; ENRIQUEZ, J. A.; SCORRANO, L. Mitochondrial Cristae: Where Beauty Meets Functionality. **Trends Biochem Sci,** v. 41, n. 3, p. 261-273, Mar 2016. ISSN 0968-0004 (Print)
0968-0004.

COGLIATI, S. et al. Mitochondrial cristae shape determines respiratory chain supercomplexes assembly and respiratory efficiency. **Cell,** v. 155, n. 1, p. 160-71, Sep 26 2013. ISSN 0092-8674.

CONNOLLY, N. M. C. et al. Guidelines on experimental methods to assess mitochondrial dysfunction in cellular models of neurodegenerative diseases. **Cell Death & Differentiation,**

v. 25, n. 3, p. 542-572, 2018/03/01 2018. ISSN 1476-5403. Disponível em: < https://doi.org/10.1038/s41418-017-0020-4 >.

CORNELIUS, C. et al. **Traumatic Brain Injury: Oxidative Stress and Neuroprotection**. 2013.

CORREIA, S. C. et al. Mitochondrial preconditioning: a potential neuroprotective strategy. **Frontiers in aging neuroscience,** v. 2, p. 138, 2010. ISSN 1663-4365. Disponível em: < https://www.ncbi.nlm.nih.gov/pubmed/20838473
https://www.ncbi.nlm.nih.gov/pmc/PMC2936931/ >.

CORREIA, S. C. et al. Mitochondria: the missing link between preconditioning and neuroprotection. **Journal of Alzheimer's disease : JAD,** v. 20 Suppl 2, n. Suppl 2, p. S475-S485, 2010. ISSN 1875-8908
1387-2877. Disponível em: < https://www.ncbi.nlm.nih.gov/pubmed/20463394
https://www.ncbi.nlm.nih.gov/pmc/PMC2923830/ >.

CYRAN, E. Hypophysenschadigung durch schadelbasisfraktur. **Dtsch. Med. Wochenschr.,** v. 44, p. 1261, 1918.

DASH, P. K. et al. Biomarkers for the diagnosis, prognosis, and evaluation of treatment efficacy for traumatic brain injury. **Neurotherapeutics,** v. 7, n. 1, p. 100-14, Jan 2010. ISSN 1878-7479 (Electronic)
1878-7479 (Linking). Disponível em: < http://www.ncbi.nlm.nih.gov/pubmed/20129502 >.

DAULATZAI, M. A. Cerebral hypoperfusion and glucose hypometabolism: Key pathophysiological modulators promote neurodegeneration, cognitive impairment, and Alzheimer's disease. **J Neurosci Res,** v. 95, n. 4, p. 943-972, Apr 2017. ISSN 0360-4012.

DAVIS, L. M. et al. Fasting is neuroprotective following traumatic brain injury. **J Neurosci Res,** v. 86, n. 8, p. 1812-22, Jun 2008. ISSN 0360-4012.

DAWSON, V. L.; DAWSON, T. M. Neuronal ischaemic preconditioning. **Trends Pharmacol Sci,** v. 21, n. 11, p. 423-4, Nov 2000. ISSN 0165-6147 (Print)
0165-6147.

DEMETRIADOU, A.; DROUSIOTOU, A.; PETROU, P. P. The “sweet” side of ER-mitochondria contact sites. **Communicative & Integrative Biology,** v. 10, n. 4, p. e1329787, 2017. ISSN 1942-0889. Disponível em: < https://www.ncbi.nlm.nih.gov/pmc/articles/PMC5595418/
https://www.ncbi.nlm.nih.gov/pmc/PMC5595418/ >.

DESCAMPS, O. et al. Mitochondrial production of reactive oxygen species and incidence of age-associated lymphoma in OF1 mice: effect of alternate-day fasting. **Mech Ageing Dev,** v. 126, n. 11, p. 1185-91, Nov 2005. ISSN 0047-6374 (Print)
0047-6374 (Linking). Disponível em: < http://www.ncbi.nlm.nih.gov/pubmed/16126250 >.

DIAZ-ARRASTIA, R. et al. Pharmacotherapy of traumatic brain injury: state of the science and the road forward: report of the Department of Defense Neurotrauma Pharmacology Workgroup. **Journal of neurotrauma,** v. 31, n. 2, p. 135-158, 2014. ISSN 1557-9042
0897-7151. Disponível em: < https://www.ncbi.nlm.nih.gov/pubmed/23968241 https://www.ncbi.nlm.nih.gov/pmc/PMC3900003/ >.

ELGASS, K. et al. Recent advances into the understanding of mitochondrial fission. **Biochimica et Biophysica Acta (BBA) - Molecular Cell Research,** v. 1833, n. 1, p. 150-161, 2013/01/01/ 2013. ISSN 0167-4889. Disponível em: < http://www.sciencedirect.com/science/article/pii/S0167488912001097 >.

ESCOBAR-HENRIQUES, M.; ANTON, F. Mechanistic perspective of mitochondrial fusion: Tubulation vs. fragmentation. **Biochimica et Biophysica Acta (BBA) - Molecular Cell Research,** v. 1833, n. 1, p. 162-175, 2013/01/01/ 2013. ISSN 0167-4889. Disponível em: < http://www.sciencedirect.com/science/article/pii/S0167488912002248 >.

FANAEI, H. et al. Testosterone enhances functional recovery after stroke through promotion of antioxidant defenses, BDNF levels and neurogenesis in male rats. **Brain Res,** v. 1558, p. 74-83, Apr 16 2014. ISSN 0006-8993.

FISHER-WELLMAN, K. H. et al. Mitochondrial Diagnostics: A Multiplexed Assay Platform for Comprehensive Assessment of Mitochondrial Energy Fluxes. **Cell Reports,** v. 24, n. 13, p. 3593-3606.e10, 2018/09/25/ 2018. ISSN 2211-1247. Disponível em: < http://www.sciencedirect.com/science/article/pii/S2211124718314104 >.

FRANKENFELD, S. P. et al. The Anabolic Androgenic Steroid Nandrolone Decanoate Disrupts Redox Homeostasis in Liver, Heart and Kidney of Male Wistar Rats. **PLOS ONE,** v. 9, n. 9, p. e102699, 2014. Disponível em: < https://doi.org/10.1371/journal.pone.0102699 >.

FRANKENFIELD, D.; SMITH, J. S.; COONEY, R. N. Validation of 2 approaches to predicting resting metabolic rate in critically ill patients. **JPEN J Parenter Enteral Nutr,** v. 28, n. 4, p. 259-64, Jul-Aug 2004. ISSN 0148-6071 (Print)
0148-6071.

FREY, T. G.; MANNELLA, C. A. The internal structure of mitochondria. **Trends Biochem Sci,** v. 25, n. 7, p. 319-24, Jul 2000. ISSN 0968-0004 (Print)
0968-0004.

FUKUJIMA, M. M. O Traumatismo Cranioencefálico na Vida do Brasileiro. doi:10.4181/RNC.2013.21.855ed.2p (2013). **Rev Neurocienc,** v. 21, n. 2, p. 173-174, 2013.

GAJAVELLI, S. et al. Evidence to support mitochondrial neuroprotection, in severe traumatic brain injury. **Journal of Bioenergetics and Biomembranes,** v. 47, n. 1, p. 133-148, 2015/04/01 2015. ISSN 1573-6881. Disponível em: < https://doi.org/10.1007/s10863-014-9589-1 >.

GARBER, C. E. et al. American College of Sports Medicine position stand. Quantity and quality of exercise for developing and maintaining cardiorespiratory, musculoskeletal, and neuromotor fitness in apparently healthy adults: guidance for prescribing exercise. **Med Sci Sports Exerc,** v. 43, n. 7, p. 1334-59, Jul 2011. ISSN 0195-9131.

GEYER, H.; SCHÄNZER, W.; THEVIS, M. Anabolic agents: recent strategies for their detection and protection from inadvertent doping. **British Journal of Sports Medicine**, BMA House, Tavistock Square, London, WC1H 9JR**,** v. 48, n. 10, p. 820-826, 03/14
02/20/accepted 2014. ISSN 0306-3674
1473-0480. Disponível em: < http://www.ncbi.nlm.nih.gov/pmc/articles/PMC4033149/ >.

GIAGULLI, V. A. et al. Serum Testosterone and Cognitive Function in Ageing Male: Updating the Evidence. **Recent Pat Endocr Metab Immune Drug Discov,** v. 10, n. 1, p. 22-30, 2016. ISSN 1872-2148.

GILMER, L. K. et al. Early mitochondrial dysfunction after cortical contusion injury. **Journal of neurotrauma,** v. 26, n. 8, p. 1271-1280, 2009. ISSN 1557-9042
0897-7151. Disponível em: < https://www.ncbi.nlm.nih.gov/pubmed/19637966
https://www.ncbi.nlm.nih.gov/pmc/PMC2850255/ >.

GLANCY, B.; BALABAN, R. S. Role of Mitochondrial Ca2+ in the Regulation of Cellular Energetics. **Biochemistry,** v. 51, n. 14, p. 2959-2973, 2012/04/10 2012. ISSN 0006-2960. Disponível em: < https://doi.org/10.1021/bi2018909 >.

GOODRICK, C. L. et al. Effects of intermittent feeding upon body weight and lifespan in inbred mice: interaction of genotype and age. **Mech Ageing Dev,** v. 55, n. 1, p. 69-87, Jul 1990. ISSN 0047-6374 (Print)
0047-6374.

GORGEY, A. S. et al. Effects of Testosterone and Evoked Resistance Exercise after Spinal Cord Injury (TEREX-SCI): study protocol for a randomised controlled trial. **BMJ open,** v. 7, n. 4, p. e014125-e014125, 2017. ISSN 2044-6055. Disponível em: < https://www.ncbi.nlm.nih.gov/pubmed/28377392
https://www.ncbi.nlm.nih.gov/pmc/PMC5387951/ >.

GOURAS, G. K. et al. Testosterone reduces neuronal secretion of Alzheimer's beta-amyloid peptides. **Proc Natl Acad Sci U S A,** v. 97, n. 3, p. 1202-5, Feb 01 2000. ISSN 0027-8424 (Print)
0027-8424.

GURER, B. et al. Neuroprotective effects of testosterone on ischemia/reperfusion injury of the rabbit spinal cord. **Injury,** v. 46, n. 2, p. 240-8, Feb 2015. ISSN 0020-1383.

HALLIWELL, B. Oxidative stress and neurodegeneration: where are we now? **Journal of Neurochemistry,** v. 97, n. 6, p. 1634-1658, 2006/06/01 2006. ISSN 0022-3042. Disponível em: < https://doi.org/10.1111/j.1471-4159.2006.03907.x >. Acesso em: 2019/02/04.

HANTEN, G. et al. Updating memory after mild traumatic brain injury and orthopedic injuries. **J Neurotrauma,** v. 30, n. 8, p. 618-24, Apr 15 2013. ISSN 0897-7151.

HARTL, R. et al. Effect of early nutrition on deaths due to severe traumatic brain injury. **J Neurosurg,** v. 109, n. 1, p. 50-6, Jul 2008. ISSN 0022-3085 (Print)
0022-3085.

HATANAKA, Y. et al. Rapid increase of spines by dihydrotestosterone and testosterone in hippocampal neurons: Dependence on synaptic androgen receptor and kinase networks. **Brain Res,** v. 1621, p. 121-32, Sep 24 2015. ISSN 0006-8993.

HEMPHILL, M. A. et al. Traumatic brain injury and the neuronal microenvironment: a potential role for neuropathological mechanotransduction. **Neuron,** v. 85, n. 6, p. 1177-92, Mar 18 2015. ISSN 1097-4199 (Electronic)
0896-6273 (Linking). Disponível em: < http://www.ncbi.nlm.nih.gov/pubmed/25789754 >.

HIEBERT, J. B. et al. Traumatic brain injury and mitochondrial dysfunction. **Am J Med Sci,** v. 350, n. 2, p. 132-8, Aug 2015. ISSN 0002-9629.

HIOKI, T. et al. Brain testosterone deficiency leads to down-regulation of mitochondrial gene expression in rat hippocampus accompanied by a decline in peroxisome proliferator-activated receptor-gamma coactivator 1alpha expression. **J Mol Neurosci,** v. 52, n. 4, p. 531-7, Apr 2014. ISSN 0895-8696.

HORWITZ, B.; DUARA, R.; RAPOPORT, S. I. Intercorrelations of glucose metabolic rates between brain regions: application to healthy males in a state of reduced sensory input. **J Cereb Blood Flow Metab,** v. 4, n. 4, p. 484-99, Dec 1984. ISSN 0271-678X (Print)
0271-678x.

HUA, J. T.; HILDRETH, K. L.; PELAK, V. S. Effects of Testosterone Therapy on Cognitive Function in Aging: A Systematic Review. **Cognitive and behavioral neurology : official journal of the Society for Behavioral and Cognitive Neurology,** v. 29, n. 3, p. 122-138, 2016. ISSN 1543-3641
1543-3633. Disponível em: < https://www.ncbi.nlm.nih.gov/pubmed/27662450
https://www.ncbi.nlm.nih.gov/pmc/PMC5079177/ >.

HYDER, F.; ROTHMAN, D. L.; BENNETT, M. R. Cortical energy demands of signaling and nonsignaling components in brain are conserved across mammalian species and activity levels. **Proc Natl Acad Sci U S A,** v. 110, n. 9, p. 3549-54, Feb 26 2013. ISSN 0027-8424.

ISHIHARA, N. et al. Regulation of mitochondrial morphology by membrane potential, and DRP1-dependent division and FZO1-dependent fusion reaction in mammalian cells. **Biochem Biophys Res Commun,** v. 301, n. 4, p. 891-8, Feb 21 2003. ISSN 0006-291X (Print)
0006-291x.

JAFRI, M. S.; KUMAR, R. Modeling Mitochondrial Function and Its Role in Disease. **Progress in molecular biology and translational science,** v. 123, p. 103-125, 2014. ISSN 1877-1173

1878-0814. Disponível em: < http://www.ncbi.nlm.nih.gov/pmc/articles/PMC4219577/ >.

JANOFF, A. ALTERATIONS IN LYSOSOMES (INTRACELLULAR ENZYMES) DURING SHOCK; EFFECTS OF PRECONDITIONING (TOLERANCE) AND PROTECTIVE DRUGS. **Int Anesthesiol Clin,** v. 2, p. 251-69, Feb 1964. ISSN 0020-5907 (Print)
0020-5907.

JENSEN, G. L. et al. Adult starvation and disease-related malnutrition: a proposal for etiology-based diagnosis in the clinical practice setting from the International Consensus Guideline Committee. **JPEN J Parenter Enteral Nutr,** v. 34, n. 2, p. 156-9, Mar-Apr 2010. ISSN 0148-6071.

JI, J. et al. Mitochondrial injury after mechanical stretch of cortical neurons in vitro: biomarkers of apoptosis and selective peroxidation of anionic phospholipids. **J Neurotrauma,** v. 29, n. 5, p. 776-88, Mar 20 2012. ISSN 0897-7151.

JOHNSON, V. E.; STEWART, W. Traumatic brain injury: age at injury influences dementia risk after TBI. **Nat Rev Neurol,** v. 11, n. 3, p. 128-30, Mar 2015. ISSN 1759-4766 (Electronic)
1759-4758 (Linking). Disponível em: < http://www.ncbi.nlm.nih.gov/pubmed/25534914 >.

JOHNSON, V. E. et al. SNTF immunostaining reveals previously undetected axonal pathology in traumatic brain injury. **Acta Neuropathol,** v. 131, n. 1, p. 115-35, Jan 2016. ISSN 0001-6322.

JOHNSON, V. E. et al. Mechanical disruption of the blood–brain barrier following experimental concussion. **Acta Neuropathologica,** v. 135, n. 5, p. 711-726, 2018/05/01 2018. ISSN 1432-0533. Disponível em: < https://doi.org/10.1007/s00401-018-1824-0 >.

KALININE, E. et al. Nandrolone-induced aggressive behavior is associated with alterations in extracellular glutamate homeostasis in mice. **Horm Behav,** v. 66, n. 2, p. 383-92, Jul 2014. ISSN 0018-506x.

KANG, L. et al. Dihydrotestosterone treatment delays the conversion from mild cognitive impairment to Alzheimer's disease in SAMP8 mice. **Horm Behav,** v. 65, n. 5, p. 505-15, May 2014. ISSN 1095-6867 (Electronic)
0018-506X (Linking). Disponível em: < http://www.ncbi.nlm.nih.gov/pubmed/24717850 >.

KHACHO, M.; HARRIS, R.; SLACK, R. S. Mitochondria as central regulators of neural stem cell fate and cognitive function. **Nature Reviews Neuroscience,** v. 20, n. 1, p. 34-48, 2019/01/01 2019. ISSN 1471-0048. Disponível em: < https://doi.org/10.1038/s41583-018-0091-3 >.

KICMAN, A. T. Pharmacology of anabolic steroids. **Br J Pharmacol,** v. 154, n. 3, p. 502-21, Jun 2008. ISSN 0007-1188 (Print)
0007-1188.

KLOSE, M.; FELDT-RASMUSSEN, U. Hypopituitarism in Traumatic Brain Injury-A Critical Note. **Journal of clinical medicine,** v. 4, n. 7, p. 1480-1497, 2015. ISSN 2077-0383. Disponível em: < https://www.ncbi.nlm.nih.gov/pubmed/26239687 https://www.ncbi.nlm.nih.gov/pmc/PMC4519801/ >.

KÜHLBRANDT, W. Structure and function of mitochondrial membrane protein complexes. **BMC biology,** v. 13, p. 89-89, 2015. ISSN 1741-7007. Disponível em: < https://www.ncbi.nlm.nih.gov/pubmed/26515107 https://www.ncbi.nlm.nih.gov/pmc/PMC4625866/ >.

KULBE, J. R.; HALL, E. D. Chronic traumatic encephalopathy-integration of canonical traumatic brain injury secondary injury mechanisms with tau pathology. **Prog Neurobiol,** v. 158, p. 15-44, Nov 2017. ISSN 0301-0082.

LANGLOIS, J. A.; RUTLAND-BROWN, W.; WALD, M. M. The epidemiology and impact of traumatic brain injury: a brief overview. **J Head Trauma Rehabil,** v. 21, n. 5, p. 375-8, Sep-Oct 2006. ISSN 0885-9701 (Print)
0885-9701.

LE GREVES, P. et al. Effects of an anabolic-androgenic steroid on the regulation of the NMDA receptor NR1, NR2A and NR2B subunit mRNAs in brain regions of the male rat. **Neurosci Lett,** v. 226, n. 1, p. 61-4, Apr 18 1997. ISSN 0304-3940 (Print)
0304-3940 (Linking). Disponível em: < http://www.ncbi.nlm.nih.gov/pubmed/9153642 >.

LEVIN, H. S.; DIAZ-ARRASTIA, R. R. Diagnosis, prognosis, and clinical management of mild traumatic brain injury. **Lancet Neurol,** v. 14, n. 5, p. 506-17, May 2015. ISSN 1474-4422.

LÓPEZ-LLUCH, G. et al. Calorie restriction induces mitochondrial biogenesis and bioenergetic efficiency. **Proceedings of the National Academy of Sciences of the United States of America,** v. 103, n. 6, p. 1768, 2006. Disponível em: < http://www.pnas.org/content/103/6/1768.abstract >.

LOPEZ-RODRIGUEZ, A. B. et al. Profiling Neuroactive Steroid Levels After Traumatic Brain Injury in Male Mice. **Endocrinology,** v. 157, n. 10, p. 3983-3993, Oct 2016. ISSN 0013-7227.

MA, F.; LIU, D. 17beta-trenbolone, an anabolic-androgenic steroid as well as an environmental hormone, contributes to neurodegeneration. **Toxicol Appl Pharmacol,** v. 282, n. 1, p. 68-76, Jan 1 2015. ISSN 0041-008x.

MAGISTRETTI, P. J. Neuron-glia metabolic coupling and plasticity. **J Exp Biol,** v. 209, n. Pt 12, p. 2304-11, Jun 2006. ISSN 0022-0949 (Print)
0022-0949.

MATTSON, M. P. Calcium and neurodegeneration. **Aging Cell,** v. 6, n. 3, p. 337-350, 2007/06/01 2007. ISSN 1474-9718. Disponível em: < https://doi.org/10.1111/j.1474-9726.2007.00275.x >. Acesso em: 2019/02/04.

MATTSON, M. P. et al. Intermittent metabolic switching, neuroplasticity and brain health. **Nat Rev Neurosci,** v. 19, n. 2, p. 63-80, Feb 2018. ISSN 1471-003x.

MCEVOY, C. T. et al. Resting energy expenditure in non-ventilated, non-sedated patients recovering from serious traumatic brain injury: comparison of prediction equations with indirect calorimetry values. **Clin Nutr,** v. 28, n. 5, p. 526-32, Oct 2009. ISSN 0261-5614.

MEANEY, D. F.; MORRISON, B.; DALE BASS, C. The mechanics of traumatic brain injury: a review of what we know and what we need to know for reducing its societal burden. **J Biomech Eng,** v. 136, n. 2, p. 021008, Feb 2014. ISSN 1528-8951 (Electronic)
0148-0731 (Linking). Disponível em: < http://www.ncbi.nlm.nih.gov/pubmed/24384610 >.

MEIER, R. et al. Differential temporal profile of lowered blood glucose levels (3.5 to 6.5 mmol/l versus 5 to 8 mmol/l) in patients with severe traumatic brain injury. **Crit Care,** v. 12, n. 4, p. R98, 2008. ISSN 1364-8535.

MENG, Q. et al. Traumatic Brain Injury Induces Genome-Wide Transcriptomic, Methylomic, and Network Perturbations in Brain and Blood Predicting Neurological Disorders. **EBioMedicine,** v. 16, p. 184-194, Feb 2017. ISSN 2352-3964.

MEZ, J. et al. Clinicopathological Evaluation of Chronic Traumatic Encephalopathy in Players of American FootballEvaluation of Chronic Traumatic Encephalopathy in Football PlayersEvaluation of Chronic Traumatic Encephalopathy in Football Players. **JAMA,** v. 318, n. 4, p. 360-370, 2017. ISSN 0098-7484. Disponível em: < https://dx.doi.org/10.1001/jama.2017.8334 >. Acesso em: 2/21/2019.

MILLS, J. D. et al. Anabolic steroids and head injury. **Neurosurgery,** v. 70, n. 1, p. 205-9; discussion 209-10, Jan 2012. ISSN 0148-396x.

MOTA, B. C. et al. Exercise pre-conditioning reduces brain inflammation and protects against toxicity induced by traumatic brain injury: behavioral and neurochemical approach. **Neurotox Res,** v. 21, n. 2, p. 175-84, Feb 2012. ISSN 1029-8428.

MÜLLER, J.; HENLE, J. **Systematische Beschreibung der Plagiostomen**. Berlin :: Veit, 1841. Disponível em: < https://www.biodiversitylibrary.org/item/30065 >.

MÜLLER, M. et al. Constitutive cAMP response element binding protein (CREB) activation by Alzheimer's disease presenilin-driven inositol trisphosphate receptor (InsP<sub>3</sub>R) Ca<sup>2+</sup> signaling. **Proceedings of the National Academy of Sciences,** v. 108, n. 32, p. 13293, 2011. Disponível em: < http://www.pnas.org/content/108/32/13293.abstract >.

NAKASHIMA, T. et al. Focal brain glucose hypometabolism in patients with neuropsychologic deficits after diffuse axonal injury. **AJNR Am J Neuroradiol,** v. 28, n. 2, p. 236-42, Feb 2007. ISSN 0195-6108 (Print)
0195-6108.

NAMJOSHI, D. R. et al. Chronic Exposure to Androgenic-Anabolic Steroids Exacerbates Axonal Injury and Microgliosis in the CHIMERA Mouse Model of Repetitive Concussion. **PLoS One,** v. 11, n. 1, p. e0146540, 2016. ISSN 1932-6203.

NICHOLLS, D. G. Bioenergetics and transmitter release in the isolated nerve terminal. **Neurochem Res,** v. 28, n. 10, p. 1433-41, Oct 2003. ISSN 0364-3190 (Print)
0364-3190.

NOVAES GOMES, F. G. et al. The beneficial effects of strength exercise on hippocampal cell proliferation and apoptotic signaling is impaired by anabolic androgenic steroids. **Psychoneuroendocrinology,** v. 50, p. 106-17, Dec 2014. ISSN 1873-3360 (Electronic)
0306-4530 (Linking). Disponível em: < http://www.ncbi.nlm.nih.gov/pubmed/25202830 >.

OBERLANDER, J. G.; HENDERSON, L. P. The Sturm und Drang of anabolic steroid use: angst, anxiety, and aggression. **Trends Neurosci,** v. 35, n. 6, p. 382-92, Jun 2012. ISSN 0166-2236.

ORTEGA-MARTÍNEZ, S. A new perspective on the role of the CREB family of transcription factors in memory consolidation via adult hippocampal neurogenesis. **Frontiers in Molecular Neuroscience,** v. 8, n. 46, 2015-August-26 2015. ISSN 1662-5099. Disponível em: < https://www.frontiersin.org/article/10.3389/fnmol.2015.00046 >.

PANDYA, J. D.; NUKALA, V. N.; SULLIVAN, P. G. Concentration dependent effect of calcium on brain mitochondrial bioenergetics and oxidative stress parameters. **Front Neuroenergetics,** v. 5, p. 10, 2013. ISSN 1662-6427 (Print)
1662-6427.

PANI, G. Neuroprotective effects of dietary restriction: Evidence and mechanisms. **Seminars in Cell & Developmental Biology,** v. 40, p. 106-114, 2015/04/01/ 2015. ISSN 1084-9521. Disponível em: < http://www.sciencedirect.com/science/article/pii/S1084952115000476 >.

PANTZIARKA, P.; PIRMOHAMED, M.; MIRZA, N. New uses for old drugs. **BMJ,** v. 361, p. k2701, 2018. Disponível em: < http://www.bmj.com/content/361/bmj.k2701.abstract >.

PEREL, P. et al. Nutritional support for head-injured patients. **Cochrane Database Syst Rev**, n. 4, p. Cd001530, Oct 18 2006. ISSN 1361-6137.

PFANNER, N.; WARSCHEID, B.; WIEDEMANN, N. Mitochondrial proteins: from biogenesis to functional networks. **Nature Reviews Molecular Cell Biology**, 2019/01/09 2019. ISSN 1471-0080. Disponível em: < https://doi.org/10.1038/s41580-018-0092-0 >.

PHELPS, M. E. et al. Tomographic measurement of local cerebral glucose metabolic rate in humans with (F-18)2-fluoro-2-deoxy-D-glucose: validation of method. **Ann Neurol,** v. 6, n. 5, p. 371-88, Nov 1979. ISSN 0364-5134 (Print)
0364-5134.

PICARD, M. et al. Trans-mitochondrial coordination of cristae at regulated membrane junctions. **Nature Communications,** v. 6, p. 6259, 02/17/online 2015. Disponível em: < https://doi.org/10.1038/ncomms7259 >.

PONGKAN, W.; CHATTIPAKORN, S. C.; CHATTIPAKORN, N. Chronic testosterone replacement exerts cardioprotection against cardiac ischemia-reperfusion injury by attenuating mitochondrial dysfunction in testosterone-deprived rats. **PLoS One,** v. 10, n. 3, p. e0122503, 2015. ISSN 1932-6203.

POPE, H. G., JR. et al. Adverse health consequences of performance-enhancing drugs: an Endocrine Society scientific statement. **Endocr Rev,** v. 35, n. 3, p. 341-75, Jun 2014. ISSN 0163-769x.

QIU, X. et al. Calorie restriction reduces oxidative stress by SIRT3-mediated SOD2 activation. **Cell Metab,** v. 12, n. 6, p. 662-7, Dec 1 2010. ISSN 1550-4131.

ROOZENBEEK, B.; MAAS, A. I.; MENON, D. K. Changing patterns in the epidemiology of traumatic brain injury. **Nat Rev Neurol,** v. 9, n. 4, p. 231-6, Apr 2013. ISSN 1759-4766 (Electronic)
1759-4758 (Linking). Disponível em: < http://www.ncbi.nlm.nih.gov/pubmed/23443846 >.

ROSENFELD, J. V. et al. Early management of severe traumatic brain injury. **Lancet,** v. 380, n. 9847, p. 1088-98, Sep 22 2012. ISSN 1474-547X (Electronic)
0140-6736 (Linking). Disponível em: < http://www.ncbi.nlm.nih.gov/pubmed/22998718 >.

SALEHI, F. et al. Histologic study of the human pituitary gland in acute traumatic brain injury. **Brain Inj,** v. 21, n. 6, p. 651-6, Jun 2007. ISSN 0269-9052 (Print)
0269-9052.

SCHOLL, M. et al. Early astrocytosis in autosomal dominant Alzheimer's disease measured in vivo by multi-tracer positron emission tomography. **Sci Rep,** v. 5, p. 16404, Nov 10 2015. ISSN 2045-2322.

SCHON, E. A.; PRZEDBORSKI, S. Mitochondria: the next (neurode)generation. **Neuron,** v. 70, n. 6, p. 1033-1053, 2011. ISSN 0896-6273
1097-4199. Disponível em: < http://www.ncbi.nlm.nih.gov/pmc/articles/PMC3407575/ >.

SHI, J. et al. Review: Traumatic brain injury and hyperglycemia, a potentially modifiable risk factor. **Oncotarget,** v. 7, n. 43, p. 71052-71061, 09/10
05/27/received
09/02/accepted 2016. ISSN 1949-2553. Disponível em: < http://www.ncbi.nlm.nih.gov/pmc/articles/PMC5342608/ >.

SIEBOLD, L.; OBENAUS, A.; GOYAL, R. Criteria to define mild, moderate, and severe traumatic brain injury in the mouse controlled cortical impact model. **Experimental Neurology,** v. 310, p. 48-57, 2018/12/01/ 2018. ISSN 0014-4886. Disponível em: < http://www.sciencedirect.com/science/article/pii/S0014488618302188 >.

SIMON, P. et al. Antidoping Science: Important Lessons From the Medical Sciences. **Curr Sports Med Rep,** v. 17, n. 10, p. 326-331, Oct 2018. ISSN 1537-890x.

SIMS, N. R.; ANDERSON, M. F. Isolation of mitochondria from rat brain using Percoll density gradient centrifugation. **Nat Protoc,** v. 3, n. 7, p. 1228-39, 2008. ISSN 1750-2799.

SIVANANDAM, T. M.; THAKUR, M. K. Traumatic brain injury: a risk factor for Alzheimer's disease. **Neurosci Biobehav Rev,** v. 36, n. 5, p. 1376-81, May 2012. ISSN 0149-7634.

SMITH, D. H. et al. Chronic traumatic encephalopathy - confusion and controversies. **Nat Rev Neurol**, Jan 21 2019. ISSN 1759-4758.

SMITH, D. H. et al. Chronic traumatic encephalopathy — confusion and controversies. **Nature Reviews Neurology**, 2019/01/21 2019. ISSN 1759-4766. Disponível em: < https://doi.org/10.1038/s41582-018-0114-8 >.

STAUCH, K. L.; PURNELL, P. R.; FOX, H. S. Quantitative proteomics of synaptic and nonsynaptic mitochondria: insights for synaptic mitochondrial vulnerability. **J Proteome Res,** v. 13, n. 5, p. 2620-36, May 2 2014. ISSN 1535-3893.

SUNDARAM, K. et al. Different patterns of metabolism determine the relative anabolic activity of 19-norandrogens. **J Steroid Biochem Mol Biol,** v. 53, n. 1-6, p. 253-7, Jun 1995. ISSN 0960-0760 (Print)
0960-0760.

TANRIVERDI, F. et al. High risk of hypopituitarism after traumatic brain injury: a prospective investigation of anterior pituitary function in the acute phase and 12 months after trauma. **J Clin Endocrinol Metab,** v. 91, n. 6, p. 2105-11, Jun 2006. ISSN 0021-972X (Print)
0021-972x.

TARASOV, A. I.; GRIFFITHS, E. J.; RUTTER, G. A. Regulation of ATP production by mitochondrial Ca(2+). **Cell calcium,** v. 52, n. 1, p. 28-35, 2012. ISSN 1532-1991
0143-4160. Disponível em: < https://www.ncbi.nlm.nih.gov/pubmed/22502861 https://www.ncbi.nlm.nih.gov/pmc/PMC3396849/ >.

TINSLEY, G. M.; LA BOUNTY, P. M. Effects of intermittent fasting on body composition and clinical health markers in humans. **Nutr Rev,** v. 73, n. 10, p. 661-74, Oct 2015. ISSN 0029-6643.

TÖLLI, A. et al. Pituitary function within the first year after traumatic brain injury or subarachnoid haemorrhage. **Journal of Endocrinological Investigation**, p. 1-13, 2016// 2016. ISSN 1720-8386. Disponível em: < http://dx.doi.org/10.1007/s40618-016-0546-1 >.

TORO-URREGO, N. et al. Testosterone Protects Mitochondrial Function and Regulates Neuroglobin Expression in Astrocytic Cells Exposed to Glucose Deprivation. **Frontiers in**

**aging neuroscience,** v. 8, p. 152-152, 2016. ISSN 1663-4365. Disponível em: < https://www.ncbi.nlm.nih.gov/pubmed/27445795 https://www.ncbi.nlm.nih.gov/pmc/PMC4921852/ >.

TWIG, G. et al. Fission and selective fusion govern mitochondrial segregation and elimination by autophagy. **Embo j,** v. 27, n. 2, p. 433-46, Jan 23 2008. ISSN 0261-4189.

VASILAKI, F. et al. Cardiotoxicity in rabbits after long-term nandrolone decanoate administration. **Toxicol Lett,** v. 241, p. 143-51, Jan 22 2016. ISSN 0378-4274.

VEKARIA, H. J. et al. Targeting mitochondrial dysfunction in CNS injury using Methylene Blue; still a magic bullet? **Neurochem Int,** v. 109, p. 117-125, Oct 2017. ISSN 0197-0186.

WEBER, J. T. Altered calcium signaling following traumatic brain injury. **Frontiers in pharmacology,** v. 3, p. 60-60, 2012. ISSN 1663-9812. Disponível em: < https://www.ncbi.nlm.nih.gov/pubmed/22518104 https://www.ncbi.nlm.nih.gov/pmc/PMC3324969/ >.

WINKLHOFER, K. F.; TATZELT, J.; HAASS, C. The two faces of protein misfolding: gain- and loss-of-function in neurodegenerative diseases. **Embo j,** v. 27, n. 2, p. 336-49, Jan 23 2008. ISSN 0261-4189.

XIE, K. et al. Every-other-day feeding extends lifespan but fails to delay many symptoms of aging in mice. **Nature Communications**, London**,** v. 8, p. 155, 07/24 11/01/received 06/08/accepted 2017. ISSN 2041-1723. Disponível em: < http://www.ncbi.nlm.nih.gov/pmc/articles/PMC5537224/ >.

YANG, T. et al. Brain ischemic preconditioning protects against ischemic injury and preserves the blood-brain barrier via oxidative signaling and Nrf2 activation. **Redox Biol,** v. 17, p. 323-337, Jul 2018. ISSN 2213-2317.

YARANA, C. et al. Synaptic and nonsynaptic mitochondria demonstrate a different degree of calcium-induced mitochondrial dysfunction. **Life Sci,** v. 90, n. 19-20, p. 808-14, May 22 2012. ISSN 0024-3205.

ZHAO, Z. et al. Voluntary Exercise Preconditioning Activates Multiple Antiapoptotic Mechanisms and Improves Neurological Recovery after Experimental Traumatic Brain Injury. **J Neurotrauma,** v. 32, n. 17, p. 1347-60, Sep 1 2015. ISSN 0897-7151.

ZOCCARATO, F.; CAVALLINI, L.; ALEXANDRE, A. Respiration-dependent Removal of Exogenous H2O2 in Brain Mitochondria: INHIBITION BY Ca2+. **Journal of Biological Chemistry,** v. 279, n. 6, p. 4166-4174, February 6, 2004 2004. Disponível em: < http://www.jbc.org/content/279/6/4166.abstract >.

**Anexo I: Nandrolone decanoate triggers neuroenergetics alterations and memory deficits through NMDA receptor**

**Nandrolone decanoate triggers neuroenergetics alterations and memory deficits through NMDA receptor**

Randhall B Carteri, *MSc*,[1] Afonso Kopzynski,[1] Nathan Ryzewski Strogulski, *MSc*,[1] Marcelo Salimen Rodolphi *MSc*,[1] Wesley Cotta,[1] Mônia Sartor,[1] Marcelo Ganzella,[2] Luis Valmor Portela, *PhD*[1*]

[1] Laboratório de Neurotrauma e Biomarcadores - Departmento de Bioquímica, Programa de Posgraduação em Bioquímica, ICBS, Universidade Federal do Rio Grande do Sul - UFRGS, Porto Alegre, RS, Brazil.

[2] Max Planck Institute for Biophysical Chemistry, Department of Neurobiology, 37077, Goettingen, Germany.

**Correspondence:**

* Dr. Luis V. Portela,

Department of Biochemistry,

ICBS, UFRGS. Rua Ramiro Barcelos, 2600 anexo

90035-003, Porto Alegre, RS, Brazil.

Tel: 55 51 33085558; Fax: 55 51 33085544;

E-mail: roskaportela@gmail.com

***Paper in preparation***

*Abstract*

Nandrolone (ND) is an anabolic steroid, which in high doses may cause neurochemical modifications and behavioral changes by mechanisms not well defined. Here we show that 19 days of ND induced object recognition memory deficits and decreased glutamate release by hippocampal synaptosomes of mice. There was also, disturbances in mitochondrial energy production associated with disrupt calcium homeostasis. Using a NMDAr channel blocker memantine, we partially prevented these undersirable effects, evidencing a role of steroids in mediating calcium-dependent glutamatergic receptor interplay with bioenergetics and behavior.

## Introduction

Anabolic Androgen Steroid (AAS) abuse is a growing public health concern, due to uncontrolled use for professional athletes and general population [1]. AAS pharmacological therapy is of clinical importance for diverse catabolic conditions including HIV infection and severe burned patients. Further, AAS like testosterone has been suggested as replacement therapy, and for delay neurodegenerative disorders including Alzheimer's disease[2].

Nonetheless, it has been well established that AAS abuse can induce undesirable psychiatric effects, such as mood swings, increased aggressive, anxious and depressive behaviors, which may be mechanistically associated with impaired glutamate uptake, increased N-methyl-D-Aspartate receptor (NMDAr) activity and calcium influx [3, 4]. In addition, preclinical studies have demonstrated that AAS supra physiological doses may impair spatial memory performance in hippocampal dependent behavioral tasks [5-7]. Particularly in rodents, AAS exposure can induce neuronal apoptosis [9], and impaired hippocampal neurogenesis [6], albeit its effects in mitochondrial function remains to be fully elucidated.

Conceptually, mitochondrial electron transfer system is physiologically coupling with oxidative phosphorylation (OxPhos) generating (ATP) whereas energy deficits and redox imbalance due to mitochondrial uncoupling, ultimately contributes to brain disorders and cognitive deficits [8]. The metabolic effects of AAS are widely studied in heart, liver and skeletal muscle. However, few studies have addressed the potential effects on brain metabolism Therefore, we treated male 90 days old C57BL/6J mice with a daily 50uL injection of vehicle (corn oil, Veh) or 15 mg/kg nandrolone decanoate from Organon ® (Nand) diluted in 50 uL of vehicle, combined with a 500ul intraperitoneal injection of saline (Sal) or a 10 mg/kg dose of memantine from Aventis ® diluted in 500uL of saline (Mem). A total of 5-6 animals per group were used in each experiment (Veh+Sal, Nand+Sal and Nand+Mem). This study was designed to unravel whether nandrolone decanoate, a worldwide used AAS, affects hippocampal mitochondrial bioenergetics through NMDA receptor mechanism involving NMDA in hippocampus of adult mice.

**Results**

*Nandrolone-induced cognitive impairment is prevented by memantine co-treatment*

The novel object recognition task was used to assess memory. During training, no differences for object preference was found between groups (Figure 1A). The short-term memory testing with a novel object indicated that ND treated mice did not explore the novel object as VEH group (Figure 1B) implying in memory deficits. This effect was prevented by MEM co-treatment (Figure 1B). The NOR index confirms this result (Figure 1C).

*Decreased glutamate release by Nandrolone was not prevented by memantine*

Glutamate release from hippocampi synaptosomes is indicated in Figure 2A. After addition of NADP (time 0) the percent of variation in fluorescence (Figure 2B) was similar to all group. The fluorescence from GDH until K+addition, was significantly

higher in both ND and NDMEM groups compared to VEH. The potassium addition to the induce glutamate release to the medium resulted in decreased variation of fluorescence in both ND and NDMEM compared to VEH, indicating decreased vesicular glutamate release after depolarization. This could indicate a desensitization of potassium channels. Glutamate was then added to confirm the functionality of the system.

*Nandrolone induces GluN2B phosphorilation and Tau phosphorilation at ser$^{396}$*

Imunnocontent of pGLuN2B$^{Tyr1472}$ (Figure 2C) showed that both ND and NDMEM increased this subunit phosphorylation. We further explored phosphorylation of Tau at ser$^{396}$ (Figure 2D) indicating a significant increase comparing ND with VEH, and a prevention by NDMEM. No effects were observed in alpha-spectrin cleavage (Figure 2E).

*Nandrolone induced increased mitochondrial calcium uptake was not prevented by memantine co-treatment*

In Figure 3A, we showed that both ND and NDMEM significantly increased mitochondrial calcium uptake, but does not altered calcium efflux. Memantine prevented exacerbated mitochondrial calcium swelling induced by ND.

*Nandrolone impaired mitochondrial membrane potential dynamics*

We further explored mitochondrial membrane potential dynamics in different mitochondrial coupling states (Figure 3B). After addition of mitochondrial substrates to induce leak respiration, a decreased variation in ND-MEM compared to VEH was observed, indicating a decreased $\Delta\psi m$ formation. Following ADP addition to induce OxPhos, it was notice a significant impairment comparing both ND and NDMEM with VEH. The same effect was observed with the addition of oligomycin to inhibit ATP synthase. After uncoupling, a decreased variation in ND compared to both VEH and ND-MEM indicated impaired dissipation of $\Delta\psi m$. Since no differences comparing VEH to

ND-MEM were observed, MEM co-treatment prevented this effect. No differences were observed after inhibition of complex IV by cyanide.

*Nandrolone induced mitochondrial hydrogen peroxide increase was partially prevented by memantine co-treatment*

While no effects were observed in hippocampi synaptosomes oxygen consumption rates and OxPhos coupling efficiency among groups (Figure 4A and B), decreased cell viability was observed in ND compared to both VEH and ND-MEM (Figure 4C). Finally, mitochondrial hydrogen peroxide production in different coupling states was increased by ND, while this effect was partially prevented in ND-MEM (Figure 4D). Higher levels of $H_2O_2$ when comparing ND to VEH were observed in routine, Leak and Leak(omy) states without differences of NDMEM to neither VEH or ND. Only in OxPHOS state, stimulating maximal activity, ND showed increased production compared to both ND and NDMEM.

## Discussion

Here, we investigated whether the interaction of ND with the NMDAR could explain the undesirable effects of ND in the cognitive function, mitochondrial OXPHOS and survival. To counteract these effects, we used memantine (MEM), a non-competitive antagonist with low affinity for the GluN2B subunit of the NMDAR. Nandrolone treatment induced a short-term memory impairment and mitochondrial dysfunction. Although concomitant treatment with memantine prevented the memory impairment and decresed OxPhos it does not preserve membrane potential or avoid decrease glutamate release.

Memantine acts as an NMDAR open-channel blocker, commonly prescribed to treatment of several Alzheimer-like diseases [10]. Memantine preferentially blocks excessive (considered pathological and mainly extrasynaptic) NMDAR activity while relatively sparing normal physiological synaptic activity [11]. Furthermore, memantine treatment prevent several mechanisms involved in neurodegeneration and memory

deficits [12] and could act as a cholinergic stimulant in the hippocampus [13], resulting in neuroprotection [14]. The high level of expression of androgen receptor partially mediates its sensitivity to glutamate-induced excitatory stimuli, thereby elucidating how synthetic AAS like ND could promote such prominent effects within the brain.[15-17] Nandrolone decanoate induces hyperactivation of glutamatergic synapses in the hypothalamus, hippocampus and cerebral cortex, which correlates with behavioral alterations [4] and increased NMDAr activity [18] [3]. Previous studies reported that NMDAr is possibly involved in the effects of AAS treatment in behavior [3]. A single injection of nandrolone induced phosphorylation of GluN2A at Ser1232 and GluN2B at Tyr1472 [18]. Moreover, chronic nandrolone treatment has been shown to interfere in neurosteroids actions via the sigma receptors, which in turn could modulate NMDAr signaling [19] and NMDAr antagonist Memantine has been shown to reduce aggressive behavior in mice induced by increased glutamatergic signaling [3]. Taken together, these findings indicate that Nandrolone decanoate actually activates NMDAr via phosphorylation, however the blockade with memantine reduces detrimental effects in brain function and memory. Although the increased extracellular levels of glutamate could be related to decreased expression of GLT-1 transport, a possible increased synaptosomal release of glutamate was not previously ruled out [3]. Therefore, glutamate release from synaptic vesicles was investigated. Our data demonstrated that short-term ND decreases the release of glutamate from synaptosomes.

Extracellular glutamate clearence impairment is a potential mechanism leading to neuronal cell death, resulting from decrease in ATP which would enhance the release of cytoplasmic glutamate through reversal of the glutamate carrier and inhibit the exocytotic $Ca^{2+}$-dependent release[20] coupled with increased oxidative processes [21]. Notably, Extracelular glutamate levels is increased with long-term nandrolone treatment and associated with decreased GLT-1 expression [3]. In addition, glutamate release modulates EAAC1/EAAT3 translocation to neuronal cell surface, evidencing a significant role in glutamate reuptake and homeostasis in synapses despite the relative smaller expression of glutamate transporters EAAC1/EAAT3 compared to glial cells. [22] Impairment in this mechanism is of paramount importance in AAS induced

glutamatergic excitotocixity previously demonstrated in the literature. Therefore, the decreased glutamate release observed in the present study associated with high level of NMDAR Gun2B subunit activation, may suggest impaired gltamate uptake by astrocytes.

Glutamate binding to NMDAr promotes calcium influx through the ion channel [23, 24] and hippocampal androgen receptor activation results in changes in calcium concentrations.[25] Additionally, persistent increased $Ca^{2+}$ levels are associated with impaired mitochondrial ATP synthesis and increased apoptotic signaling.[26, 27] Interestingly, it was previously demonstrated that AAS treatment results in increased stores of calcium and higher peak of calcium concentration after glutamate stimulation [25] and also that NCLX can be modulated by androgens [28]. This response could be explained by the aforementioned mechanisms (increased AR activation and extracellular glutamate levels).

Impaired glutamate and calcium homeostasis leading to glutamatergic excitotocixity could also impact mitochondrial function within the presynaptic neuron, which is intimately related to neurotransmitter release from synaptic vesicles [30]. Therefore using high-resolution respirometry we evaluated mitochondrial function in brain synaptosomes. Although we found no effects in OCR, the increase in hydrogen peroxide production in different coupling states as well as impaired cell viability induced by ND and partially prevented by memantine indicates early bioenergetic changes that underlie cognitive dysfunction. As hypothesized, the combined treatment with nandrolone and memantine prevented the bioenergetic deficits and decreased cell viability. Additionally, the observed recognition memory impairment induced by nandrolone was also prevented by combined memantine treatment.

## Conclusion

The combined results demonstrated that Nandrolone treatment induced impaired mitochondrial metabolism and reduced cell viability associated with recognition memory deficit. These effects are modulated by NMDAr signaling and were prevented by association with memantine. The present data confirms the interaction of AAS treatment with cognitive function and extends current literature, indicating that mitochondrial

bioenergetics in the hippocampus is also affected by AAS treatment, via an NMDAr dependent mechanism.

## References


1. Pope, H.G., Jr., et al., *Adverse health consequences of performance-enhancing drugs: an Endocrine Society scientific statement.* Endocr Rev, 2014. **35**(3): p. 341-75.
2. Kang, L., et al., *Dihydrotestosterone treatment delays the conversion from mild cognitive impairment to Alzheimer's disease in SAMP8 mice.* Horm Behav, 2014. **65**(5): p. 505-15.
3. Kalinine, E., et al., *Nandrolone-induced aggressive behavior is associated with alterations in extracellular glutamate homeostasis in mice.* Horm Behav, 2014. **66**(2): p. 383-92.
4. Le Greves, P., et al., *Effects of an anabolic-androgenic steroid on the regulation of the NMDA receptor NR1, NR2A and NR2B subunit mRNAs in brain regions of the male rat.* Neurosci Lett, 1997. **226**(1): p. 61-4.
5. Magnusson, K., et al., *Nandrolone decanoate administration elevates hippocampal prodynorphin mRNA expression and impairs Morris water maze performance in male rats.* Neurosci Lett, 2009. **467**(3): p. 189-93.
6. Novaes Gomes, F.G., et al., *The beneficial effects of strength exercise on hippocampal cell proliferation and apoptotic signaling is impaired by anabolic androgenic steroids.* Psychoneuroendocrinology, 2014. **50**: p. 106-17.
7. Pieretti, S., et al., *Brain nerve growth factor unbalance induced by anabolic androgenic steroids in rats.* Med Sci Sports Exerc, 2013. **45**(1): p. 29-35.
8. Lin, M.T. and M.F. Beal, *Mitochondrial dysfunction and oxidative stress in neurodegenerative diseases.* Nature, 2006. **443**(7113): p. 787-795.
9. Ma, F. and D. Liu, *17beta-trenbolone, an anabolic-androgenic steroid as well as an environmental hormone, contributes to neurodegeneration.* Toxicol Appl Pharmacol, 2015. **282**(1): p. 68-76.
10. Zimmer, E.R., et al., *Long-term NMDAR antagonism correlates reduced astrocytic glutamate uptake with anxiety-like phenotype.* Front Cell Neurosci, 2015. **9**: p. 219.
11. Chen, H.S., et al., *Open-channel block of N-methyl-D-aspartate (NMDA) responses by memantine: therapeutic advantage against NMDA receptor-mediated neurotoxicity.* J Neurosci, 1992. **12**(11): p. 4427-36.
12. Figueiredo, C.P., et al., *Memantine rescues transient cognitive impairment caused by high-molecular-weight abeta oligomers but not the persistent impairment induced by low-molecular-weight oligomers.* J Neurosci, 2013. **33**(23): p. 9626-34.

13. Drever, B.D., et al., *Memantine acts as a cholinergic stimulant in the mouse hippocampus.* J Alzheimers Dis, 2007. **12**(4): p. 319-33.
14. Park, D., et al., *Improvement of cognitive function and physical activity of aging mice by human neural stem cells over-expressing choline acetyltransferase.* Neurobiol Aging, 2013. **34**(11): p. 2639-46.
15. Sar, M., et al., *Immunohistochemical localization of the androgen receptor in rat and human tissues.* Endocrinology, 1990. **127**(6): p. 3180-6.
16. Pouliot Wendy, A., J. Handa Robert, and G. Beck Sheryl, *Androgen modulates N ‐ methyl ‐ D ‐ aspartate ‐ mediated depolarization in CA1 hippocampal pyramidal cells.* Synapse, 1996. **23**(1): p. 10-19.
17. Leranth, C., O. Petnehazy, and N.J. MacLusky, *Gonadal hormones affect spine synaptic density in the CA1 hippocampal subfield of male rats.* J Neurosci, 2003. **23**(5): p. 1588-92.
18. Rossbach, U.L., et al., *Nandrolone-induced hippocampal phosphorylation of NMDA receptor subunits and ERKs.* Biochem Biophys Res Commun, 2007. **357**(4): p. 1028-33.
19. Elfverson, M., et al., *Chronic administration of the anabolic androgenic steroid nandrolone alters neurosteroid action at the sigma-1 receptor but not at the sigma-2 or NMDA receptors.* Neuropharmacology, 2011. **61**(7): p. 1172-81.
20. Kauppinen, R.A., H.T. McMahon, and D.G. Nicholls, *Ca2+-dependent and Ca2+-independent glutamate release, energy status and cytosolic free Ca2+ concentration in isolated nerve terminals following metabolic inhibition: Possible relevance to hyoglycaemia and anoxia.* Neuroscience, 1988. **27**(1): p. 175-182.
21. Greenamyre, J.T. and A.B. Young, *Excitatory amino acids and Alzheimer's disease.* Neurobiol Aging, 1989. **10**(5): p. 593-602.
22. Nieoullon, A., et al., *The neuronal excitatory amino acid transporter EAAC1/EAAT3: does it represent a major actor at the brain excitatory synapse?* J Neurochem, 2006. **98**(4): p. 1007-18.
23. Danbolt, N.C., *Glutamate uptake.* Prog Neurobiol, 2001. **65**(1): p. 1-105.
24. Aalders, T.T. and J. Meek, *The hypothalamic aggression region of the rat: observations on the synaptic organization.* Brain Res Bull, 1993. **31**(1-2): p. 229-32.
25. Foradori, C.D., et al., *Activation of the androgen receptor alters the intracellular calcium response to glutamate in primary hippocampal neurons and modulates sarco/endoplasmic reticulum calcium ATPase 2 transcription.* Neuroscience, 2007. **149**(1): p. 155-164.
26. Boyman, L., et al., *NCLX: the mitochondrial sodium calcium exchanger.* J Mol Cell Cardiol, 2013. **59**: p. 205-13.
27. Jafri, M.S. and R. Kumar, *Modeling Mitochondrial Function and Its Role in Disease.* Progress in molecular biology and translational science, 2014. **123**: p. 103-125.
28. Zup, S.L., N.S. Edwards, and M.M. McCarthy, *Sex- and age-dependent effects of androgens on glutamate-induced cell death and intracellular calcium regulation in the developing hippocampus.* Neuroscience, 2014. **281**: p. 77-87.

29. Sanchez‐Prieto, J. and P. González, *Occurrence of a Large Ca2+‐Independent Release of Glutamate During Anoxia in Isolated Nerve Terminals (Synaptosomes).* Journal of Neurochemistry, 1988. **50**(4): p. 1322-1324.
30. Verstreken, P., et al., *Synaptic mitochondria are critical for mobilization of reserve pool vesicles at Drosophila neuromuscular junctions.* Neuron, 2005. **47**(3): p. 365-78.

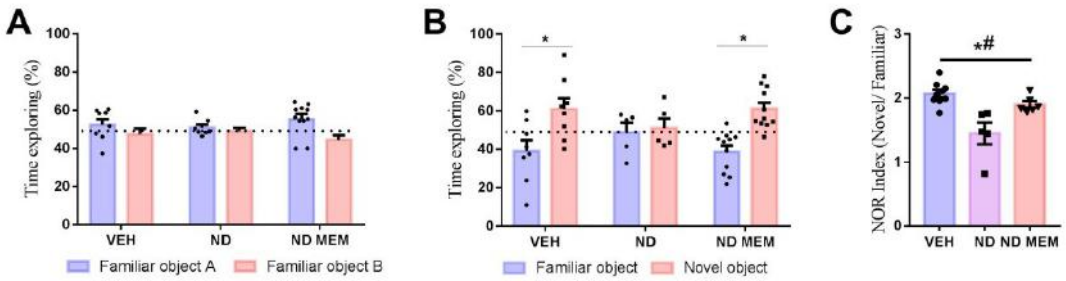


**Figure 01. Nandrolone-induced cognitive impairment is prevented by memantine co-treatment.** The novel object recognition task was used to assessment of cognition. During training, no differences for object preference was found (A). However, during short-term memory testing with a novel object indicated that ND treated animals did not explore the novel object, and indicative of impaired cognition (B). This effect was reversed by MEM co-treatment. The NOR index (C) confirms this result.

* Significant difference comparing familiar to novel object ($p < 0.005$, Student's t test)

*# Significant difference comparing ND to both VEH and NDMEM ($p < 0.005$, One-Way ANOVA, Tukey's *post hoc*)

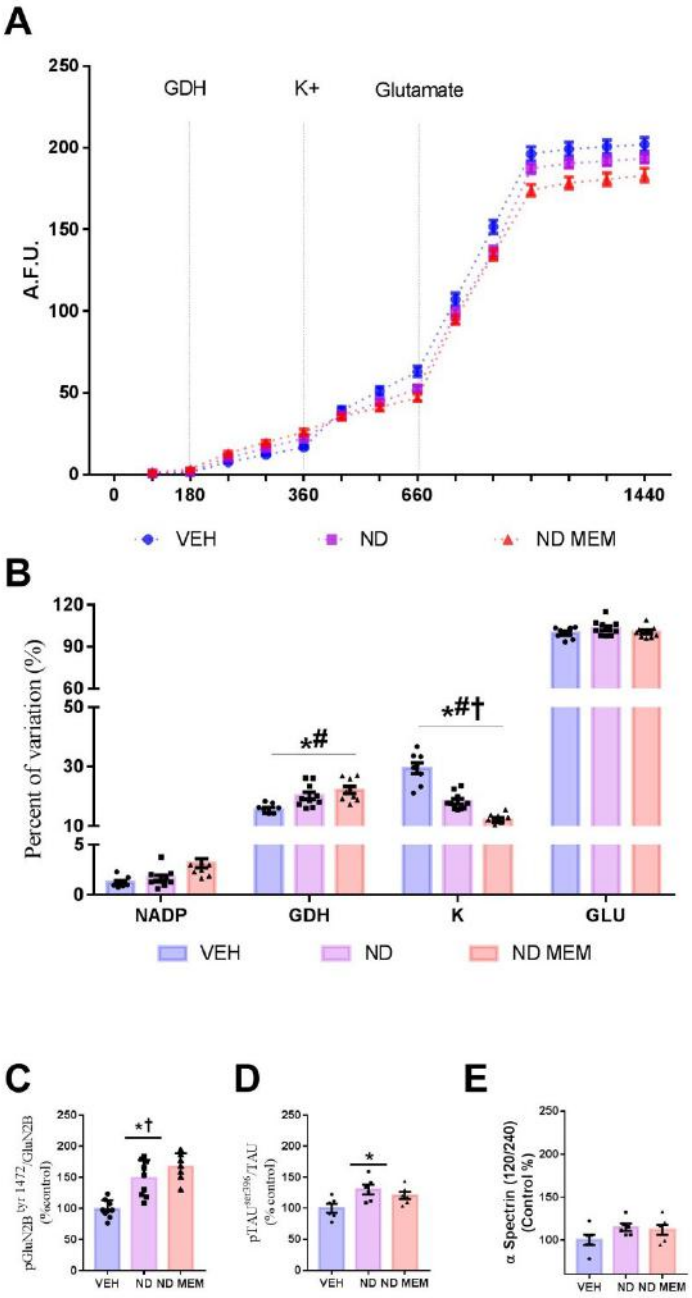


**Figure 2. Nandrolone increases glutamate release and GluN2B phosphorylation and Tau phosphorylation at ser$^{396}$are partially prevented by memantine.** Glutamate release from hippocampi synaptosomes (A) was monitored spectrophotometrically. Addition of NADP was performed at 0 and monitored until GDH addition. The variation of fluorescence was similar to all groups (B, analyzed by Two-Way ANOVA, with Tukey's *post hoc*) for all comparisons. After addition of GDH until $K^+$ addition, fluorescence variation was higher in both ND and NDMEM compared to VEH, indicating increased glutamate release. Potassium addition to induce glutamate release resulted in decreased variation of fluorescence in both ND and NDMEM

compared to VEH, indicating decreased glutamate release due to depolarization. This could indicate a desensitization of potassium channels. Glutamate was then added to confirm the functionality of the system. Moreover, comparisons of protein immunocontent was performed with One-Way ANOVA, with Tukey's *post hoc.* The evaluation of GLuN2B phosphorylation (C) showed that both ND and NDMEM increased this subunit phosphorylation. We further explored phosphorylation of Tau at ser $^{396}$ (D) indicating a significant increase comparing both ND and NDMEM to VEH, indicating a partial prevention of this effect in NDMEM. No effects were observed in alpha-spectrin cleveage (E).

* Significant difference comparing ND to VEH($p < 0.005$)

$^{\#}$ Significant difference comparing ND to NDMEM ($p < 0.005$)

$^{\dagger}$ Significant difference comparing VEH to NDMEM ($p < 0.005$)

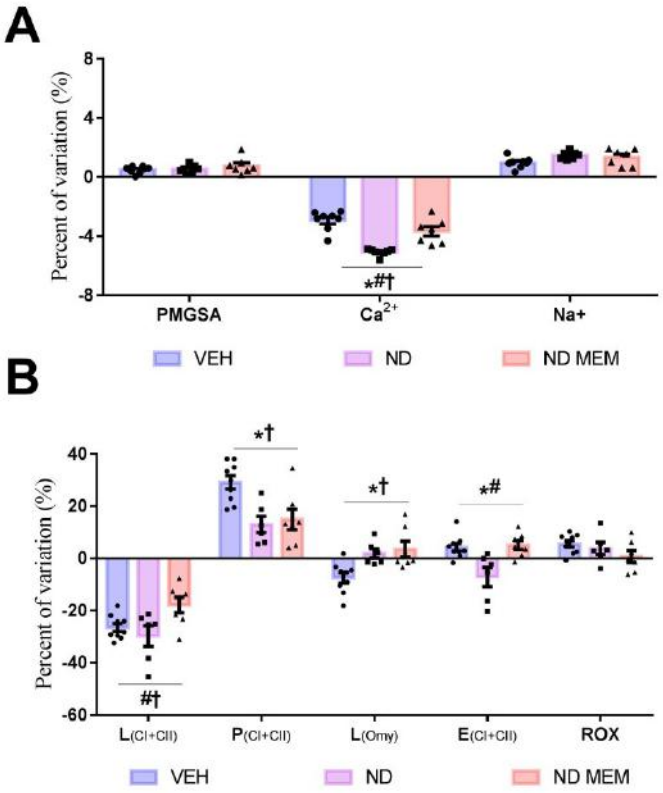


**Figure 03. Nandrolone impairment in mitochondrial calcium homeostasis and membrane potential dynamics was not prevented by memantine co-treatment.** The evaluation calcium uptake (A, analyzed by Two-Way ANOVA, with Tukey's *post hoc*) showed that both ND and NDMEM increased calcium uptake, without effects on

calcium efflux. This results indicates that MEM co-treatment was not able to prevent impaired mitochondrial calcium homeostasis induced by ND. We further explored mitochondrial membrane potential dynamics (B, analyzed by Two-Way ANOVA, with Tukey's *post hoc*) in different mitochondrial coupling states. After addition of mitochondrial substrates to induce leak respiration, a decreased variation in NDMEM compared to VEH was observed, indicating a decreased $\Delta\psi m$ formation. Following ADP addition to induce OxPhos, a significant impairment comparing both ND and NDMEM to VEH. The same effect was observed with the addition of oligomycin to inhibit ATP synthase. After uncoupling, a decreased variation in ND compared to both VEH and NDMEM indicated impaired dissipation of $\Delta\psi m$. Since no differences comparing VEH to NDMEM were observed, MEM co-treatment prevented this effect. No differences were observed after inhibition of complex IV by cyanide.

***** Significant difference comparing ND to VEH($p < 0.005$)

[#] Significant difference comparing ND to NDMEM ($p < 0.005$)

[†] Significant difference comparing VEH to NDMEM ($p < 0.005$)

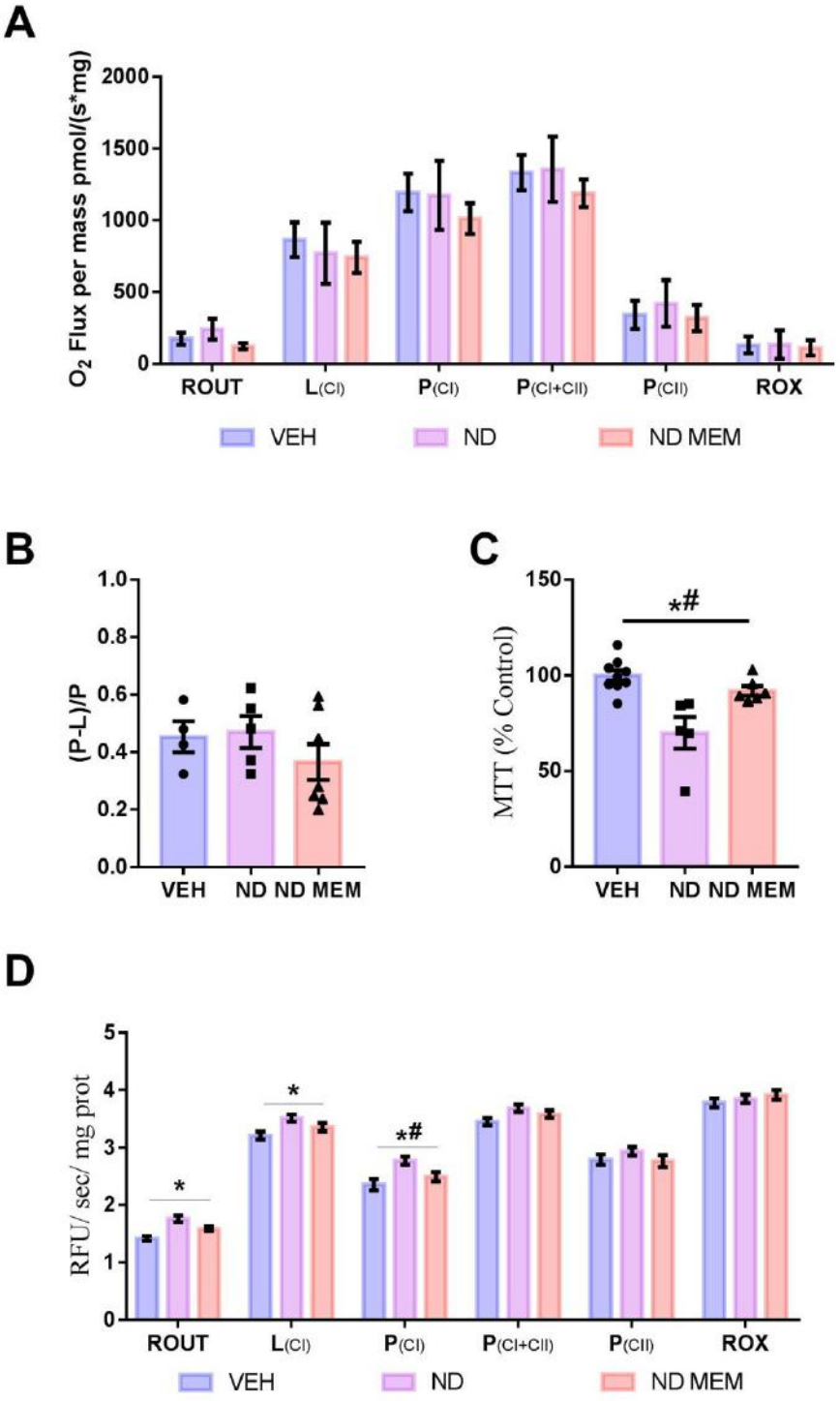


**Figure 4. Nandrolone induced mitochondrial hydrogen peroxide increase was partially prevented by memantine co-treatment.** No effects were observed in hippocampal synaptosomes oxygen consumption rates (A, analyzed by Two-Way ANOVA, with Tukey's *post hoc*) and OxPhos coupling efficiency (B, analyzed by One-Way ANOVA, with Tukey's *post hoc*) among groups. Decreased cell viability was observed in ND compared to both VEH and ND-MEM (C, analyzed by One-Way

ANOVA, with Tukey's *post hoc*). Finally, mitochondrial hydrogen peroxide production in different coupling states was increased by ND, while this effect was partially prevented in ND-MEM (D, analyzed by Two-Way ANOVA, with Tukey's *post hoc*). Higher levels of $H_2O_2$ when comparing ND to VEH were observed in routine and Leak states ($L_{(CI)}$), without differences of NDMEM to neither VEH or ND. Only in the phosphorylating state ($P_{(CI)}$), stimulating maximal activity, ND showed increased production compared to both ND and NDMEM.

* Significant difference comparing ND to VEH($p < 0.005$)

[#] Significant difference comparing ND to NDMEM ($p < 0.005$)

[†] Significant difference comparing VEH to NDMEM ($p < 0.005$)

## Anexo II: Intermittent fasting promotes anxiolytic-like effects unrelated to mitochondrial function

**FULL TITLE: Intermittent fasting promotes anxiolytic-like effects unrelated to mitochondrial function**

Randhall B Carteri, *MSc*,[1*] Lizia Nardi Menegassi,[1] Marceli Feldmann,[1] Afonso Kopzynski,[1] Marcelo Salimen Rodolphi *MSc*,[1] Nathan Ryzewski Strogulski, *MSc*,[1] Amanda Staldoni Almeida,[2] Daniela Melo Marques *MSc*,[2] Lisiane O. Porciúncula *PhD*,[2] Luis Valmor Portela *PhD,*[1]

[1] Laboratório de Neurotrauma e Biomarcadores - Departamento de Bioquímica, Programa de Pós-Graduação em Bioquímica, ICBS, Universidade Federal do Rio Grande do Sul - UFRGS, Porto Alegre, RS, Brazil.
[2] Laboratório de Estudos sobre o Sistema Purinérgico - Departamento de Bioquímica, Programa de Pós Graduação em Bioquímica, ICBS, Universidade Federal do Rio Grande do Sul - UFRGS, Porto Alegre, RS, Brazil.

**Correspondence:**
*** MsC, Randhall B Carteri**
Department of Biochemistry,
ICBS, UFRGS. Rua Ramiro Barcelos, 2600 anexo
90035-003, Porto Alegre, RS, Brazil.
Tel: 55 51 33085558; Fax: 55 51 33085544;
E-mail: rcarteri@hotmail.com

## INTRODUCTION

Anxiety and depression are highly prevalent, complex disorders involving multiple brain regions and feedback loops. During 2010 alone, anxiety and depressive disorders together comprise the second largest cause of years lived with disability globally, thereby posing a major economic burden.[1] Brazil is the country with the

highest rate of people with anxiety disorders in the world reaching 9.3% of the population.[1] Yet, these conditions are mostly undiagnosed and remain untreated because of lack of effective therapies. Anxiety disorders represent a maladaptive state of a normal response to threat, marked by excessive fear and avoidance in the absence of real danger.[1]

The emerging advances achieved in the understanding of mitochondria roles in the central nervous system (CNS) have shed lights on how bioenergetics are particularly connected with psychiatric disorders. Actually, emerging findings indicate a robust relationship between impaired mitochondrial metabolism and anxiety disorders.[2, 3] Particularly, deficient mitochondrial ATP production via Oxidative Phosphorylation (OxPHOS) negatively impacts synaptic plasticity and increases vulnerability to anxiety disorders.[4, 5] Accordingly, anxiolytic drugs such as monoamine oxidase I inhibitors (MAO-I),[6, 7] neurosteroids [8, 9] and mitochondrial benzodiazepine receptor ligands are recognized to promote a markedly improvement in the energy production by mitochondria linked with decreased anxious behavior. [10, 11]

Based on this mechanistic link it is reasonable to propose that non-pharmacological approaches addressed to increase mitochondrial metabolism may cause parallel behavioral benefits against anxiety disorders. Indeed, standard treatment for anxiety disorders consist in pharmacotherapy alone or associate with psychotherapy.[12] In this context, dietary interventions manipulating caloric intake or specific macronutrients may arise as potential non-pharmacological therapies.[13-17]

In agreement with this framework, the alternate day intermittent fasting (IF), in which animals are submitted to 24 h cycles of food deprivation and *ad libitum* consumption has been a suitable paradigm of caloric restriction (CR).[18] Different paradigms of calorie restriction are associated with cognitive improvements,[19] albeit the influence in anxiety-like behavior is controversial, probably due to differences in the mice strains, age and behavioral assessments.[20-23] Withal, intermittent fasting (IF) is associated with improved oxidative energy metabolism and antioxidant defenses in different tissues,[24, 25] including the brain.[13, 14] In fact, anxious rodents exhibit reduced expression of mitochondrial complex I and II proteins, reduced total respiratory capacity coupled with decreased ATP synthesis and increased production of reactive

oxygen species in the nucleus accumbens.[5] However, there are limited data exploring interactions between IF-induced mitochondrial adaptations, particularly in specific respiratory complexes and the anxious behavior. Further, mitochondrial function is associated to the expression of proteins of the Bcl-2 family. Aside from its role in apoptosis, Bcl-2 overexpression is associated to reduced anxiety-like behavior in rodents.[26] In addition, neurotrophic factors play particularly prominent roles in the adaptive and neuroprotective responses of brain cells to calorie restriction models [27]. Caloric restriction may increase brain-derived neutrotrophic factor (BDNF) levels, which may contribute to improve neuronal function [28, 29] and mitochondrial oxidative efficiency [30, 31]. Therefore, the objective of the present study is to investigate whether a chronic IF regimen could exert anxiolytic-like effects in behavior concomitantly to mitochondrial bioenergetics modulation in mice brain.

## METHODS

### *Animals and treatment protocol*

Male 180 days old C57BL/6J mice were obtained from Foundation for Health Science Research (FEPPS, Porto Alegre/RS, Brazil). Animals (4-5 per cage) were placed into a controlled temperature room (22 ºC ± 1) under a 12 h light/12 h dark cycle (lights on at 7 a.m.) and had free access to food and water. Animals were assigned to two different dietary regimens: a normal, ad libitum diet (AL group) and an alternate-day fasting (IF group), where animals had no food access during 24 h and ad libitum food access in the following day. Animals underwent a total of 10 cycles of food restriction and access. Subsequently, 48h after the last fasting day for the IF group, animals were submitted to the behavioral assessments and were euthanized for tissue dissection and neurochemical analysis. All experiments were in agreement with the Committee on the Care and Use of Experimental Animal Resources, UFRGS, Brazil number 22436.

### *Food consumption and Body Mass Assessment.*

Total food consumption as measured every day. In three separated AL days (after the first, fifth and tenth fast), food consumption was monitored every 2h to evaluate food consumption patterns. Body mass was accessed in 6 different time-points, in AL days.

*Total Blood Ketones and Blood Glucose concentrations*

Total Ketones and blood glucose were assessed using specific meters and test strips in tail-tip blood samples (FreeStyle Optium Neo and β-Ketone Monitoring System; Abbott, Brazil and On Call® Plus glucose meter; ACON Laboratories, Inc., US, respectively). Blood samples were collected by skilled personnel using the routine tail-tip technique.

*Open Field*

Animals were submitted to an open field task 24 h after treatment (48 h after the last fast day). All the cages containing mice were transferred to the behavior testing room 60 min before the first trial. The experiments were conducted in a quiet room under low-intensity light (12 lux), between 9:00 a.m. and 11:00 a.m. The apparatus was made of a black-painted box measuring 50 cm × 50 cm and was surrounded by 50 cm high walls. Each mouse (n=10 per group) was placed in the same site in the arena and the distance travelled (total and central zone), time spent in central zone and mean speed were measured during 5 min.[32] After each trial, all chambers are cleaned with super hypochlorous water to prevent a bias based on olfactory cues. The experiment was recorded with a video camera positioned above the arena and analysis was performed using a computer-operated tracking system (Any-maze, Stoelting, Woods Dale, IL).

*Light Dark Box*

The experiments were conducted in a quiet room under low-intensity light (12 lux), between 11:00 a.m. and 12:00 p.m. The apparatus used for the light/dark transition test consisted of a cage (21 x 42 x 25 divided into two sections of equal size by a partition

with door. One chamber was brightly illuminated by white light (~300 lux), whereas the other chamber is dark (~2 lux). Mice were placed into the dark side and were allowed to move freely between the two chambers with door open for 5 min. The experiment was recorded with a video camera positioned above the arena and analysis was performed using a computer-operated tracking system (Any-maze, Stoelting, Woods Dale, IL). After each trial, all chambers are cleaned with super hypochlorous water to prevent a bias based on olfactory cues. [33]

*Elevated Plus Maze*

The cross-shaped MDF fiberboard apparatus used for the elevated plus maze test comprises two open arms (25 x 5 x 0.5 cm) across from each other and perpendicular to two closed arms (25 x 5 x 16 cm) with a center platform (5 x 5 x 0.5 cm). The open arms have a very small (0.5 cm) wall to decrease the number of falls, whereas the closed arms have a high (16 cm) wall to enclose the arm. The entire apparatus is 50 cm above the floor and was surrounded by a dark curtain to protect the mice that fall/ escape during the experiment and to prevent contact with the operator. All the experimental mice are transferred to the behavior testing room 60 min prior to beginning the first trial to habituate to the condition of the behavior testing room (illumination level was maintained at 100 lux). The order of trials was randomized. Mice were placed in the center area of the maze with its head directed toward a closed arm. After each trial, the apparatus was cleaned with super hypochlorous water to prevent a bias based on olfactory cues. A video camera positioned above the arena recorded the experiment and analysis was performed using a computer-operated tracking system (Any-maze, Stoelting, Woods Dale, IL). Time spent in the open and closed arms, total distance and number of entries in each arm were recorded. The ratio of time spent in the open arms relative to closed arms serve as an index of anxiety-like behavior [34].

*Preparation of brain hemisphere synaptosomes and tissue homogenates*

Isolated nerve terminals were obtained from the left hemisphere of mice brain following a standard centrifugation in discontinuous Percoll gradient protocol [35, 36], the resulting synaptosome-enriched bands were resuspended in a sucrose and Tris buffer (320 mM sucrose, 10 mM Tris, pH 7.4) and immediately used for respirometry. The remaining samples were frozen at − 80 °C for protein quantification (Pierce™ BCA Protein Assay Kit; Catalog number: 23225) and western blotting.

*Mitochondrial respiratory protocol*

Oxygen consumption rates (OCR) per tissue mass was obtained following a modified multi-substrate titration [37] protocol using the high-resolution Oxygraph-2k system and recorded real-time using DatLab software (Oroboros, Innsbruck, Austria). Experiments were performed at 37°C in a 2-ml chamber filled with standard respiration buffer (100 mM KCI, 75 mM mannitol, 25 mM sucrose, 5 mM phosphate, 0.05 mM EDTA, and 10 mM Tris-HC1, pH 7.4). The defined coupling states were ROUTINE ( baseline OCR recorded for 5 minutes); LEAK (L), obtained after pyruvate, malate, and glutamate (PMG; 10, 10, and 20 mM, respectively); CI – linked OxPHOS capacity (CI-P) was obtained after addition of Adenosine diphosphate (ADP, 2.5 mM); Maximal OxPHOS capacity ($P_{max}$) was obtained with addition of Succinate (S, 10 mM) in saturating ADP concentrations; Complex II OxPHOS capacity (CII-P), obtained with Rotenone (ROT, 2.0mM) and non-mitochondrial respiration (ROX) after cyanide (KCN, 5 mM). Tissue-mass specific oxygen fluxes were corrected for ROX and compared in different coupling states. In addition we calculated the biochemical coupling efficiency (P-L)/P = 1-L/P; The stimulation of CII-linked OCR by CI-linked substrates (rotenone effect, 1 – CII/CI&II) and CII-linked substrate stimulating CI-linked OCR (succinate effect, 1 – CI/CI&II), determined in the OXPHOS state in the protocol.[37, 38]

*Western Blot*

After defrosting, the protein content from synaptosome-enriched samples was determined using the bicinchoninic acid assay (BCA) (Pierce, São Paulo/ Brazil). The

samples were diluted to a final protein concentration of 2 μg/uL in SDS solution and the amount of protein applied for SDS–PAGE analysis was as follows: 40 μg for Bax, Bcl-2, BDNF, proBDNF and Synaptophysin. The proteins, together with pre-stained molecular weight standards (Bio-Rad, São Paulo/Brazil), were applied to a 12% SDS–PAGE running gel with a 4% concentrating gel. After electrotransfer, membranes were blocked with Tris-buffered saline containing 0.1% Tween-20 and 3% bovine serum albumin (BSA) during 2 h. The nitrocellulose membranes (Amersham, São Paulo/Brazil) were then incubated overnight at 4 °C with rabbit anti-Bax (1:1000; ab7977, São Paulo/Brazil), rabbit anti-Bcl-2 (1:500; ab7973, São Paulo/Brazil), rabbit anti-BDNF (1:500; sc-546, São Paulo/ Brazil), rabbit anti-proBDNF (1:500; ab72440, São Paulo/Brazil) and rabbit anti-synaptophysin (1:5000; ab32127, São Paulo/Brazil). The membranes were washed and incubated with horseradish peroxidase conjugated secondary antibodies for 1.5 h at room temperature and developed with chemiluminescence ECL kit (Amersham, São Paulo/Brazil). Densitometric analyses were performed using the NIH ImageJ software after images acquisition in the ImageQuant LAS 4000 (Amersham, São Paulo/Brazil). After stripping, ß-actin was quantified as a loading control using a mouse anti-ß-actin antibody (1:10000; sc-81178, São Paulo/Brazil), as described above.

*Statistical Analysis*

Results were calculated and expressed as the mean ± S.E.M. To analyze the differences between groups, we used the student's t-test, or multiple t-tests followed by the Holm-Sidak method when necessary. In addition, two-way ANOVA with bonferroni post hoc tests were used when appropriate. All procedures were performed using GraphPad Prism 6.0 software. The differences were considered statistically significant at $p < 0.05$.

## RESULTS

### *Alternate Fasting promotes alterations in food consumption patterns*

We showed that IF significantly alters total daily food intake and food consumption patterns in mice (Figure 1). It was observed a sharp peak of food intake after food availability on the feeding days. The pattern then followed a more normal and nocturnal intake until the food availability is turned off. Remarkably, IF mice consumed more food during the day and less food during the night, a pattern accentuated after the fifth and last IF cycle (Figure 2 C and E, respectively). Additionally, IF mice showed increased total daily food consumption (Figure 2 B, D and F).

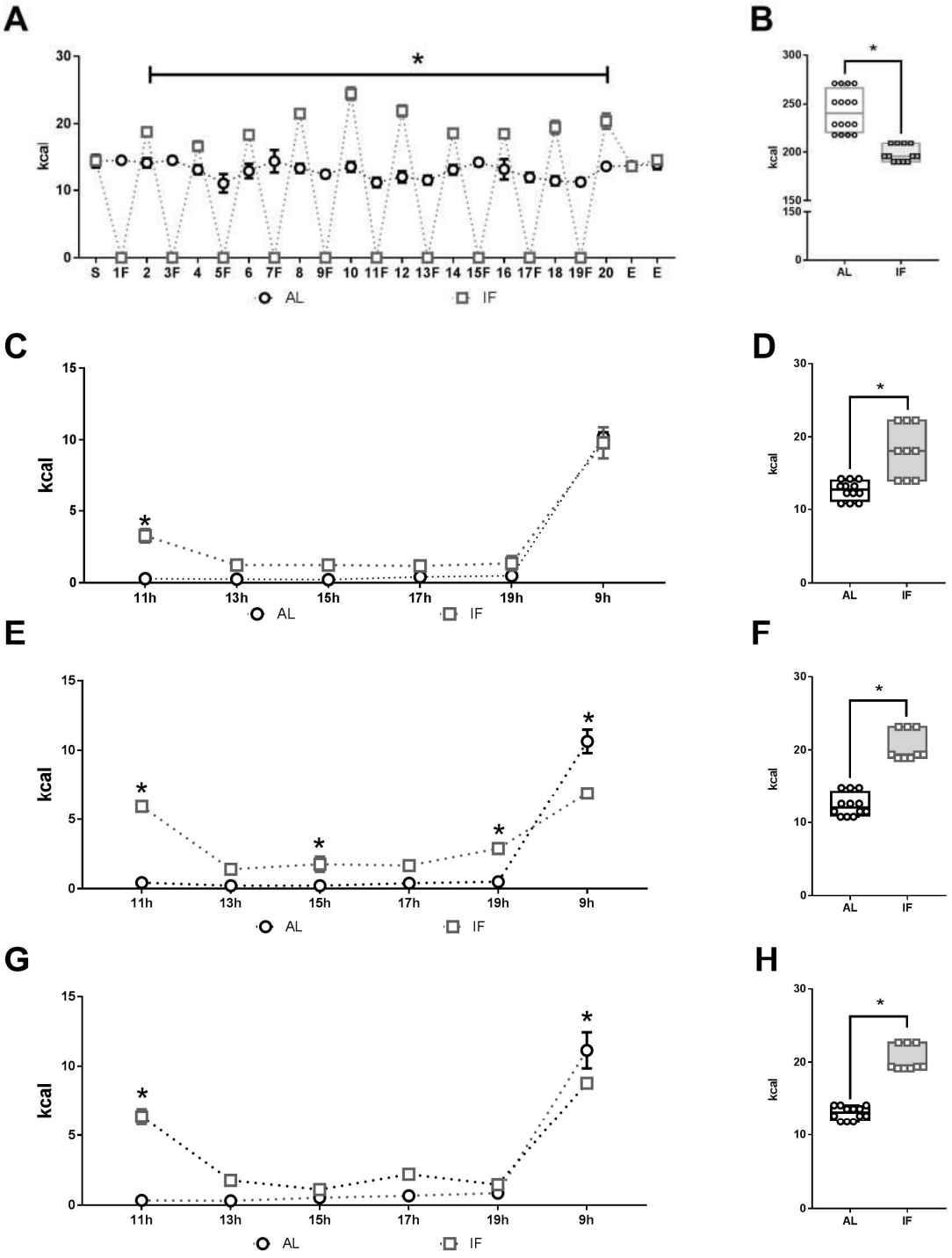


**Figure 1. Food consumption patterns assessed during the protocol (n = 9-15).** The IF protocol altered daily food intake throughout evaluated days (A) albeit IF showed lower total caloric consumption at the end of the experiment (B). It was observed a sharp peak of food intake after food availability on the feeding days. The pattern then followed a

more normal and nocturnal intake until the food availability is turned off. Remarkably, IF mice consumed more food during the day and less food during the night, a pattern accentuated after the fifth and last IF cycle (Figure 2 C and E, respectively). Additionally, IF mice showed increased total daily food consumption (Figure 2 B, D and F).

* Denotes significant difference between AL and IF groups.

***Alternate Fasting promotes metabolic shift without effects in body mass***

Regarding total ketones and blood glucose measured 2 h after a fast day, IF group showed increased levels of ketone bodies and decreased levels of blood glucose (Figure 1 A and B). When total ketones and blood glucose was assessed 24 h after the last ad-libitum day, the groups were not different (Figure 1 A and B). Body mass was accessed in 5 different time-points. After treatment, body mass was not different among groups (Figure 1C). However a significant effect for time was detected (Two-Way ANOVA: $F(5.45) = 3.072$; $p = 0.01$). Therefore, treatment promoted substrate shifts which did not influenced body mass. In addition animals showed no differences in epididymal (0.2527 ± 0.02 for AL, n = 7 and 0.2784 ± 0.04 for IF, n=6; p = 0.616) and visceral mass (0,8466 ± 0,08 for AL, n = 7 and 0,916 ± 0,07 for IF, n=6; p = 0.537).

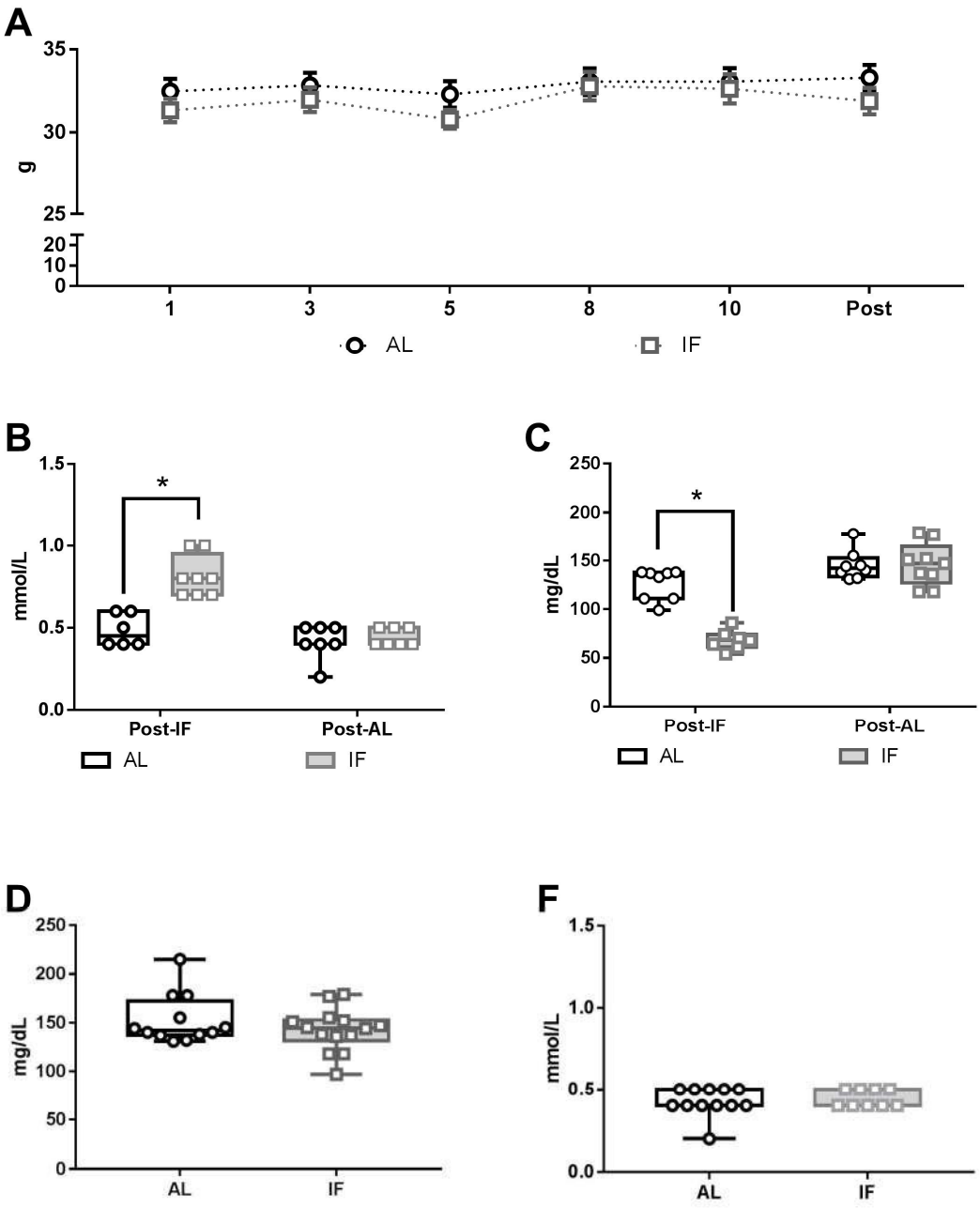


**Figure 2.** Total body mass, total ketones and blood glucose (n = 7-10).LEGENDA

* Denotes significant difference between AL and IF groups.

***Intermittent Fasting decreases anxiety-like behavior in mice without changes in overall locomotor activity***

We assessed locomotion and exploratory behaviors in the open field task, prior to the light/dark box to evaluate anxiety-like behavior. There were no differences in the parameters of exploratory and locomotor behavior assessed: total distance travelled, time in periphery area and time in the central area (Figure 3 A, B and C, respectively). However, when mice were submitted to the light/dark box, there was a significant higher percent of time in the light area for the IF group (Figure 3 D). The combination of this results indicates that IF decreased anxiety-like behavior, and this changes were independent of locomotor and exploratory alterations.

To further explore these results, we submitted a second set of animals to the open field to assess exploratory and locomotor behavior and the elevated plus maze task to evaluate anxiety-like behavior. As previously observed, there were no differences in the same parameters of exploratory and locomotor behavior (Figure 3 E, F and G) and no differences between the distance travelled between the first and second set of animals (One-Way ANOVA: $F(3.48) = 0.186$; $p = 0.9$). However, when mice were submitted to the EPM, there was a significant higher time in the total distance, time in the open arms, time in the closed arms and the ratio between open to total time for the IF group when compared to the AL group. Taking together, our combined results indicate that IF decreased anxiety-like behavior in different paradigms, and this changes were independent of locomotor and exploratory alterations.

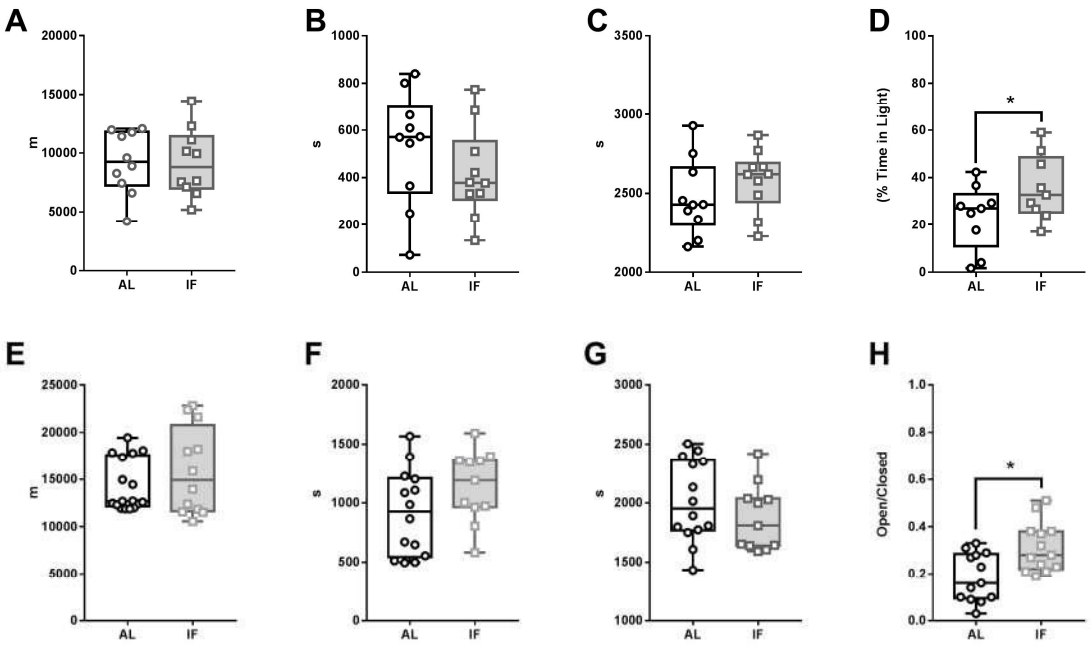


**Figure 3. Behavioral Assessment parameters.** Animals from both AL (n= 9-12) and IF (10-14) were submitted to the open field task, showing no differences in total distance travelled (A), time spent in the periphery area (B) or central area (C). However, animals from IF spent higher time in the lighter area in the Light/Dark box, indicating reduced anxiety-like behavior (D). A second set of animals were submitted to the open field task showing no differences in in total distance travelled (E), time spent in the periphery area (F) or central area (G), albeit showing increased ratio of time spent in the open arm related to closed arm in the elevated plus maze (H), another indicator of reduced anxiety-like behavior. * Denotes significant difference between AL and IF groups.

***Intermittent Fasting exerts no effects in mitochondrial function***

We explored whether intermittent fasting promotes alterations in mitochondrial bioenergetics. Initially we assessed phosphate consumption in synaptosomes, were we found no significant differences (Figure 4 A) Assessment of mitochondrial oxygen consumption rate (OCR) in different coupling states were statistically similar (Figure 4 B). Also, no differences were observed for non-mitochondrial OCR (Figure 4 C). To

further explore this result, we investigated specific mitochondrial function parameters: There were no differences between groups in OxPhos Coupling efficiency and Reserve Respiratory capacity (Figure 4 D and E, respectively).

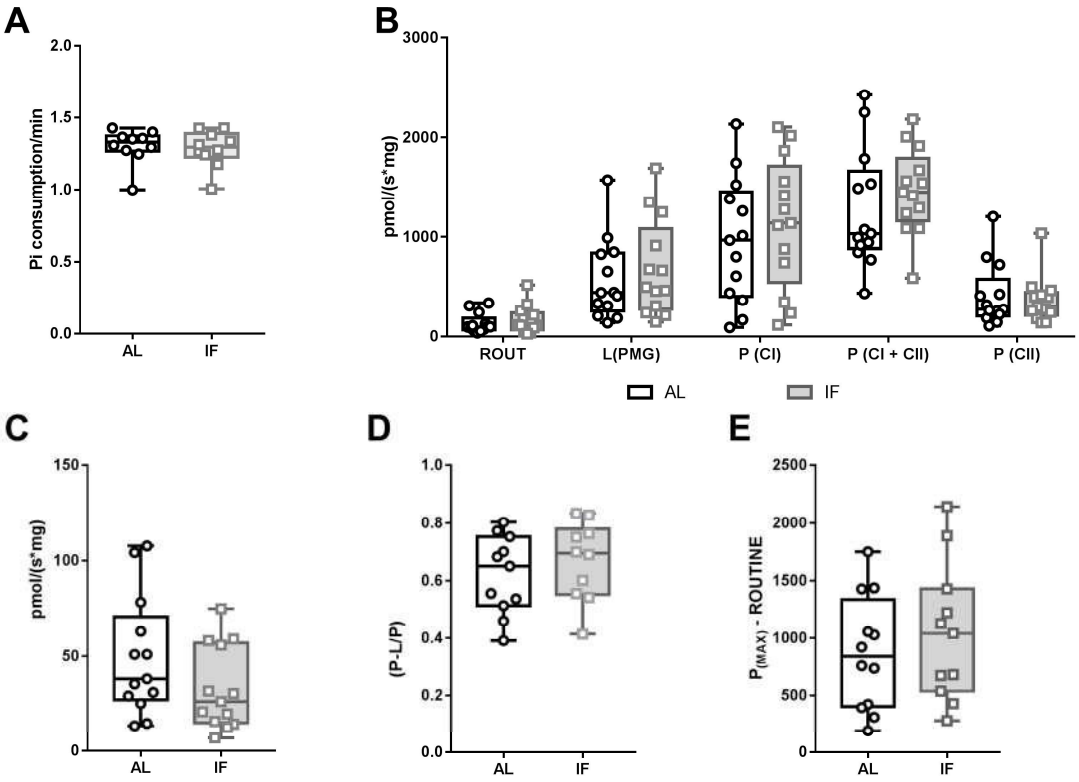


**Figure 4. Mitochondrial Metabolic Parameters (*n*=8-10).** Phosphate consumption was not different between AL and IF (A), Also, no differences were detected in OCR in different coupling states (B) and for non-mitochondrial OCR (C). Accordingly no differences were detected in the OxPhos Coupling Efficiency (D) or Reserve Respiratory Capacity (E).

***Intermittent Fasting exerts no effects in hydrogen peroxide production, membrane potential dynamics or calcium handling***

Owing that mitochondria is a predominant source of ROS production, we evaluated hydrogen peroxide production in different coupling states, which were statistically similar (Figure 5 A). Also, no differences were observed for mitochondrial membrane potential dynamics in different coupling states (Figure 5 B). Finally, we evaluated mitochondrial calcium influx after the addition of mitochondrial substrates (PMGSA) and a calcium load, showing no differences in calcium uptake. After the addition of $Na^+$, efflux was also similar between groups (Figure 5 C).

***Intermittent Fasting exerts no effects in apoptotic and neurotrophic signalling***

We explored whether intermittent fasting promotes alterations in mitochondria-associated molecular indicators of apoptotic balance (Bax/Bcl-2 ratio) showing no differences (Figure 6 A). Further we assessed neurotrophic factors (proBDNF/BDNF) showing similar responses (Figure 6 B). Finally, no differences were observed for synaptophysin, a classic indicator of synaptic plasticity (Figure 7 C).

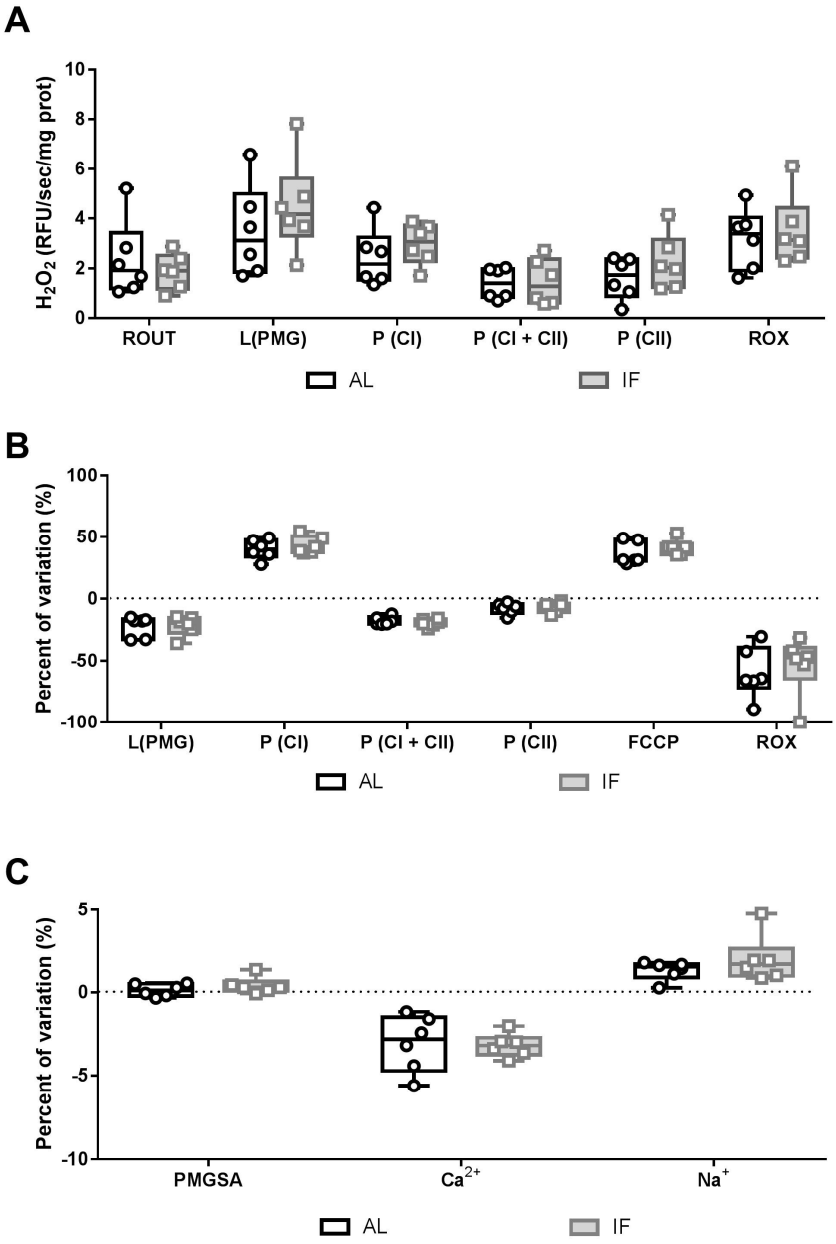


**Figure 5. Mitochondrial hydrogen peroxide production, membrane potential dynamics and calcium handling (*n*=6-8).** Owing that mitochondria is a predominant source of ROS production, we evaluated hydrogen peroxide production in different coupling states, which were statistically similar (Figure 5 A). Also, no differences were observed for mitochondrial membrane potential dynamics (Figure 5 B) or mitochondrial calcium influx and efflux in fully energized synaptosomes (Figure 5 C).

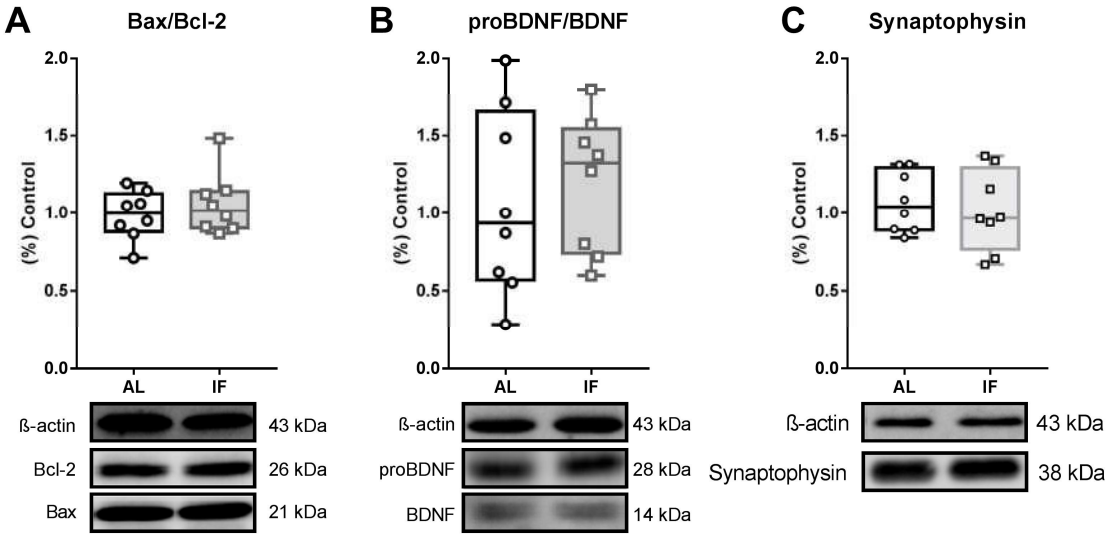


**Figure 6. Immunocontent of mitochondria-associated proteins (*n*=6-8).** Indicators of apoptotic balance (Bax/Bcl-2 ratio; A), neurotrophic factors (proBDNF/BDNF; B) and synaptic plasticity (synaptophysin; C) showed no differences.

## DISCUSSION

The beneficial effects for brain function associated to chronic IF are related to the adaptive responses to the repeating cycle of dietary restriction (causing a metabolic stress liver glycogen stores depletion, increasing circulating ketone levels) followed by a recovery period (eating, resting and sleeping), namely "Intermittent Metabolic Switching" (IMS). Although the effects of different dietary restriction paradigms on liver, muscle, and fat bioenergetics are relatively well described, studies focusing on behavioral changes related to brain bioenergetics and mitochondrial adaptability to dietary restriction are limited. Based on this, we investigated if a chronic intermittent fasting regimen aiming to induce IMS could modulate anxiety-like behavior changes and brain mitochondrial function. The present results indicate that intermittent fasting promotes anxiolytic-like behavior without detectable changes in mitochondrial oxygen consumption and metabolic parameters in brain synaptosomes.

The protocol used in our study was composed of 10 cycles of 24-hour intervals of food deprivation followed by 24-hour ad libitum food access (IF). This induced IMS (as indicated by significant differences in total ketones concentration after a fast day and no differences after 48 h of *ad libitum* feeding) without significant changes in total body mass. Although a similar protocol can induce body mass reduction,[39] differences of age could influence body mass changes. This result corroborate with Gotthardt et al., [40] reporting no body mass alterations after up to 30 days of IF in comparison to normal diets.[40] Additionally, this result was also recently reported using forty days of IF.[41] We demonstrated that male C57BL/6 mice compensate for periods of fasting by increasing their food intake, maintaining body mass similar to mice fed AL.[42-44] Strikingly, IF significantly altered the food consumption patterns and total daily food intake. This alteration in IF mice culminated in 24h food consumption comparable to the amount that AL would consume in a 48h period. Further, this adaptation in rodents has been hypothesized to reflect the learning of new feeding schedules imposed.[45] It is important to note that we limited our analysis to total body mass and fat mass weight, a limitation compared to sensible methods to detect changes in body mass composition, an important factor in IF associated benefits.[39, 46]

Chronic IF is associated with cognitive improvement.[19] However, the influence of paradigms of dietary restriction in anxiety-like behavior is contentious.[20-23] In addition, there is a temporal relationship between age and anxiogenic-like behavior [47, 48]. Considering these aspects, we used 6 months old mice in different paradigms to assess anxiety-like behavior. The light/dark paradigm is a classic method to predict anxiolytic-like or anxiogenic-like activity in mice, based on the innate aversion of rodents to brightly illuminated areas.[49] In the Light/Dark box paradigm we observed that IF promoted anxiolytic effects, as indicated by increased time in the lighted chamber. The elevated plus maze is a widely used behavioral task for anxiety behavior of rodents. The elevated plus maze relies upon the proclivity of rodents toward dark and enclosed spaces together with an unconditioned fear of open spaces and heights, instead of the presentation of noxious stimuli.[50] The evaluated parameters confirmed the anxiolytic effects promoted by IF. This is in accordance with chronic food restriction induced anxiolytic-like changes in behavior that persisted for days beyond the normalization of

food availability.[51] Additionally, our results are similar to the reported by Cabral-Costa et al.[52], were IF increased the exploration of open arms in EPM without locomotion or exploratory behavior alterations. Although both paradigms do not require prior training of animals, we assessed specific spontaneous exploratory behavior using the open field task. Our combined results indicate that IF induced an anxiolytic-like behavior without affecting spontaneous exploratory activity. To optimize our behavioral phenotyping, we implied EPM and LD in different animals, avoiding the long-lasting influences of previous test experiences and the need for inter-test intervals (of a few days or weeks) to ensure minimal effects of test history.[53] Notwithstanding, a single anxiety-related paradigm is unable to provide, a comprehensive emotional profile of animals. The observed convergence of results among the imposed behavioral paradigms assures anxiolytic effects induced by IF, as opposed to often indefinable influence of this intervention in anxiety-like behavior idiosyncratically revealed using a single paradigm.[54]

The anxiolytic-like effects of different drugs is often related to their effects on brain bioenergetics and mitochondrial mechanisms reportedly modulated by dietary restriction regimens. Our results indicated that oxygen consumption rates and biochemical coupling efficiency was not beneficially modulated by the imposed IF protocol. Additionally, no effects were detected in mitochondrial hydrogen peroxide production, calcium homeostasis or membrane potential dynamics. Modulation of mitochondrial metabolism induced by different paradigms of CR, including IF in brain are still a matter of debate. Remarkably, early reports of increased mitochondrial biogenesis and oxygen consumption in mice fed of alternate days [55] were followed by several studies expanding the controversy regarding brain metabolism.[56] Additionally, the heterogeneity of brain mitochondrial should be considered, since different mitochondrial populations (i.e. synaptic and non-synaptic) could respond differently to IF as they differ in overall bioenergetics, redox status and calcium homeostasis. [57, 58] Thus, it could be assumed that although CR paradigms or IF does not necessarily increase oxygen consumption in different mitochondrial coupling states,[15, 59] these paradigms are strongly associated to an overall mitochondrial metabolism improvement, related to redox homeostasis,[60] insulin action[61] and mitochondrial biogenesis.[62]

To further explore potential mitochondria-associated mechanism in the observed behavioral effects we evaluated the Bcl-2/Bax ratio and found no significant differences which is in accordance to recent findings with CR models. [63] The lack of difference found in proBDNF to BDNF ratio was contrary to recent findings using longer IF regimens.[64] In addition, synaptophysin levels also showed no differences. Since synaptophysin is expressed in almost all neurons in the CNS, it is often referred as an indirect indicator of synapse number.[65] Our results regarding BDNF and synaptophysin are similar to those recently reported after 11 months of IF in mice.[66] Therefore, although there is evidence that long-term caloric restriction increases Bcl-2 expression [63] and BDNF expression,[67] we believe that the differences of our protocol regarding to its duration and restriction regimen can explain these differences indicating that more severe restriction (50% of AL group) could be necessary to induce these specific trophic responses. Nevertheless, several reports indicated enhanced cognitive function after IF paradigms, without necessarily affecting other metabolic parameters. [19, 42, 68] The present results expand current literature indicating a cognitive benefit associated to IF are beyond brain bioenergetics, and can be assessed in different paradigms of anxiety-like behavior. Therefore, owing that the neuropharmacological and neuroanatomical parallels between rodent emotionality and human anxiety,[69] the present results reinforces the applicability of IF regimens to promote anxiolytic-like effects in order to reverse anxiogenic pharmacological stimuli [70] or in anxiety-related chronic conditions.[71]

In conclusion, intermittent fasting exerts anxiolytic-like behavior without affecting spontaneous exploratory activity. These behavioral responses were not associated with bioenergetic improvement in synaptosomes or the expression of neurotrophic proteins. These results highlights the necessity to explore different mechanisms promoting the benefits associated with intermittent fasting.

## REFERENCES


1. *Depression and Other Common Mental Disorders*. Global Health Estimates, ed. W.H. Organization. 2017: World Health Organization. 24.
2. Streck, E.L., et al., *Mitochondria and the central nervous system: searching for a pathophysiological basis of psychiatric disorders.* Rev Bras Psiquiatr, 2014. **36**(2): p. 156-67.
3. Shao, L., et al., *Mitochondrial involvement in psychiatric disorders.* Annals of medicine, 2008. **40**(4): p. 281-295.
4. Gardner, A., et al., *Alterations of mitochondrial function and correlations with personality traits in selected major depressive disorder patients.* J Affect Disord, 2003. **76**(1-3): p. 55-68.
5. Hollis, F., et al., *Mitochondrial function in the brain links anxiety with social subordination.* Proc Natl Acad Sci U S A, 2015. **112**(50): p. 15486-91.
6. Hauptmann, N., et al., *The metabolism of tyramine by monoamine oxidase A/B causes oxidative damage to mitochondrial DNA.* Arch Biochem Biophys, 1996. **335**(2): p. 295-304.
7. Marcocci, L., et al., *Tyramine and monoamine oxidase inhibitors as modulators of the mitochondrial membrane permeability transition.* J Membr Biol, 2002. **188**(1): p. 23-31.
8. Aikey, J.L., et al., *Testosterone rapidly reduces anxiety in male house mice (Mus musculus).* Horm Behav, 2002. **42**(4): p. 448-60.
9. Reddy, D.S. and S.K. Kulkarni, *Role of GABA-A and mitochondrial diazepam binding inhibitor receptors in the anti-stress activity of neurosteroids in mice.* Psychopharmacology (Berl), 1996. **128**(3): p. 280-92.
10. Bitran, D., et al., *Activation of peripheral mitochondrial benzodiazepine receptors in the hippocampus stimulates allopregnanolone synthesis and produces anxiolytic-like effects in the rat.* Psychopharmacology, 2000. **151**(1): p. 64-71.
11. Thiffault, C., R. Quirion, and J. Poirier, *The effect of L-deprenyl, D-deprenyl and MDL72974 on mitochondrial respiration: a possible mechanism leading to an adaptive increase in superoxide dismutase activity.* Brain Res Mol Brain Res, 1997. **49**(1-2): p. 127-36.
12. Devane, C.L., et al., *Anxiety disorders in the 21st century: status, challenges, opportunities, and comorbidity with depression.* Am J Manag Care, 2005. **11**(12 Suppl): p. S344-53.
13. Amigo, I., et al., *Caloric restriction increases brain mitochondrial calcium retention capacity and protects against excitotoxicity.* Aging Cell, 2017. **16**(1): p. 73-81.
14. López-Lluch, G., et al., *Calorie restriction induces mitochondrial biogenesis and bioenergetic efficiency.* Proceedings of the National Academy of Sciences of the United States of America, 2006. **103**(6): p. 1768.
15. Chausse, B., et al., *Intermittent Fasting Results in Tissue-Specific Changes in Bioenergetics and Redox State.* PLoS ONE, 2015. **10**(3): p. e0120413.

16. Greco, T., et al., *Ketogenic diet decreases oxidative stress and improves mitochondrial respiratory complex activity.* J Cereb Blood Flow Metab, 2016. **36**(9): p. 1603-13.
17. Gano, L.B., M. Patel, and J.M. Rho, *Ketogenic diets, mitochondria, and neurological diseases.* Journal of Lipid Research, 2014. **55**(11): p. 2211-2228.
18. Xie, K., et al., *Every-other-day feeding extends lifespan but fails to delay many symptoms of aging in mice.* Nature Communications, 2017. **8**: p. 155.
19. Singh, R., et al., *Late-onset intermittent fasting dietary restriction as a potential intervention to retard age-associated brain function impairments in male rats.* Age (Dordr), 2012. **34**(4): p. 917-33.
20. Kuhla, A., et al., *Lifelong caloric restriction increases working memory in mice.* PLoS One, 2013. **8**(7): p. e68778.
21. Riddle, M.C., et al., *Caloric restriction enhances fear extinction learning in mice.* Neuropsychopharmacology, 2013. **38**(6): p. 930-7.
22. Yamamoto, Y., et al., *Changes in behavior and gene expression induced by caloric restriction in C57BL/6 mice.* Physiological Genomics, 2009. **39**(3): p. 227-235.
23. Parikh, I., et al., *Caloric restriction preserves memory and reduces anxiety of aging mice with early enhancement of neurovascular functions.* Aging (Albany NY), 2016. **8**(11): p. 2814-2826.
24. Descamps, O., et al., *Mitochondrial production of reactive oxygen species and incidence of age-associated lymphoma in OF1 mice: effect of alternate-day fasting.* Mech Ageing Dev, 2005. **126**(11): p. 1185-91.
25. Qiu, X., et al., *Calorie restriction reduces oxidative stress by SIRT3-mediated SOD2 activation.* Cell Metab, 2010. **12**(6): p. 662-7.
26. Einat, H., P. Yuan, and H.K. Manji, *Increased anxiety-like behaviors and mitochondrial dysfunction in mice with targeted mutation of the Bcl-2 gene: further support for the involvement of mitochondrial function in anxiety disorders.* Behav Brain Res, 2005. **165**(2): p. 172-80.
27. Mattson, M.P., *Energy Intake and Exercise as Determinants of Brain Health and Vulnerability to Injury and Disease.* Cell metabolism, 2012. **16**(6): p. 706-722.
28. Raefsky, S.M. and M.P. Mattson, *Adaptive Responses of Neuronal Mitochondria to Bioenergetic Challenges: Roles in Neuroplasticity and Disease Resistance.* Free radical biology & medicine, 2017. **102**: p. 203-216.
29. Rich, N.J., et al., *Chronic caloric restriction reduces tissue damage and improves spatial memory in a rat model of traumatic brain injury.* J Neurosci Res, 2010. **88**(13): p. 2933-9.
30. Markham, A., et al., *BDNF increases rat brain mitochondrial respiratory coupling at complex I, but not complex II.* Eur J Neurosci, 2004. **20**(5): p. 1189-96.
31. Markham, A., et al., *Brain-derived neurotrophic factor-mediated effects on mitochondrial respiratory coupling and neuroprotection share the same molecular signalling pathways.* Eur J Neurosci, 2012. **35**(3): p. 366-74.
32. Kazlauckas, V., et al., *Enriched environment effects on behavior, memory and BDNF in low and high exploratory mice.* Physiology & Behavior, 2011. **102**(5): p. 475-480.

33. Takao, K. and T. Miyakawa, *Light/dark transition test for mice.* J Vis Exp, 2006(1): p. 104.
34. Komada, M., K. Takao, and T. Miyakawa, *Elevated plus maze for mice.* Journal of visualized experiments : JoVE, 2008(22): p. 1088.
35. Sims, N.R., *Rapid isolation of metabolically active mitochondria from rat brain and subregions using Percoll density gradient centrifugation.* J Neurochem, 1990. **55**(2): p. 698-707.
36. Sims, N.R. and M.F. Anderson, *Isolation of mitochondria from rat brain using Percoll density gradient centrifugation.* Nat Protoc, 2008. **3**(7): p. 1228-39.
37. Gnaiger, E., *Mitochondrial pathways and respiratory control. An introduction to OXPHOS analysis.* . 4th ed, ed. M.P. Network. 2014, Innsbruck: OROBOROS MiPNet Publications. 80.
38. Burtscher, J., et al., *Differences in mitochondrial function in homogenated samples from healthy and epileptic specific brain tissues revealed by high-resolution respirometry.* Mitochondrion, 2015. **25**: p. 104-112.
39. Li, G., et al., *Intermittent Fasting Promotes White Adipose Browning and Decreases Obesity by Shaping the Gut Microbiota.* Cell Metab, 2017. **26**(4): p. 672-685.e4.
40. Gotthardt, J.D., et al., *Intermittent Fasting Promotes Fat Loss With Lean Mass Retention, Increased Hypothalamic Norepinephrine Content, and Increased Neuropeptide Y Gene Expression in Diet-Induced Obese Male Mice.* Endocrinology, 2016. **157**(2): p. 679-691.
41. Acosta-Rodríguez, V.A., et al., *Mice Under Caloric Restriction Self-Impose a Temporal Restriction of Food Intake as Revealed by an Automated Feeder System.* Cell metabolism, 2017. **26**(1): p. 267-277.e2.
42. Halagappa, V.K.M., et al., *Intermittent fasting and caloric restriction ameliorate age-related behavioral deficits in the triple-transgenic mouse model of Alzheimer's disease.* Neurobiology of Disease, 2007. **26**(1): p. 212-220.
43. Rusli, F., et al., *A weekly alternating diet between caloric restriction and medium fat protects the liver from fatty liver development in middle-aged C57BL/6J mice.* Mol Nutr Food Res, 2015. **59**(3): p. 533-43.
44. Anson, R.M., et al., *Intermittent fasting dissociates beneficial effects of dietary restriction on glucose metabolism and neuronal resistance to injury from calorie intake.* Proc Natl Acad Sci U S A, 2003. **100**(10): p. 6216-20.
45. Krizova, E., et al., *Food intake and body weight in rats with daily food-availability restrictions.* Physiol Behav, 1996. **60**(3): p. 791-4.
46. Brandhorst, S., et al., *A periodic diet that mimics fasting promotes multi-system regeneration, enhanced cognitive performance and healthspan.* Cell metabolism, 2015. **22**(1): p. 86-99.
47. Shoji, H., et al., *Age-related changes in behavior in C57BL/6J mice from young adulthood to middle age.* Molecular brain, 2016. **9**: p. 11-11.
48. Bedrosian, T.A., et al., *Altered temporal patterns of anxiety in aged and amyloid precursor protein (APP) transgenic mice.* Proceedings of the National Academy of Sciences of the United States of America, 2011. **108**(28): p. 11686-11691.

49. Hascoët, M., M. Bourin, and B.Á. Nic Dhonnchadha, *The mouse ligth-dark paradigm: A review.* Progress in Neuro-Psychopharmacology and Biological Psychiatry, 2001. **25**(1): p. 141-166.
50. Walf, A.A. and C.A. Frye, *The use of the elevated plus maze as an assay of anxiety-related behavior in rodents.* Nature protocols, 2007. **2**(2): p. 322-328.
51. Inoue, K., et al., *Reduction of anxiety after restricted feeding in the rat: implication for eating disorders.* Biological Psychiatry, 2004. **55**(11): p. 1075-1081.
52. Cabral-Costa, J.V., et al., *Intermittent fasting uncovers and rescues cognitive phenotypes in PTEN neuronal haploinsufficient mice.* 2018. **8**(1): p. 8595.
53. Paylor, R., et al., *The use of behavioral test batteries, II: effect of test interval.* Physiol Behav, 2006. **87**(1): p. 95-102.
54. Ramos, A., *Animal models of anxiety: do I need multiple tests?* Trends Pharmacol Sci, 2008. **29**(10): p. 493-8.
55. Nisoli, E., et al., *Calorie restriction promotes mitochondrial biogenesis by inducing the expression of eNOS.* Science, 2005. **310**(5746): p. 314-7.
56. Hancock, C.R., et al., *Does calorie restriction induce mitochondrial biogenesis? A reevaluation.* Faseb j, 2011. **25**(2): p. 785-91.
57. Stauch, K.L., P.R. Purnell, and H.S. Fox, *Quantitative proteomics of synaptic and nonsynaptic mitochondria: insights for synaptic mitochondrial vulnerability.* J Proteome Res, 2014. **13**(5): p. 2620-36.
58. Yarana, C., et al., *Synaptic and nonsynaptic mitochondria demonstrate a different degree of calcium-induced mitochondrial dysfunction.* Life Sci, 2012. **90**(19-20): p. 808-14.
59. Ferguson, M., et al., *Effect of long-term caloric restriction on oxygen consumption and body temperature in two different strains of mice.* Mechanisms of ageing and development, 2007. **128**(10): p. 539-545.
60. Cerqueira, F.M., et al., *Calorie restriction increases cerebral mitochondrial respiratory capacity in a NO•-mediated mechanism: Impact on neuronal survival.* Free Radical Biology and Medicine, 2012. **52**(7): p. 1236-1241.
61. Lu, J., et al., *Alternate Day Fasting Impacts the Brain Insulin Signaling Pathway of Young Adult Male C57BL/6 Mice.* Journal of neurochemistry, 2011. **117**(1): p. 154-163.
62. Cassano, P., et al., *Tissue-specific effect of age and caloric restriction diet on mitochondrial DNA content.* Rejuvenation Res, 2006. **9**(2): p. 211-4.
63. Lončarević-Vasiljković, N., et al., *Dietary restriction suppresses apoptotic cell death, promotes Bcl-2 and Bcl-xl mRNA expression and increases the Bcl-2/Bax protein ratio in the rat cortex after cortical injury.* Neurochemistry International, 2016. **96**: p. 69-76.
64. Arumugam, T.V., et al., *Age and energy intake interact to modify cell stress pathways and stroke outcome.* Ann Neurol, 2010. **67**(1): p. 41-52.
65. Schmitt, U., et al., *Detection of behavioral alterations and learning deficits in mice lacking synaptophysin.* Neuroscience, 2009. **162**(2): p. 234-243.
66. Li, L., Z. Wang, and Z. Zuo, *Chronic intermittent fasting improves cognitive functions and brain structures in mice.* PloS one, 2013. **8**(6): p. e66069-e66069.

67. Lee, J., W. Duan, and M.P. Mattson, *Evidence that brain-derived neurotrophic factor is required for basal neurogenesis and mediates, in part, the enhancement of neurogenesis by dietary restriction in the hippocampus of adult mice.* J Neurochem, 2002. **82**(6): p. 1367-75.
68. Hu, Y. and M. Zhang, *Postoperative intermittent fasting prevents hippocampal oxidative stress and memory deficits in a rat model of chronic cerebral hypoperfusion.* 2018.
69. Wegener, G., A.A. Mathe, and I.D. Neumann, *Selectively bred rodents as models of depression and anxiety.* Curr Top Behav Neurosci, 2012. **12**: p. 139-87.
70. Ebrahimian, Z., et al., *Behavioral and Stereological Analysis of the Effects of Intermittent Feeding Diet on the Orally Administrated MDMA ("ecstasy") in Mice.* Innov Clin Neurosci, 2017. **14**(1-2): p. 40-52.
71. Levay, E.A., et al., *Effects of adult-onset calorie restriction on anxiety-like behavior in rats.* Physiology & Behavior, 2007. **92**(5): p. 889-896.

## Anexo III: Elevated glutamate and lactate predict brain death after severe head trauma

ANNALS of Clinical and Translational Neurology
Open Access
ANA American Neurological Association since 1875

RESEARCH ARTICLE

# Elevated glutamate and lactate predict brain death after severe head trauma

Marco A. Stefani[1], Rafael Modkovski[1], Gisele Hansel[2], Eduardo R. Zimmer[2,3], Afonso Kopczynski[2], Alexandre P. Muller[4], Nathan R. Strogulski[2], Marcelo S. Rodolphi[2], Randhall K. Carteri[2], André P. Schmidt[2], Jean P. Oses[5], Douglas H. Smith[6] & Luis V. Portela[2]

[1]Laboratory of Neuroanatomy, Department of Morphological Sciences, Federal University of Rio Grande do Sul (UFRGS), Porto Alegre, RS, Brazil
[2]Laboratory of Neurotrauma, Department of Biochemistry, Post-graduation Program in Biochemistry, Federal University of Rio Grande do Sul (UFRGS), Porto Alegre, RS, Brazil
[3]Brain Institute of Rio Grande do Sul (BraIns), Pontifical Catholic University of Rio Grande do Sul (PUCRS), Porto Alegre, RS, Brazil
[4]Laboratory of Exercise, Biochemistry and Physiology, University of Southern Santa Catarina (UNESC), Criciúma, Santa Catarina, Brazil
[5]Graduate Program in Health and Behavior, Catholic University of Pelotas, Pelotas, RS, Brazil
[6]Penn Center for Brain Injury and Repair and Department of Neurosurgery, Perelman School of Medicine, University of Pennsylvania, Philadelphia, Pennsylvania 19104

**Correspondence**
Luis V. Portela, Department of Biochemistry, ICBS, UFRGS, 2600 Ramiro Barcelos Street, 90035-003, Porto Alegre, RS, Brazil.
Tel: 55 51 33085558; Fax: 55 51 33085544;
E-mail: roskaportela@gmail.com

**Funding Information**
This work was supported by Coordenação de Aperfeiçoamento de Pessoal de Nível Superior PNPD 1663, Fundação de Amparo à Pesquisa do Estado do Rio Grande do Sul 1010267, Conselho Nacional de Desenvolvimento Científico e Tecnológico 4011645/2012-6, 5465346/2014-6

Received: 23 February 2017; Accepted: 31 March 2017

***Annals of Clinical and Translational Neurology*** **2017; 4(6): 392–402**

doi: 10.1002/acn3.416

## Abstract

**Objective**: Clinical neurological assessment is challenging for severe traumatic brain injury (TBI) patients in the acute setting. Waves of neurochemical abnormalities that follow TBI may serve as fluid biomarkers of neurological status. We assessed the cerebrospinal fluid (CSF) levels of glutamate, lactate, BDNF, and GDNF, to identify potential prognostic biomarkers of neurological outcome. **Methods**: This cross-sectional study was carried out in a total of 20 consecutive patients (mean [SD] age, 29 [13] years; M/F, 9:1) with severe TBI Glasgow Coma Scale ≤ 8 and abnormal computed tomography scan on admission. Patients were submitted to ventricular drainage and had CSF collected between 2 and 4 h after hospital admission. Patients were then stratified according to two clinical outcomes: deterioration to brain death (nonsurvival, $n = 6$) or survival (survival, $n = 14$), within 3 days after hospital admission. CSF levels of brain-derived substances were compared between nonsurvival and survival groups. Clinical and neurological parameters were also assessed. **Results**: Glutamate and lactate are significantly increased in nonsurvival relative to survival patients. We tested the accuracy of both biomarkers to discriminate patient outcome. Setting a cutoff of >57.75, glutamate provides 80.0% of sensitivity and 84.62% of specificity (AUC: 0.8214, 95% CL: 54.55–98.08%; and a cutoff of >4.65, lactate has 100% of sensitivity and 85.71% of specificity (AUC: 0.8810, 95% CL: 54.55–98.08%). BDNF and GDNF did not discriminate poor outcome. **Interpretation**: This early study suggests that glutamate and lactate concentrations at hospital admission accurately predict death within 3 days after severe TBI.

## Introduction

Traumatic brain injury (TBI) is a leading cause of mortality and morbidity among young individuals in low- and middle-income countries. In Brazil, the estimated incidence of TBI is 400 cases per 100.000 inhabitants.[1] TBI survivors, commonly suffer persisting cognitive dysfunction, and have a heightened risk of premature death, progressive neurodegeneration, and Alzheimer's disease.[2,3] The pathophysiological mechanisms governing short- and long-term TBI outcomes include axonal injury[3], blood-brain barrier disruption[4], glutamate neurotoxicity[5], neuroenergetic deficits[6], and lack of neurotrophic support.[7] These neurochemical signatures also provide an opportunity for identifying molecules in body fluids that may serve as candidate biomarkers with putative clinical relevance.[8,9]

Glutamate, the predominant excitatory neurotransmitter in the mammalian brain, may become excitotoxic at high extracellular concentrations through overstimulation of glutamate receptors.[5,10] Remarkably, high concentrations of extracellular glutamate are commonly observed after severe TBI, the magnitude of which correlates with increased intracranial pressure (ICP) and poor clinical outcomes.[11–14] Immediately after TBI, there is an exacerbated glutamate-induced neuronal calcium influx and ionic imbalance, which evokes membrane depolarization and further glutamate release. As consequence, the membrane pumps work to rapidly restore the membrane gradients thereby increasing the glucose flux through glycolytic pathway and lactate production.[8,10] However, extracellular lactate may arise not only from neuronal glycolysis. The astrocyte-neuron lactate shuttle model proposes a metabolic coupling between astrocytes and neurons based on the glutamate-stimulated glycolysis in astrocytes, and the extrusion of lactate to support the energy demands associated with increased neuronal activity.[15] Based on this concept, one could argue that increased extracellular brain lactate concentrations after TBI may reflect increased astrocytic metabolic responsiveness to high glutamate concentrations. This mechanism seems to be important for the survival of severe TBI patients since hypertonic sodium lactate infusion improves ICP, hemodynamic, and energetic parameters[16,17], whereas disturbances in this metabolic coupling are associated with worse prognosis.[18]

Moreover, experimental studies have demonstrated that in response to increased extracellular glutamate levels, astrocytes and neurons release brain-derived neurotrophic factor (BDNF) and the glial cell line-derived neurotrophic factor (GDNF). Notably, both of these neurotrophins modulate the activity of glutamatergic neurotransmission, which includes neuronal synaptic release and astrocytic glutamate uptake transporters activity/expression[19,20], while BDNF specifically modulates the expression of the high-affinity monocarboxylate transporters 2 (MCT2) in neurons.[21] The MCT2 controls the influx of energetic substrates including lactate to the oxidative metabolism in neurons.[21] Based on the aforementioned, increased concentration of these molecules could likely indicate trophic responses intending to halt glutamatergic toxicity and improve metabolic support.

Although not yet shown in TBI patients, demonstration of a mechanistic interaction between neurotrophins, lactate, and glutamate neurotransmission may shed light on the high incidence of death in the initial days after a severe TBI. In addition, this interaction may provide an opportunity to evaluate relative concentrations of neurotrophins and glutamate levels as potential biomarkers with prognostic value. Indeed, since clinical neurological assessment is challenging for severe TBI patients in the acute setting, due to the common comatose state, etc., fluid biomarkers are being vigorously pursued.

Therefore, in this study, we assessed the cerebrospinal fluid (CSF) concentrations of glutamate, lactate, BDNF, and GDNF at hospital admission, to identify prognostic biomarkers of clinical outcomes.

## Subjects and Methods

### Study population and clinical management

The cohort used in this study was previously established in Böhmer et al., 2011[2]. Briefly, a cross-sectional study was carried out between 2006 and 2009 with a total of 20 consecutive patients with severe TBI, presenting score 8 or less in Glasgow Coma Scale (GCS) and abnormal computed tomography (CT) scan on their admission to the Emergency Unit of Cristo Redentor Hospital (Porto Alegre, RS, Brazil). CT classification was performed according to Eisenberg et al., 1990[22]. Further details regarding patient's CT on admission were available on Böhmer et al., 2011[2]. The TBI patients were predominantly young male (mean [SD] age, 29 [13] years; M/F, 9:1) and were admitted to emergency mainly because of motor vehicle accidents. The inclusion criteria for participating in this study was patients with isolated severe TBI, with no previous history of inflammatory, metabolic, and neuropsychiatric disorders that could influence the biomarkers' concentrations and clinical outcomes. The exclusion criteria were diabetes, drug abuse, and neuropsychiatric disorders. The characteristics of patients are shown in Table 1. Severe TBI patients were submitted to Hospital Cristo Redentor emergency clinical protocol as previously reported by our group[2]. Briefly, after intubation, patients were supported with continuous mild hyperventilation induced with arterial carbon dioxide tension (PaCO2 between 30 and 35 mmHg). Mean arterial pressure was kept at satisfactory levels to allow cerebral perfusion pressure (mean arterial blood pressure minus intracerebral pressure) above 60 mmHg. Immediately after initial resuscitation, one intracranial pressure monitor (Codman® microsensor) was introduced into the brain parenchyma through a right frontal trepanation. Ventriculostomy was performed to monitor ICP and to allow drainage of CSF when the ICP exceeded 20 mmHg, which was the proposed protocol of Brain Trauma Foundation for clinical management of severe TBI patients with GCS of 8 or less and abnormalities on the computed tomography. The clinical management followed the same standard protocol for ICP management in all patients. CSF drained from the intraventricular catheter was collected via an extraventricular drainage system. The

 

intraventricular catheter was removed when patients died, or when survival patients presented stable ICP for 24 h. The primary ventricular CSF samples collected between 2 and 4 h after hospitalization were used to determine biomarkers' concentrations. For an overview about advantages and disadvantages of CSF as a matrix to measure candidate biomarkers of brain injury, please see Zetteberg et al., 2016.[23]

Intracranial mass lesions associated with midline displacement greater than 5 mm were surgically removed when necessary. No undesirable complications associated with intraventricular catheter placement or ICP monitoring including intracranial hemorrhage or infection were observed. Intracranial hypertension was managed initially in all patients by conventional ICP reduction therapy, such as CSF drainage, mannitol bolus, and mild hyperventilation (PaCO2 up to 30 mmHg). In patients with sustained high ICP (from 20 mmHg) and unresponsive to conventional therapy, other alternatives were employed, including barbiturate coma, hyperventilation ($PaCO_2$ < 30 mmHg), control with jugular bulb monitoring, and decompress craniotomy.

Moreover, 20 healthy subjects (ASA I status) scheduled for elective urological, gynecological, general, or vascular procedures were selected as age and sex-matched controls. Surgeries essentially included inguinal or umbilical herniorrhaphy, perineoplasty, abdominal hysterectomy, vaginal hysterectomy, myomectomy, transurethral prostate or bladder resection, prostatectomy, and saphenectomy. These subjects were interviewed for the absence of cognitive or neurological disorders.[2] Control subjects received a spinal anesthesia technique. Experienced anesthesiologists collected the CSF. The first 0.5 mL of CSF aspirated was discarded to reduce cells contamination. The CSF samples were inspected visually and discarded if blood contamination was present. A total of 0.5 mL of CSF was collected from the patients after successful subarachnoid puncture and before the intrathecal injection of anesthetics or analgesics. The CSF samples from patients and controls were immediately centrifuged at 10,000*g* in an Eppendorf centrifuge during 5 min to obtain cell-free supernatants and stored at −70°C within 30 min of collection.

Informed consent for participating in this study was obtained from patients' family members and directly from healthy individuals, according to the Declaration of Helsinki. At the moment when the consent form was applied, family members were also questioned about patient's lifestyle and preexistent diseases. The local institutional Ethics Committee approved this protocol (project number 0038.0.164.165-05).

**Table 1.** Demographics and clinical characteristics of patients.

| Variables | Survival ($n$ = 14) (median ± range) | NonSurvival ($n$ = 6) (median ± range) | $P$ -value |
|---|---|---|---|
| Age | 29 (17–53) | 21.5 (16–38) | $P$ = 0.140 |
| ICP | 8.5 (3–20) | 10 (2–45) | $P$ = 0.095 |
| MAP | 93 (70–124) | 92.5 (63–113) | $P$ = 0.534 |
| CPP | 87.5 (57–114) | 82 (21–88) | $P$ = 0.149 |
| GCS | 6 (4–8) | 4 (4–7) | $P$ = 0.085 |
| CSF glucose (mg/dL)[1] | 108.2 (75.9–129.4) | 118.3 (80.7–191.9) | $P$ = 0.341 |

ICP, intracranial pressure; MAP, mean arterial pressure; CPP, cerebral perfusion pressure; GCS, Glasgow coma scale.
[1]CSF glucose levels (controls): median: 55.29 range: 29.8–94.1 mg/dL.

## Outcome measures

Considering that patients died up to 3 days from hospital admission, we decided to use 3 days as an arbitrary cutoff point. Patients were then stratified according to two clinical outcomes: deterioration to brain death (nonsurvival $n$ = 6) or survival (survival, $n$ = 14), within 3 days after hospital admission. The ICP, hemodynamic, and metabolic variables including mean arterial blood pressure and cerebral perfusion pressure were daily assessed.[22] Two years after discharge, phone calls were placed to confirm that survival patients remained alive, and to investigate the grade of long-term functional disability. TBI patients were then assessed for the modified Rankin Scale (mRS) and scored by an experienced neurologist (R.M). The mRS score is the commonly used outcome classification scale for disabilities and handicaps after cerebral stroke or other causes of neurological disability. The scale has six grades ranging from 0 (fully independent) to grade 6 (dead), and is considered a reliable endpoint for clinical neurological studies.[24]

## CSF Biomarkers analysis

### Glutamate assay

Glutamate concentration in TBI patients and controls were analyzed in 25 $\mu$L of the CSF cell-free supernatant samples through high-performance liquid chromatography (HPLC). Briefly, samples were filtered and derivatized with o-phthalaldehyde and mercaptoethanol. CSF samples were separated by reverse phase column (Supelcosil LC-18, 250 mm × 4.6 mm, Supelco) in a Shimadzu Instruments liquid chromatograph. The mobile phase flowed at a rate of 1.4 mL/min at 24°C. Buffer composition is A:

 

0.04 mol/L sodium dihydrogen phosphate monohydrate buffer, pH 5.5, containing 20% of methanol; and B: 0.01 mol/L sodium dihydrogen phosphate monohydrate buffer, pH 5.5, containing 80% of methanol. The gradient profile was modified according to the content of buffer B in the mobile phase: 0% at 0.00 min, 25% at 13.75 min, 100% at 15.00–20.00 min, and 0% at 20.01–25.00 min. Absorbance was read in a Shimadzu fluorescence detector, with excitation and emission being 360 nm and 455 nm, respectively. The concentration was expressed in $\mu$mol/L.[22]

### Lactate, BDNF, and GDNF assays

The lactate level was measured using a commercial kit manufactured by Interteck-Katal Biotechnology, Brasil. Calibration factors were determined using a standard of lithium lactate (4.44 mmol/L). Lactate concentration is expressed as mmol/L (24). The levels of BDNF and GDNF were assayed using commercially available enzyme-linked immunosorbent assay kits (ELISA) (BDNF ref. DBNT00 and GDNF ref. DY212; R&D Systems Inc., Minneapolis, MN, USA.). The CSF concentrations of BDNF or GDNF were determined by measuring the absorbance of standard and samples at 450 nm with a SpectraMax M5 (Molecular Devices). The calibration curve was linear up to 1000 pg/mL for BDNF, and up to 2000 pg/mL to GDNF (25). The concentrations are expressed as pg/mL. All samples and standards were carried out in duplicate within the same experiment, and the variation within each duplicate was <5%.

### Statistical analysis

We submitted data to Kolmogorov–Smirnov testing for normality evaluation. Glutamate, lactate, BDNF, and GDNF values were fitted in a standard distribution curve and were therefore subjected to nonparametric analyses. Comparisons between groups were performed by two-tailed Mann–Whitney test. ROC curves were created to explore the ability of biomarkers to predict survival and nonsurvival patients after severe TBI. Estimates of the areas under the curves (AUCs) were obtained, with an AUC of 0.5 indicating no discrimination and an AUC of 1.0 indicating a perfect diagnostic test. Bivariate correlations among biomarkers were performed by Spearman correlation test. Spearman cross-correlation analyses among biomarkers was also performed and corrected by Bonferroni Method. All numerical variables are presented as mean $\pm$ standard deviation (S.D.). $P$ values at $\leq 0.05$ were considered statistically significant. All analyses were performed using GraphPad Prism 5.0 or Matlab 2014b.

## Results

### CSF biomarkers glutamate, lactate, BDNF, and GDNF

The level of the excitatory neurotransmitter glutamate in TBI patients (nonsurvival: median [IQR]: 61.25 [41.40–88.20] $\mu$mol/L and survival: 25.35 [5.00–93.70] $\mu$mol/L) was significantly higher than control group (median [IQR]: 2.6 [2.1–3.3] $\mu$mol/L) ($P < 0.0001$). Also, glutamate levels were significantly increased in nonsurvival relative to survival patients ($P = 0.0256$) (Fig. 1A).

Similarly, we found that CSF lactate levels in TBI group were significantly increased compared with control group (median [IQR]: 1.5 [0.4–2.8] mmol/L) ($P < 0.0001$). Further, there was a significant difference in lactate level between nonsurvival (median [IQR]: 6.05 [5.00–9.10] mmol/L) relative to survival group (median [IQR]: 3.6 [1.6–8.1] mmol/L) ($P = 0.0060$) (Fig. 1B).

In contrast to glutamate and lactate, while CSF BDNF levels in TBI patients were significantly different from control group (median [IQR]: 190.8 [161.0–210.4] pg/mL ($P = 0.0001$), BDNF levels in nonsurvival (median [IQR]: 263.0 [216.5–311.9] pg/mL) were not significantly different from survival group (median [IQR] 231.7 [174.0–552.6] pg/mL) ($P = 0.4072$) (Fig. 1C).

Moreover, there was no significant difference in CSF GDNF levels between control (median [IQR]: 338.9 [306.8–440.9] pg/mL) and TBI, and between nonsurvival (median [IQR]: 317.7 [303.0–473.9] pg/mL) and survival patients (median [IQR] 351.7[287.6–788.7] pg/mL ($P = 0.3015$) (Fig. 1D).

The dynamic heat map (Fig. 1E) provides a visualization of the biomarker signatures. We can visualize that both lactate and glutamate displayed a distinct profile in the survival and nonsurvival patients, whereas BDNF and GDNF showed no evident discriminatory profile.

### CSF biomarkers and bivariate correlation analysis

To provide insights regarding the quantitative relationship between biomarkers, we tested the correlation coefficient in the TBI and Control groups pooled together. There was significant statistical correlation between CSF levels of glutamate and lactate ($r = 0.7051$; $P = 0.053$; Fig. 2A), glutamate and BDNF ($r = 0.6983$; $P = 0.024$) (Fig. 2B), and BDNF and lactate ($r = 0.7491$; $P = 0.039$) (Fig. 2D). The correlations between GDNF and glutamate ($r = -0.01794$; $P = 0.462$) (Fig. 2C), GDNF and BDNF ($r = -0.004$; $P = 0.574$) (Fig. 2F), and GDNF and lactate ($r = 0.1368$; $P = 0.513$) (Fig. 2E) did not reach statistical significance.

 

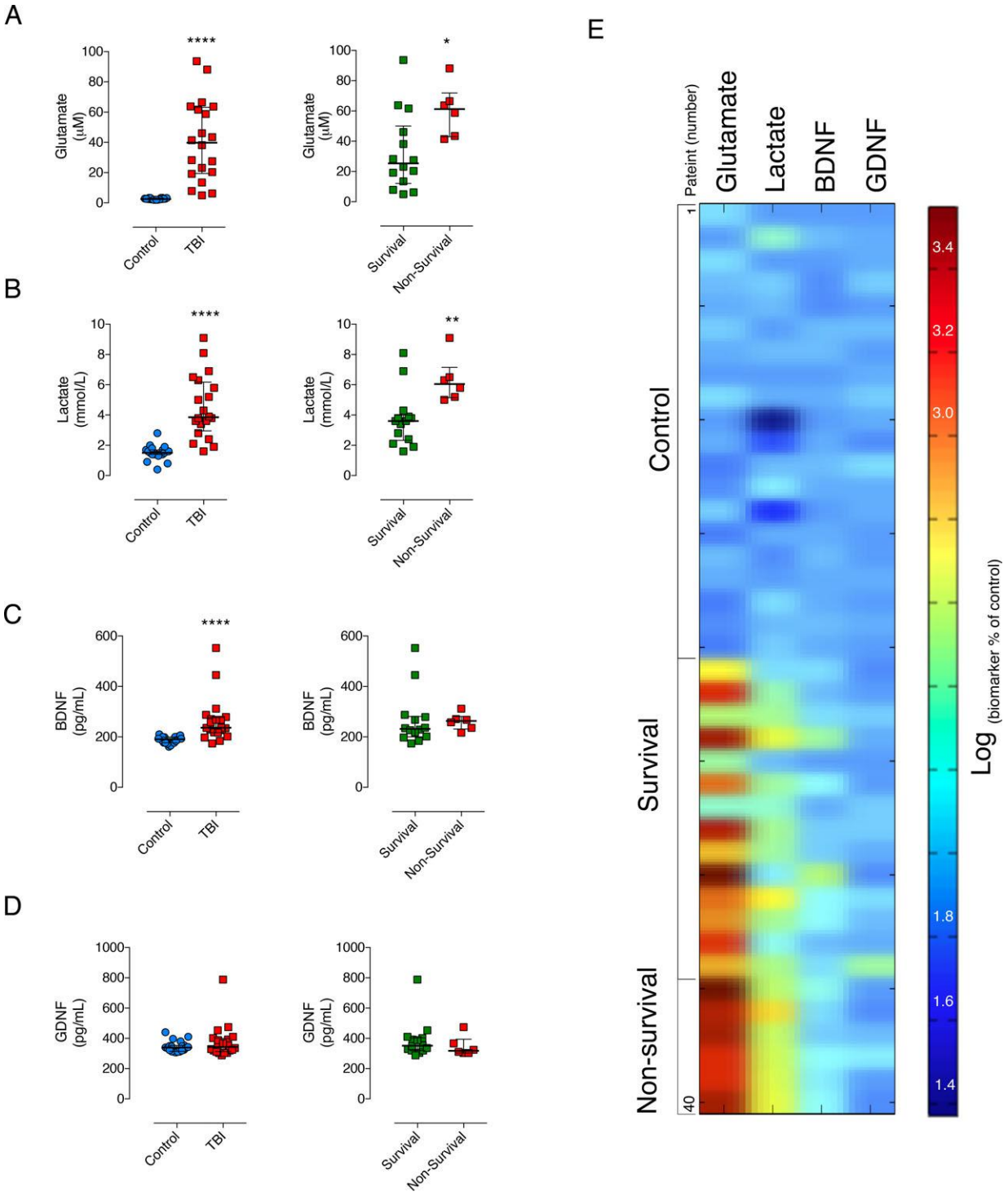


**Figure 1.** Cerebrospinal fluid biomarkers in controls and severe TBI patients (survival and nonsurvival). The CSF levels of glutamate (A), lactate (B), and BDNF (C) in TBI group at hospital admission were significantly different than control group ($n = 20$ per group, $^{****}P > 0.0001$). In addition, glutamate and lactate levels were significantly higher in nonsurvival ($n = 6$) relative to survival patients ($n = 14$) ($^{*}P = 0.0256$ and $^{**}P = 0.0060$, respectively). The GDNF level was not different between control and TBI groups, (D). Both BDNF (C, right panel) and GDNF (D, right panel) were not different between survival and nonsurvival TBI patients. The dynamic heatmap shows a neurochemical signature regarding the profile of the biomarkers in control subjects and TBI patients (E). Horizontal lines indicate median and interquartile range. The dynamic heatmap scale represents normalized (log) percent of change in relation to controls.

 

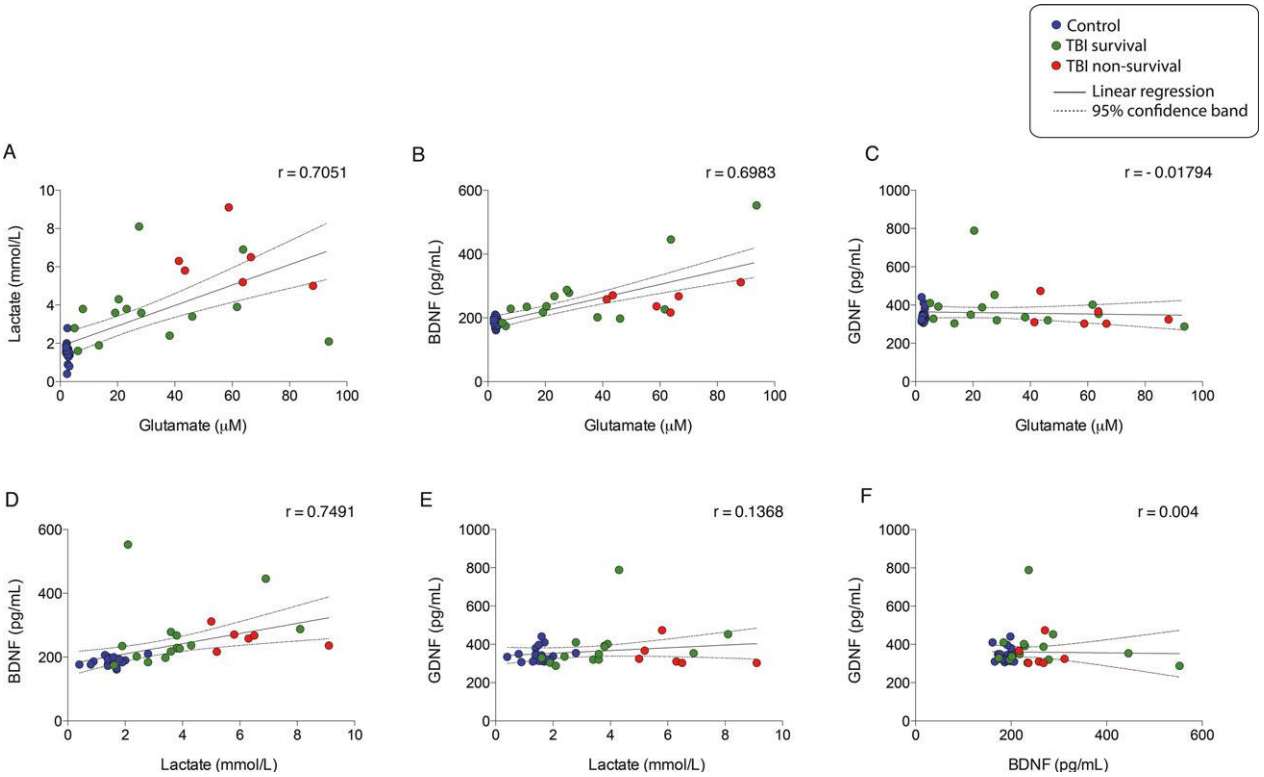


**Figure 2.** Spearman bivariate correlation analyses between cerebrospinal fluid biomarkers. There were statistically significant correlations between glutamate and lactate (A) ($r$ = 0.7051; $P$ = 0.053), glutamate and BDNF (B) ($r$ = 0.6983; $P$ = 0.024), Lactate and BDNF (D)($r$ = 0.7491; $P$ = 0.039). GDNF did not show statistically significant correlations with glutamate (C), lactate (E), and BDNF (F).

The statistical correlations between the CSF biomarkers and clinical outcomes are showed in Table 2. There were no significant correlations between fluid biomarkers concentrations at admission and clinical outcomes measured up to 3 days after hospital admission. In contrast, glutamate and lactate were significantly correlated with modified Rankin Scale (mRS). Correlation coefficients for Glutamate vs. mRS, and Lactate vs. mRS were ($r$ = 0.6427, $P$ = 0.002) and ($r$ = 0.4635, $P$ = 0.03), respectively.

## ROC curves and biomarkers associations

Given the CSF concentrations of glutamate and lactate showed the highest level in nonsurvival patients, we evaluated the accuracy of those tests as early prognostic biomarkers of neurological deterioration. The area under the ROC curve (AUC) indicate how well glutamate and lactate can discriminate patients that will survive from patients that will evolve to death up 3 days in the intensive unit care. The ROC curve was achieved from glutamate and lactate up to 3 days from admission in relation to death (Fig. 3A and B). The specificity rate is showed in function of sensitivity rate at different cutoff points. Setting

**Table 2.** Correlation between CSF biomarkers and clinical outcomes in TBI survival and nonsurvival groups.

| Variables | Spearman ($r$) | $P$ -value |
|---|---|---|
| Glutamate vs. ICP | 0.34 | 0.15 |
| Lactate vs. ICP | 0.09 | 0.72 |
| BDNF vs. ICP | 0.16 | 0.50 |
| GDNF vs. ICP | 0.20 | 0.41 |
| Glutamate vs. MAP | −0.21 | 0.37 |
| Lactate vs. MAP | 0.01 | 0.98 |
| BDNF vs. MAP | −0.05 | 0.84 |
| GDNF vs. MAP | 0.21 | 0.37 |
| Glutamate vs. CPP | −0.36 | 0.12 |
| Lactate vs. CPP | −0.15 | 0.53 |
| BDNF vs. CPP | −0.18 | 0.46 |
| GDNF vs. CPP | 0.01 | 0.96 |
| Glutamate vs. GCS | −0.15 | 0.54 |
| Lactate vs. GCS | −0.39 | 0.09 |
| BDNF vs. GCS | 0.13 | 0.58 |
| GDNF vs. GCS | −0.16 | 0.49 |

ICP, Intracranial pressure; BDNF, brain-derived neurotrophic factor; GDNF, glial cell line-derived neurotrophic factor; MAP, Mean arterial pressure; CPP, Cerebral perfusion pressure; GCS, Glasgow coma scale.

 

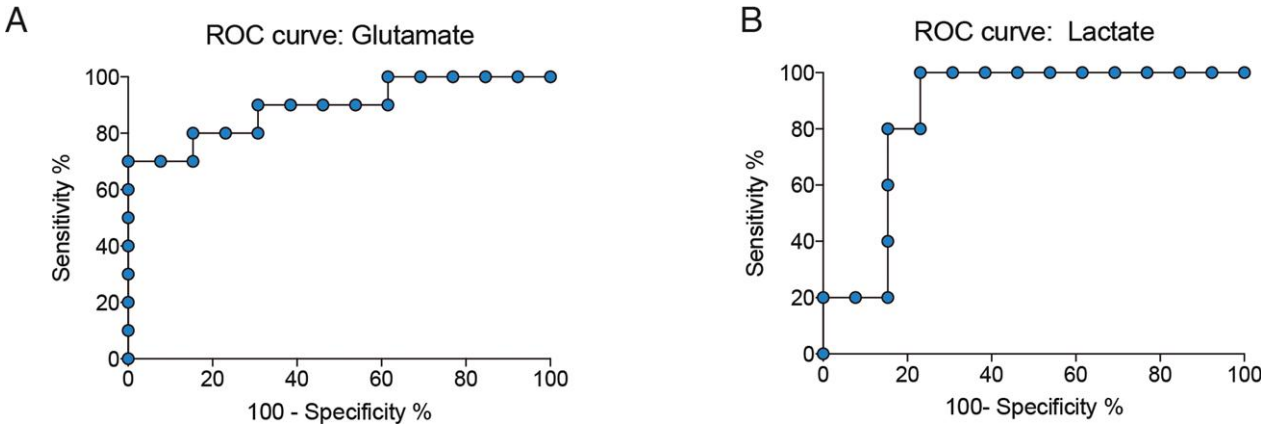


**Figure 3.** Diagnostic accuracy of biomarkers predicts brain death. Area under the receiver-operating characteristic curve (AUC) for CSF glutamate (A) and lactate (B) concentrations. ROC curves based on glutamate and lactate were used as a predictor of death in TBI patients. The cutoff for glutamate was set at >57.75, providing 80% of sensitivity and 84.62% of specificity (AUC: 0.8214, 95% CI, CL: 54.55–98.08%). The cutoff for lactate was set at >4.650, providing 100% of sensitivity and 85.71% of specificity (AUC: 0.8810, 95% CI, CL: 54.55–98.08%). Both biomarkers presented high specificity and sensitivity for discriminating TBI survival and nonsurvival patients.

a cutoff of >57.75, glutamate provides 80% of sensitivity and 84.62% of specificity (AUC: 0.8214, 95% CI, CL: 54.55% to 98.08%) and with a cutoff of >4.650, lactate has 100% of sensitivity and 85.71% of specificity (AUC: 0.8810, 95% CI, CL: 54.55–98.08%). Glutamate and lactate provide high specificity and sensitivity, with almost identical power, for predicting brain death in TBI patients.

Additionally, aiming to corroborate the proposed functional interplay among biomarkers, we have developed a network using cross-correlation analysis. We identified statistically significant associations among glutamate, lactate, and BDNF. One may propose that these associations suggest reactive neuronal and glial responses to injury, and ultimately may reflect some level of functional coupling (Fig. 4).

## Discussion

This study used a multi-biomarker approach in the CSF of severe TBI patients searching for neuroactive substances with potential clinical and prognostic relevance. Our results demonstrated that CSF levels of glutamate, lactate, and BDNF at hospital admission have potential value as biomarkers of severe head injury. Further, glutamate and lactate levels were able to predict with high sensitivity and specificity patients who will die within 3 days following severe TBI. Also, up to 3 days, the clinical outcomes including intracranial pressure (ICP), mean arterial pressure, cerebral perfusion pressure, and GCS were similar between TBI groups (nonsurvival *vs*. survival) and did not correlate with CSF biomarkers.

The role of glutamate as biomarker of brain injury and clinical outcomes has previously been explored in studies with severe TBI patients. In contrast to our findings, Brown et al., 1998[25] showed that despite the persistent increase in the CSF glutamate levels up to 5 days after severe TBI, these changes did not predict brain death or correlate with GCS and electrophysiological deterioration. However, the majority of clinical studies indicate that increased brain extracellular glutamate levels in association with comorbidities may predict poor functional outcomes and brain death.[11–14] For instance, secondary mechanisms associated with the brain tissue deformation including global ischemia, sustained increased intracranial pressure and focal contusions[11,13], and spontaneous brain hypothermia (<36°C)[26] have been implicated in the increase in glutamate levels and acute neuronal death. Also, increased extracellular brain glutamate concentration after TBI is also influenced by decreased astrocytic glutamate uptake.[27] This might indicate that different players associated to the tripartite glutamatergic synapse, likely contribute for the deterioration of brain function after severe TBI, such as disrupted energy support rapidly triggering neuronal death.

We found that CSF lactate levels at hospital admission predict severe TBI patients who will die within 3 days after hospitalization. As previously stated, astrocytes take up glutamate in the synaptic space thereby triggering glycolysis and lactate production, which is shuttled to neurons.[15] The flux of these substrates in the body fluids has been explored in the clinical setting as biomarkers of neuroenergetic support, neuron-to-astrocyte interactions, and clinical outcomes.[28] Recently, Thelin et al., 2014 showed that an increased brain extracellular levels of lactate and pyruvate after TBI were correlated with unfavorable neurological outcome based on Glasgow Outcome Scale[29].

 

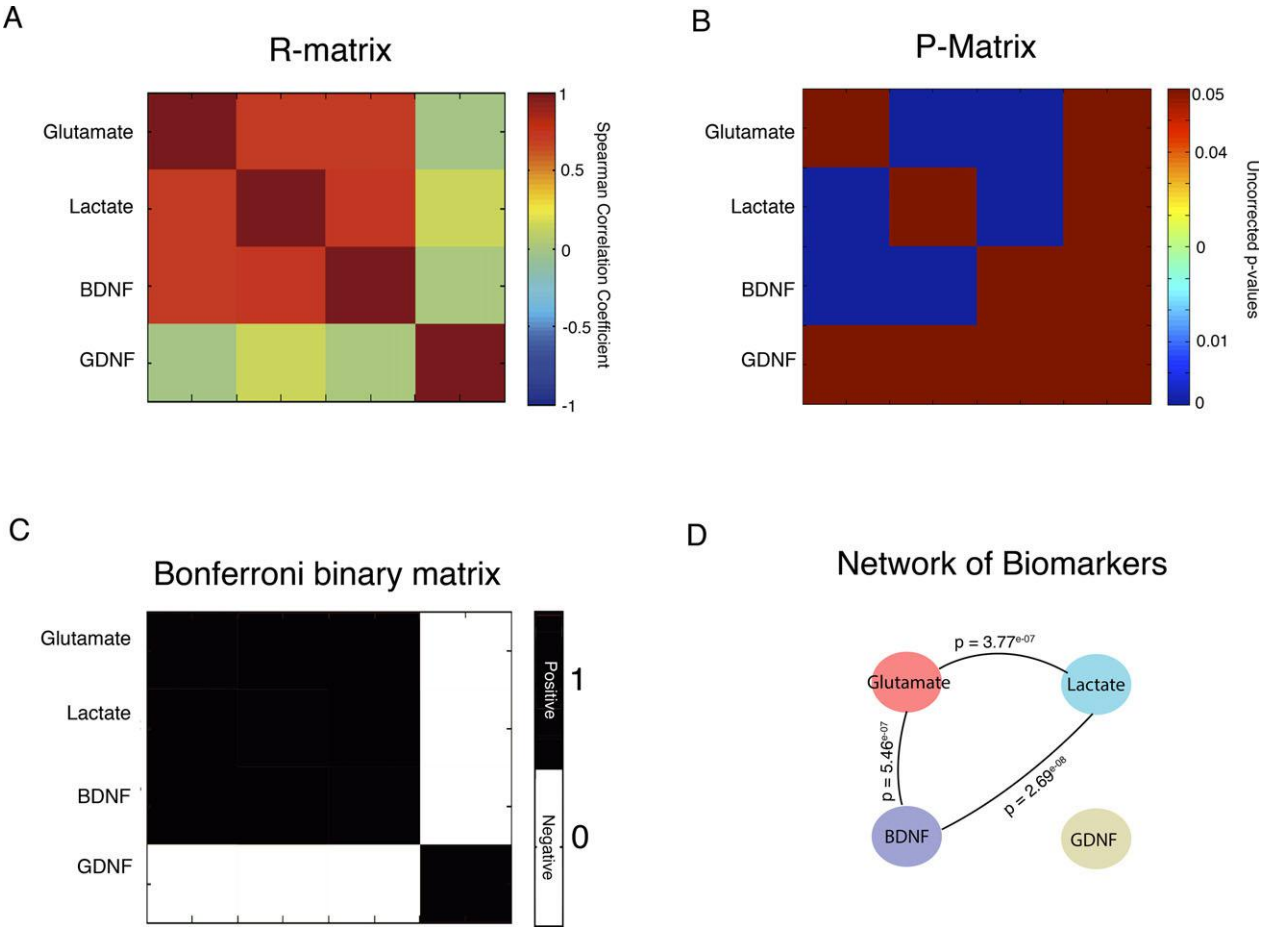


**Figure 4.** Association between biomarkers indexed by cross-correlation analyses. (A) Symmetric matrix of correlation coefficient values between biomarkers; (B) Symmetric matrix of – values between biomarkers; (C) Binary matrix corrected by Bonferroni method at $P < 0.05$; (D) Network for the biomarkers indicating high levels of associations between glutamate, lactate and BDNF.

Moreover, there is strong evidence showing that impaired cerebrovascular pressure reactivity, and decreased brain perfusion and oxygenation, are forces driving metabolic abnormalities related to lactate/pyruvate ratio. However, this oxygen deficiency is more pronounced in the perilesional tissue[26,30] and apparently does not explain the metabolic alterations in the whole brain after a TBI. Indeed, increased lactate production in the injured brain seems to be independent of oxygen availability, and therefore cannot be considered as a direct ischemic and hypoxic metabolic marker[30]. Instead, experimental and clinical studies highlight the existence of an acute hyperglycolysis after severe TBI followed by subacute decrease in glucose metabolism.[31,32] The early hyperglycolytic phase seems to reflect the energy demands for reversal of ionic imbalances caused by massive release of glutamate[33], while in subacute phase, the decrease in glucose utilization may indicate impaired mitochondrial function.[33,34]

Interestingly, we found a significant correlation between lactate and glutamate levels indicating they are strongly and positively associated. In comparison to our findings in CSF, Bouzat et al., 2014[16] demonstrated that hypertonic infusion of lactate in severe TBI patients improved metabolic profile and decreased glutamate levels in the brain extracellular microdyalisate. In addition, a previous study in severe TBI patients showed that brain glucose availability decreases locally and lactate increases in the absence of ischemia. In contrast, our study, suggests that lactate production may significantly increase even in the presence of a satisfactory glucose supply (Table 1) to attend brain metabolic needs. However, as proposed by Lama et al., 2014[28], the acute increase in the brain tissue lactate concentrations after severe TBI is associated to decreased neuronal uptake, probably leading to irreversible injury and pan-necrosis. Therefore, although the high extracellular availability of lactate suggests that

 

the metabolic machinery in astrocytes was responsive to the increased energy demands after TBI, neurons were apparently not capable of using lactate as substrate, ultimately contributing to the patient's death. This highlights a putative role for the monocarboxylated transporters expression in the metabolic uncoupling and neuronal death after severe TBI. From the clinical perspective, we propose that short-term elevation of CSF glutamate and lactate levels after severe TBI has strong predictive value for unfavorable neurological outcome. Moreover, lactate and glutamate positively correlated with long-term disability grade scale mRS).

In addition, we also assessed the ability of neurotrophins BDNF and GDNF in interrogate clinical outcomes in severe TBI patients. Data from preclinical studies indicate that BDNF modulates vesicular glutamate release and NMDA receptor sensitivity[35,36], and the availability of lactate for neurons through the monocarboxylate transporters-2.[21] As a CSF biomarker, BDNF displayed significant correlations with both glutamate and lactate; however, it was not predictive of imminent death within 3 days of hospitalization as were glutamate and lactate levels. Actually, measurements of BDNF levels in plasma and serum of severe TBI patients have provided controversial results. Simon et al., 2016 reported no predictive value for BDNF to discriminate survival and non-survival patients.[37] Similar to our findings, day-of-injury serum BDNF was associated with TBI diagnosis; however, the authors also showed 6-month prognostic value regarding recovery from TBI.[38] Further, the CSF levels of BDNF predicted mortality within 7 days of hospitalization after severe TBI.[39] Though preclinical studies proposes GDNF as therapeutic strategy to treat TBI, which highlights a neurobiological importance, its clinical value as fluid biomarker in patients has been little explored. In our study, CSF GDNF level was not a good diagnostic or predictive biomarker of poor clinical outcome. The main limitation of this study was the small sample size. Further, due to logistic difficulties, we did not have access to the biological samples of patients posthospitalization.

The CSF levels of glutamate and lactate have potential prognostic value to discriminate with high sensitivity and specificity severe TBI patients who will evolve to death within 3 days after hospitalization. Glutamate and lactate are promising CSF biomarkers of death after severe TBI.

## Acknowledgements

The authors thank Dr. Ana Elisa Böhmer (Department of Pharmacology, Institute of Biomedical Sciences, University of São Paulo) for the technical support in HPLC analysis. This research was funded by resources from FAPERGS # 1010267, CAPES PNPD # 1663, Science without borders CNPQ # 4011645/2012-6 and CNPQ INCTen Excitotoxicity and Neuroprotection # 573677/2008-5. The authors have no financial, personal or scientific conflict of interest.

## Author Contribution

Dr. Stefani: study concept and design; revising the manuscript; patient's care, data and interpretation. Dr. Modkovski: study concept and design; revising the manuscript patient's care and data collection. Dr. Hansel: study concept and design; revising the manuscript; biological fluids processing and analyses, neurobiochemical assays and data interpretation. Dr. Zimmer: study concept and design; revising the manuscript; data analysis and interpretation. Ms. Kopczynski: study concept and design; revising the manuscript; neurobiochemical assays and data interpretation. Dr. Muller: study concept and design; revising the manuscript; data collection and analysis. Ms. Strogulski: study concept and design; revising the manuscript; analysis and interpretation. Ms. Rodolphi: study concept and design; revising the manuscript; analysis and interpretation. MSc. Carteri: study concept and design; revising the manuscript; statistical analysis and data interpretation. Dr. Schmidt: study concept and design; revising the manuscript; selection of control individuals; clinical and neurological evaluation and cerebrospinal fluid sampling. Dr. Oses: study concept and design; revising the manuscript; study supervision, data acquisition and interpretation. Dr. Smith: study concept and design; drafting the manuscript, study concept and design, analysis and interpretation of data. Dr. Portela: study concept and design; drafting the manuscript, interpretation of data and obtaining funding. All authors critically revised and approved the final version of the manuscript.

## Conflict of Interest

Dr. Marco A. Stefani, Dr. Rafael Modkovski, Dr. Gisele Hansel, Dr. Eduardo R. Zimmer, Ms. Afonso Kopczynski, Dr. Alexandre P. Muller, Ms. Nathan R. Strogulski, Ms. Marcelo S. Rodolphi, Ms. Randhall K. Carteri, Dr. André P. Schmidt, Dr. Jean P. Oses, Dr. Douglas H. Smith and Dr. Luis V. Portela report no financial, personal or scientific conflict of interest.

### References

1. Roozenbeek B, Maas AI, Menon DK. Changing patterns in the epidemiology of traumatic brain injury. Nat Rev Neurol 2013;9:231–236.
2. Bohmer AE, Oses JP, Schmidt AP, et al. Neuron-specific enolase, S100B, and glial fibrillary acidic protein levels as

 

outcome predictors in patients with severe traumatic brain injury. Neurosurgery 2011;68:1624–1630; discussion 30-1.
3. Johnson VE, Stewart W, Smith DH. Axonal pathology in traumatic brain injury. Exp Neurol 2013;246:35–43.
4. Hay JR, Johnson VE, Young AM, et al. Blood-brain barrier disruption is an early event that may persist for many years after traumatic brain injury in humans. J Neuropathol Exp Neurol 2015;74:1147–1157.
5. Faden AI, Demediuk P, Panter SS, Vink R. The role of excitatory amino acids and NMDA receptors in traumatic brain injury. Science 1989;244:798–800.
6. Moro N, Ghavim SS, Harris NG, et al. Pyruvate treatment attenuates cerebral metabolic depression and neuronal loss after experimental traumatic brain injury. Brain Res 2016;1642:270–277.
7. Rostami E, Krueger F, Plantman S, et al. Alteration in BDNF and its receptors, full-length and truncated TrkB and p75(NTR) following penetrating traumatic brain injury. Brain Res 2014;1542:195–205.
8. Zetterberg H, Smith DH, Blennow K. Biomarkers of mild traumatic brain injury in cerebrospinal fluid and blood. Nat Rev Neurol 2013;9:201–210.
9. Shahim P, Tegner Y, Wilson DH, et al. Blood biomarkers for brain injury in concussed professional ice hockey players. JAMA Neurol 2014;71:684–692.
10. Bonfoco E, Krainc D, Ankarcrona M, et al. Apoptosis and necrosis: two distinct events induced, respectively, by mild and intense insults with N-methyl-D-aspartate or nitric oxide/superoxide in cortical cell cultures. Proc Natl Acad Sci USA 1995;92:7162–7166.
11. Zauner A, Bullock R, Kuta AJ, et al. Glutamate release and cerebral blood flow after severe human head injury. Acta Neurochir Suppl 1996;67:40–44.
12. Bullock R, Zauner A, Woodward JJ, et al. Factors affecting excitatory amino acid release following severe human head injury. J Neurosurg 89:507–518.
13. Koura SS, Doppenberg EM, Marmarou A, et al. Relationship between excitatory amino acid release and outcome after severe human head injury. Acta Neurochir Suppl 1998;71:244–246.
14. Chamoun R, Suki D, Gopinath SP, et al. Role of extracellular glutamate measured by cerebral microdialysis in severe traumatic brain injury. J Neurosurg 2010;113:564–570.
15. Pellerin L, Magistretti PJ. Glutamate uptake into astrocytes stimulates aerobic glycolysis: a mechanism coupling neuronal activity to glucose utilization. Proc Natl Acad Sci USA 1994;91:10625–10629.
16. Bouzat P, Sala N, Suys T, et al. Cerebral metabolic effects of exogenous lactate supplementation on the injured human brain. Intensive Care Med 2014;40:412–421.
17. Quintard H, Patet C, Zerlauth JB, et al. Improvement of neuroenergetics by hypertonic lactate therapy in patients with traumatic brain injury is dependent on baseline cerebral lactate/pyruvate ratio. J Neurotrauma 2016;33:681–687.
18. Glenn TC, Kelly DF, Boscardin WJ, et al. Energy dysfunction as a predictor of outcome after moderate or severe head injury: indices of oxygen, glucose, and lactate metabolism. J Cereb Blood Flow Metab 2003;23:1239–1250.
19. Almeida RD, Manadas BJ, Melo CV, et al. Neuroprotection by BDNF against glutamate-induced apoptotic cell death is mediated by ERK and PI3-kinase pathways. Cell Death Differ 2005;12:1329–1343.
20. Farrand AQ, Gregory RA, Scofield MD, et al. Effects of aging on glutamate neurotransmission in the substantia nigra of Gdnf heterozygous mice. Neurobiol Aging 2015;36:1569–1576.
21. Robinet C, Pellerin L. Brain-derived neurotrophic factor enhances the expression of the monocarboxylate transporter 2 through translational activation in mouse cultured cortical neurons. J Cereb Blood Flow Metab 2010;30:286–298.
22. Schmidt AP, Tort AB, Silveira PP, et al. The NMDA antagonist MK-801 induces hyperalgesia and increases CSF excitatory amino acids in rats: reversal by guanosine. Pharmacol Biochem Behav 2009;91:549–553.
23. Zetterberg H, Blennow K. Fluid biomarkers for mild traumatic brain injury and related conditions. Nat Rev Neurol 2016;12:563–574.
24. Huisman TA, Schwamm LH, Schaefer PW, et al. Diffusion tensor imaging as potential biomarker of white matter injury in diffuse axonal injury. AJNR Am J Neuroradiol 2004;25:370–376.
25. Brown JI, Baker AJ, Konasiewicz SJ, Moulton RJ. Clinical significance of CSF glutamate concentrations following severe traumatic brain injury in humans. J Neurotrauma 1998;15:253–263.
26. Timofeev I, Carpenter KL, Nortje J, et al. Cerebral extracellular chemistry and outcome following traumatic brain injury: a microdialysis study of 223 patients. Brain 2011;134(Pt 2):484–494.
27. Goodrich GS, Kabakov AY, Hameed MQ, et al. Ceftriaxone treatment after traumatic brain injury restores expression of the glutamate transporter, GLT-1, reduces regional gliosis, and reduces post-traumatic seizures in the rat. J Neurotrauma 2013 Aug;30:1434–1441.
28. Lama S, Auer RN, Tyson R, et al. Lactate storm marks cerebral metabolism following brain trauma. J Biol Chem 2014;289:20200–20208.
29. Thelin EP, Nelson DW, Ghatan PH, Bellander BM. Microdialysis monitoring of csf parameters in severe traumatic brain injury patients: a novel approach. Front Neurol 2014;5:159.
30. Lazaridis C, Andrews CM. Brain tissue oxygenation, lactate-pyruvate ratio, and cerebrovascular pressure reactivity monitoring in severe traumatic brain injury:

 

systematic review and viewpoint. Neurocrit Care 2014;21:345–355.
31. Bergsneider M, Hovda DA, Shalmon E, et al. Cerebral hyperglycolysis following severe traumatic brain injury in humans: a positron emission tomography study. J Neurosurg 1997;86:241–251.
32. Yoshino A, Hovda DA, Kawamata T, et al. Dynamic changes in local cerebral glucose utilization following cerebral conclusion in rats: evidence of a hyper- and subsequent hypometabolic state. Brain Res 1991;561:106–119.
33. Katayama Y, Becker DP, Tamura T, Hovda DA. Massive increases in extracellular potassium and the indiscriminate release of glutamate following concussive brain injury. J Neurosurg 1990;73:889–900.
34. Verweij BH, Muizelaar JP, Vinas FC, et al. Impaired cerebral mitochondrial function after traumatic brain injury in humans. J Neurosurg 2000;93:815–820.
35. Black IB. Trophic regulation of synaptic plasticity. J Neurobiol 1999;41:108–118.
36. Kohara K, Kitamura A, Morishima M, Tsumoto T. Activity-dependent transfer of brain-derived neurotrophic factor to postsynaptic neurons. Science 2001;291:2419–2423.
37. Simon D, Nascimento RI, Filho EM, et al. Plasma brain-derived neurotrophic factor levels after severe traumatic brain injury. Brain Inj 2016;30:23–28.
38. Korley FK, Diaz-Arrastia R, Wu AH, et al. Circulating brain-derived neurotrophic factor has diagnostic and prognostic value in traumatic brain injury. J Neurotrauma 2016;33:215–225.
39. Failla MD, Conley YP, Wagner AK. Brain-derived neurotrophic factor (BDNF) in traumatic brain injury-related mortality: interrelationships between genetics and acute systemic and central nervous system BDNF profiles. Neurorehabil Neural Repair 2016;30:83–93.

 

**Anexo IV: Serum Biomarkers and Clinical Outcomes in Traumatic Spinal Cord Injury: Prospective Cohort Study**

World Neurosurg. 2019 Feb;122:e1028-e1036. doi: 10.1016/j.wneu.2018.10.206. Epub 2018 Nov 7.

# Serum Biomarkers and Clinical Outcomes in Traumatic Spinal Cord Injury: Prospective Cohort Study

Marcelo de Mello Rieder [1], Jean Pierre Oses [2], Fernanda Machado Kutchak [1], Mônia Sartor [3], André Cecchini [4], Marcelo Salimen Rodolphi [3], Carolina David Wiener [2], Afonso Kopczynski [3], Alexandre Pastoris Muller [5], Nathan Ryzewski Strogulski [3], Randhall B Carteri [3], Gisele Hansel [6], Marino Muxfeldt Bianchin [7], Luis Valmor Portela [8]

Affiliations
PMID: 30414523 DOI: 10.1016/j.wneu.2018.10.206

## Abstract

**Background:** A plethora of reactive cellular responses emerge immediately after a traumatic spinal cord injury (SCI) and may influence the patient's outcomes. We investigated whether serum concentrations of neuron-specific enolase, interleukin-6, glial-derived neurotrophic factor, and neurotrophic growth factor reflect the acute-phase responses to different etiologies of SCI and may serve as predictive biomarkers of neurologic and functional outcomes.

**Methods:** Fifty-two patients were admitted to the intensive care unit after SCI due to traffic accidents, falls, and firearm wounds and had blood samples collected within 48 hours and 7 days after SCI. Thirty-six healthy subjects with no history of SCI were included as controls. Neurologic and functional status was evaluated on the basis of American Spinal Injury Association and Functional Independence Measure scores over a period of 48 hours and 6 months after SCI.

**Results:** Serum NSE increased significantly 48 hours and 7 days after SCI compared with controls, while interleukin-6 increased only at 48 hours. In contrast, the neurotrophic growth factor level significantly decreased 48 hours and 7 days after SCI. Serum glial-derived neurotrophic factor level did not differ from control at any time point. Also, there was no significant difference in biomarker concentrations between the etiologies of SCI or the level of spinal injury. There were no correlations between biomarker levels at 48 hours with neurologic or functional outcomes 7 days and 6 months after SCI.

**Conclusions:** Our results suggest expansive axonal damage coupled with an acute proinflammatory response after SCI. However, in our study biomarker concentration did not correlate with short- or long-term prognosis, such as survival rate or sensory and motor function.

**Keywords:** GDNF; IL-6; NGF; NSE; Serum biomarkers; Spinal cord injury.



## LinkOut - more resources